Forays in Process Analytical Technologies and Theory of Sampling:

1. Feasibility of handheld NIR characterization in small-scale berry wineries (PAT)

2. Variographic analysis of standard procedures for industrial waste water characterization (TOS)

Dorthe Vognstoft Kristensen
M. Sc. Eng. Dissertation
15th July 2009 – 14th June 2010
Esbjerg Institute of Technology Aalborg University

Title Sheet

Project Title: (English)

Forays in Process Analytical Technologies and Theory of Sampling:

1. Feasibility of handheld NIR characterization in small-scale berry wineries (PAT)
2. Variographic analysis of standard procedures for industrial waste water characterization (TOS)

Project Title: (Danish)

Bidrag til anvendt Process Analytical Technologies og Theory of Sampling

1. Indledende undersøgelse af NIR karakterisering hos en lokal bærvinsproducent
2. Variografisk analyse af standard procedurer for spildevandskarakterisering

Supervisor: Professor Kim H. Esbensen, Esbjerg Institute of Technology Aalborg University

Collaborator: Guttorm Isaksen, De 5 Vinmakeran, Tromsø, Norway

Ulla O. Lund, Eurofins Environment A/S, Vejen, Denmark

Period: 15th July 2009 – 14th June 2010

School of Education: Esbjerg Institute of Technology Aalborg University

Abstract

Local, small-scale wineries can today employ fast, easy-to-use, inexpensive techniques for measuring chemical constituents for process and product control to guard against failed fermentations as early as possible and to further optimal wine quality. NIR is a reliable, fast, accurate, and precise method for measuring a. o. sugars, acids, glycerol, and ethanol using newly developed, robust, *hand-held* short- and long-wave NIR equipment. Two general Phazir™ sensor systems (short- and long-wave NIR), were employed, based on chemometric multivariate calibration on three low-alcohol wines made from locally harvested berry and fruits in a local winery, Tromsø, Norway. For each wine a PLS-regression calibration model for selected components of wine-making interest was optimized; all PLS-regression models were validated with test-set validation exclusively. Satisfactory individual models were obtained for sucrose, glucose, fructose, glycerol, ethanol, citric, tartaric, malic, succinic, lactic, and acetic acid, and excellent models for total sugar and total acid, when using the short-wave NIR region (890 – 1690 nm); 1.st derivative pre-treatment was applied to all parameters except for ethanol where full MSC is used. There is a high likelihood of carrying over these results also to table wines and fermentation broths.

Variographic analysis (Theory of Sampling) evaluates process variability and uncertainties associated with sampling of waste water. This study analysed both incremental samples and 24-hour composite samples from the Bramming Waste Water Treatment Facility North including total phosphorus (TP), conductivity, and ammonium (NH_4-N). For 48 hours, short-term increments were extracted at two selected sampling points to evaluate the total sampling error and effects from periodicity; these increments were analyzed individually and their variogram showed a cyclic variation of approx 420 m^3, which corresponds to day-to-night load variations. The 24 hour composite samples were concluded to be reliable results for emission monitoring. Also, for a period of 39 days, standard composite samples (24-hour intervals) were collected from seven different locations in the standard sampling outlet facility and compared. Variographic analysis of TP and conductivity from these alternative outlet locations result in a marked cyclic variation of 7 days (TP) and 9 days (conductivity). This cycle equals week vs. weekend variations in composition. The indicated 9-day period remains unexplainable. The present study confirms that the standard sampling point F, directly after the weir, is representative, but an equally good alternative was found in sampling point B. Total Sampling Error (TSE) for TP and conductivity could be estimated as 12.3 % and 12.4 % respectively, while the Total Analytical Error (TAE) was insignificant. Variographic analysis of NH_4-N in increments indicates a 12-lag cyclic variation, interpreted as a possible *pseudo-variation* due to systematic analysis delays.

Resumé

For at imødekomme problemer i forbindelse med produktion af vin er det ønskeligt at kunne implementere en hurtig, lettilgængelig og rentabel teknik til at måle koncentrationen af vigtige kemiske parametre. NIR er en relativ billig løsning, som samtidig er både let at anvende og hurtig til at analysere prøver uden at en egentlig prøveforberedelse er nødvendig. NIR er en spektroskopisk teknik, som er nøjagtig og præcis. I dette projekt blev to håndholdte og nyligt udviklede NIR spektrofotometre (Phazir™) anvendt, målende spektre i områderne 890 nm – 1690 nm og 1596 nm – 2396 nm. Tre bærvine fra en lille vinproducent i Tromsø, Norge, hvor vinene er baseret på råmaterialer høstet i lokalområdet, blev karakteriseret mht. koncentration af sukrose, glukose, fruktose, glycerol, ethanol, citron- , vin- , æble-, rav-, mælke- og eddikesyre. For alle tre vine blev der vha. kemometri og NIR spektre udviklet og optimeret PLS kalibreringsmodeller, som er valideret udelukkende vha. test set validering. De bedste modeller blev opnået ved at anvende NIR intervallet 890 nm – 1690 nm og anvende matematisk modellering af spektrene; MSC til modellering af ethanol og 1. afledede til sukre, glycerol og syrer. Der blev fundet tilfredsstillende resultater for de individuelle kemiske stoffer og endnu bedre modeller for total-sukker og total-syre.

Variografi blev anvendt til at bestemme usikkerhedsbidraget ved prøvetagningen af spildevand og samtidig evaluere om placering af prøvetageren har betydning for repræsentativiteten og prøvetagningsusikkerheden. Den variografiske analyse er udført på både delprøver og døgnprøver fra Bramming Renseanlæg Nord. Total fosfat (TP), konduktivitet og ammonium (bestemt som NH_4-N) er blevet anvendt som analyseparametre. Over en periode på 48 timer blev der udtaget delprøver fra to punkter (før og efter v-overfald) i udløbet fra renseanlægget. Alle delprøver blev analyseret for TP og konduktivitet og evalueret variografisk. Variografisk evaluering af TP og konduktivitet i delprøver viste en cyklisk variation på ca. 420 m^3 H_2O. Denne cyklus svarer til variationer mellem dag og nat, hvorfor en døgnprøver vil give et realistisk mål for den mængde, som bliver udledt fra renseanlægget i løbet af et døgn. Variografisk evaluering af døgnprøver udtaget over en periode på 39 dage viste en cyklisk variation på 7 og 9 dage for hhv. TP og konduktivitet. En cyklus på 7 dage svarede til variationerne mellem weekender og hverdage, men en cyklus på 9 dage var uforklarlig ved afslutning af dette projekt. Sammenligningen mellem syv punkter har vist at punkt F er repræsentativt og resulterede i en mindre prøvetagningsusikkerhed end de andre, men punkt B kunne være et anvendeligt alternativ, da dette punkt viste lignende resultater. Prøvetagningsusikkerheden for pukt F blev fundet til at være 12.3 % og 12.4 % for hhv. TP og konduktivitet. Variografisk evaluering af NH_4-N i delprøver viste en cyklisk variation svarende til ca. 12 delprøver (= 84 m^3 H_2O). Denne variation kan forklares som en pseudo-variation pga. praktiske problemer i forbindelse med prøvetagningen og analysering i felten.

Preface

This project was a dissertation for the M. Sc. (Eng.) degree. The dissertation was divided in two parts;

1. Method development for measuring taste constituents in low-alcohol berry wine and
2. Quantitation of sampling uncertainty when doing automated sampling of waste water

The first part was done in collaboration with the local winery "*De 5 Vinmakeran*", Tromsø, and the second part was carried out in collaboration with Eurofins Environment A/S, Vejen.

Figures and tables are called "Figure x" and "Table x". If nothing else is stated, the figure and table are my own production. References are marked as [number]. A table of contents for appendices is found after the bibliography.

Regarding the first part of the project of the dissertation I would like to thank the laboratory staff at Esbjerg Institute of Technology Aalborg University; Dorte Spangsmark and Linda Madsen, for doing the analysis of many of the reference analysis for the method development.

Regarding the second part of the dissertation I would like to thank the laboratory staff at Eurofins Environment A/S for doing the analysis on many samples and Perry Hansen for setting up the sampler units, and especially Ulla Oxenboll Lund, for both practical and theoretical help regarding the project. Also I would like to thank Mia-Maria Hellestrup, laboratory trainee, and Charlotte Nørkær Hansen, fellow student, at Esbjerg Institute of Technology Aalborg University for their help and company during the experimental period, and especially Mia-Maria for doing analysis on many more samples in the laboratory.

A very special thanks to my supervisor professor Kim H. Esbensen, Esbjerg Institute of Technology Aalborg University, for his endless patience and help with questions regarding the project.

Esbjerg, June 14th 2010

Dorthe Kristensen

Table of Contents

Part 1 – Feasibility of Handheld NIR Characterization in Small-scale Berry Wineries (PAT)

Introduction

Many conventional analytical methods are applied in the production of wine to determine the content of different important parameters during fermentation and storage of a produced wine. Nearly all these analytical methods are time consuming, expensive and/or use potentially dangerous reagents. This is a problem for both small- and large-scale wineries and for the laboratories which services winemaking and quality control. Therefore, to meet the demands from wineries and laboratories quick, in-expensive, and easy-to-use methods are desired. As an alternative to conventional methods a spectroscopic technique may be applied.

The main disadvantages of spectroscopic techniques are that they are *indirect methods*, meaning that there is a need for calibration and validation, and only a few spectroscopic methods exist which are fully calibrated and validated directly off the shelf.

Some of the advantages with a spectroscopic technique compared to conventional methods are [1,2]:

- Quick analysis
- No reagents are required
- Non-destructive and non-invasive
- None or limited sample preparation
- Sample form, size, and physical state (solid, liquid, or gas) is no restriction
- Economic (relative high purchase, but low cost when in use)
- Qualitative and quantitative analysis
- Easy-to-use for trained and untrained personal

One of the most important advantages in spectroscopic instrumentation is the possibility and potential for the development and commercializing of an easy-to-use instrumentation. Many spectroscopic techniques are complex and sophisticated for untrained personal and require trained personal to develop the calibration and validation of the technique. When the calibration and validation are made, then with the set up of dedicated instruments (including sample preparation) and fully programmed for target analysis, the spectroscopic instrument is ready as a “push-button” easy-to-use instrument, which does not require specially trained personal. This feature will make spectroscopic techniques a potential alternative to the conventional analytical methods [1,2].

This first part of the project first gives an overview of similar studies for alcoholic beverages. Next there is an overview of the winery and the wines studied. Later a discussion of a replicate experiment to find a representative sampling process and to determine the uncertainty contribution of the sampling process is made. Lastly chemometric PLS-models were made to compare the NIR spectra with concentrations of wine samples to find the optimal models and to make recommendations as to variable selection i.e., which regions of the NIR spectra serves to result in optimal models.

Previous Studies

Different Techniques and Equipment

The quality of wine for the consumers is primarily related to the odour and taste of the bottled wine. For both small- or large-scales wineries the quality is related to the above, but of a more complex nature related to the specific chemical components in the wine.

In previous studies [3-19], different techniques have been used for measuring the content especially of ethanol, but also to measure the content of sugars, acids, and other components which are of importance for the quality of wine. A list of examples of some of the techniques follows.

Determination of one component at a time with conventional methods

- Pycnometry [3,4,5]: Ethanol
- GC-FID [5]: Ethanol
- Distillation and densiometry [6,7]: Ethanol
- Refractometry [8]: Sugar

Determination of several components at a time with conventional methods

- Capillary Electroforese [9]
- HPLC (High Performance Liquid Chromatography) [10,11,12]: Citric, tartaric, malic, succinic, lactic, and acetic acid, glucose, fructose, glycerol, and ethanol
- HPICE (High Performance Ion Chromatography Exclusion) [13]: Tartaric, citric, and succinic acid
- GC-MS (Gas Chromatography – Mass Spectrometer) [14]: Volatile compounds

Many of the above are time consuming, expensive and/or demand trained personal. Therefore, it is desirable to develop an inexpensive, easy-to-use, and quick method for measuring as many components as possible, where the method shown to be just as effective and give the same results as the more conventional methods. A desirable alternative could be a relatively inexpensive IR method.

Possibility for determination of many components at a time through spectrometry

- NMR [12,15]
- FT-IR [1,7,11,16,12]
- UV/VIS/NIR [5,8]
- NIR [17]
- MIR [18]
- ATR and IR[6,19]

Comparison of Previous Studies of IR Methods

A comparison of obtained results from previous studies are listed in Table 1, where models are developed for IR through chemometric evaluation with one or more from the above listed methods used as reference analysis,. The components evaluated in the present comparison are sugars, glycerol, ethanol, and acids.

All the studies listed are using IR spectroscopy in different combinations of ATR, FT, NIR, and MIR. For some of the studies it was not possible to find values for both slope, R^2, number of PLS components, and the error of prediction. These missing values are marked with "-" in the table.

Table 1 Overview of previous studies with regards to determination of chemical components in wine by IR spectroscopy

Component	Range	Technique	Slope	R^2	# PLS	Error	Literature
Reducing sugar[1]	0.6 - 14.4 g/L	NIR	0.983	0.712	-	0.33 [3]	[17]
Sucrose[2]	0.8 - 8.8 % vol.	ATR and NIR	-	0.996	5	0.1142 [4]	[19]
Glucose[2]	0 - 125 g/L	FT-IR	-	0.994	3	3.4 [7]	[11]
Glucose[1]	0 – 4 g/L	FT-MIR	-	0.9951	6	0.207 [8]	[12]
Fructose[2]	0 - 133 g/L	FT-IR	-	0.994	9	4.9 [7]	[11]
Fructose[1]	0 - 64.5 g/L	ATR FT-NIR	1.04	0.987	-	1.606 [3]	[6]
Fructose[1]	0 – 4 g/L	FT-MIR	-	0.9978	6	0.138 [8]	[12]
Glycerol[2]	0 - 11 g/L	FT-IR	-	0.988	9	0.66 [7]	[11]
Glycerol[1]	2.1 - 15.5 g/L	ATR FT-NIR	0.796	0.864	-	0.824 [3]	[6]
Glycerol[1]	2.0 - 14.6 g/L	NIR	0.871	0.845	-	0.72 [3]	[17]
Glycerol[1]	0 – 6 g/L	FT-MIR	-	0.9941	6	0.297 [8]	[12]
Ethanol[2]	0 - 15.4 % vol.	FT-IR	-	0.99	9	1.1 [7]	[11]
Ethanol[2]	10 - 50 % vol.	ATR and NIR	-	0.99	5	0.2193 [4]	[19]
Ethanol	0 - 45 % vol.	IR	0.995	0.9996	-	0.279 [5]	[3]
Ethanol[1]	7.3 - 17 % vol.	ATR FT-NIR	1.02	0.997	-	0.099 [3]	[6]
Ethanol[1]	9.6 - 15.2 % vol.	NIR	0.971	0.978	-	0.24 [3]	[17]
Ethanol[2]	0 - 20 % vol.	NIR	-	0.999	3	0.09 [5]	[22]
Ethanol[2]	5 - 26 % vol.	FT-NIR	-	0.998	4	0.26 [5]	[23]
Ethanol[1]	25.0 - 78.1 % vol.	FT-MIR	-	0.94	5	0.21 [3]	[7]
Ethanol[1]	0 – 10 g/L	FT-MIR	-	0.9940	4	0.562 [8]	[12]
Citric acid[2]	0 - 0.85 g/L	FT-IR	-	0.985	10	0.08 [7]	[11]
Citric Acid[1]	0 - 3.37 g/L	ATR FT-NIR	0.081	0.384	-	0.104 [3]	[6]
Citric Acid[1]	0 – 0.88 g/L	FT-MIR	-	0.9710	6	0.107 [8]	[12]
Tartaric acid[2]	0 - 2.62 g/L	FT-IR	-	0.987	12	0.24 [7]	[11]
Tartaric Acid[2]	0.5 - 8.2 % vol.	ATR and NIR	-	0.989	4	0.1699 [4]	[19]
Tartaric Acid[1]	0.4 - 3.8 g/L	ATR FT-NIR	0.764	0.709	-	0.388 [3]	[6]
Tartaric Acid[1]	1.5 - 4.6 g/L	NIR	0.675	0.428	-	0.39 [3]	[17]
Tartaric Acid[1]	0 – 0.75 g/L	FT-MIR	-	0.9095	7	0.184 [8]	[12]
Malic acid[2]	0 - 4.57 g/L	FT-IR	-	0.985	13	0.32 [7]	[11]
Malic Acid[1]	0 - 4.5 g/L	ATR FT-NIR	0.7	0.768	-	0.651 [3]	[6]
Malic Acid[1]	0.03 - 1.8 g/L	NIR	0.91	0.441	-	0.36 [3]	[17]
Malic Acid[1]	0 – 1.75 g/L	FT-MIR	-	0.9772	7	0.191 [8]	[12]
Succinic acid[2]	0 - 10.97 g/L	FT-IR	-	0.982	9	0.67 [7]	[11]
Lactic acid[2]	0 - 1.03 g/L	FT-IR	-	0.989	13	0.12 [7]	[11]
Lactic Acid[1]	0.03 - 3.5 g/L	ATR FT-NIR	0.821	0.901	-	0.291 [3]	[6]
Lactic Acid[1]	0.06 - 5.3 g/L	NIR	0.941	0.814	-	0.41 [3]	[17]
Lactic Acid[1]	0 – 1.75 g/L	FT-MIR	-	0.9791	6	0.183 [8]	[12]
Acetic acid[2]	0 - 2.3 g/L	FT-IR	-	0.988	14	0.18 [7]	[11]
Acetic Acid[1]	Mole fraction: 0 - 0.8	NIR	-	-	4	3.1 % [6]	[24]
Acetic acid[1]	0 – 0.32 g/L	FT-MIR	-	0.9791	6	0.0615 [8]	[12]

1: Calibration: cross-validation, validation: test set and 2: Cross-validation, 3:SEP, 4: RMSEP, 5: RMSECV, 6: relSEP, 7: SECV, and 8: RMSEE

The most evaluated component in wine is without doubt ethanol, and then secondary an evaluation of different taste and colour components are evaluated. The taste components evaluated in the previous studies were different types of sugars and acids. Additionally, in some of the studies different kinds of amino acids were evaluated, but these are not discussed in this project.

It can be seen from Table 1 that the most prominent validation technique used is test set validation, but calibration is made with cross-validation on a calibration set. By this method the cross-validation is used to find the optimal PLS component for the model, and then the model is applied to test set for validation. Since cross validation usually gives an over-optimistic estimate of the prediction error, real test-set validation should rather have been used for evaluation of the models. In this way, the most realistic optimal PLS component and error of prediction for the model are found through test set validation. [1, 43]

Overall, models for sugars, glycerol, and ethanol provided good results with regards to R^2, since the values were above 0.90 with only a few exceptions. Only a few models for acids had R^2 values above 0.90, showing that it could be difficult to model some acids from IR spectra. The same tendency with regards to accuracy of the models was seen, where the slopes for sugars, glycerol and ethanol were closer to 1, than the slopes from the modelling of acids. One study showed that a model for total organic acids (sum of all the acids determined in the study) gave a better result than when the organic acids were modelled individually. This might be due to differences in the precision and accuracy of the reference methods as well as to possible inadequacy of the FT-NIR method in differentiating among the various organic acids.[6]

With regards to the number of PLS components used in the models, a number of 3 to 5 PLS components were generally considered acceptable for modelling of pulp, must, or wine. In one study [7] the number of PLS components for the calibration models show a number of PLS components of 5 to 13 found through cross validation. By applying the models to a test set, the validation gave a number of PLS components of 5 to 9. In general the number of PLS components used for the individual chemical components were lowered by 1 to 2 PLS components and in one case even by 8 PLS components – all a clear sign of adhesive model over fitting by cross-validation.

The tolerance allowed in the indication of the alcoholic strength in wines made from grapes is ± 0.5 % vol. and for fruit wines the tolerance is ± 1.0 % vol. [20,21]. With regards to this the root mean square error of prediction and cross-validation and the standardized error of prediction in the previous studies of ethanol were below the allowed threshold.

For the other components of interest in this project; sugars, glycerol, and acids, there are not stated an allowed tolerance for the labelling of the wine. Instead for the level of residual sugar an interval coding is listed

- **Dry**: maximum 4 g/L or 9 g/L, if the total acidity is not more than 2 g (expressed as g/L of tartaric acid) below the residual sugar content
- **Medium dry**: 4 g/L to 12 g/L or 4 g/L to 18 g/L, where the minimum total acidity level is set by the local regulations
- **Medium sweet**: 12 g/L to 45 g/L
- **Sweet**: minimum 45 g/L

For the acids a maximum level of acid, expressed as tartaric acid, used for acidification of the wine is stated, depending on the wine type and the origin of the wine. The level of both residual sugar and

acids are not important for this project, but the tolerance is, since this is consistent with the uncertainty in the modelling of the components. Since no regulations are made for the labelling, the tolerance should be as low as possible to make the error of prediction as low as possible.

The relative uncertainty in the models for sugars in the previous studies gave a result of approx 2.5 % compared to the range of concentration used in the models. For the glycerol the results was approx 5.5 %, and for the acids the results were approx 2 % to 20 %. This uncertainty for sugar and glycerol were within acceptable limits, where the range for the acids was very large. This might be due to the previous mentioned reasons as to the difficulties with the precision and accuracy of the reference methods, or possible inadequacy of the IR method in differentiating between the different acids, or due to the limited concentration range of the acids.

Overall the models for sugars, glycerol, and ethanol were good when evaluating slope, R^2, and the error of prediction. The models for acids were not quite as good, since both slope and R^2 shows low values and the error of prediction was high for many of the models compared to the concentration range used in the models.

Of particular interest for this project are three of the previous studies [11,12,3]. The first two are studies where many parameters were evaluated at the same time: the first using NIR, the second using MIR, and the third was a study using a portable NIR equipment.

The first study [11] evaluated all the parameters interesting for this project using NIR for the determination, only sucrose was not included. All the models obtained acceptable results using cross-validation for the calibration. The results showed precision between 0.98 and 0.99. By applying test set validation to the models, the models gave an average relative error in the range of 1.5 % to 8.7 %. The absolute error was defined as the average difference between the predicted value and the reference value. When evaluating the number of PLS components used in the cross-validation, only the model for glucose showed acceptable results. The rest of the models were using 9 to 14 PLS components, which indicates that the models were significantly over fitted and over optimistic in their prediction. Therefore optimization should have been applied before using the model for prediction. The study also showed that a calibration model made for one wine type could not necessarily be used for other wine types without including the other wine types in the calibration.

The second study [12] evaluated almost the same as the first study [11], only this time FT-MIR was used. All the models obtained acceptable results using cross-validation for the calibration. The result showed precision between 0.9095 and 0.9978. By applying test set validation to the models, they gave an average deviation in the range of 1.0 % to 17.4 %. When evaluating the number of PLS components used in the cross-validation, only the model for ethanol showed acceptable results with the use of four PLS components. The rest were using six or seven PLS components, which made the models over optimistic in their predictions.

A special feature of this study [12] was that it showed that ethanol severely influences the quantitative determination of the other parameters, as they have spectral features characteristic for those of ethanol. The solution was to use water as a reference during modelling and then use a solution of 35 g/L ethanol in distilled water as a reference, when predicting the other parameters in the real wine samples. In this way the apparent absorbance of ethanol in the real wine samples were reduced to a degree where it was possible to quantitatively determine the concentration of the other parameters.

Another special feature of the study [12] was that it evaluated the ability of the models to detect an increase in concentration of one single parameter in a real wine sample. The study showed that an increase could easily be detected; furthermore, the determination of the other parameters was hardly affected by the change in concentration of one single parameter.

The third study [3] was an evaluation of an inexpensive, easy-to-use, and portable equipment, with an identical purpose to the present feasibility study. The previous study measured the content of ethanol in the range of 0 % to 45 % vol. using different types of alcoholic beverages (beers, wines, and spirit drinks) as the matrix. It showed very good results with a slope of 0.995, R^2 of 0.9996, and a root mean square of error of 0.279 % vol. In the study only ethanol was determined, where as in the present study a simultaneous determination of several sugars and acids, glycerol, and ethanol will be made.

Temperature Effect on NIR Spectra

The lack of robustness, which was seen in several of the previous studies, could be due to several causes of the temperature effect on NIR spectra such as the varying temperature of the sample, the spectrometer, and/or the surroundings. The factor, which has been most widely studied, was the sample temperature. The previous studies showed that the sample temperature affects the result of both classification and calibration models when NIR spectra are used. [24 - 30]

The NIR spectra of liquids are by nature a vibrational spectra of the liquid sample; the vibrational features arises from chemical structure of functional groups. The Theory of IR is described in Appendix 1. The secondary molecular features could be the result of hydrogen bonding. These forces which influence the molecular bonds and their vibration modes, are highly affected by conditions like temperature and pressure.

The NIR spectra of different alcohols are depending on the temperature, because the self-associated forms of the alcohols dissociates into oligomers, dimers, and monomers as a function of the temperature of the liquid [28]. The absorption intensity of the molecular bonds is also affected by the temperature changes, since the spectrum changes according to the temperature variation [30].

The temperature of the sample can also cause shifts in absorption bands. As an example, when increasing the temperature of a wine sample from 30 °C to 50 °C, the band at 978 nm shifted to 972 nm, and the band at 1454 nm shifted to 1444 nm [25]. The temperature also affects the width of a band due to different cluster sizes formed by the hydrogen bonding. An increase in temperature of the sample, decreases the average cluster size and increases the relative absorbance of the free groups of O-H stretches [28,29].

Due to the effects of the temperature on the NIR spectra a systematic trend were found in previous studies [25, 27], to that an increase in the temperature would give an increase in the standard error to the calibration models. Therefore, the temperature in the samples when in a prediction situation should be identical to the temperature in the samples used for calibration of the model.

The Winery in Tromsø

The Beginning of "De 5 Vinmakeran"

Take five unemployed Norwegian men, all with a passion for wine, and put them in the same room, add Norwegian raw materials of berries and fruit, and finally a little help from an experienced oenologist from Toscana, Italy. Well, that equals the start of the first professional wine making business in northern Norway. The company were called Scimus Polarvin and located in what used to be an old dairy building in Tromsø.

Picture 1 The old diary building

The commercial concept was developed in a business entrepreneur group which redefined itself as a micro credit group. This group quickly assumed the name Scimus Nettverkskredittgruppe. When the establishment project reached the point of formally registering as an "AS" (Limited) company, the name *Scimus Polarvin AS* was registered. Scimus Polarvin was started as a private limited company with 20 % to each partner. The company was financed with help from "Innovation Norway". The plan was to make three types of wine from berries found in Northern Norway, preferably from the area around Tromsø.

The five men had very different backgrounds and didn't know each other before, but had the same interest in establishing their own business. They met in 2004 within the context of Troms Næringsservice (Troms Business Service), a Consulting and Development company. The focus was on starting up a private business enterprise. The five new business men were

- Guttorm Isaksen, previously a chief municipal executive
- Terje Vassbotn, engineer in IT and telecom
- Alfred Granmo, doctor in mycological botany
- Jarle Aas, tele service man
- Erling-Tore Andreassen, senior salesman

Picture 2 The five business men before the facilities were ready for production [31]

In 2006 this group took over the buildings and tanks from a former dairy in Tromsø and started to renovate the inner surroundings. New floors were made, windows were mounted, and the office was repainted. The five men did it nearly all on their own. Later the bottling equipment, bottles, and labels came on-line and they were ready to begin production. They only needed the most important thing – the local berries. [31]

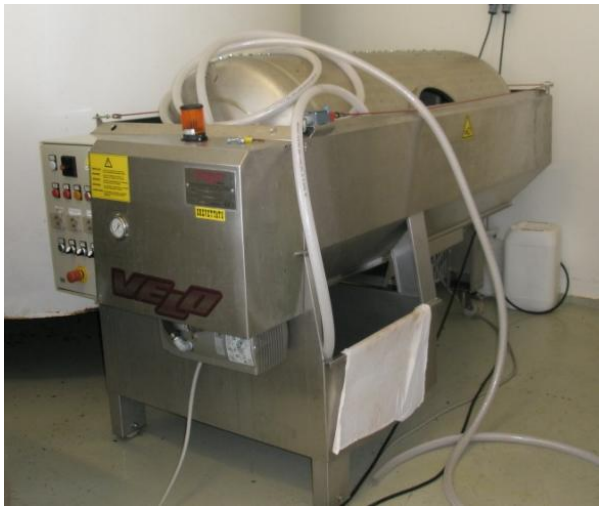

Picture 3 The press for the must

Picture 4 Filtering of wine before bottling

Picture 5 Tank used for cold stabilization

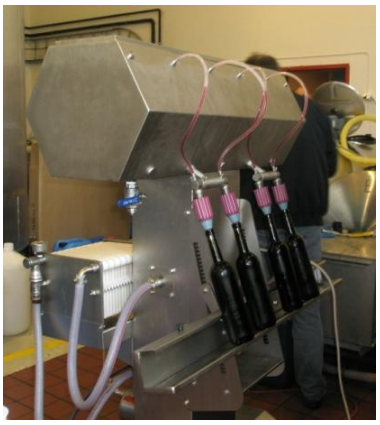

Picture 6 Bottling of the wine

To get the right taste in the wine, help was coming from Italy. *De 5 Vinmakeran* had started a corporation with an oenologist from Italy, Alessandro Spartafora. He helped tailor a wine with the optimal taste, odour, and look, with regards to colour and turbidity.

In January 2007 the company changed its name to *De 5 Vinmakeran* in order to focus on local ambiance in Tromsø and the surrounding regions.

The old name "Scimus" proved to be rather incomprehensible for most consumers. "De 5" indicated the amount of people involved in the company. "Vinmakeran" (Winemakers) was chosen because in Norway it is not allowed to advertise directly for alcohol. So when a wine making company wants to herald its line of business, it can only be done in the company name.

Picture 7 The logo for "*De 5 Vinmakeran*"

"*Vinmakeran*" is a northern dialect (the proper norwegian word would be: "*Vinmakerne*". Using a local dialect in name emphasizes that the company is working with products that has a local identity. This is related to a growing trend, nationally and internationally, that foods and specially wines should have a specific location. Hence, the company name promotes wines with a history and with a clear originate context.

They started out as a five person company, but today there are only two of the original "grounders" left– Guttorm Isaksen and Terje Vassbotn.

De 5 Vinmakeran is a beautiful proof that you don't need to have a great place in France, a large vineyard, and many grapes of a specific class and sort to start a winery and produce a good wine.[32]

Picture 8 The five business men after the first wine was ready for consumption [31]

The Idea

The original plan was to make three types of table wine – White, red, and rosé. The white wine was based on rhubarb and cloudberries, the rosé wine on blackcurrant and raspberries, and the red wine on crowberries and blueberries. The rhubarb came from local farmers and the rest of the berries came from hobby farmers or was picked in the forest around Troms. The rhubarb and berries were frozen on arrival to the winery and stored in the freezer until they were needed.

The market for table wine made from fruit was not as good as expected, so *De 5 Vinmakeran* reduced the alcohol content from 12 % to 15 % down to 4.7 % and produced a wine, which was directed more to the common Norwegian than that of an exclusive wine drinker. They called the low-alcohol wine a "mild wine", signifying that the alcohol percentage was lower, but at the same time it was still a wine and not a non-alcoholic fruit juice.

The Production Plan

With regards to table wine "De 5" produced and sold 7000 bottles in 2007 and 3000 bottles in 2008. The market was more interested in the mild wine than the table wine, so the production of table wine was temporarily suspended, but the plan is to re-establish production in the future.

Picture 9 Wine bottles ready for labelling and packaging

"De 5" produced and sold 20,000 bottles of mild wine during seven months of 2008. In 2009 they initially planned to produce and sell 60,000 to 120,000 bottles, but in the shadow of pending financial recession that objective was down-scaled to 40,000 to 60,000 during first half of 2009.

Since 2006 "De 5" have expanded the production to be able to produce 60,000 bottles in 2009, and with a few marginal investments increased to 120,000 bottles. The plan for the period of 2009 – 2012 is to be able to develop the capacity to produce 1,000,000 bottles in 2012 [33].

The Wines

The original wines were made from local berries and had an alcohol content of 12 % vol. to 15 % vol. The sales for these wine were not as good as expected, so *De 5 Vinmakeran* decided to make a mild wine with a alcohol content of 4.7 % vol. instead. The wines were intended for the everyday market, and the mild wine had proven to be more successful than originally foreseen. The common signature item for all the wines are that the raw materials are harvested above the Arctic Circle from regional areas in Northern Norway, especially Troms. [35]

The General Production Protocol

Each wine has its own production protocol depending on the type of berries and the desired taste and colour, but some general elements are the same for all wines [34].

1. The berries are frozen after receiving and stored until use
2. The berries are thawed, crushed, and pressed
3. Water, enzymes, and sulphite are added to the must
4. For the white and rosè wines the skins are removed and the juice is pumped into the fermentation tank. For the red wine, the berries are fermented with the skins (fermented maceration).
5. Add sugar and yeast to the juice
6. Ferment for 8 days to 10 days. The fermented red wine is pumped into the juice press, where the must is taken out.
7. The fermented wine is pumped to a new tank for one month of maturing and clarification
8. After clarification the wines are pumped over and blended into a new tank
9. Finings: add sugar, metabitatrate, supplementary tannins (for the mild wines), plant extracts, enzymes and ascorbic acid
10. Cold stabilization: 10 days at approx 0 °C
11. Bottling

The table wine can get better with storage, where as the mild wine should be served within the first two years after production.

The Table Wines

The names of the table wines were inspired from the novels of Nobel Prize winning North Norwegian author Knut Hamsun, famous for his poetic description of the nature and characters of the north: Victoria, Rosa, and August.

The White Wine – Victoria

The name was also inspired from the fact that the most common species of rhubarb in the north carries the botanic name of Victoria (in addition to Hamsun's famous love story). This wine was a blend of 90 % rhubarb and 10 % cloudberries. Only 10 % of the raw materials came from Sweden, the rest was from Norway. The wine had an alcohol content of 12 % vol. and a slightly brown tan. The wine goes well with seafood.

The Rosé Wine – Rosa

The name indicates the rosé character of the wine, (in addition to one of Hamsun's heroines). The wine was a blend of 45 % raspberries, 45 % blackcurrant and 10 % arctic crowberries. Only 15 % of the raw materials came from Sweden, the rest was from the

area of Troms. The wine was semisweet and was excellent when served with desserts like chocolate, fresh strawberries, or raspberries. It also went well with duck's breast or lamb roast. The wine had an alcohol content of 15 % vol.

The Red Wine – August

The name was inspired from Hamsun's novel by the same name, in addition to the fact that August was a month where most of the raw materials could be harvested. It was made from a blend of 50 % arctic crowberries and the other 50 % were a co-fermented mix of bilberries, red- and blackcurrants. Like a table wine made of grapes the colour was deep dark red. The fruit wine should be served slightly colder than a grape red table wine, and the taste was preserved best at 10 °C to 12 °C. The wine had an alcohol content of 15 % vol. and goes well with red meat, fish, especially red fish, and a well matured soft cheese.

The Mild Wines

The term "mildvin" (mild wine) was coined by the company to indicate that these wines had a milder degree of alcohol and thus a milder taste. These wines were made from the same protocol as the table wines, except for the lesser amount of sugar added to the must before fermentation.

In the finings (the after treatment, where the final taste was achieved with addition of different taste constituents), however, the protocols differ significantly, due to the fact that alcohol is a strong aroma-carrier. Therefore, reducing the alcohol would reduce the aroma of the wine. The finings of the mild wines were altered to compensate for that. This was done mostly by raising acidity/sweetness balance.

As a general rule, the aroma of the mild wines blossoms best at temperatures significantly below those considered normal for comparable table wines.

The White Mild Wine – Lofoten

The name comes from a group of islands south of Tromsø, where a very beautiful site is called Lofoten. Lofoten is made with the same protocol as Victoria. Extracts of rhodiola roseum (rose root) are added to the wine to enhance the taste of the raw materials. The Lofoten wine taste's best if the wine is served at 4 °C to 10 °C, straight from the refrigerator, preferably with frosty dew on the glass. Lofoten goes well with seafood and light meat.

The Rosé Mild Wine – Tana

The name comes from the river Tana, which has its spring in Finland. Tana is by far the Norwegian river with the largest water flow and the largest yield of wild salmon in the northern Europe. The rosé wine is made from 45 % raspberries, 45 % blackcurrant, and 10 % arctic crowberries. Tana is made with the same protocol as Rosa. Like Lofoten, Tana is added extracts of rose root to enhance the taste. The slightly sweet taste of the wine makes it perfect as an aperitif or dessert wine. Its freshness and fruitiness blossoms best when served at 4 °C to 10 °C, cold from the fridge.

The Red Mild Wine – Senja

The name comes from a beautiful island south of Tromsø. The red wine is made from 50 % crowberries and 50 % bilberries,

redcurrants and blackcurrants. Senja is made with the same protocol as August. Like Lofoten and Tana, extracts of rose root are added to enhance the taste. The wine goes well with red meat, dishes with soy sauce, pasta and pizza. The taste is best preserved when the wine is served at 9 °C to 14 °C, chilled from the cellar.

Raw Materials

The following is a short description of the different berries used for the three wine types evaluated in this project.

Rhubarb

Rhubarb *(Latin name: Rheum rhabarbarum, Danish: Rabarber, Norwegian: Rabarbra)* is an approx 1.5 m high plant with green or red stalks. The species "*Victoria*" has very rough and green stalks. The level of acids depend on the species, but they are generally low. The species "*Victoria*" contains e.g., malic acid in low concentrations and oxalic acid in moderate concentrations. The sugar content is low for all species [36].

Cloudberries

Cloudberry (*Latin: Rubus chamaemorus, Danish: Multebær, Norwegian: Multe*) are an usually growing in arctic climates, especially along the northern coast of Norway, producing a berry similar to raspberry and blackberry. The plants are 10 cm to 25 cm high with white flowers, which after pollination form the berries. The berries are red when they are initially formed and turn amber in the early autumn during ripening. The ripe berries are golden-yellow, soft and juicy, and have a high content of sugar. Its high content of benzoic acid acts as a natural preservative. The cloudberries are used for winemaking in many regions of the northern arctic areas of Scandinavia and Canada. [37]

Raspberries

Raspberry (*Latin: Rubus Edaeus, Danish: Hindbær, Norwegian: Bringebær*) is a red berry that demands ample sun and water for optimal development. As a cultivated plant in moist temperate regions, it is easy to grow and has a tendency to spread unless pruned. The fruit is harvested in the mid-summer when it is easily removed from the plant and has turned a deep red colour. It is at this point that the berries are ripest and sweetest.

Blackcurrant

Blackcurrant *(Latin: Ribes nigrum, Danish: Solbær, Norwegian: Solbær)* are found in the northern cold climate. The plant is a bush of 1 m to 2 m high, and the berry is approx 1 cm in diameter and has a very dark purple colour. They have a distinctive sweet and sharp taste and are used for jam and juice.

Crowberries

Crowberry *(Latin: Empetrum nigrum, Danish: Sortebær, Norwegian: Krøkebær*) is a small dwarf bush, commonly found in the northern hemisphere in the cool climate. The berries are black and approx 4 mm to 8 mm in diameter. The berries are mature and ready for harvesting in July to August, but may be left on the bush to be harvested in the spring. Crowberries consist mainly of water; therefore, they are almost tasteless. The levels of both acids and sugar are low, and they are mainly used for colouring. [37]

Bilberries

Bilberry *(Latin: Vaccinium myrtillus L. , Danish: Vilde blåbær, Norwegian: Blåbær)* is a low-growing bush. Bilberries are a wild berry found throughout the cool climate regions of the world. Bilberries produce a single berry or paired berries on the bush. Bilberries are dark in colour, and usually appear almost black with a slight shade of blue. The bilberries fruit pulp is red to purple, and severely stains anything coming in contact with it. Bilberries are typically collected from wild plants. The berries are soft and contain much water, and are mainly used for colouring.

Redcurrant

Red currant (Latin: *Ribes rubrum, Danish: Ribs, Norwegian: Ripser*) are growing in the northern hemisphere. It is a bush of 1 m to 1.5 m high. The berries are located in racemes, where the berries mature and end up as bright red translucent berries of 8 mm to 12 mm in diameter. There are 3 to 10 berries on each raceme. Red currants have a high level of acids and a low level of sugars.

The Chemical Parameters

The important parameters for winemakers are the ones defining the taste, odour, and stability of the wine. In this project different sugars, glycerol, ethanol, and acids are evaluated. Aspects of the parameters with regards to the wines are described in the following.

Sugars

Sucrose is converted by naturally occurring enzymes in the raw materials to glucose and fructose, which are then used in the fermentation. The amount of sugar added depends on the desired end concentration of ethanol. The amount of sugar added also depends on the natural content of sugar in the raw material.

When the fermentation has stopped, there may be some remaining sugar left in the wine. The sum of all the sugar components remaining is called the "*residual sugar*" and gives the wine its sweetness. If the taste after fermentation is not sweet enough, more sugar is added during stabilization of the wine and before bottling to ensure the right sweetness of the finished wine.

Glycerol and Ethanol

Glycerol is a useful by-product of the fermentation. It is produced by the yeast, in order to protect the yeast cells against high osmotic pressure as the concentration of ethanol increases [38]. Glycerol is important for the wine, since this is the component which ensures that the wine has its soft feeling in the mouth.

Ethanol is produced during fermentation, where the sugars are converted to ethanol. First step is conversion of glucose to pyruvate through glycolysis, see Figure 1.

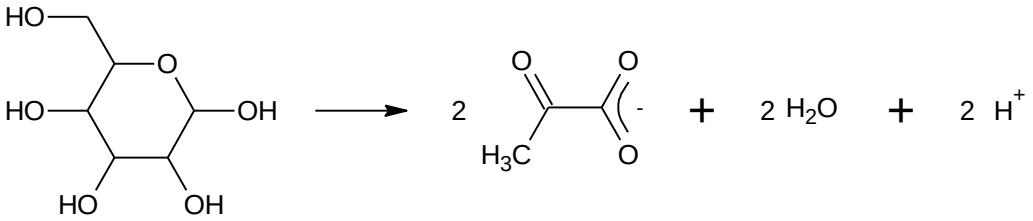

Figure 1 Net Glycolysis: One glucose converts to two pyruvate,two2 H_2O, and two H^+

The next step is the fermentation, where pyruvate is converted to acetaldehyde, and then this is reduced into ethanol, see Figure 2.

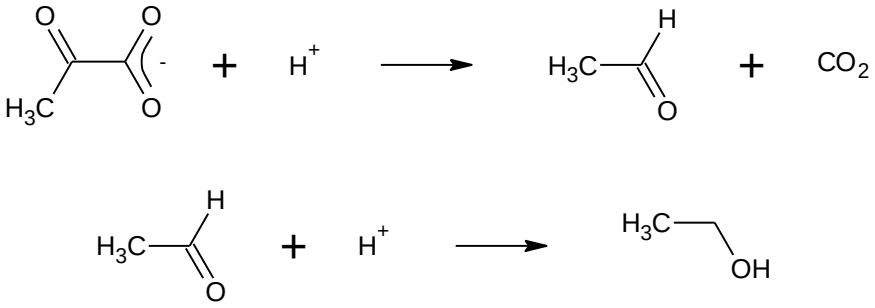

Figure 2 Fermentation: Conversion of pyruvate to acetaldehyde (top) and reduction of acetaldehyde into ethanol (bottom)

The overall reaction for glycolysis and fermentation are $C_6H_{12}O_6$ to two CH_3CH_2OH and two CO_2, see Figure 3.

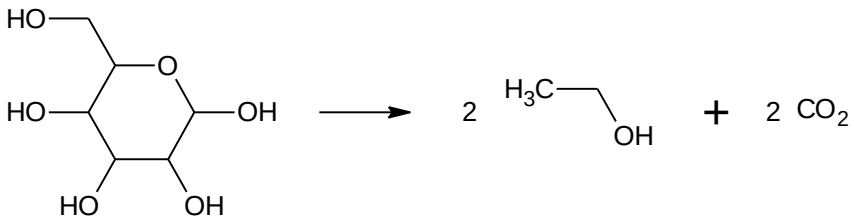

Figure 3 Overall reaction of the glycolysis and fermentation of glucose into ethanol

If the content of ethanol is too low, the taste of the wine for some consumers may be described as "flat" and lacking of taste.

Acids

Some acids occur naturally in the raw materials, and some are by-products of the fermentation. They may also be produced during production and storage, and may spoil the production. Acids evaluated in this project are shown in Figure 4, where citric, tartaric, and malic acid come from the raw materials, and succinic, lactic, and acetic acid are produce during the fermentation. [39]

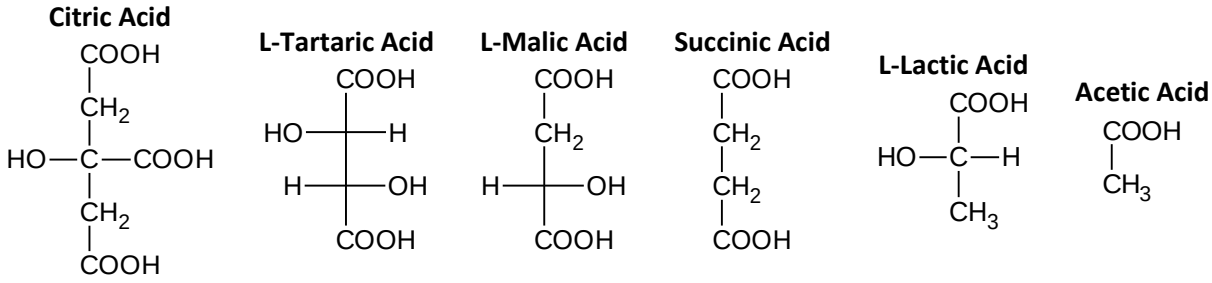

Figure 4 The acids evaluated in this study

Acids are used to ensure that the pH of the wine is in the desired range (approx pH 3.5) to prevent bacterial growth during production and storage. Different acids are also used to smooth the sweetness of the wine. If some acids are present in too high a concentration they may have the opposite effect on the taste, creating an undesired sour taste or smell. This is the reason why acetic acid in high concentrations is undesired, as it gives the wine a smell and taste similar to vinegar. [39]

Another problem with having acids with concentrations that are too high is that they may crystallize during storage in the consumers home., especially for tartaric acid. To prevent this, the wine undergoes a process called cold-stabilization: a process where the wine for a period of several days is held at temperatures around 0 °C. This temperature allows the crystallization process to speed up, and later the crystals are filtered from the wine during the bottling process. [39]

If the concentration of malic acid is too high and the taste of the acid in the wine is to distinct, it may be smoothened by malolactic fermentation. In malolactic fermentation the malic acid is converted to lactic acid and carbon dioxide through decarboxylation, Figure 5.

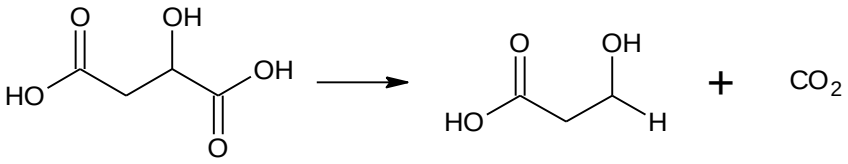

Figure 5 Malolactic fermentation: Decarboxylation of malic acid to lactic acid and carbon dioxide

Lactic acid has a softer taste than malic acid. The malolactic fermentation is made by lactic acid bacteria, which may be naturally present or may be added intentionally. [39]

Thesis Problem

The purpose with the project is to make a feasibility study to determine if handheld easy-to-use short- and long-wave NIR equipment can be used to determine different parameters in low-alcohol berry wine.

The thesis problem is as follows:
"Is it possible to make a satisfactory model for the prediction of different sugars and acids, glycerol, and ethanol on the basis of data obtained from NIR-spectra?"

The aim of this first part of the report is to bridge the spectral information from a wine sample with the chemometric applications of quantitative analysis of the wine sample. The mild wines, hereafter referred to as wine, were delivered directly from "*De 5 Vinmakeran*" by air-flight.

Results and Discussion

The results of the individual experiments and modelling campaigns made during this project are presented in the following together with related discussions.

Replicate Experiment

Before samples for the modelling of parameters were extracted from the mild wines, it had to be determined if the sampling process was representative. This was determined through a replication experiment where 10 samples from each wine type were extracted, analyzed, and the results evaluated. The replicate experiment is described in Appendix 2.

Sampling process

The sampling of wine during a production process is done by the use of a wine thief, which is a cylinder made of plastic or glass with small holes on both ends. It is similar to a pipette and functions in the same way. When it is lowered into the wine, wine enters at the one end. Samples are then extracted by closing the other end with a finger, and the wine stays inside the wine thief until the finger is removed (capillary action).

Due to practical reasons at the winery, the samples for the replicate experiment were extracted from the three types of wine at different times in the production process. Samples from the white wine (Lofoten) were extracted from a storage tank during cold stabilization. Samples from the rosé wine (Tana) were extracted before addition of sugar and acids also during cold stabilization. Samples from the red wine (Senja) were extracted after cold stabilization just before the wine was to be bottled.

Measured Concentrations

The measured concentrations in the replicate experiment for parameters evaluated in this project are listed in Table 2. The listed values are a mean value of 10 samples with triplicate analytical measurement of each sample. The raw data are shown on the enclosed CD-rom. The concentrations are measured by the reference method HPLC, where the sugars, glycerol, and ethanol are detected by their refractive index and the acids are detected by an UV/VIS detector. The samples were diluted 10 times for sugars, glycerol, and ethanol, and three times for acids. This resulted in some of the diluted samples having concentrations close to the limit of detection of the methods. The concentrations listed are the calculated concentrations taking the dilution factor into account. Ethanol is listed in both g/L and % vol. A conversion table for later use is shown in Appendix 3.

Table 2 Concentration of sugars, glycerol, ethanol and acids

	White Wine	Rosé Wine	Red Wine
Sucrose	38.8 g/L ± 1.43 g/L	-	29.7 g/L ± 0.56 g/L
Glucose	9.95 g/L ± 0.90 g/L	11.7 g/L ± 1.27 g/L	4.89 g/L ± 0.93 g/L
Fructose	7.86 g/L ± 0.41 g/L	11.5 g/L ± 1.25 g/L	3.99 g/L ± 0.24 g/L
Glycerol	2.85 g/L ± 0.05 g/L	12.4 g/L ± 1.38 g/L	3.24 g/L ± 0.06 g/L
Ethanol	33.8 g/L ± 0.55 g/L	30.0 g/L ± 0.50 g/L	30.6 g/L ± 0.45 g/L
	4.30 % vol. ± 0.07 % vol.	3.82 % vol. ± 0.06 % vol.	3.89 % vol .± 0.06% vol.
Citric acid	169.3 mg/L ± 26.7 mg/L	2583 mg/L ± 38.0 mg/L	1279 mg/L ± 30.5 mg/L
Tartaric acid	-	1682 mg/L ± 17.4 mg/L	-
Malic acid	1891 mg/L ± 271 mg/L	1016 mg/L ± 34.5 mg/L	537.5 mg/L ± 22.0 mg/L
Succinic acid	437.6 mg/L ± 53.6 mg/L	1374 mg/L ± 37.4 mg/L	899.0 mg/L ± 56.6 mg/L
Lactic acid	506.9 mg/L ± 85.3 mg/L	258.6mg/L ± 53.4 mg/L	-
Acetic acid	281.9 mg/L ± 52.0 mg/L	4564 mg/L ± 43.6 mg/L	1867 mg/L ± 49.6 mg/L

Relative Sampling Variance Compared to Total Analytical Uncertainty

To determine if the sampling process is representative, the Relative Sampling Variance (RSV), see Appendix 2 for theory about RSV, of the measurements is calculated, evaluated, and compared to the Total Analytical Uncertainty (TAE) which is determined independently. These data are shown on the CD-rom. The RSV is the sum of errors from the sampling process including TAE. The RSV are calculated from data from both triplicate and duplicate measurements of each of 10 samples from three types of berry wine, seeTable 3. Outliers in the dataset were removed before calculation of RSV and TAE. The measurements used for the calculations of RSV and TAE for duplicated measurements were the 2nd and 3rd measurements. The first measurement was intended to be used for flushing the column to minimize contamination from the previous sample.

Table 3 RSV and TAE for three or two measurements of sugars, glycerol, ethanol, and acids

	White Wine		Rosé Wine		Red Wine	
	RSV(3) RSV(2) %	TAE %	RSV(3) RSV(2) %	TAE %	RSV(3) RSV(2) %	TAE %
Sucrose	3.69 3.86	0.62	- -	-	1.88 2.07	3.12
Glucose	9.05 7.66	0.15	1.83 1.75	0.75	12.1 10.9	2.26
Fructose	5.18 4.42	0.12	1.48 1.26	0.44	6.11 5.89	0.71
Glycerol	1.72 2.64	0.24	1.42 1.42	1.53	1.88 2.15	1.95
Ethanol	1.63 1.76	0.44	1.67 1.50	0.43	1.48 1.47	0.47
Citric Acid	17.1 21.3	2.36	1.47 1.70	1.77	2.39 3.21	2.60
Tartaric Acid	- -	1.82	1.04 1.03	-	- -	0.90
Malic Acid	3.55 4.11	1.67	3.39 3.17	5.02	4.10 8.66	5.49
Succinic Acid	5.24 5.55	3.88	2.72 4.16	3.43	3.41 4.14	1.94
Lactic Acid	10.2 14.3	8.64	3.71 5.19	1.31	- -	6.75
Acetic Acid	12.4 12.3	-	0.96 1.23	-	2.66 3.24	3.49

Red signifies that concentrations are close to the limit of detection. Blue signify that RSV is smaller than TAE. RSV(3): three analytical measurements on each sample, RSV(2): two analytical measurements on each sample

Illustrations of the information in Table 3 are shown in Figure 6 to Figure 16, where the RSV and TAE are compared for each parameter. The bars in the figures are an overview of the RSV divided in two parts; 1) TAE and 2) Sampling Error ($\sqrt{(RSV)^2 - (TAE)^2}$) . The total height of the bars equals the RSV. Where no result is stated for the wine type, it means that the parameter is not detected. For all figures: a blue bar = TAE; a red bar= sampling error; and a green bar = RSV < TAE (value stated is equal to TAE). The number under the wine type represents triplicated or duplicated measurement taken on each sample.

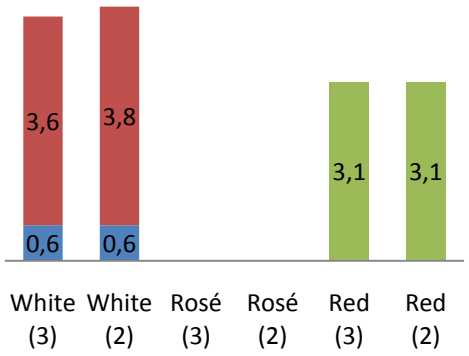

Figure 6 Sampling Error and TAE for sucrose

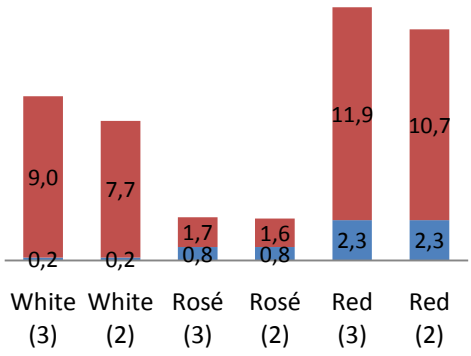

Figure 7 Sampling Error and TAE for glucose

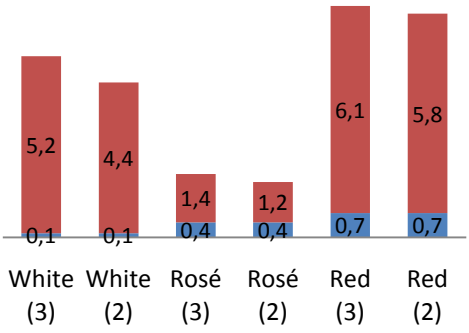

Figure 8 Sampling Error and TAE for fructose

Figure 9 Sampling Error and TAE for glycerol

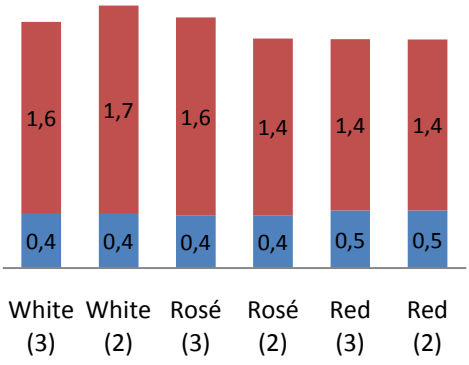

Figure 10 Sampling Error and TAE for ethanol

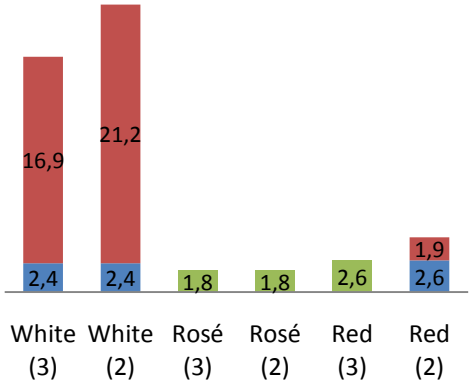

Figure 11 Sampling Error and TAE for citric acid

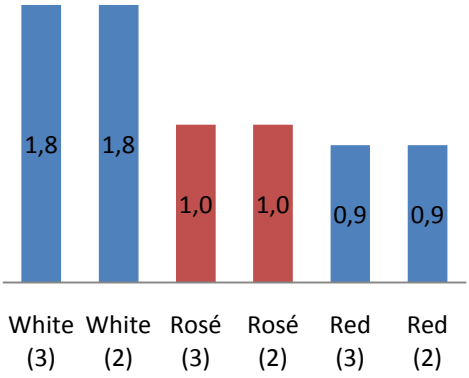

Figure 12 Sampling Error and TAE for tartaric acid

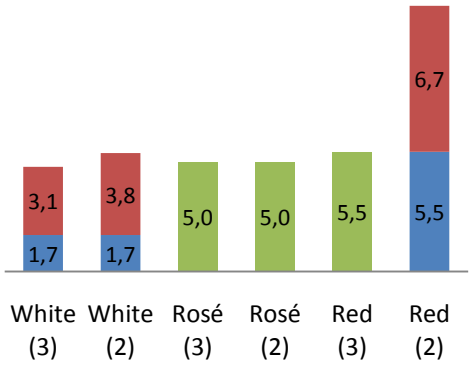

Figure 13 Sampling Error and TAE for malic acid

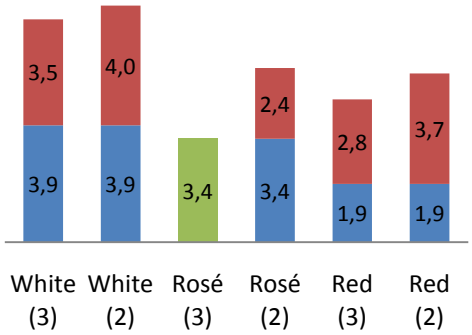

Figure 14 Sampling Error and TAE for succinic acid

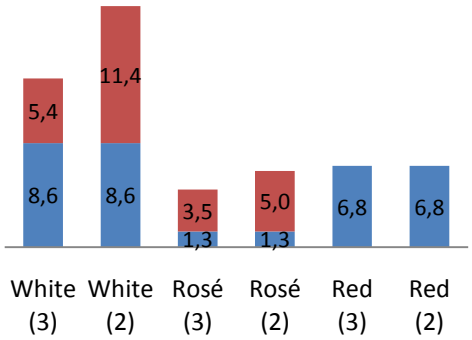

Figure 15 Sampling Error and TAE for lactic acid

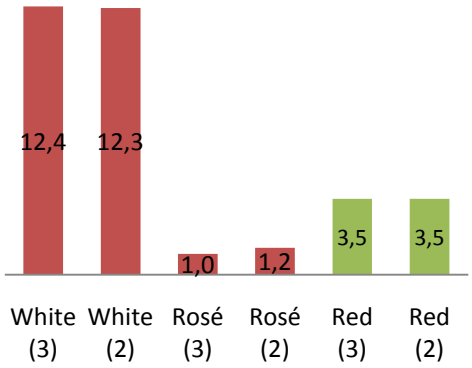

Figure 16 Sampling Error and TAE for acetic acid

Discussion

For sucrose the sampling errors are in the same range for the white wine, although using all three measurements gave a slightly smaller sampling error. Sucrose was not detected in the rosé wine. In the red wine the TAE was higher than the RSV. This is also seen for some of the other parameters, both glycerol and different acids (blue values in Table 3 and green bars in Figure 6 to Figure 16). In all of them the RSV and TAE were at the same level, so it might be due to coincidences and analytical difficulties in determination and separation of the parameters in the HPLC columns.

In the evaluation of the sampling and analysis for sugars, it was found that glucose and fructose had the smallest sampling errors when only the 2nd and 3rd measurements were used. This applies for all three wine types. For both glucose and fructose the RSV was largest in for the red wine and smallest in the rosé wine, stating that the sampling process had the largest difficulties with the red wine. However, the overall values are within acceptable ranges.

For glycerol in the white wine the sampling error was smallest when using all three measurements. In the rosé and the red wine the TAE was slightly higher than the RSV, but with a deviation of ± 0.1 %, they were almost equal to each other.

For ethanol the RSV was in the same range for all wine types as was the TAE. Comparing the RSV and TAE for ethanol with those for the other parameters, it was found that ethanol had the smallest sampling and analytical error.

Regarding acids, it was found that the sampling error and analytical uncertainty was higher than for sugars, glycerol, and ethanol. This may be due to difficulties in separating and detecting the acids, by

HPLC. Wine is a complex matrix, which also contains other components that are detectable at the used wavelength in the UV/VIS detector. This was seen by the detection of other peaks in the chromatograms, see example in Figure 17. In the shown chromatogram there isn´t a good baseline separation between the peaks, which makes it difficult to determine when a peak begin and end.

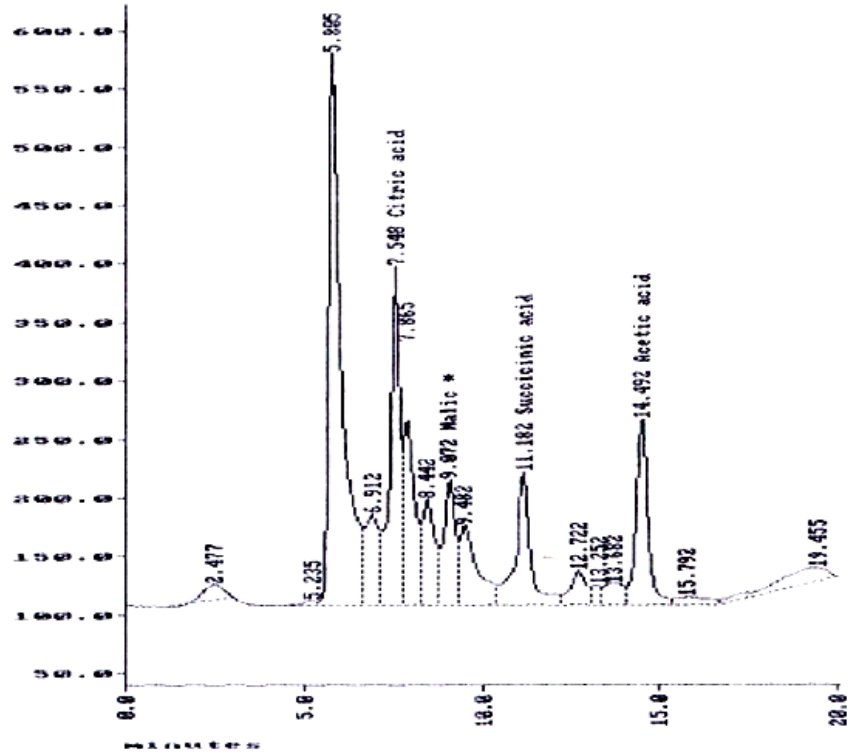

Figure 17 Chromatogram for determination of acids in the red wine

RSV are largest for citric, succinic, lactic, and acetic acid, where the concentrations measured (after dilution of the samples) were in the range of the limit of detection for the method. Therefore, it can be stated that RSV increases when the concentration decreases. This is as expected, since the small variance in the samples will have a large influence on the mean concentration and standard deviation, and then again on the RSV.For tartaric, lactic, and acetic acid only RSV or TAE are stated. The reason for this is that TAE and RSV are determined in wines from two different fermentations. Therefore, the parameters and the concentrations detected may not be the same due to differences in the chemical composition of the raw materials.

Overall for the acids, with a few exceptions, it was found that the smallest RSV are obtained by using all three measurements in determining the concentrations. The differences between using three or two measurements are very small and it may simply be due to difficulties in separating the components and not be a real difference.

Conclusion

It was found that the uncertainty from sampling is within a reasonable range where the concentration is above the limit of detection for the parameters, so the sampling procedure can be said to be representative for all parameters.

The conclusion to the sampling process and the analytical measurements was that each sample was measured in triplicate, and since the differences in RSV are small, only the 2nd and 3rd measurement was used for determination of the concentration.

The Data Set Used for Modelling

Context and Problem

The conventional method used for measuring the content of the different winemaking parameters can be time-consuming, expensive, and demand trained personnel. Therefore, it is desirable to have an inexpensive, long-time basis technique and develop a method that is fast and easy-to-use. If it is possible to replace the traditional methods for measurement of content of different sugars and acids, glycerol and ethanol with the quick and inexpensive NIR-spectroscopy technique money could be saved for small scale wineries. Ideally the method developed should be able to characterize the wine during different stages of fermentation to ensure a more uniform wine from one fermentation to another.

This was precisely the case for the small-scale winery “De 5” in Tromsø; therefore, their mild wines were evaluated with hand-held NIR equipment. The wines were treated in a dilution experiment that was meant to simulate the different concentrations obtained during fermentation and further production.

Sampling

The dilution and sampling process used when extracting wine samples for the modelling were as follows:

1. Each wine bottle was shaken a few times to ensure that there were no precipitates. If precipitates were present, the bottle were shaken to ensure that the precipitates were “equally distributed” in the bottle.
2. With a pipette, 200 ml of wine was extracted and transferred to a 5 L Erlenmeyer flask.
3. 200 ml of distilled water was added and the solution mixed
4. 20 ml of diluted wine was extracted
5. 50 ml distilled water was added to the first solution and the solution was mixed.
6. Points 4 – 5 are repeated, where an increasing volume of distilled water was added until the theoretical concentrations were close to or below the limit of detection.

Analytical Methods

The wine samples were analyzed for sugars, glycerol and ethanol with HPLC equipment from Perkin Elmer (Series 200 Autosampler and Pump, Series 200a Refractive Index Detector, NCI 900; Network Chromatography Interface). The column used was a Aminex HPX-87C (HPLC Carbohydrate Column, 300 mm x 7.8 mm) with water as the eluent at a temperature of 85 °C and a flow of 0.6 ml/min. The method was calibrated with concentrations ranging from 0 g/L to 10 g/L for all parameters.

The wine samples were analyzed regarding acids with HPLC equipment from Perkin Elmer (Binary Pump 250, Diode Array Detector 235C, Nelson PC Integrator). The column used was an Aminex HPX-87H (HPLC Organic Acid Analysis Column, Ion Exclusion Column, 300 mm x 7.8 mm) with 0.005 M H_2SO_4 as eluent at a temperature of 50 °C and a flow of 0.6 ml/min. The wavelength used in the detector was 210 nm. The method was calibrated with concentration ranges as follows:

- Citric Acid: 20 mg/L to 1000 mg/L
- Tartaric Acid: 20 mg/L to 1000 mg/L
- Malic Acid: 20 mg/L to 1000 mg/L
- Succinic acid: 20 mg/L to 1000 mg/L
- Lactic Acid: 24 mg/L to 1210 mg/L
- Acetic Acid: 41 mg/L to 2040 mg/L

The actual concentration results for all wine samples are listed in Appendix 4 and shown in Table 4.

Table 4 Concentration ranges for calibration (top) and test set (bottom)

		White Wine	Rosé Wine	Red Wine
Sucrose	**[g/L]**	0.0 – 4.0	–	0.1 – 5.9
		0.3 – 4.6	–	0.2 – 6.1
Glucose	**[g/L]**	0.0 – 12.4	0.2 – 11.0	0.1 – 5.8
		0.7 – 15.0	0.4 – 10.8	0.1 – 4.1
Fructose	**[g/L]**	0.0 – 12.0	0.2 – 10.7	0.1 – 4.5
		07 – 14.3	0.4 – 10.3	0.1 – 3.7
Glycerol	**[g/L]**	0.0 – 11.1	0.0 – 3.0	0.4 – 2.9
		0.7 – 13.9	0.1 – 2.4	0.1 – 2.8
Ethanol	**[g/L]**	0.0 – 16.1	0.5 – 25.2	0.4 – 24.1
		0.8 – 19.7	0.7 – 17.0	0.7 –16.3
Citric Acid	**[mg/L]**	4 – 68	173 – 1617	57 – 547
		3 – 82	61 – 1492	21 – 554
Tartaric Acid	**[mg/L]**	74 – 939	–	122 – 1075
		54 – 887	12 – 312	50 – 1010
Malic Acid	**[mg/L]**	81 – 1255	74 – 711	38 – 365
		73 – 124	24 – 602	13 – 324
Succinic acid	**[mg/L]**	14 – 328	91 – 830	83 – 826
		17 – 341	24 – 878	39 – 920
Lactic Acid	**[mg/L]**	3 – 58	14 – 104	19 – 240
		3 – 64	4 – 106	9 – 153
Acetic Acid	**[mg/L]**	31 – 535	–	23 – 206
		35 – 540	10 – 145	8 – 160

The NIR spectra were obtained by handheld Phazir™ equipment from Polychromix with an adaptor for measuring liquids. The mean spectra of five scans was used for modelling. The temperature of the samples was 20 °C to 25 °C. The technique used in Phazir™ was based upon Micro-Electromechanical Systems (MEMS). The theory of MEMS is described in Appendix 5. The obtained spectra and data are on the enclosed CD.

Data Set

The data set arises from an experimental design formed diluting the three types of low-alcohol wines to obtain samples with different concentrations. The concentrations obtained should describe the concentrations ranging from almost zero to the content obtained during fermentation.

Calibrations were developed by using Partial Least Squared regression (PLS) with *test-set validation* [40]. A short introduction to the theory of PLS is given in Appendix 6. The number of samples for each wine type is listed in Table 5.

Table 5 The number of samples for calibration and test set for each wine type

Wine type	Calibration set		Test set
	Sugars, glycerol, ethanol	Acids	
White Wine	30	20	10
Rosé Wine	22	14	14
Red Wine	22	14	14

The calibration set and the test set for the white wine did not contain the same number of samples as the set for the rosé and the red wine. This was because the white wine was used for a exploratory preliminary survey to see if modelling was possible, and to see if the number of samples was adequate. The results from the first modelling trials showed that the number of samples in the calibration set could be lowered, while more samples were desirable for the test set.

The **X**-variables are NIR-spectra consisting of short- and long-wave NIR transmission spectra with 100 variables from 890 nm to 1691 nm (short-wave NIR region) and another 100 variables from 1596 nm to 2396 nm(long-wave NIR region) respectively. The interval between each wavelength was approx 10 nm. The spectral data were recorded as the logarithms of the reflectance reciprocal (log(1/R)), and was included on the enclosed CD-rom. The **Y**-variables were the reference concentration of sucrose, glucose, fructose, glycerol, ethanol, citric, tartaric, malic, succinic, lactic, and acetic acid.

Data Analysis

The data are analyzed with The Unscrambler® v. 9.8 from CAMO Software AS. A short- and a long-wave NIR spectrum was acquired for all samples and then used to make a PLS-model for the prediction of the individual concentration of sugars, glycerol, ethanol, and acids. The method development for one PLS-model using ethanol as an example is described below. All other models are described in tabular form by their appropriate parameters and statistics.

Partial Least Squared Regression Model for the *Exemplar* analyte Ethanol

Ethanol in the white wine was selected as the modelled parameter to be described in more detail. The NIR region selected was the short-wave region. The model described was first calibrated and validated with test set validation on the spectra, without any pre-treatment, but with scaling of the variables.

Representability and Distribution of Samples

The representability and distribution of samples over the measured concentration range is shown in Figure 18 and Figure 19, respectively.

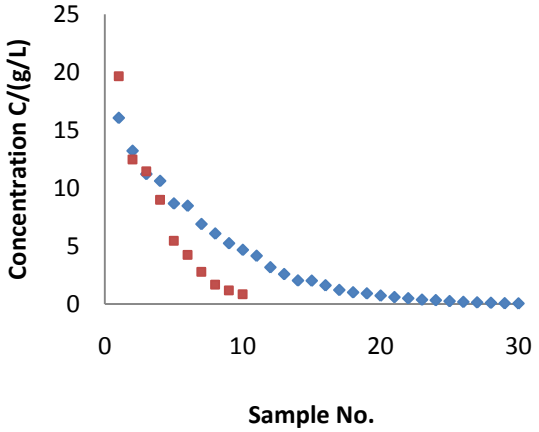

Figure 18 Representability of the samples.
Blue: Calibration set, red: Test set

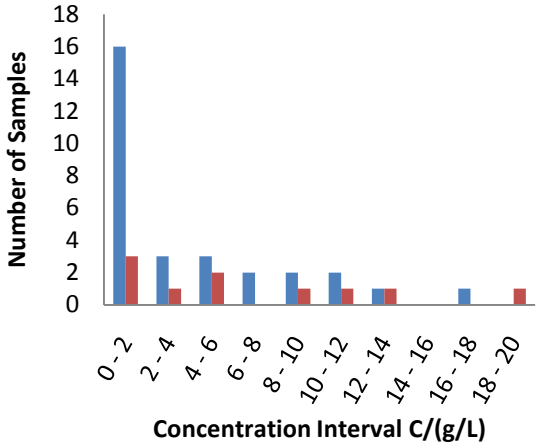

Figure 19 Distribution of the samples
Blue: Calibration set, red: Test set

The distribution of sample concentrations was acceptable since it was desired to have some samples distributed in a high concentration range and some in a lower concentration range. The calibration set showed that there were many samples in the interval 0 g/L to 2 g/L. This was because these samples were used for determination of the limit of detection for the used NIR technique. The representability and distribution of samples with regards to concentration was similar for all other parameters.

The Spectra

When visually comparing the spectra for all samples from the calibration and test sets, one sample stands out as being very different, see Figure 20. This was the sample from the test set, with the highest concentration (LT01), and since this was an outlier, it was removed from the test set before modelling. The status as an outlier was confirmed in the U scores vs. T scores plot, where the sample was located far away from the rest of the samples.

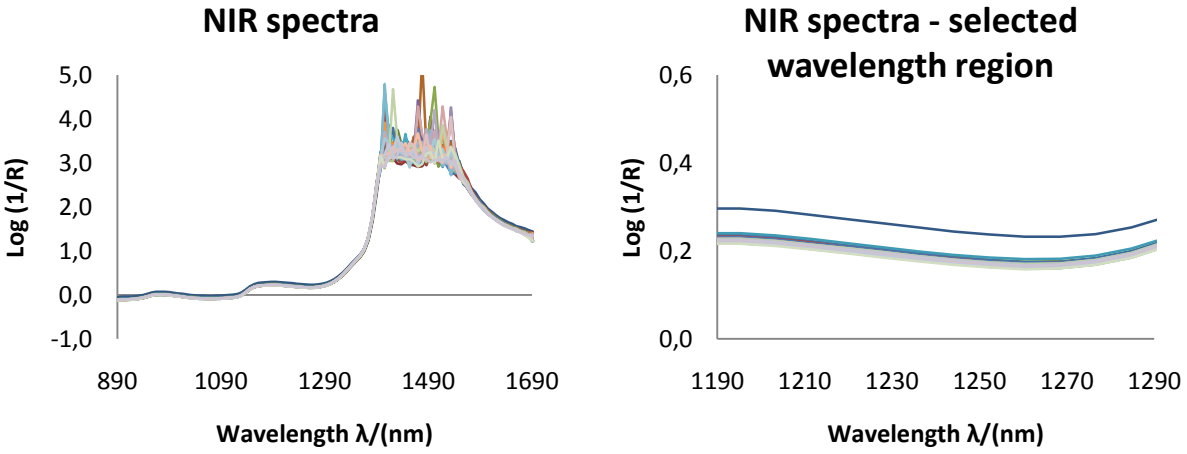

Figure 20 Short-wave NIR spectra for all samples of the white wine.
Left: the whole spectra , right: part of the spectra clearly showing an outlier

Outliers

The first part of any multivariate modelling is to remove outliers from both the calibration and test set. In the U scores vs. T scores plot the model was approximately linear, see Figure 21. To make this relation more distinct, the most distant “transverse outliers” are sometimes deleted (if significantly identified and documented as outliers). In the t_4-u_4 plot, Figure 21, the most prominent outliers are

marked with green (LT03 and LT10). A new model was made, which did not create other new, less pronounced outliers in the U scores vs. T scores plots.

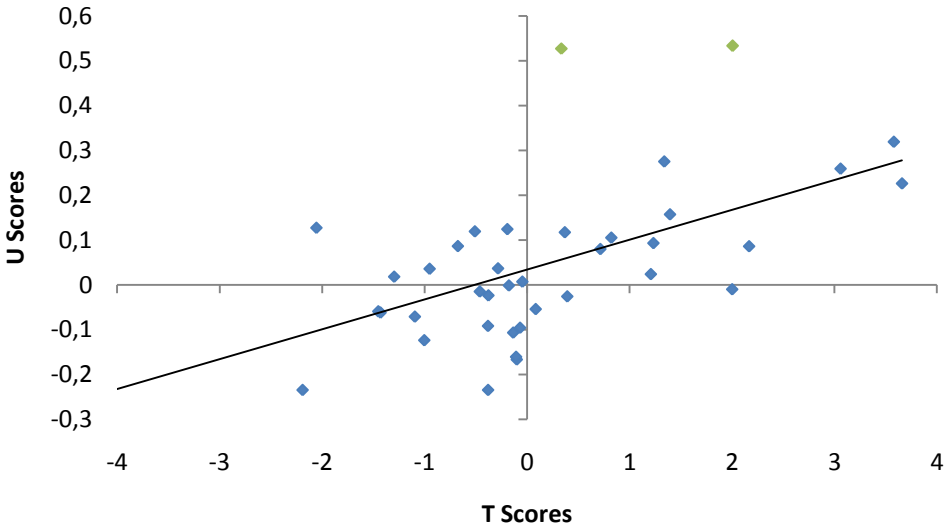

Figure 21 U scores vs. T scores for PLS4.
Green marking of outliers (LT03 and LT10)

From the predicted Y vs. reference Y plot, in Figure 22, some of the samples are predicted to be negative, marked with green in the figure (L25, L28, L29, and L30). There are many other samples in the calibration and test set with a value close to zero; therefore, it is a stochastic probability that some of them will always be predicted to have a negative value. When removing these samples there are still enough samples to anchor the model around zero. A new model is made, which produced one more sample (L23), which was predicted to be negative; hence, similarly removed from the calibration set.

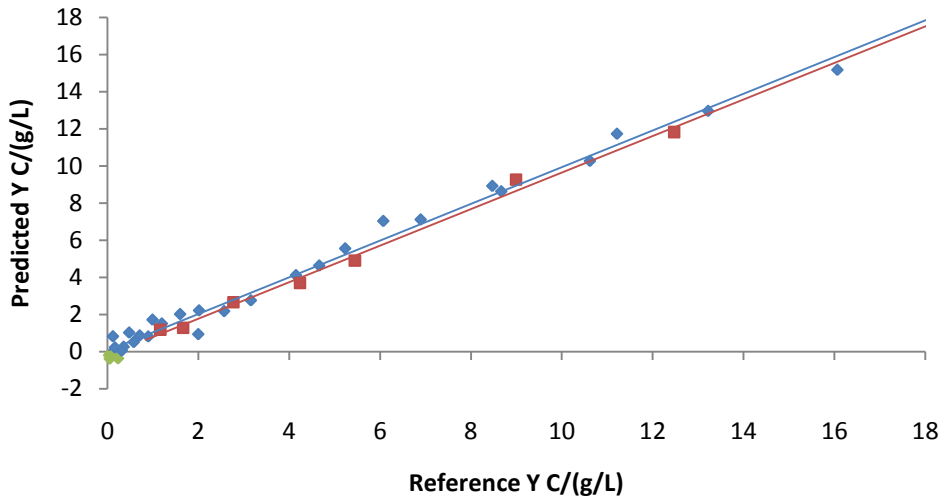

Figure 22 Predicted Y vs. Measured Y for PLS4.
Blue: calibration set, red: test set, green: predicted negative

After this removal, a final model was made as there were no more outliers left in any of the T-U plots, nor any samples which were predicted to be negative.

The Final Model for Ethanol

After removal of the eight outliers (five from the calibration set and three from the test set), a final model was made. This resulted in the model described below.

The Residual Validation Y-variance plot shows that the optimal number of PLS-components was four (possibly three), Figure 23, which gave a validated 98.4 % modelling (prediction) variance, corresponding to a prediction error variance fraction of 1.6 % for ethanol. The reason to why four was chosen is because the RMSEP decreases from using three to using four components. Since test set validation almost always give a higher RMSEP in a prediction situation, it would be desired to lower the RMSEP as much as possible in the validation.

Figure 23 shows that the first and second PLS components have the largest degree of explanation; therefore, they are the most important for the model. The related loading weights are discussed further below.

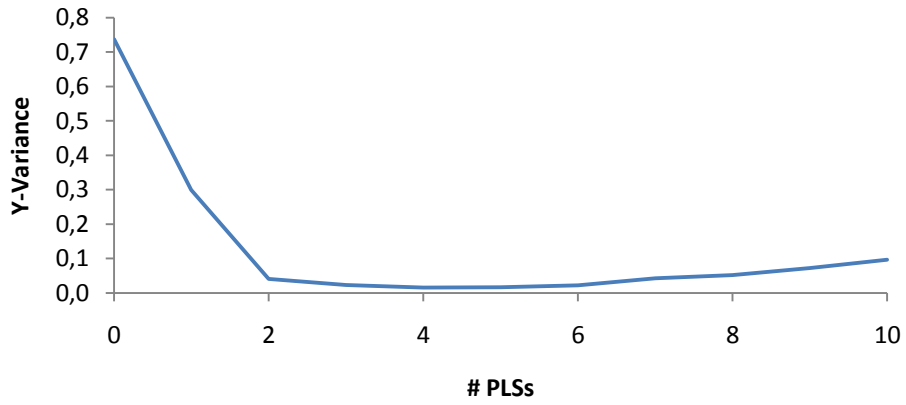

Figure 23 The residual validation variance

The Explained Validation X-variance plot shows that a model with four components explains 37.5 % of the variance in the short-wave NIR spectra, Figure 24. This means that < 40 % of the information in the NIR spectra are used to construct this prediction model. This indicates that only a small selected part of the NIR spectra have importance for the model, and the rest may be removed from the model to make it simpler. This is discussed later.

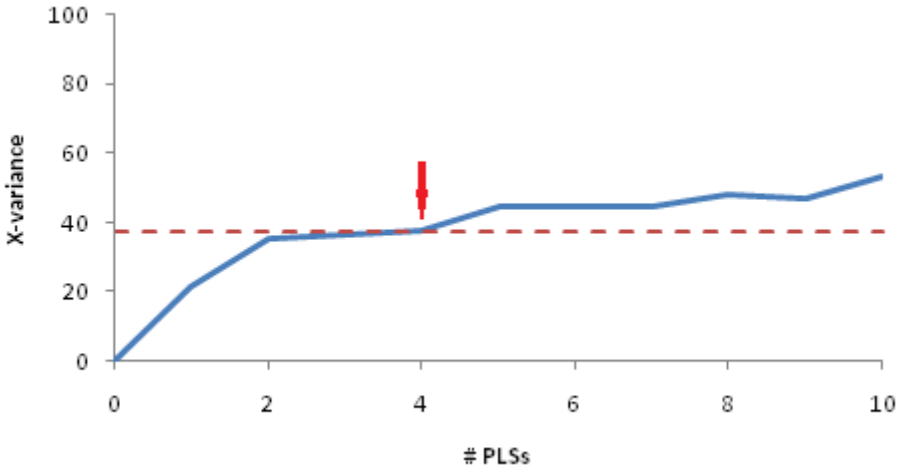

Figure 24 The explained validation variance

From the final validation plot: "Predicted vs. Reference", see Figure 25, the slope of the model was 1.01 for the test set, which was an excellent prediction accuracy covering the entire ethanol interval in the data set. The R^2 is 0.98 for the test set indicating a similarly very good precision. The RMSEP was in the order of 0.57 g/L for the test set. The corresponding relative RMSEP was then approx 10 %. RMSEP can be viewed as corresponding to an estimate of ± 1 x standard deviation. Thus, predicted ethanol values will be characterised by a 95 %-tile prediction error interval of ± 2 x RMSEP = approx 1.10 g/L, corresponding 0.15 % vol.

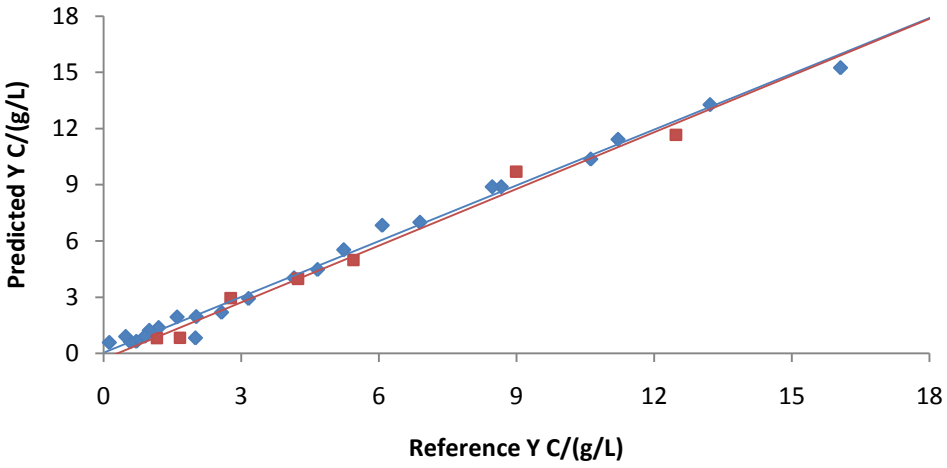

Figure 25 The predicted Y vs. Reference Y for PLS4.
Blue: calibration set, red: test set

To see how far the predicted values are from the reference, a plot of the predicted and the measured values vs. the sample number is shown in Figure 26. It is seen from the plot of the calibration set that the values for the predicted and the reference are very similar indeed, which is a visual confirmation of a R^2 value of 0.99. For the test set, where the R^2 value is 0.98, the prediction only differs slightly from the reference. Overall it can be said that the prediction validation offers a very good confirmation of validity of the method.

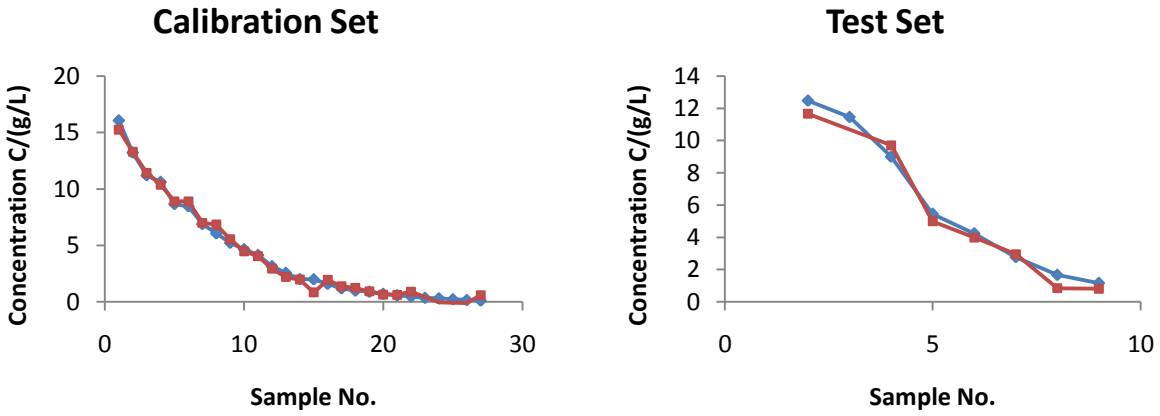

Figure 26 Comparison of range: Measured and predicted vs. sample number for calibration set (left) and test set (right)
Blue: Measured, red: Predicted

Insignificant Wavelengths in the Spectra

By evaluating the relevant w_1 and w_2 loading-weight plots, see Figure 27, it can be seen that the wavelength regions from approx 890 nm to 1400 nm and 1540 nm to 1691 nm were the most important regions for the model. This is seen in the large absolute w-values in these regions. In the intervening interval the X-loading weights differ only a little from the value zero. This region can safely be deleted from the model (variable selection) and a new model can be made.

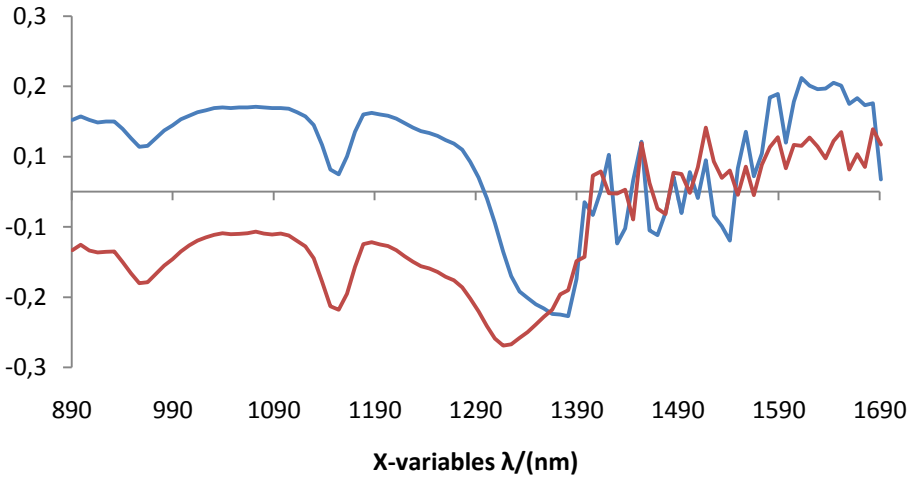

Figure 27 X-loading weights for PLS1
Blue: w_1 , red: w_2

A comparison of the regression coefficients and the raw spectra is shown in Figure 28, where both the regression coefficients and the raw spectra is shown as un-weighted. Here it is directly shown that the region with vanishing influence (1400 nm – 1540 nm), marked with red lines) was related to the region where water had a high influence on the spectra and causing noise rather than information for the model. This is again a confirmation that this region is of no importance to the model. The spectral data are neighbour covariate, which means that the spectral shape is a smooth curve, and the curve of the regression coefficients also curves smoothly. This is another reason to remove this region of the spectra from the model.

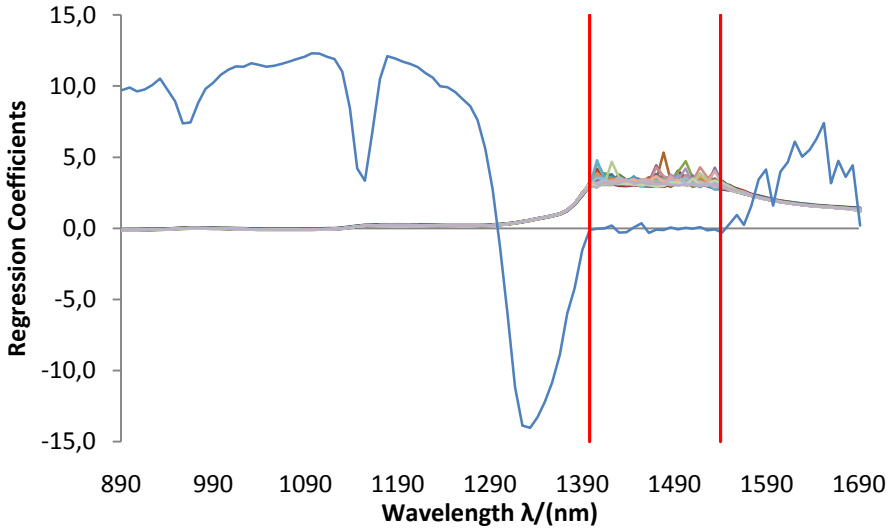

Figure 28 Regression Coefficients for PLS-model based on raw spectra. The raw spectra are plotted for direct comparison. Red lines marked the variable selection interval

Removal of these variables with little influence to the model was done in the first step of the modelling process. As seen from the explained validation variance the model use < 40 % of the spectral data for the modelling therefore more variables could be removed.

In the second modelling process more variables were deleted to obtain a simpler model. It will not be described here, since the process of obtaining the best model was the same.

Different types of pre-treatment was also applied to the spectra and used in the modelling steps to find the best model, see more below.

Conclusion

From the above considerations I conclude that a four PLS-component model, validated through test set validation, gives a satisfactory prediction with an uncertainty of ± 0.57 g/L (±1 x RMSEP). This model explains 98.4 % of the Y-variance (ethanol), i.e., a prediction error variance of only of 1.6 %, and a degree of explanations of the variance in the X-spectra of 37.5 %. This indicates that only a third of the spectra have importance for the model; therefore, a model with fewer and relevant variables would give an even better model.

Modelling

Before the first modelling campaign are evaluated a description of the datasets and the conditions under which they were obtained are listed in

Table 6. The table also lists the variables used for each modelling process after removal of insignificant variables.

Table 6 Experimental and modelling conditions

Conditions for calibration and test set	
White wine	Calibration and test set obtain from the same bottle, but made in two different experiments. All samples obtained and measured in November 2009.
Rosé wine	Calibration and test set is from two different fermentations. N.B. Calibration set obtained and measured in January 2010. Test set obtained and measured in December 2009.
Red wine	Calibration and test set is from two different fermentations. N.B. Calibration set is obtained and measured in January 2010. Test set is obtained and measured in December 2009

	Included variables	
	Short-wave NIR	**Long-wave NIR**
Raw spectra	890 nm to 1691 nm	1596 nm to 2396 nm
Reduced raw spectra – first modelling campaign	890 nm to 1398 nm 1542 nm to 1691 nm	1596 nm to 1861 nm
Reduced raw spectra – second modelling campaign	1163 nm to 1382 nm 1581 nm to 1644 nm	1596 nm to 1861 nm

The reason the calibration and the test set for the white wine was from the same bottle was because the white wine was a preliminary survey study. When it was established that the technique and equipment worked as intended, the calibration and test set for the rosé and the red wine was made from two different fermentations to make the study as realistic for the winery as possible.

In August 2009 a calibration set was made for the rosé and the red wine, but due to practical problems and change in conditions a new calibration set was made in January 2010. Since the calibration and test set for the rosé and the red wine was made *from different fermentations* there may be larger variations in the chemical composition of the wine due to variability in the raw material. In addition, if the raw material is from different harvests there may be differences due to climate and cultivation variations etc. Previous studies of grape wines have shown that the wines differ in chemical composition from one year to another, both with regards to components and to the concentration of the components [10, 14]. The same may be expected in berry wines. The present test set study (rosé and red) can be said to be (much) more relevant with regards to realistic process monitoring conditions in a winery during routine operations.

In the first and second modelling campaigns, variables were excluded from the spectra to obtain a simpler model. The regions included in the models were the same areas used in a previous study.[5]

With regards to applying pre-treatment to the spectra from the three wine types, it was expected that none or only a simple pre-treatment was needed to model the parameters for the white wine. This was because white wine is very translucent with only the slightest colouring. For the red wine it is expected that a more complex pre-treatment may be needed, since the wine is less transparent with its deep dark red colour. The rosé wine is somewhere between the two and the spectra may need a simple or complex pre-treatment. The above is only based upon the colour of the wines and it may not be of importance, since the spectra is only recorded in the NIR region. Instead the expectation of the use of pre-treatment should be based upon the chemical composition of the wines. The white wine was the less complex then the red wine, which was the most complex and compiles to the previous description of the use of raw materials. This gave the same expectations with regards to pre-treatment as described for the colouring of the wine. A pre-treatment may also be able to compensate for any temperature variations in the samples and surroundings that could have an impact on the spectra. [43]

Requirements to the Models

In general a model is considered acceptable if the slope (accuracy) is between 0.85 – 1.15, the R^2 (precision) value is above 0.85, and the relative RMSEP value is below 10 %. The number of PLS is preferable to be below four and the percentage of outliers is preferable below 10 %, ACABS specifications for feasibility calibrations [40]. Theoretical calculations of slope, R^2, and RMSEP are shown in Appendix 6.

Variable Selection

In Figure 29 the spectra for the short-wave and the long-wave NIR ranges are shown, where the white wine is used as an example.

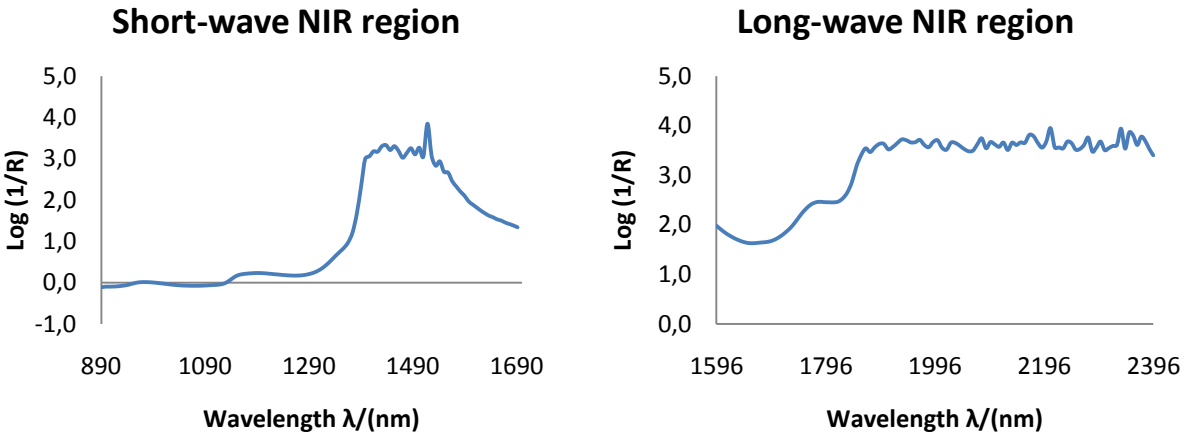

Figure 29 Raw spectra for the white wine. Left: 890-1691 nm, right: 1596-2396 nm.

The above figure shows that not all regions in the spectra are equally suitable for use in this method development also as previously mentioned. This is seen as the the spectra in some regions has no reflectance, a lot of noise is disturbed by the spectra for water, which is the main constituents of the wines.

The difficulties in interpretation of NIR spectra is that the absorption bands in this region are broad and overlapping, see Table 7 for some typical absorption bands for selected functional groups. By combining the information from Figure 29 and Table 7 it can be confirmed that the region of the NIR spectra excluded are due to overlapping of water and C-H bands.

Table 7 Absorption bands for selected functional groups in NIR [41]

Group	Combinations [nm]	1st overtone [nm]	2nd overtone [nm]	3rd overtone [nm]
CH	2270 – 2440	1690 – 1780	1170 – 1230	905 – 935
CH_2	2250 – 2410	1670 – 1750	1150 – 1210	900 – 925
CH_3	2200 – 2400	1630 – 1710	1120 – 1195	870 – 910
H_2O	1850 – 1920	1393 – 1445	955 – 990	740 – 765
R-OH	2060 – 2090	1410 – 1480	925 – 940	725 – 748

As seen from Table 6 the variables in the spectra that are removed in the first modelling step are:

- 1400 nm to 1540 nm in the short-wave NIR region
- 1860 nm to 2396 nm in the long-wave NIR region

In the second modelling step the excluded variables are:

- 890 nm to 1160 nm, 1380 nm to 1580 nm, and 1645 nm to 1690 nm in the short-wave NIR region
- 1860 nm to 2396 nm in the long-wave NIR region

These particular regions are mainly excluded based upon evaluating the important loading weights for the models, as previous described in the modelling of ethanol. In the second modelling step the first region excluded from the short-wave region are due to only a small complements of chemical information, since the absorbance is below or close to zero. The second region excluded was due to the absorbance band of water, and the third region are removed due to noise in the spectra.

For ease of use of the models in practice, it was decided that the regions to exclude should be the same for all parameters for the three wine types.

Pre-processing of Spectra

By applying pre-treatment to the spectra it was possible to compensate for chemical and physical interferences that would otherwise have an adverse influence on the models. Factors one would like to compensate for might be, for example:

- Temperature (- of samples, -spectrometer, -surroundings)
- "False light" in the surroundings, when measuring NIR spectra
- Sample pH
- Sample colour
- Particle size, differential compaction

After pre-treatment was applied to the spectra involved, the conventional chemometric auto-scaling was often also applied (if/when needed). It was here decided to use auto-scaling, since the absorbance at different wavelengths vary in value. By correcting each absorbance value with the standard deviation of the given variable, see equation below, each scaled variable got the same total variance as all other variables.

$$X_{scaled} = X \cdot \frac{1}{s_X}$$

Where
x_{scaled}: scaled x value
x: original x value
s_x: standard deviation

Centering is always needed for data analytical reasons, otherwise the first PLS-component is wasted for this translation in the coordinate system used for modelling. [43]

Pre-treatment of Spectra

In this work, calibration models were made both with and without several alternative types of pre-treatment as follows: raw data, raw data reduced, 1st derivative, 2nd derivative, and Multiplicative Scatter Correction (MSC). Each pre-treatment principle was designed to remove as much interference or background noise as possible without degrading the underlying chemical information.

1st and 2nd Derivative

The 1st derivative of a spectrum is often used to remove differential offsets. The 2nd derivative is often used to remove offset as well as varying baseline slopes. Both 1st and 2nd derivative in this project are applied after a smoothening of the spectra using the Savitsky-Golay algorithm. [42 – 45]

The algorithm for mathematical calculating a smoothening of the spectra was defined by evaluating a set of spectral values both with lower as well as higher wavelengths, and then use the method of least squares to find an optimised curve through these spectral points. This is Savitsky-Golay filtering, which works as a smoothing of the spectra. It was not possible to make a completely general statement on how many points should be used for smoothing, but typical filters used were 3, 5, 7, and 9 points (half before and half after the central point). The same goes for which polynomial order to use, but usually 1st, 2nd, or 3rd order was used – this was claimed to depend on the shape of the original spectra [42 – 45]. In this project a filter of 3 points and 2nd polynomial order was used.

A 2nd order polynomial has the equation[44]

$$y = \hat{a} + \hat{b}x + \hat{c}x^2$$

Where
x: wavelength
y: spectral absorbance
$\hat{a}$, $\hat{b}$, and $\hat{c}$: parameters estimated by the least squares fit

The slope of the equation is the tangent to the curve

$$\frac{dy}{dx} = \hat{b} + 2\hat{c}x$$

And the 2nd derivative is the rate of change of the slope as one move along the curve

$$\frac{dy^2}{dx^2} = 2\hat{c}$$

With Savitsky-Golay smoothing, using 1st or 2nd derivative pre-treatment, the spectral value of interest (the center of the filter) is *replaced* with the derivative arising from the smoothening algorithm [44].

With continuous spectra, the 1st derivative results in a spectrum were the points are the slope at each wavelength of the original spectra. This will change the whole shape of the spectra leaving peaks in the original spectra to become zero crossing in the derivative spectra, see Figure 30. In Figure 30 the red line is the function, the black line represents a zero line, and the blue line is where the raw function has the largest slope, the 1st derivative has a peak, and the 2nd derivative is zero crossing. The 2nd derivative pre-treatment can be explained by repeating the 1st derivative pre-treatment two times: taking the 1st derivative to the 1st derivative spectra.[44]

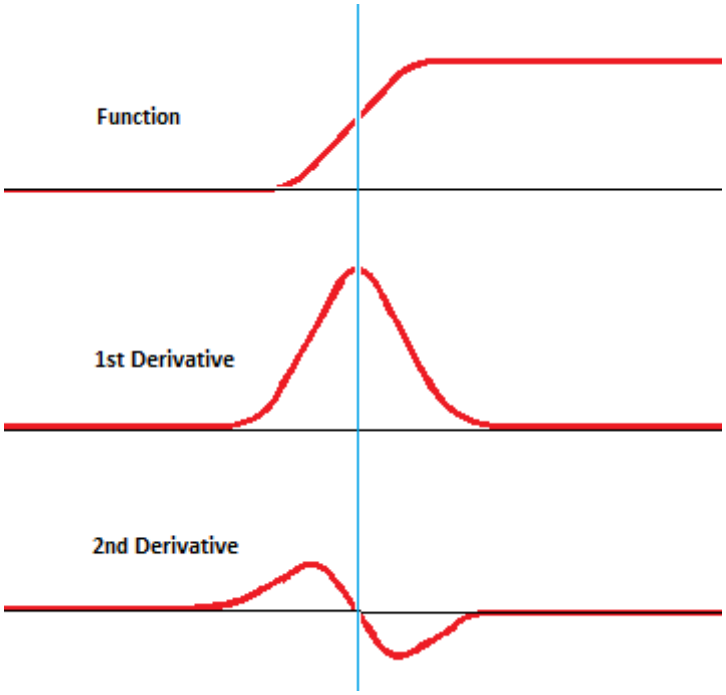

Figure 30 A function and its 1st and 2nd derivative

The 1st derivative pre-treatment removes offset from the spectra as is seen from the equations above, in which $\hat{a}$ denotes such features. If the baseline of the spectra was only comprised of an offset, the other parameters in the equation for the 2nd order polynomial would be zero. If a more complex baseline was present, where the other parameters was not equal to zero, repeated application of the derivates would remove higher order terms. F. ex. taking the 2nd derivative would removed both $\hat{a}$ and $\hat{b}$ features [45].

The raw spectra for the white wine samples from both calibration and test sets are shown in Figure 31.

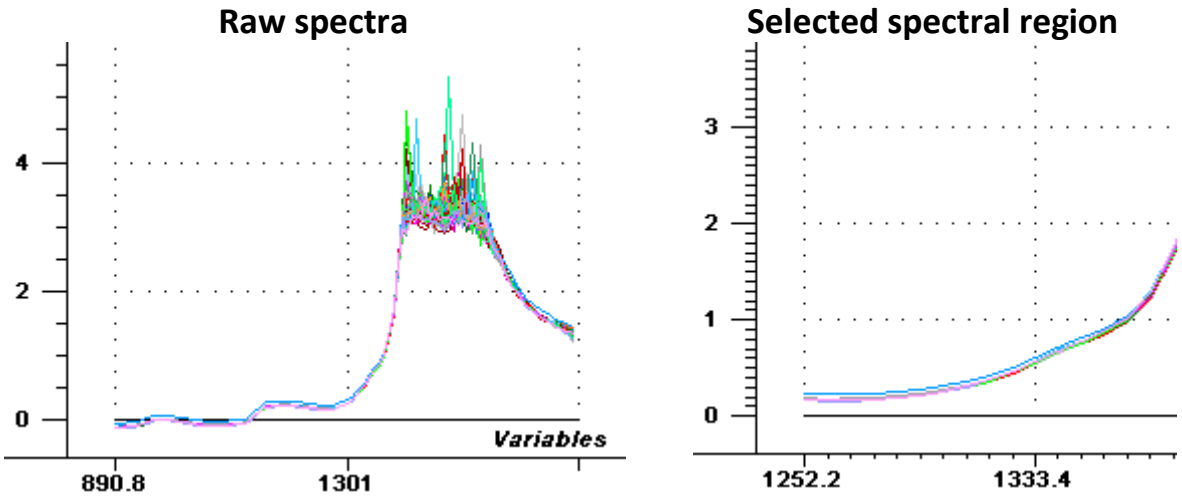

Figure 31 Raw spectra of samples from the white wine, both calibration and test set.
Left: full spectra, right: selected spectral region

The effect of applying 1st and 2nd derivative to the raw spectra can be seen in Figure 32 and Figure 33, respectively.

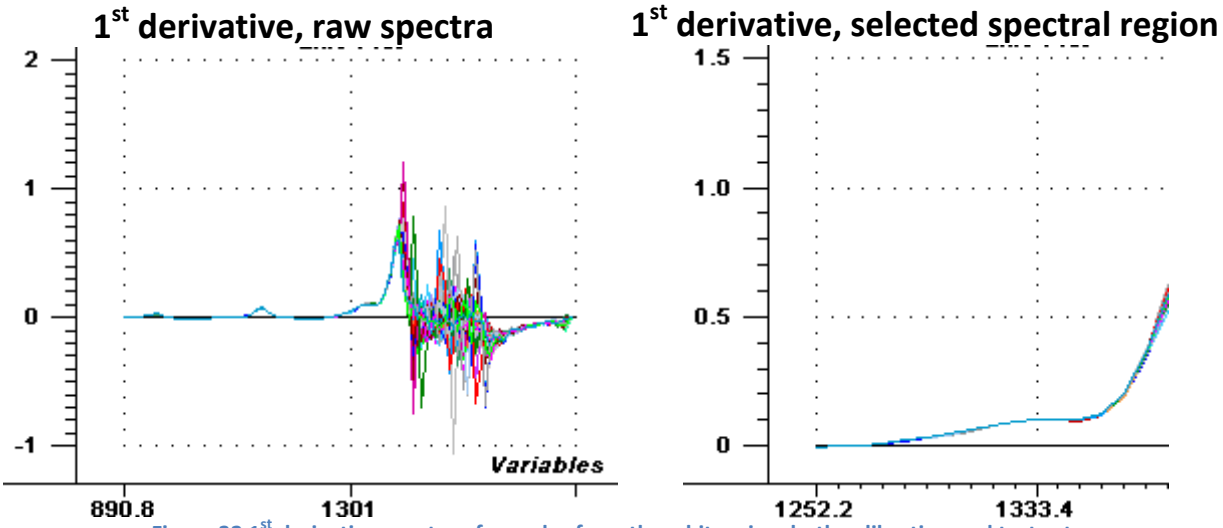

Figure 32 1st derivative spectra of samples from the white wine, both calibration and test set.
Left: full 1st derivative spectra, top right: selected spectral region

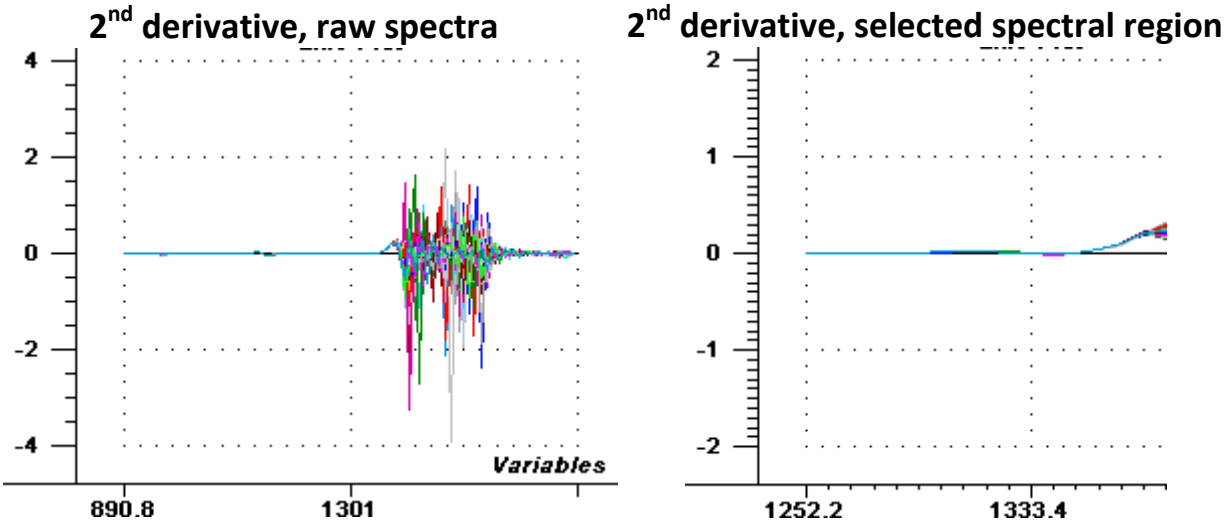

Figure 33 2nd derivative spectra of samples from the white wine, both calibration and test set.
Left: full 2nd derivative spectra, bottom right: selected spectral region

Multiplicative Scatter Correction (MSC)

A third type of pre-treatment is MSC, which was used in three different modes; common offset, common amplification, and full MSC. A short description of how MSC works is given below.

First all variables in the spectra was plotted against their average spectrum and a regression was fitted to these data, where a(*i*) was the offset and b(*i*) was the coefficient for the slope of the fitted regression line, *i* was an index for all individual objects in the data set.

Then MS correction was applied to the spectra. This meaning that the MSC pre-treatment replaced every element in the original **X**-matrix (spectra) with a new element according to the following equations. [43]

The common offset corrects additive effects according to

$$M_{new}(i,k) = M(i,k) - a(i)$$

The common amplification corrects multiplicative effects according to

$$M_{new}(i,k) = \frac{M(i,k)}{b(i)}$$

The full MSC corrects for both the additive and the multiplicative effects according to

$$M_{new}(i,k) = \frac{M(i,k) - a(i)}{b(i)}$$

A visual illustration of the MSC pre-treatments are shown in Figure 34. It is seen that the common offset moves the spectra down to a common baseline, thus correcting for additive effect and this remove the offset (red arrows). The common amplification calculates a common baseline slope for all spectra and rotates each individual spectrum to this common horizontal baseline which has the effect of correcting for multiplicative scatter effects (blue arrows). Full MSC is the combination of the common offset and common amplification.

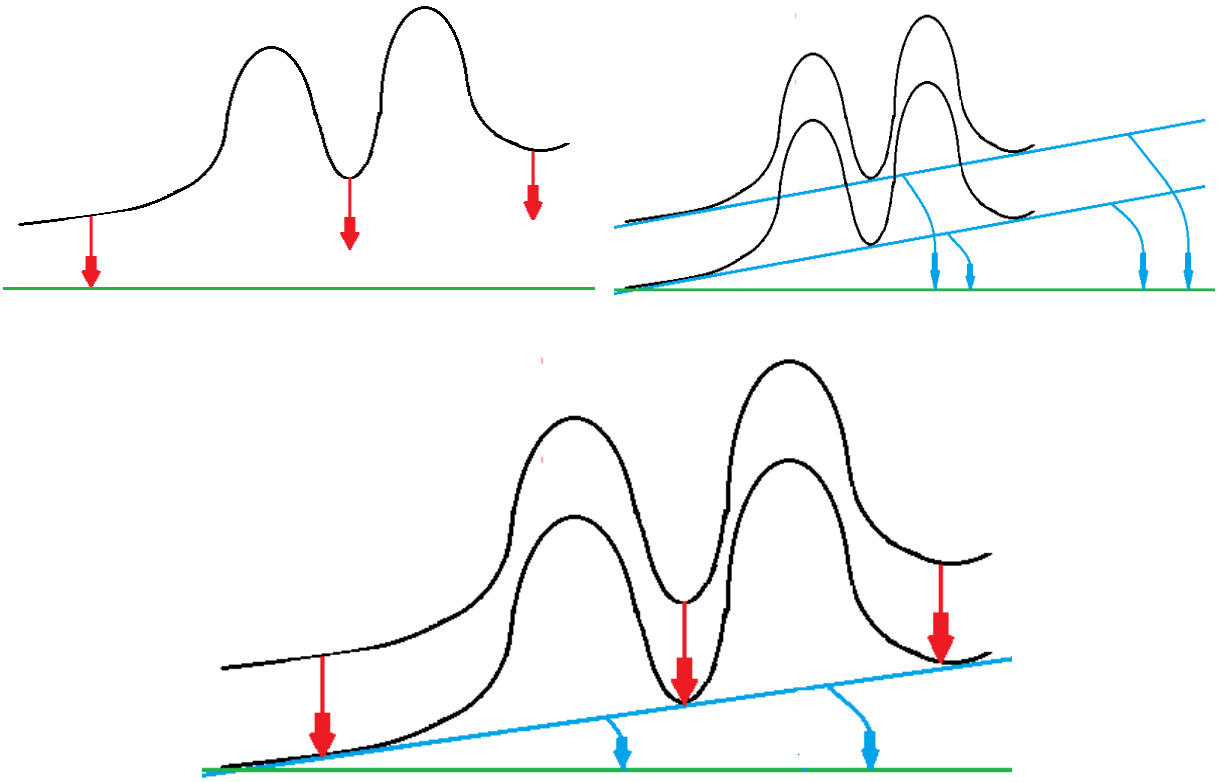

Figure 34 The effects of MSC pre-treatments
Effect of common offset (red arrows) and common amplification (blue arrows)

Preferably the MSC pre-treatment parameter estimation must be done on a part of the spectra that contains no chemical information but only (or mainly) background information. In this project the MSC pre-treatment was made on the whole spectra, though leaving out the absorption band from

water etc., since the regions which show no clear chemical information were very narrow, see Figure 31.

In Figure 35, Figure 36, and Figure 37 are shown the effect of the MSC pre-treatments on the full spectra and on a selected part of the spectra for the white wine. It is seen from the figures that the three MSC pre-treatments converts the baseline of the spectra in not so dramatically different ways.

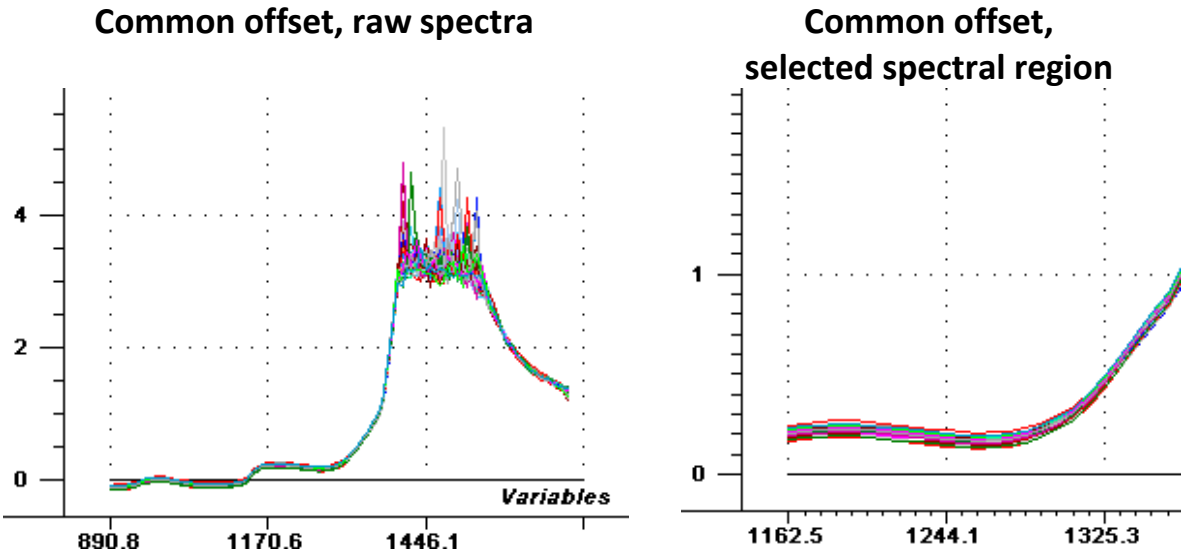

Figure 35 Effect of common offset on spectra from the white wine
Left: full spectra after common offset, right: a part of the spectra after common offset

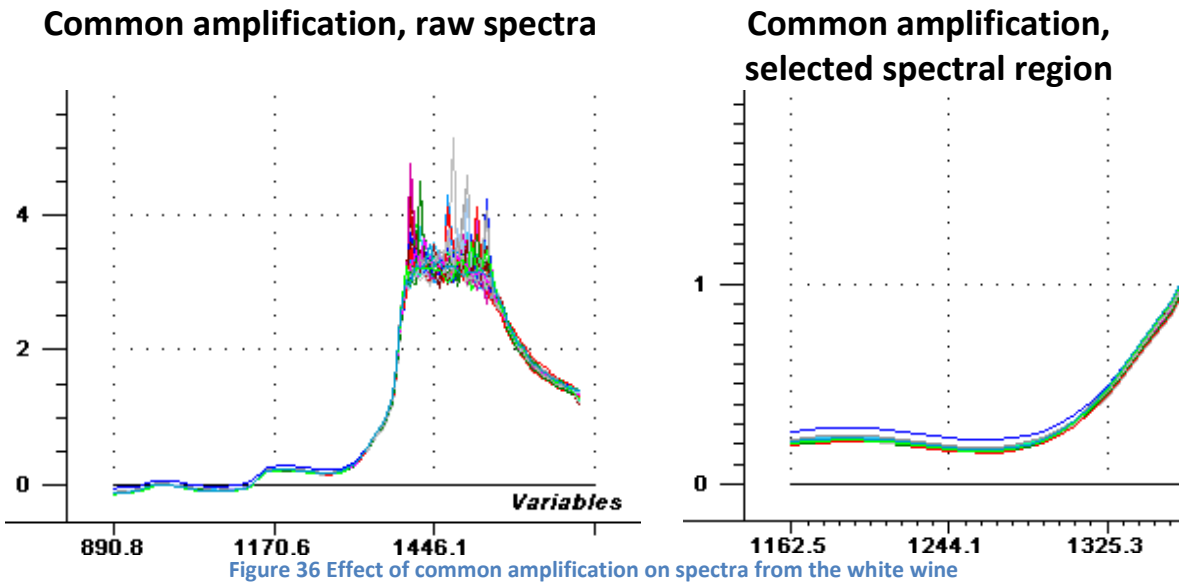

Figure 36 Effect of common amplification on spectra from the white wine
Left: full spectra after common amplification, right: a part of the spectra after common amplification

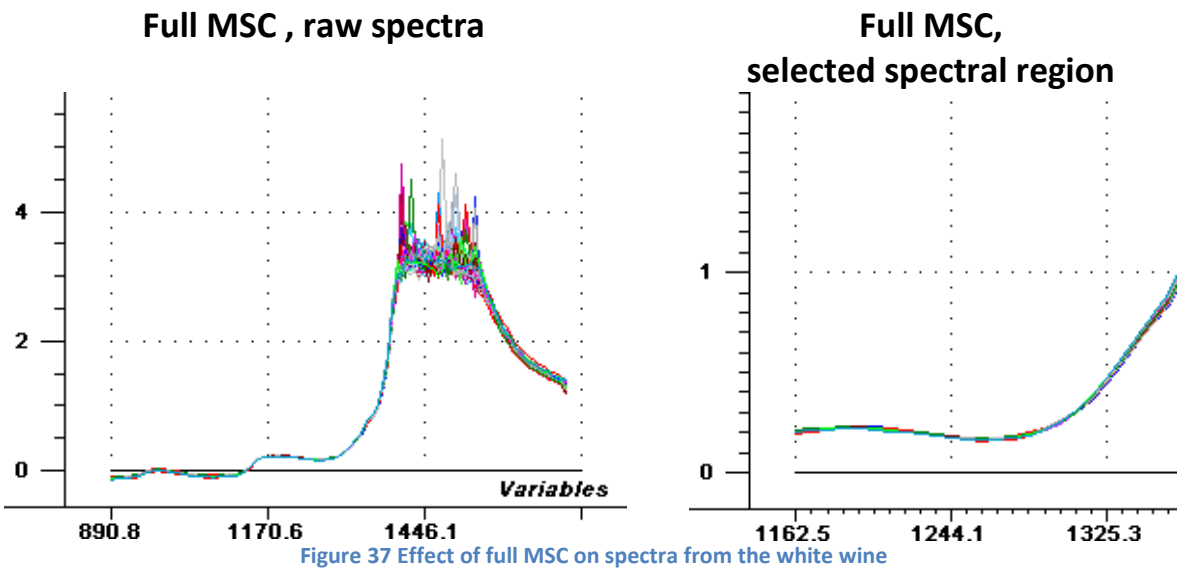

Figure 37 Effect of full MSC on spectra from the white wine
Left: full spectra after full MSC, right: a part of the spectra after full MSC

First Modelling Campaign

The first modelling was done to find the optimal pre-treatment of the spectra (if indeed any pre-treatment was needed). The modelling was applied to the raw spectra with all variables included and afterwards applied to a reduced part of the spectra, where the insignificant variables were excluded. The 1st and 2nd derivative of the spectra was also used for modelling. MSC pre-treatment was applied to the reduced spectra in means of common amplification, common offset, and full MSC. This gave a total of 462 models (3 wine types * 11 parameters * 7 pre-treatments * 2 NIR regions). All models are listed on the CD-rom, and the best models for all parameters divided by wine type are listed in Appendix 7. The type of pre-treatment which gave the best initial models are listed in Table 8.

Table 8 Best pre-treatments of spectra for the first modelling campaign

	White wine (short)	White wine (long)	Rosé wine (short)	Rosé wine (long)	Red wine (short)	Red wine (long)
Sucrose	1st	1st	-	-	MSC	Raw red.
Glucose	Raw	Ampl.	1st	2nd	MSC	2nd
Fructose	Raw red.	Ampl.	MSC	2nd	Raw	2nd
Glycerol	Raw red.	Raw red.	MSC	2nd	MSC	2nd
Ethanol	2nd	Raw	1st	Raw red.	MSC	2nd
Citric Acid	1st *	1st *	1st	2nd	MSC	Raw
Tartaric Acid	MSC	1st	-	-	MSC	Raw
Malic Acid	MSC	Ampl.	1st	2nd	MSC	Raw
Succinic acid	MSC	Raw red.	MSC	2nd	MSC	2nd
Lactic Acid	Raw red. *	1st *	Raw red. *	2nd *	Ampl. *	2nd *
Acetic Acid	1st	1st	-	-	Raw *	Raw *

Short: 890 nm to 1691 nm, long: 1596 nm to 2396 nm, raw: whole spectra, raw red.: reduced spectra, 1st: 1st derivative, 2nd: 2nd derivative, Ampl.: common amplification, Off-set: common off-set, MSC: Full MSC, and *: concentration range close to or at the Limit of Detection

Table 8 shows that there was no clear systematic in which of the NIR region or the pre-treatment resulted in best models with regards to wine type or parameter. Overall it seemed that the raw spectra, the reduced raw spectra, 1st and 2nd derivative, and full MSC gave the best models. All models were made again, this time leaving out all the variables in the spectra that did not seem to have any chemical information with regards to the parameters for the first campaign.

Second Modelling Campaign

The second modeling campaign provided a total of 264 new models (3 wine types * 11 parameters * 4 pre-treatments * 2 NIR regions). All models are listed on the CD-rom, and the best models for all parameters divided by wine type are listed in Appendix 8. Table 9 lists the best pre-treatment for the models from the second modelling campaign for each parameter and wine type (top of each cell).

Table 9 Best pre-treatment of spectra in the second modelling campaign

	White wine (short)	White wine (long)	Rosé wine (short)	Rosé wine (long)	Red wine (short)	Red wine (long)
Sucrose	1st	1st	-	-	1st MSC	Raw 2nd
Glucose	1st	Raw red. 1st	1st MSC	2nd	1st MSC	2nd
Fructose	1st	Raw red. 1st	1st MSC	2nd	1st MSC	2nd
Glycerol	1st	Raw red. 1st	MSC 1st	2nd	1st MSC	2nd
Ethanol	1st	Raw 1st	MSC Raw	Raw red	MSC	2nd
Citric Acid	1st	1st	1st MSC	2nd	MSC 1st	Raw 2nd
Tartaric Acid	1st	1st	-	-	1st MSC	Raw 2nd
Malic Acid	1st	1st	MSC 1st	2nd	MSC 1st	Raw 2nd
Succinic acid	1st	Raw 1st	1st MSC	2nd	MSC 1st	2nd
Lactic Acid	1st	1st	1st	2nd	MSC 1st	MSC 2nd
Acetic Acid	1st	1st	-	-	1st MSC	Raw 2nd

Top: Best model. Bottom: acceptable alternative model if only one, consistent pre-treatment is sought for each wine/analytical modality

There seemed to be a fairly systematic tendency that 1st derivative or full MSC would provide an acceptable model for the short-wave NIR range for all three wines and for the white wine in the long-wave range. The 2nd derivative would provide an acceptable model for the long-wave NIR range for

the rosé wine and the red wine, in fact the only exception was the ethanol for the rosé wine, which demanded a full MSC pre-treatment.

Choice of Pre-Treatment

To see if this tendency could be followed through for all of the parameters for each wine type, the derivations from this pattern were checked and also listed in Table 9 as an alternative model (bottom row in the cell). It was found that for all parameters, except ethanol, the 1st derivative could be used for the short-wave NIR range for all three wines and also for the white wine in the long-wave NIR range. For the rosé wine and the red wine the 2nd derivative could be used for all parameters in the long-wave NIR range, except ethanol in the rosé wine.

The modelling of ethanol shows deviation from the rest of the parameters in the requirements of pre-treatment. With regards to pre-treatment there was a need for a more complex and effective pre-treatment for the rosé and red wine, than for the white wine. This may be due to the higher complexity of the wines, but also because this parameter has the most similar molecular structure to that of water. This resulted in difficulties to distinguish the chemical information of ethanol clearly from that of water in the NIR spectra. This was also seen in a previous study [12]. Since ethanol required full MSC it was possible that the temperature effect on the NIR spectra was more distinct for ethanol than the rest of the parameters.

On the basis of the above discussion of the first and second modelling campaign, it was shown that the best models were obtained when 1st derivative was applied to both short- and long-wave NIR regions for the white wine. For the rosé and the red wine the best models were obtained when applying 1st derivative to the short-wave NIR region and 2nd derivative to the long-wave NIR region, except for ethanol which required full MSC pre-treatment.
For an easier overview of the chosen pre-treatments see Table 10.

Table 10 Final overview of consistent, effective pre-treatment of spectra for each wine type/analytical modality

	White wine (short)	White wine (long)	Rosé wine (short)	Rosé wine (long)	Red wine (short)	Red wine (long)
Sugars	1st	1st	1st	2nd	1st	2nd
Glycerol	1st	1st	1st	2nd	1st	2nd
Ethanol	1st	1st	MSC	Raw red.	MSC	2nd
Acids	1st	1st	1st	2nd	1st	2nd

Previous literature studies stated that the 1st and 2nd derivative was a normally used pre-treatment in the short-wave NIR region for wines made from grapes [4,10,15]. Therefore, it was to be expected that this pre-treatment would also work best here, since the main chemical components of the fruit and the grape wine are approximately identical.

Result of Modelling

In the following the optimized models will be discussed with regards to slope, R^2, outliers, PLS components, RMSEP, and relative RMSEP.

Slope and R^2

Table 11 lists the slope and R^2 values for the optimized models. Models were left out where the concentrations were at or close to the limit of detection for the parameters. These models are left out, since they are not adequate to be proper validated.

Table 11 Slope (top) and R^2 (bottom) for optimized models with regards to wine type and analytical modality

	White wine (short)	White wine (long)	Rosé wine (short)	Rosé wine (long)	Red wine (short)	Red wine (long)	Mean
Sucrose	1.09	0.97	-	-	0.93	0.86	0.96
	0.97	0.97	-	-	0.97	0.89	0.95
Glucose	0.97	0.88	0.93	1.00	1.06	1.00	0.97
	0.98	0.96	0.97	0.96	0.97	0.93	0.96
Fructose	0.97	0.87	0.95	1.04	1.01	0.92	0.96
	0.98	0.96	0.97	0.96	0.99	0.96	0.97
Glycerol	0.95	0.85	1.08	0.99	0.99	1.03	0.98
	0.98	0.96	0.92	0.97	0.99	0.97	0.97
Ethanol	0.94	0.86	1.10	1.19	1.12	1.09	1.05
	0.98	0.97	0.97	0.95	0.89	0.88	0.94
Citric Acid	-	-	1.04	0.94	0.96	0.84	0.95
	-	-	0.98	0.97	0.98	0.95	0.97
Tartaric Acid	1.07	0.98	-	-	1.02	0.91	1.00
	0.98	0.99	-	-	0.94	0.94	0.96
Malic Acid	1.10	0.93	1.06	0.99	1.03	0.96	1.01
	0.97	0.99	0.98	0.94	0.96	0.98	0.97
Succinic acid	1.09	0.91	0.89	1.00	0.93	0.82	0.94
	0.95	0.99	0.97	0.98	0.93	0.92	0.96
Lactic Acid	-	-	-	-	-	-	-
	-	-	-	-	-	-	-
Acetic Acid	0.99	0.99	-	-	-	-	0.99
	0.99	0.99	-				0.99
Mean	1.03	0.93	1.01	1.02	1.01	0.94	
	0.97	0.97	0.96	0.96	0.96	0.93	

From Table 11 it can be seen that the slopes are between 0.82 to 1.19 and the R^2 values are between 0.89 to 0.99. This shows that almost all models are within the range which was stated as acceptable ($0.85 < \text{slope} < 1.15$, $0.85 < R^2 < 1.00$). Only three models did not meet the requirements. Those models are for ethanol (slope = 1.19) in the long-wave NIR region for the rose wine, and for succinic acid (slope = 0.82) and citric acid (slope = 0.84) in the long-wave NIR region for the red wine.

From the mean values of the key statistics for all models, see Table 11, it shows that the mean quality of the models, when compared with regards to parameter and wine type, are very good overall. This means that the slopes were between 0.91 to 1.02 and the R^2 values were between 0.94 to 0.99.

From Figure 38 it is seen that the result of the high slope could be because of random stochastic fluctuations, and the solution could be to add samples to the test set especially in the high end of the concentration range. This would give fluctuations in the whole concentrations range and give a more valid result of the prediction.

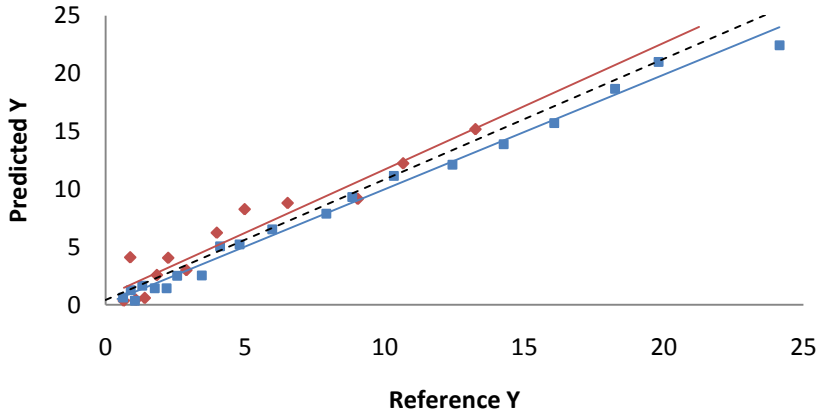

Figure 38 Example of a model with a high slope (Red wine, ethanol, long-wave NIR range). Blue: Calibration set, Red: Test set, Black: Mean between calibration and test set

Optimal Number of PLS Components

In Table 12 the optimal number of PLS components are listed. The table shows that all models had an optimal number PLS components below four, which most likely signified that the models were not over-fitted. Only the model for succinic acid in the red wine in the short-wave NIR region was at the limit of preferably requirements with a value of four. The models are seen to be simple, since most of the models only need one or two components to be good and acceptable with regards to the number of PLS components needed.

Table 12 Optimal number of PLS components for optimized models

	White wine (short)	White wine (long)	Rosé wine (short)	Rosé wine (long)	Red wine (short)	Red wine (long)	Mean
Sucrose	1	1	-	-	2	1	1
Glucose	1	2	2	2	2	1	2
Fructose	1	2	2	2	1	2	2
Glycerol	1	3	2	2	1	2	2
Ethanol	1	2	1	3	1	2	2
Citric Acid	-	-	2	1	3	2	2
Tartaric Acid	2	1	-	-	3	2	2
Malic Acid	1	1	2	2	1	2	2
Succinic acid	1	2	3	2	4	2	2
Lactic Acid	-	-	-	-	-	-	-
Acetic Acid	1	2	-	-	-	-	2
Mean	1	2	2	2	2	2	

RMSEP and Relative RMSEP

The RMSEP for the models are the mean uncertainty of the model and are expressed in the same unit as the concentration of the samples. Therefore, it is directly seen how large the uncertainty is to the determination of concentration in each sample.
The relative RMSEP is calculated as

$$relRMSEP = \frac{RMSEP}{\bar{Y}} \cdot 100\ [\%]$$

Where
$\bar{Y} = \frac{Y_{highest} - Y_{lowest}}{2}$, Y: Concentration measured for the test set

Since the relative RMSEP is in percentage points it can be compared across all models without taking into account the differences in concentrations. The relative RMSEP should preferably be below 10 % in a feasibility study, indeed it should always be as small as possible.

Table 13 lists the RMSEP (top) and the corresponding relative RMSEP (bottom) for each model.

Table 13 RMSEP (top) and relative RMSEP (bottom) for optimized models

	White wine (short)	White wine (long)	Rosé wine (short)	Rosé wine (long)	Red wine (short)	Red wine (long)	Mean
Sucrose	0.191	0.183	-	-	0.320	0.669	0.341
	12.9	11.8	-	-	10.8	22.6	14.5
Glucose	0.692	0.561	0.443	0.625	0.226	0.302	0.475
	9.66	12.1	11.0	12.0	11.9	15.9	12.1
Fructose	0.628	0.575	0.413	0.611	0.100	0.211	0.423
	9.22	13.1	10.7	12.3	6.29	13.3	10.8
Glycerol	0.641	0.742	0.199	0.108	$9.94 \cdot 10^{-2}$	0.160	0.324
	9.67	16.7	17.1	17.7	7.27	11.7	13.4
Ethanol	0.829	0.819	0.819	1.23	1.27	1.81	1.13
	8.81	14.1	10.3	15.5	20.1	28.8	16.3
Citric Acid	-	-	$7.16 \cdot 10^{-2}$	$8.94 \cdot 10^{-2}$	$2.72 \cdot 10^{-2}$	$4.26 \cdot 10^{-2}$	$4.64 \cdot 10^{-2}$
	-	-	10.0	12.5	10.3	16.0	12.2
Tartaric Acid	$2.89 \cdot 10^{-2}$	$3.12 \cdot 10^{-2}$	-	-	$8.69 \cdot 10^{-2}$	$8.55 \cdot 10^{-2}$	$5.81 \cdot 10^{-2}$
	12.1	7.48	-	-	18.1	17.8	13.9
Malic Acid	$4.51 \cdot 10^{-2}$	$4.40 \cdot 10^{-2}$	$2.95 \cdot 10^{-2}$	$4.40 \cdot 10^{-2}$	$2.27 \cdot 10^{-2}$	$1.57 \cdot 10^{-2}$	$3.35 \cdot 10^{-2}$
	13.9	7.46	10.5	20.2	14.6	10.1	12.8
Succinic acid	$1.47 \cdot 10^{-2}$	$1.09 \cdot 10^{-2}$	$4.63 \cdot 10^{-2}$	$4.00 \cdot 10^{-2}$	$7.68 \cdot 10^{-2}$	$8.10 \cdot 10^{-2}$	$4.50 \cdot 10^{-2}$
	17.1	6.76	13.5	11.9	17.7	18.7	14.3
Lactic Acid	-	-	-	-	-	-	-
	-	-	-	-	-	-	-
Acetic Acid	$1.21 \cdot 10^{-2}$	$1.95 \cdot 10^{-2}$	-	-	-	-	$1.58 \cdot 10^{-2}$
	10.0	7.74	-	-	-	-	8.9
Mean	0.281	0.272	0.254	0.344	0.204	0.311	
	10.7	11.1	13.2	14.4	13.1	18.9	

RMSEP: g/L and relRMSEP: %

For sucrose the largest RMSEP were found for the red wine. For glucose, fructose, and glycerol the largest RMSEP was found for the white wine and the least for the red wine. For ethanol the largest RMSEP was found for the rosé wine and the red wine in the short-wave NIR region, and the least in the long-wave NIR region for the red wine. For the acids the RMSEP were generally small for all wine types and parameters, but there was a tendency that the largest RMSEP were found in the red wine.

Approximately half of the models met the acceptable requirements, but taking into account which samples are excluded as outliers, see Appendix 8, there was an explanation to the high values. This was due to the exclusion of samples with high concentrations or exclusion of several samples with low values. Both these reasons will decrease the size of the concentration ranges accounted for in the models. The concentration range could be increased by including more samples in the test set, both with high and low concentrations, to ensure that the concentration differences between the individual samples are lowered. In this way the concentration range will only be reduced slightly for each outlier excluded.

Due to the small test set size in this feasibility study which only can give indications of the uncertainty in more fully calibrated models, it was concluded that the models were acceptable with regards to RMSEP even though the relative RMSEP was high for some models.

Proportion of Excluded Outliers

The proportion of outliers excluded should preferably be below 10 %. In Table 14 are listed the proportion of outliers excluded from the models. It shows that for some models this was much higher than preferred. This can be explained by the fact that both the calibration and test set were small in number of samples, so by excluding more than just a few samples it resulted in dramatic percentages. This is the case for the model for sucrose in the white wine, where the proportion of outliers is twice the preferred. This was also seen for sucrose in the red wine in the short-wave NIR region and for ethanol in rosé wine in the long-wave NIR region. Otherwise, the models show a proportion of outliers that was acceptable.

Table 14 Proportion of outliers excluded from final, optimized models [%]

	White wine (short)	White wine (long)	Rosé wine (short)	Rosé wine (long)	Red wine (short)	Red wine (long)	Mean
Sucrose	23	20	-	-	17	6	17
Glucose	10	10	3	0	14	14	9
Fructose	10	10	3	0	11	8	7
Glycerol	10	10	6	8	6	8	8
Ethanol	10	8	14	14	25	6	13
Citric Acid	-	-	14	0	7	4	6
Tartaric Acid	7	7	-	-	11	7	8
Malic Acid	7	7	11	11	7	7	8
Succinic acid	7	10	7	11	14	14	11
Lactic Acid	-	-	-	-	-	-	-
Acetic Acid	10	7	-	-	-	-	9
Mean	10	10	7	7	13	8	

The proportion of outliers was not crucial for the models made in this feasibility study, since the purpose was to establish if the handheld NIR equipment was suitable for determination of the concentration of the parameters. Even though the proportion of outliers was sometimes high, the models were very much acceptable for the purpose of the study.

Choice of Wave-Length Region

When evaluating the total number of variables chosen in the short- and the long-wave NIR region, it was found that the largest number of variables and largest amount of chemical information were in the short-wave NIR region. Combining this with the choice of pre-treatment, the above discussion of the models with regards to slope, R^2, optimal number of PLS components, RMSEP, and proportion of outliers, it was concluded that the best and simplest models were obtained when using the short-wave NIR region for determination of concentrations of the sugars, glycerol, ethanol, and acids.

Overview of Models

After a selection of variables and pre-treatment of the spectra, an overview of all the models made for the parameters were listed by wine type and are shown in Table 15 (white wine), Table 16 (rosé wine), and Table 17 (red wine).

From the results shown in Table 15 it can be stated that there are no problems in modelling sugars, glycerol, ethanol, or acids in the concentration ranges listed for the white wine. With 1st derivative pre-treatment all models met the requirements listed, with only four exceptions with regards to relative RMSEP and one exception with regards to the proportion of outliers. These exceptions were discussed earlier and were concluded not to have a crucial impact on this feasibility study; therefore, all models were stated to be acceptable and properly validated.

Table 15 Overview of optimized models for white wine

	Slope	R^2	# PLS	RMSEP	relRMSEP	% Outliers	Range
Sucrose	1.09	0.965	1	0.191	12.9	23	0.50 - 3.45
Glucose	0.971	0.980	1	0.692	9.66	10	0.70 - 15.0
Fructose	0.970	0.981	1	0.628	9.22	10	0.69 - 14.3
Glycerol	0.952	0.980	1	0.641	9.67	10	0.69 - 14.0
Ethanol	0.942	0.983	1	0.829	8.81	10	0.84 - 19.7
				0.105			0.11 - 2.49
Citric acid	-	-	-	-	-	-	-
Tartaric acid	1.07	0.980	2	$2.89 \cdot 10^{-2}$	12.1	7	54.2 - 533
Malic acid	1.10	0.973	1	$4.51 \cdot 10^{-2}$	13.9	7	72.9 - 723
Succinic acid	1.09	0.952	1	$1.47 \cdot 10^{-2}$	17.1	7	17.4 - 190
Lactic acid	-	-	-	-	-	-	-
Acetic acid	0.993	0.990	1	$1.21 \cdot 10^{-2}$	10.0	10	35.2 - 279
Mean	1.03	0.976	1	0.281	10.7	10	

RMSEP: [g/L], relRMSEP: [%], range: sugars and glycerol: [g/L], acids: [mg/L], ethanol [g/L] (top) and [% vol.] (bottom)

From the results shown in Table 16 for rosé wine it can be stated that there were no problems in modelling sugars, glycerol, ethanol, or acids in the concentration range listed. With the pre-treatment used (full MSC for ethanol and 1st derivative for the rest) all models met the requirements, with only two exceptions having large deviations and four having small deviation with regards to

relative RMSEP and two exceptions with regards to the proportion of outliers. Overall the models for the rosé wine are stated to be acceptable and properly validated.

Table 16 Overview of optimized models for rosé wine

	Slope	R^2	# PLS	RMSEP	relRMSEP	% Outliers	Range
Sucrose	-	-	-	-	-	-	-
Glucose	0.929	0.971	2	0.443	11.0	3	0.42 - 8.49
Fructose	0.949	0.973	2	0.413	10.7	3	0.39 - 8.14
Glycerol	1.08	0.921	2	0.199	17.1	6	0.09 - 2.42
Ethanol	1.10	0.974	1	0.891	10.3	14	1.10 - 17.0
				0.104			0.14 - 2.15
Citric acid	1.04	0.982	2	$7.16 \cdot 10^{-2}$	10.0	4	61.1 - 1492
Tartaric acid	-	-	-	-	-	-	-
Malic acid	1.06	0.979	2	$2.95 \cdot 10^{-2}$	10.5	11	38.3 - 602
Succinic acid	0.894	0.970	3	$4.63 \cdot 10^{-2}$	13.5	7	23.8 - 707
Lactic acid	-	-	-	-	-	-	-
Acetic acid	-	-	-	-	-	-	-
Mean	1.01	0.956	2	0.254	13.2	7	

RMSEP: [g/L], relRMSEP: [%], range: sugars and glycerol: [g/L], acids: [mg/L], ethanol [g/L] (top) and [% vol.] (bottom)

From the results shown in Table 17 for the red wine it can be stated that there may have been some problems in modelling sugars, glycerol, ethanol, or acids in the concentration range listed. This is seen in the table as nearly all models having high values of relative RMSEP. Ethanol may especially be a problem since the slope is high. This was discussed earlier and may be solved by including more samples in the test set with concentration in the high end of the range.
With the pre-treatment used (full MSC for ethanol and 1st derivative for the rest) all the models for the red wine were overall stated to be acceptable and properly validated.

Table 17 Overview of optimized models for red wine

	Slope	R^2	# PLS	RMSEP	relRMSEP	% Outliers	Range
Sucrose	0.933	0.971	2	0.320	10.8	17	0.21 - 6.13
Glucose	1.06	0.970	2	0.226	11.9	14	0.14 - 3.93
Fructose	1.01	0.992	1	0.100	6.29	11	0.12 - 3.30
Glycerol	0.993	0.987	1	0.099	7.27	6	0.11 - 2.84
Ethanol	1.12	0.891	1	1.27	20.1	25	0.65 - 13.3
				0.161			0.082 - 1.68
Citric acid	0.962	0.980	3	$2.72 \cdot 10^{-2}$	10.3	7	28.2 - 554
Tartaric acid	1.02	0.942	3	$8.69 \cdot 10^{-2}$	18.1	11	50.1 - 1010
Malic acid	1.03	0.964	1	$2.27 \cdot 10^{-2}$	14.6	7	13.2 - 324
Succinic acid	0.930	0.927	4	$7.68 \cdot 10^{-2}$	17.7	14	52.8 - 920
Lactic acid	-	-	-	-	-	-	-
Acetic acid	-	-	-	-	-	-	-
Mean	1.01	0.961	2	0.204	13.1	13	

RMSEP: [g/L], relRMSEP: [%], range: sugars and glycerol: [g/L], acids: [mg/L], ethanol [g/L] (top) and [% vol.] (bottom)

Total-Sugar and Total-Acid

For wineries a parameter of total-sugar and total acid in addition to that of glycerol and ethanol may be preferred for daily use when monitoring wine during fermentation and storage. Then the model for an individual parameter could be applied when problems with the fermentation or taste etc. of the wine occur. By total-sugar or total-acid means that the concentrations modelled are the sum of all the sugars (sucrose, glucose, and fructose) and acids (citric, tartaric, malic, succinic, lactic, and acetic acid) determined, respectively. Models for total-sugar, glycerol, ethanol, and total-acid based upon the chosen model pre-treatment for the wine types are listed in Table 18 (white wine), Table 19 (rosé wine), and Table 21 (red wine). The models with a bit more information are shown in Appendix 9.

Figure 39 (white wine), Figure 40 (rosé wine), and Figure 42 (red wine) show the predicted vs. reference plot for total-sugar, glycerol, ethanol, and total-acid in the short-wave NIR region. The pre-treatment were 1st derivative for all models, except for ethanol in rosé and red wine, where full MSC was used.

It is seen from Figure 39 and Table 18 that there were no problems in modelling total sugar, glycerol, and total acid in the white wine since the models had the samples from both the calibration and test set well distributed in the whole concentration range of the models. It was also seen that the regression curve for the test set was almost equal to the regression curve for the calibration set. With regards to the slope and $R^{2,}$ the values were very close to 1 and this confirmed the visual evaluation. With regards to number of outliers and RMSEP found when making the models, they were all within an acceptable range.

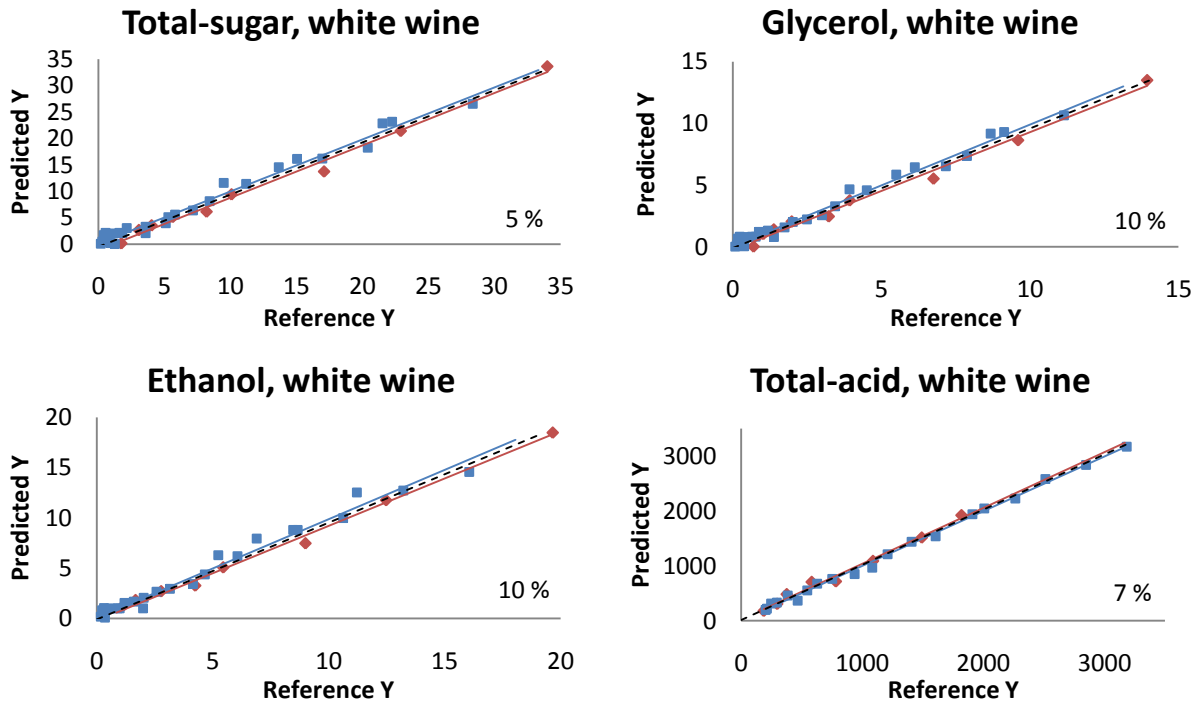

Figure 39 Predicted vs. measured for total-sugar [g/L], glycerol [g/L], ethanol [g/L], and total-acid [mg/L] in white wine. Blue: Calibration set, Red: Test set, Black: Mean between calibration and test set. The proportion of outliers is shown in the bottom right corner of the figures

Table 18 Overview of optimized models for total-sugar, glycerol, ethanol, and total-acid for white wine

	Slope	R^2	# PLS	RMSEP	relRMSEP	% outliers	Range
Total Sugar	0.992	0.980	1	1.57	9.7	5	1.7 - 34.0
Glycerol	0.952	0.980	1	0.641	9.7	10	0.69 - 13.9
Ethanol	0.942	0.983	1	0.829	8.8	10	0.84 - 19.7
				0.105			0.11 - 2.49
Total Acid	1.02	0.989	3	0.0721	8.8	7	0.19 - 1.82

RMSEP: [g/L], relRMSEP: [%], range: sugars and glycerol: [g/L], acids: [mg/L], ethanol [g/L] (top) and [% vol.] (bottom)

Just as for the white wine it is seen from Figure 40 and Table 19 that there were no problems in modelling total sugar and total acid in the rosé wine. For glycerol the R^2 were a little low, which is seen in the regressions curves as the samples from the calibration set and test set are located in what may be two groups.

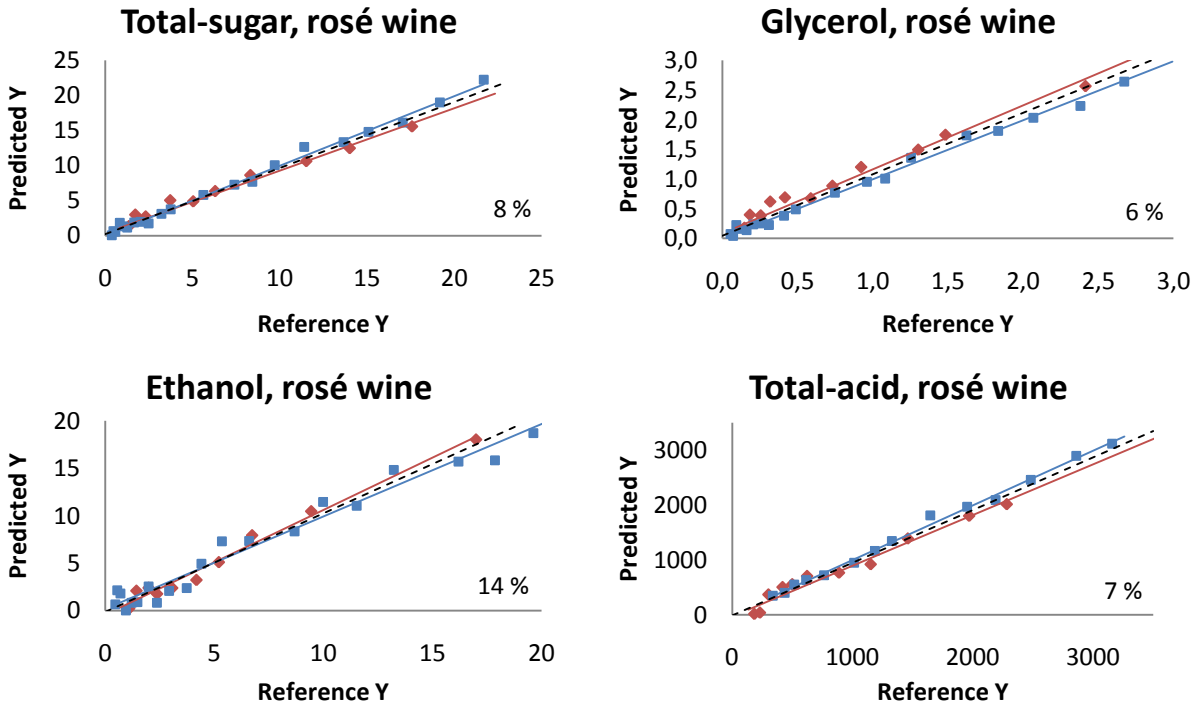

Figure 40 Predicted vs. measured for total-sugar [g/L], glycerol [g/L], ethanol [g/L], and total-acid [mg/L] in rosé wine. Blue: Calibration set, Red: Test set, Black: Mean between calibration and test set. The proportion of outliers is shown in the bottom right corner of the figures

Table 19 Overview of the optimized models for total-sugar, glycerol, ethanol, and total-acid for rosé wine

	Slope	R^2	# PLS	RMSEP	relRMSEP	% outliers	Range
Total Sugar	0.892	0.961	2	1.07	12.8	8	0.81 - 17.6
Glycerol	1.08	0.921	2	0.199	17.1	6	0.086 - 2.42
Ethanol	1.10	0.974	1	0.819	10.3	14	1.1 - 17.0
				0.104			0.14 - 2.15
Total Acid	0.923	0.972	3	0.156	14.6	7	0.13 - 2.28

RMSEP: [g/L], relRMSEP: [%], range: sugars and glycerol: [g/L], acids: [mg/L], ethanol [g/L] (top) and [% vol.] (bottom)

Glycerol was modelled again, but this time by removing a few more possible outliers. This was done to see if the model would be improved with regards to slope, R^2, and RMSEP. The result is visually shown in Figure 41. The results of the model are listed in Table 20.

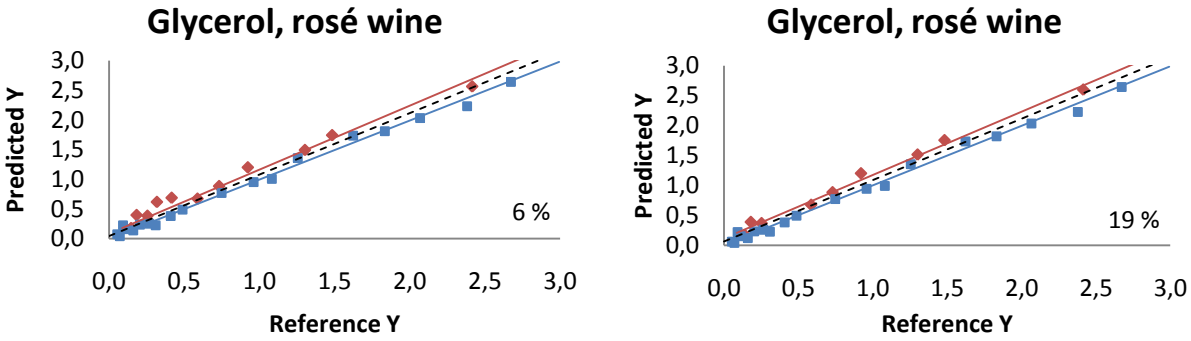

Figure 41 Comparison of models for glycerol before (left) and after (right) removal of additional outliers. The proportion of outliers is shown in the bottom right corner of the figures

Table 20 Results for the modelling of ethanol in the rosé wine before and after removal of potential last stage outliers

	Slope	R^2	# PLS	RMSEP	relRMSEP	% outliers	Range
Glycerol – before	1.08	0.921	2	0.199	17.1	6	0.0860 - 2.42
Glycerol – after	1.06	0.930	2	0.187	16.5	19	0.144 - 2.42

RMSEP [g/L], relRMSEP [%] and range [g/L]

It is seen that the new model is slightly better with regard to slope and R^2 and a little better with regards to RMSEP, but it still does not meet the requirements. This remodelling gives indication that the model can be improved by using more samples in the test set over the entire concentration range. The new model is still simple since only two PLS components were needed for the model.

Parallel to the results for the other wines it is seen from Figure 42 and Table 21 that it is possible to model total sugar and glycerol in the red wine. The described situation for glycerol in rosé wine is not visible in the red wine, but it is seen for total acid. The model for total acids showed a relatively high relative RMSEP, otherwise the model is good.

The model for ethanol showed a high slope and a low R^2 value which is due to the small amount of samples left in the model. 25 % has been removed, so only left is a few samples in the low concentration range. This results in a model with a high relRMSEP. An approach by removing more outliers would not give a better result in this case since there were no obvious outliers to remove. An approach which might help to optimize the model would be to include more samples with high concentrations in the test set, since these samples all have been concluded to be outliers and are removed from the model. The model is acceptable, but it is desired to do the validation on a test set including more samples.

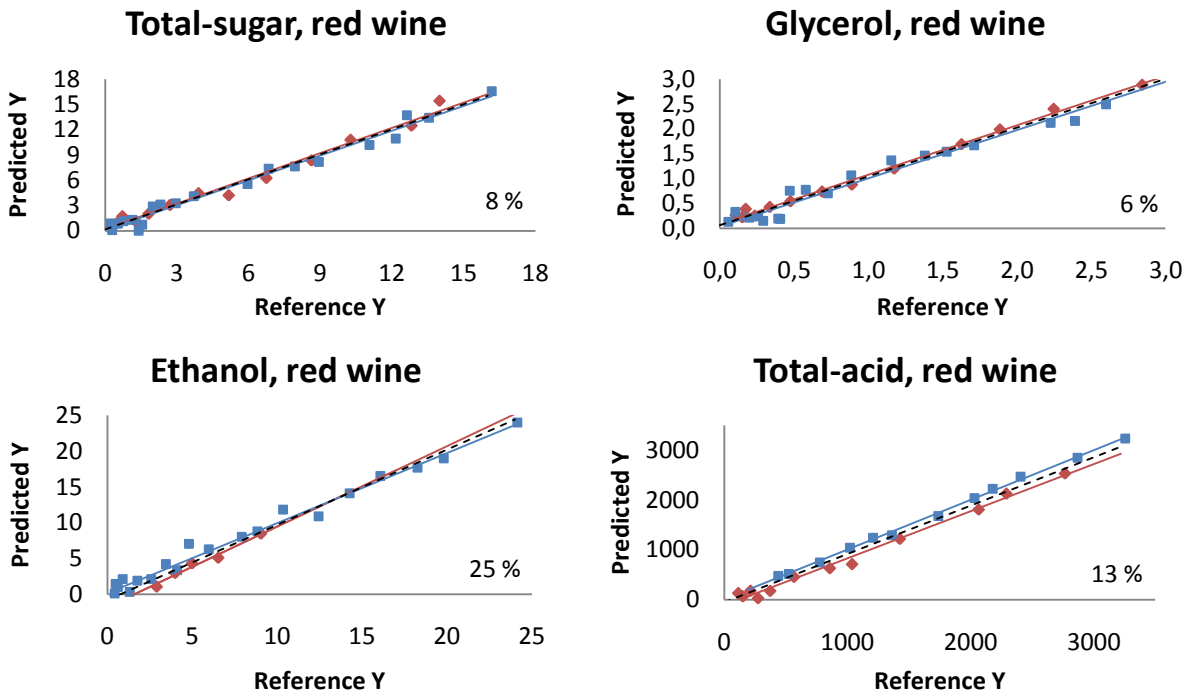

Figure 42 Predicted vs. measured for total-sugar [g/L], glycerol [g/L], ethanol [g/L], and total-acid [mg/L] in red wine. Blue: Calibration set, Red: Test set, Black: Mean between calibration and test set. The proportion of outliers is shown in the bottom right corner of the figures.

Table 21 Overview of the optimized models for total-sugar, glycerol, ethanol, and total-acid for red wine

	Slope	R^2	# PLS	RMSEP	relRMSEP	% outliers	Range
Total Sugar	1.00	0.979	2	0.659	9.76	8	0.48 - 14.0
Glycerol	0.993	0.987	1	0.099	7.27	6	0.11 - 2.84
Ethanol	1.12	0.891	1	1.27	31.9	25	1.08 - 9.04
				0.161			0.14 - 1.15
Total Acid	0.944	0.967	3	0.198	15.1	13	0.14 - 2.77

RMSEP: [g/L], relRMSEP: [%], range: sugars and glycerol: [g/L], acids: [mg/L], ethanol [g/L] (top) and [% vol.] (bottom)

The results for the modelling of total sugar and total acids showed that the models gave better results than when modelling the individual parameters. This may be due to inadequacy of the NIR equipment differentiating among the various components, since the components were similar in molecular structure and the absorption bands were overlapping. It may also be due to differences in the precision of the reference methods such as those seen for the acids. The models gave better results when modelling total parameters instead of the individual was seen in a previous study [6].

The most difficult parameters to model were glycerol and ethanol in the individual models, but this was as expected since the components are the most similar to H_2O in molecular structure and have absorption bands in almost the same regions of the NIR spectra. Another difficulty in modelling glycerol and ethanol is the reference analysis. It is the experience that it is difficult for the HPLC column to distinguish between glycerol and ethanol in rosé and red wine. This compared with the fact that the white wine is the simplest matrix, the models for white wine is simple, precise, and accurate. This is supported by the fact that the number of PLS components was increasing from the white to the red wine. The slope increases and the R^2 decreases from the white wine to the red wine. The RMSEP was the least in the white wine and so was the relative RMSEP.

Conclusion

It was possible in this feasibility study to obtain satisfactory individual prediction models for sucrose, glucose, fructose, glycerol, ethanol, citric, tartaric, malic, succinic, lactic, and acetic acid, and, perhaps of even higher direct importance for berry wine making, to obtain highly satisfactory models for *total sugar* and *total acid*, based on the short-wave NIR region (890 nm to 1690 nm). A conventional data analytical pre-treatment was needed for optimized models, full MSC was used for ethanol, while 1st derivative was used for all other parameters.

The accuracy and precision of these models all lie in the range 0.894 – 1.12 and 0.896 – 0.992, respectively. Absolute RMSEP lie in the range 0.100 – 0.692 g/L for sugars, 0.099 – 0.641 g/L for glycerol, 0.819 – 1.27 g/L for ethanol, and 0.0121 – 0.0869 g/L for acids. Of more general comparison value, the corresponding *relative RMSEP* lie in the range 6.3 – 20.1 %, the highest characterising ethanol. The number of PLS components used were maximum 4, and the proportion of outliers were in the range of 3 - 25 %.

Modelling results for *total sugar* and *total acid* (sum of all individual compounds analysed) signifies even better models, with accuracy and precision ranging 0.892 to 1.02 and 0.961 to 0.989, respectively. RMSEP for these models are in the range of 0.659 g/L to 1.57 g/L for total sugar and 0.0721 g/L to 0.199 g/L for total acid. The relative RMSEP span 7.3 % to 15 %. The number of PLS components used are here maximum 3, and the proportion of outliers are maximum 13 %.

It could be concluded that acceptable models to very good accuracy and precision could be obtained based on a relatively small feasibility data set; it was of critical importance that all results in this work were based on proper test set validation [46]. There were no reservations in claiming that the prospects for hand-held, robust NIR equipment were very good for routine process monitoring for key wine-making parameters in this small-scale berry winery. There is without doubt also a significant carrying-over potential to many other wine and must types as well, but this endeavour must be based on sound multivariate calibration practises. With raw materials of ever-varying composition and non-constant production site ambient temperatures, informed use of multivariate calibration and general chemometric competence is a must, at least as calibration goes. On the other hand, there were every reason to believe that it should be possible to establish a small set of calibration models for use for all types of personnel, also without chemometric training, due to the very user-friendly nature of the hand-held spectroscopic equipment employed.

Perspective

The need for further studies seem clear and may be identified with regard to both the evaluated parameters as well as the analytical equipment.

Expanding the Feasibility Study

This feasibility study was based on a minimum number of samples for the modelling campaign (10-14 levels to span 0 % to 100%), and it was therefore desirable to expand to use more samples in both the calibration and the test set. These additional samples should also be distributed over the entire range, but with a special focus on the high end of the range. It was also wanted to expand the concentration ranges, especially for ethanol, which is present in high(er) concentration after fermentation. By making dedicated models covering higher concentrations more comprehensively, it would be significantly easier with regard to sample preparation, since sample dilution would no longer be needed. This will ensure that the parameters present are measurable and detected.

Interference from High Concentration of Ethanol

When ethanol was present in high concentrations it was seen in a previous study [12] that ethanol had a large influence on the general spectra causing a significant interference when measuring other parameters. This was especially so when evaluating parameters of comparable molecular structure to ethanol. In the previous study this effect was evaluated when measuring malic acid. It was observed that when comparing the use of water and ethanol as alternative references, the spectra showed different shapes in the regions of importance for malic acid. When using ethanol as a reference the models for malic acid actually became both more accurate and more precise. Therefore it could also be of interest to evaluate the interference from ethanol on other parameters.

Additional Parameters

A suggestion for further studies may also be an evaluation of other parameters, such as sulphur, methanol, and other aroma compounds of importance to the quality of the wines. Also, pH and bacterial content may be of interest since this is of special importance to the wine's ability to change chemical composition both during production and storage. It might not be possible to have a monitoring of all wanted parameters by using a singular type of equipment however, but it is desirable to use as few as possible to keep expenses at a minimum. From the winery's perspective it was desirable to measure as many parameters as possible, so the expenses for external sample evaluation could be kept at a minimum.

Model Selectivity for Individual Parameters

The present models were based on diluting wines to obtain different concentration levels of the analyzed parameters. This was done to *simulate* the chemical changes during fermentation. This was of course only a simulation, the models may, or may not be completely identical in the real-world of fermentation monitoring, but this was expected to be of only minor importance for the accuracy of the models. Previously it had be found that models were robust to changes in chemical composition due to increasing values of one parameter. By standard addition of one single substance this addition could easily be detected of the model, and also the determination of the other parameters was not affected to a degree which was detectable [12]. This was highly promising in the present context.

Monitoring of Fermentation

Before, during, and after fermentation it was desirable to be able determine the concentration of the relevant set of parameters selected by the winery. This to ensure that the finished, bottled wine meets the absolute quality requirements set by the winemaker, and also to ensure that the wine was of as uniform quality as possible from one production to another.

Before fermentation it was highly desirable to be able to determine the concentration of sugars in the raw material, to make sure that only the necessary amount of sugar was added to the must to obtain the desired final ethanol content. This points to the interesting area of monitoring of both intermediates as well as final products as well as raw materials, all must be based on simple, robust and inexpensive NIR technologies.

During fermentation it was equally desirable to be able to monitor other parameters to detect problematic fermentations as early as possible. This would make the winemaker able to prevent stuck fermentations, which in the worst cases had to be discarded. Proper process monitoring would also allow that the concentration of ethanol was the same from one fermentation to another. In a previous study [47] was presented a detailed evaluation of these prospects, based on extensive chemometric calibrations with regards to both absolute time, relative time, and "biological process time" [47], which could serve as a direct continuation of the present work.

After fermentation it was sometimes necessary to add a minor, appropriate amount of various accepted *additives,* needed to ensure that taste, odour, and colour etc. were on the level with claims and expectations from one production to another. Since raw materials differ in composition, different end products in general will of course not need the same amount of additives to obtain the desired wine style etc.

Mixture of Wine Types

To make the ease-of-use of NIR prediction models even easier, it would be desirable if it would be possible to establish a (more-or-less) *universal* model, which would apply for *all* wine types. This would make monitoring very easy for untrained personal. It was surely to be expected however that this goal might not be obtainable in practise for the complete set of "all wines", but there would appear to be good prospects for certain problem-dependent broad, naturally constrained contexts (winery styles, red/white/rosé wine types etc.).

Previously it has been described that this might at times cause problems [11] but might also work out well [3]. Both these latter studies showed, that by including samples in the calibration and validation set from all relevant wine types for which the models are meant to be applied, good models could be obtained. This requirement was easily obtained in individual wineries, where only a relatively small number of wine types were produced. It could in principle be obtained in two ways; 1) by mixing wine types before spectral acquisition and reference measurements, or 2) by obtaining spectra and reference measurements on the individual wines, and samples, with the aim to include all of these in the same model. The first approach have not been evaluated, but the second gives good results for both similar wine types [11] and for different alcoholic beverages, such as beer, wine, and spirit drinks[3].

There are thus several challenging objectives in a small-scale winery where inexpensive, hand-held (or at-line) NIR spectroscopic equipment could be of significant use in the future.

Part 2 – Variographic analysis of standard procedures for industrial waste water characterization (TOS)

Sampling of Waste Water

The process of sampling waste water is of importance as to obtain routine operating data for the current treatment process, data to document the performance of a treatment operation, data in case of implementing proposed new treatment technique, and data to report regulatory compliance. The data from the analysis of the samples are the basis for implementing treatment facilities and programs; therefore, the sampling process has to be planned and executed in such a fashion that the samples obtained are representative for the composition of the waste water stream. Due to these reasons the sampling process has to be planned so the resulting data are [48]

- Representative: The data must represent the composition of the waste water.
- Reproducible: The data must be reproducible by others, when the same sampling and analytical protocols are followed.
- Verifiable: The data should be documented so proper validation of the sampling process is available with a known degree of accuracy and precision.
- Relevant: The sampling process should obtain data that meet the objectives of the monitoring scheme.

The sampling process should be well considered before any sampling is done and the process should be planned in a sampling protocol and documented in a Quality Assurance Project Plan (QAPP), which can also have the function as the requisition for the laboratory. The sampling protocol should contain information about the sampling plan, the sample types and size, and the sampling procedure. The QAPP should also contain information about sample labeling and chain of custody, storage and preservation, sample constituents, and the analytical methods employed. A well planned sampling process can be worthless if the chain of tasks from sampling to analysis and data is not properly described and documented. The same goes for the analytical results; which are worthless if the samples are not representative.

Problem Statement

The most important variation problems in a flow-weighted composite sample are listed below.

1. Does the uncertainty from sampling equipment and heterogeneity at the sampling point vary depending on the location of the sampling probe - horizontal and vertical direction, before and after weir?
2. Representativity across the sampling location – What is the bias when the sampling probe is located in the center of the stream when compared to the correct concentration of the waste water?
3. Which variations in the composite sample can be expected with regards to the equipment and its use?
    a. Location of the sampling probe - located in the center of the stream and ± 50 % of the distance to the borders (normal variations of the sampling point)
    b. Lift of samples to required height – a normal lift of sample unit is typically 1m – 3 m [49]

    c. Diameter of the sampler line from intake point to delivery point – min. 9 mm internal diameter [50]
    d. Intake liquid velocity – min 0.5 m/s [50]
    e. Location before and after a weir (see 1. above)
4. Is the content with regards to concentration in the first increments unchanged when the composite sample arrives at the laboratory for analysis?
5. What is the uncertainty when the composite sample is volume-reduced and sub-sampled in the laboratory to reach the required volume for analysis?
6. What is the uncertainty contribution to the volume of the increments from measuring of total volume of the stream with regards to the signal send to the sampler unit?
7. What is the uncertainty arising from variations in volume of each increments measured at the delivery point?
8. Representativity over time – Which variations in the composition of the composite sample are to be expected depending on the time of sampling?
    a. Time of day
    b. Day of week
9. What is the influence on uncertainty arising from the sampling frequency?

Guidelines for the Sampling Process

ISO and different departments work with waste water have given guidelines, which have to be followed to ensure reproducibility and regulatory and legal compliance. To help planning the sampling process, the Theory of Sampling (TOS) gives seven sampling unit operations, which guarantee representativity.

International Standard Organization

The ISO 5667-10 (Water quality – sampling) contains guidelines on the sampling process of domestic and industrial waste water. This includes the design of sampling process and techniques for extracting the samples.

With regards to the technique for automatic extracting samples the ISO 5667-10 set recommendations for principle and frequency of sample collection, performance and possible settings of the equipment. There are also recommendations for the sampling location depending on the structure of the facility. Examples are [50]

- Principle of sample collection
    - A chain pump
    - Compressed air and/or vacuum
    - Continuous stream of effluent, or
    - Pumping (often peristaltic pump)
- Frequency
    - Samples are to be taken at regular intervals during a certain period
    - Always use composite samples (only exception is when the parameter in question demands a spot-sample determination e.g. organic matter)
    - Number of increments are to be determined statistically, see ISO 2602, ISO 2854 and ISO 5667-1 (This is more precisely described in the guide from the Danish Environmental Protection Agency, see later)
    - The duration of sampling period depend on the parameters in question, but 24-hour samples are most often used

- Performance
  - Lift increments through the required height
  - Minimum number of parts exposed or submerged in the water
  - Minimum internal diameter of 9 mm of the suction hose
  - Minimum intake velocity of water of 0.5 m/s in the suction hose
  - Ability to purge suction hose before sampling to ensure fresh water in the increments
  - The precision and accuracy of increment volumes should be at least 5 % of the intended volume
- Settings
  - Possibility of taken time-weighted composite samples
  - Possibility of taken flow-weighted composite samples
  - Possibility of time interval between increments to be adjustable from 5 min to 1 hour
  - Provide storage of sample containers in the dark at 0 °C to 4 °C during the entire sampling period
- Sampling location at waste water treatment plants
  - High turbulent flow to ensure good mixing
  - Location downstream of a weir
  - Laminar flow should be restricted to induce turbulent flow by e.g. a weir
  - The sample intake should be located at least 3 times the pipe diameter downstream a restriction
  - The sample intake should preferably face the direction of the flow
  - Permanent sampling locations should be used whenever practicable
  - The sampling intake should be 1/3 of the effluent water depth below the surface of the water

Guidelines from the Danish Environmental Protection Agency

The guide "*Teknisk anvisning for punktkilder*" contains recommendations for monitoring discharge of waste water and is used to ensure the quality and comparability of the data collected. The recommendations are similar to those previously described for ISO 5667-10, but is more elaborated. As examples for further elaborations are listed the following [49]

- Sampling point
  - The suction hose should be fixed during sampling
  - The sampling intake should be placed in the center between the lowest water surface and the bottom of the reservoir
- Sampling equipment
  - The length of the sampling hose must not be above 3 m for the vertical part of the hose
  - Internal diameter of the suction hose shall be over 9.5 mm, though for outlet from waste water treatment facilities can an internal diameter down to 6.5 mm be used
  - The equipment should be able to lift the increments to a height of 4 m to 7 m, but it is not recommendable to lift the increments more than 1 m to 3 m
- Sampling frequency
  - There should be no more than 20 min between increments, but preferably no more than 10 min to 12 min between them

- Increment size
  - The increment size should be no less than 50 ml
  - The increment volume should be checked both at the start and the end of the sampling period
  - The deviation must be no more than 5 % compared to the preselected volume
- Velocity
  - The velocity in the suction hose should be between 0.4 m/s to 1.0 m/s
- Spot sample
  - A spot sample, if needed, should be five (equal in volume) increments extracted with a minimum of 2 min between and over no longer than 2 hours in total
  - The five increments are combined in the laboratory to a composite sample before analysis
- Discharge of samples
  - Overflow of storage container
  - Too few increments to ensure representativity
  - If the automated sample stops before or after 24 ± 2 hours
- When to sample and how many samples
  - The control period is one year and the sampling should be done equally over the entire period
  - Size of facility / sampling frequency per year
    - 30 PE < X < 200 PE / 2 samples
    - 200 PE < X < 1000 PE / 4 samples
    - X ≥ 1000 PE / 12 samples

Theory of Sampling

For the sampling procedure to be carried out in a representative manner thus ensuring a reliable analytical result, a detailed plan over each step is required. As help to determine the correct approach for obtaining a representative sample for analysis, there are seven sampling unit operations (SUO) as listed below. Each of them are described in more details in Appendix 2.

SUO 1. Always perform a heterogeneity characterization of new materials
SUO 2. Mix (homogenize) well before all further sampling steps
SUO 3. Use composite sampling instead of premature focus on the min. mass of the primary sample
SUO 4. Only use representative mass reduction
SUO 5. Comminution whenever necessary (reduction in grain size)
SUO 6. Perform variographic characterization of 1-D heterogeneity
SUO 7. Whenever possible turn 2-D and 3-D lots into 1-D equivalents

The first five SUO should always be used, not necessarily in this order, when sampling is done; depending on the situation a subset of the SUO's may suffice. SUO 6 and SUO 7 are only used when 1-D sampling is performed. When the sampling of a 1-D lot is made and the data is obtained, they are analyzed through a variographic analysis.

Variography

Variography is a heterogeneity characterization of the 1-D lot and is used to characterize the autocorrelation of 1-D lots as a function of the distance between extracted increments. Variography is also used for identifying ascending or decreasing trends and cycles in the process data. The variography is described in more details in Appendix 10.

When analysis of the experimental variogram is made the first approach is to identify the form and top level of the variogram (sill). This will provide valuable information on the process variation and the quality of the sampling process.

The next approach is to identify the nugget effect and the range of the process, see Figure 122. The nugget effect describes different aspects of the process variation of to what degree the incorrect sampling errors are included in the process variation.

After the variographic analysis is made with regards to the variogram it is possible to make an estimation of the total sampling error.

Short-term Variogram vs. Long-term Variogram

A "24-hour" sample was a composite sample of increments acquired over a period of 24 hour. The resolution difference between increments and 24-hour samples is shown in Figure 43. The time interval for increments was much smaller than that for the 24-hour samples.

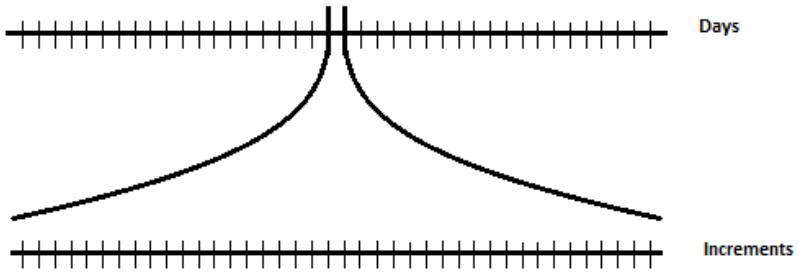

Figure 43 Diagram showing the time resolution differences between 24-hours samples and increments

The short-term variogram for increments are not comparable to the long-term variogram for 24-hour composite samples, since the samples are of two different types. The increments are so-called grab-samples with a volume of approx 50 ml and the 24-hour composite samples are many increments combined to a composite sample of 5 L to 10 L.

Total Sampling Error

The total sampling error (TSE) in TOS is split into seven error components, which characterize the material and the sampling procedure.

- FSE: Fundamental Sampling Errors
- GSE: Grouping and Segregation Errors
- ISE: Incorrect Sampling Errors
    - IDE: Incorrect Delimitation Errors
    - IEE: Incorrect Extraction Errors
    - IPE: Incorrect Preparation Errors
- TFE: Time Fluctuation Errors
- CFE: Cyclic Fluctuation Errors

FSE and GSE are always present and are material specific. The sum of the two is the Minimal Practical Error (MPE) for stationary lots (0-D, 2-D, 3-D). The variance of the MPE (s^2_{MPE}) is equal to the nugget effect in the variogram for dynamic lots (1-D). The ISE can in principle all be eliminated from the sampling procedure, which may, or may not be an easy task. They must, however, always be

minimized as much as possible. TFE and CFE are only present in 1-D sampling. When discussing TSE for a variographic experiments it is the sum of all seven errors.

$$s_{TSE} = \sqrt{s_{FSE}^2 + s_{GSE}^2 + s_{IDE}^2 + s_{IEE}^2 + s_{IPE}^2 + s_{TFE}^2 + s_{CFE}^2}$$

With regards to TSE, different combinations of lag (j) and number of increments (Q) are evaluated. The TSE is, therefore, the variance of the result for a particular combination of j and Q.

In practice when the variogram is calculated and the TSE is simulated, they are based upon one set of samples extracted in one run. The different combinations of increments or 24-hour samples are only a simulation based on the one dataset and not a new dataset for each combination.

Danish Baseline Investigation of Sampling Uncertainty

In 2005 a pilot survey was conducted using TOS and variographic analysis to estimate the uncertainties with regards to sampling [51, 52]. The purpose of the survey was to conclude whether or not a variographic experiment could be used to estimate the uncertainty from sampling increments. The survey should also quantify the uncertainty, when state-of-the-art procedures and TOS was implemented. In the survey four waste water facilities contributed with samples from both the influx and the outlet. The construction of the sampling sites are different, but the sampling equipment is of the same type and automatic sampling is used in all sites. The increments collected were analyzed for conductivity and Total Phosphorous (TP)[51]. The increments in the pilot survey were extracted automatically with a interval of 2.5 min over a total interval of 60 min.

With regards to the variograms for measuring conductivity, only one of the sites (Mejlby, 2007) showed results which fluctuates, so it was possible to make a reliable variogram. Overall the number of samples and time interval in the survey was too small to give a reliable base for estimation of the uncertainty to sampling rising from the variations in composition of the waste water. The results for conductivity from the outlet are shown in Table 22.

Table 22 Conductivity. Estimation of variance in outlet over a short interval of time.[51]

Conductivity	Variance – mass reduction, pretreatment and analysis $CV_{analysis}$ [%]	Variography from sampling each 2 min – 24 samples		Variance – material and sampling	Mean [mS/m]
		V(0)	CV(0) [%]	$CV_{sampling}$ [%]	
Lynetten, serie A	0.2	0.00000024	0.05	n.s.	358
Lynetten, serie B		0.00000074	0.09	n.s.	361
Karup		0.00000154	0.12	n.s.	50.6
Mejlby 2006		0.00000019	0.04	n.s.	66.0
Mejlby 2007		0.00000637	0.25	0.15	65.5

n.s.: not significant

From the table it is seen that uncertainty arising from the material heterogeneity and sampling ($CV_{sampling}$) for most cases was insignificant, only at one site it was found significant. This site was the only one, which gave a reliable variogram. The analytical uncertainty ($CV_{analysis}$) was found to be

0.2 %. The nugget effects were found to be $6.37 \cdot 10^{-6}$ which gave that the uncertainty was 0.25 %. These uncertainties showed that the uncertainty from sampling of one increment was in the same range as the analytical uncertainty.

With regards to the variograms for measuring TP, all the sites showed a tendency to changes in the composition of the waste water, but no significant tendency to cyclic variations. The results for TP from the outlet are shown in Table 23.

Table 23 TP. Estimation of variance in the outlet over a short time interval [51]

TP	Variance – mass reduction, pretreatment and analysis $CV_{analysis}$ [%]	Variography from sampling each 2 min – 24 samples		Variance – material and sampling	Mean [mg/L]
		V(0)	CV(0) [%]	$CV_{sampling}$ [%]	
Lynetten, serie A	3.6	0.00121	3.47	n.s.	0.219
Lynetten, serie B		0.00125	3.53	n.s.	0.207
Karup		0.00117	3.41	n.s.	0.444
Mejlby 2006		0.00517	7.19	6.2	0.225
Mejlby 2007		0.00140	3.74	1.0	0.121

n.s.: not significant

From the table it is seen that uncertainty arising from the material heterogeneity and sampling ($CV_{sampling}$) was for most cases insignificant, only at two sites was it found to be significant. The analytical uncertainty ($CV_{analysis}$) was found to be 3.6 %. The nugget effect is found to be below $5.17 \cdot 10^{-3}$ which gives that the uncertainty was below 7.19 %. This showed that the uncertainty from the sampling of one increment for most of the sites was in the same range as the analytical uncertainty.

One contribution to the sampling uncertainty, which was not taken into account in this survey, was the uncertainty arising from the variations in the composition of waste water over time depending on the flow. This was because the sampling was done proportional to time instead of flow. Whether this would provide a large contribution or not to the uncertainty arising from sampling is not known. Theoretically the uncertainty would increase when the flow increases and the time interval is kept constant. This was seen in the case of Mejlby, where the flow in 2006 was much higher than in 2007 as was the uncertainty and the nugget effect. The increase in uncertainty was due to the increasing amount of water passing the sampling point between extracting two increments; therefore, small variations in the water composition may not be found.

The conclusion to this pilot survey was that in regards to both conductivity and TP the uncertainty contributions from sampling was not significant, which confers that the material heterogeneity was modest and the sampling process was acceptable.

The nugget effect in the Danish baseline survey [51] was estimated through a geomathematical approach. The approach was calculated as a linear regression through N/2 points (N = number of increments), as a robust estimation or as a generalized additive model [53]. Both approaches were based on fitting a mathematical function to the variogram which consist of descrete points. This gave an error when dimension of non-integer was used, since this does not exist in nature. A more

practical approach to determine V(0) is to draw a line by-hand or use up to the first five points only (from TOS) and draw a line between them. The nugget effect is then described as the point of intersection with the y-axis of the variogram. This approach will give a much more reliable estimation of V(0) (the nugget effect). This TOS-approach will give the results shown in Table 24 along with the results measured in the previous study. The related variograms are shown in Appendix 11.

Table 24 TP. Estimation of variance in the outlet over a short time interval by TOS and by the technique from IMM [53]

TP	$CV_{analysis}$ [%]	TOS			IMM		
		V(0)	CV(0) [%]	$CV_{sampling}$ [%]	V(0)	CV(0) [%]	$CV_{sampling}$ [%]
Lynetten, serie A	3.6	0.00042	2.05	n.s.	0.00121	3.47	n.s.
Lynetten, serie B		0.00187	4.32	2.40	0.00125	3.53	n.s.
Karup		0.00119	3.45	n.s.	0.00117	3.41	n.s.
Mejlby 2006		0.00346	5.88	4.65	0.00517	7.19	6.2
Mejlby 2007		0.00119	3.45	1.45	0.00140	3.74	1.0

It is seen from the table that the V(0) found through the TOS-method of drawing a line through the first up to five points gives a smaller value than those calculated by IMM, except for Lynetten, serie B. These values, calculated by the software "Vario", gives a more realistic picture of the variance relationships when the distance between the extracted increments approaches zero, see the variograms in Appendix 11. For conductivity it is not possible to derive a reliable variogram based upon the data from the previously study since there is no real variation in the data.

A literature study [54], a prestudy to the above Danish baseline study [51], found a significantly different percentage for the uncertainty contribution in the sampling process of waste water. The parameters examined in this study were SS (suspended solids), COD (chemical oxygen demand), BOD (biochemical oxygen demand), Total-N, and Total-P. The results are shown in Table 25. From the table it can be seen that the expected uncertainty contributions are found in the range of 24 % to 48 % for these analytes (the square root of the sum of the squares of each uncertainty contribution for each analyte). The large difference when compared to the found result might be because the contribution from systematic errors was estimated with 24-hour samples in mind and not increments which was the sample type used in the study.

Table 25 Quantification of the systematic errors in some parts of the automatic sampling process [53]

Source of Error	SS	COD	BOD	Total-N	Total-P
Strategy of Sampling					
Flow vs. time proportional sampling	10 % to 15 %				
Choice of increment volume	10 % to 30 %				
Too low sampling frequency	4 %				
Sampling Location					
Bad mixing	5 %				
Sampling Equipment					
Length of suction hose	14 %				1 %
Diameter of suction hose	15 %				5 %
Placement of suction hose with regards to the direction of water stream	15 %	5 %	-	5 %	3 %
Too low suction velocity	19 %				13 %
Cleaning of suction hose during sampling	1.5 %				
Measurement of volume of increment	2 %				
Measurement of flow velocity	5 %				
Surroundings					
Temperature during sampling (25 °C)	10 %				
Temperature during sampling (4 °C)	< 5 %				

Thesis Problem

The purpose with the second part of the project was to evaluate the uncertainty contribution from sampling, when this is applied to waste water. The thesis problem is as follows:

"How large is the uncertainty contribution from sampling, when standard procedures is applied to sampling of waste water?"

The objective of the present project was to use variographic analysis to determine the uncertainty in the sampling of waste water. The present project tries to provide a reliable answer to all objective items listed in the previous problem statement, except items 3b, 3c, 3d, and 6. This was done by analysis of both incremental samples and 24-hour composite samples from one waste water treatment facility.

Experimental Setup

The project consists of three main experiments, and one minor experiment. All of the experiments took place at Bramming Waste Water Treatment Plant North. A picture of the outlet of the waste water is shown in Picture 10. The outlet consist of: a water reservoir before the weir where the water is flowing in from the bottom, a weir, and an oxygenation step before the water is led through a pipe to a nearby stream.

Picture 10 Outlet of waste water stream

From Bramming Waste Water Treatment Plant North there is an outlet flow of approximately 1000 m^3 waste water per day [55]. Usually sampling is conducted with 10 m^3 between extractions of increments to the 24-hour composite sample. The flow is measured with a V-weir as shown in Picture 10 and level measurement by a stationary ultrasound meter.

The parameters that were used to characterize the waste water stream system were total phosphorus (TP), conductivity, and ammonium (as NH_4-N). The conductivity is a measure of all dissolved compounds while the total phosphorus is a measure of compounds connected to suspended matter. Both parameters are considered to be stable (degradation during storage for a limited time period are not expected to be occurring), so they were analyzed in the laboratory in both the composite samples and increments. Ammonium is a parameter that is considered to be unstable (degradation during storage for a limited time period may occur), so this is only analyzed in main experiment 2, where each increment sampled over a time period of 24 hours is analyzed directly in the field.

Quality Control and Test for Analytical Uncertainty

Total Phosphorous

The analytical uncertainty for TP was examined by analyzing one sample or a control sample several times and then comparing the results. The results are shown in Appendix 12.

The quality control for TP was performed by analyzing the control samples first, last, and for each 20 real samples in each series. Each control sample should be analyzed in duplicate. When using the samples from one composite sample the results should be within the acceptable analytical uncertainty since TP is considered to be a stable parameter, which do not change during storage of the samples. By analyzing the same sample several time during the experiment both the repeatability and long term variations are monitored.

Conductivity

The analytical uncertainty and quality control for conductivity was done in the same way as for TP. The results are shown in Appendix 12.

Ammonium

To prevent mistakes in the field, the kit for measuring ammonium, should be well known and tested of all the persons involved (both for ease of use and analytical uncertainty). Ease of use was tested by analyzing samples before the experiments were conducted to get well acquainted with the kit. The analytical uncertainty of the kit and use by the persons involved in the practical part of the analysis was tested by analyzing the same sample several times and comparing the results. The results are shown in Appendix 12. The quality control of the kit was conducted by analyzing a synthetic sample with a known concentration at the beginning and the end of the experiment, and also in between for each 20 samples. A synthetic and stable sample was used for quality control since it is the possible degradation of the ammonium in the increments that were investigated.

Volume

Before each sampling starts, the volume of increments should be checked five times to ensure that the increment volume does not differ more than ± 5 % [50]. The volume of each increment should be 50 ml. The results for uncertainty contribution from the volume variation in the increments are shown in Appendix 13.

Main Experiment 1 – The Importance of the Sampling Point

This experiment covers objective item 2, 3a, and 3e and was planned to take place both before and after the V-weir in the waste water stream. The experiment was conducted as follows:

Three sampling units were placed before the weir in the stream at center, and right and left of center. The right and left sampling point represents the extremes of possible locations of sampling points. The distance to the weir was 30 cm. The vertical position of the sampling points was in the stream just below the weir and low enough so they were always covered with waste water.

One extra sampling unit was placed verticaly by the centre sampling point and below the weir. This was done in order to see if any damming took place before the weir. The vertical distance between these two centre sampling points was 30 cm.

After the weir another three sampling units were placed in the stream at centre, and again right and left of centre. The centre was the sampling point required according to DS/ISO 5667-10 [50] and "*Teknisk anvisning til punktkilder"* [49]. The sampling unit was placed in the stream where there was the most turbulence, in practice this will be straight before the water passes the oxygenations steps, see picture 1. Before placement of sampling units and regularly during the experiments the reservoir should be cleaned from sediments to avoid clotting of the hoses and sampling units.

From the seven sampling units composite samples from a time period of 24 hours (± 2 hours [50]) were collected over a 39 day period and from the data a variographic analysis was conducted. Each day the container was replaced and the sampling unit was adjusted with regards to the expected amount of rain.

This pilot survey will show any variations of composition in the waste water stream when the sample is taken right in the center of the stream, right and left of the centre, and top or bottom of the stream (Item no. 3a and 2), because of the very powerful variographic data analysis.

When the pilot survey was conducted both before and after the weir, it will also testify as to whether or not this factor is of importance to the location of sampling point (Item no. 3e).

When the samples are compared over a 39 day period they will reveal if the day of sampling is of importance to the composition of the sample (Item 8b).

Main Experiment 2 - Variographic Analysis of Waste Water After the Weir

This experiment covered objective items no. 1, 4, 7, 8a, and 9 when the sampling was done after the weir. The experiment was as follows:

Two sampling units were placed, so the sampling points were as close as acceptable and the delivery point was placed in the same height above the waste water stream. The experiment was conducted over two 24 hour periods. From the one sampling unit two composite samples were collected for each a time period of 24 hours with at least six increments per hour according to DS/ISO 5667-10. From the second sampling unit increments were collected with the same interval as for the first sampling unit, but each increment from the second sampling unit was analyzed separately (taking on the role as individual so-called grab-samples (see Appendix 2).

In the first 24 hours each increment was analyzed in the field for ammonium. Before sending the composite sample from the first sampling unit to the laboratory, it was also analyzed for ammonium using the same technique. By comparing the mean of all the increments with the results from the composite sample, it would give indications to if any decomposition might have happened in the first increments during extraction of a composite sample (Item no. 4). The container for the composite sample from the first sampling unit were fitted with a temperature logger as were the container for the increments from the second sampling unit.

In the second 24 hours, the containers, used for storage of increments, were weighed before and after they were used to collect the increments. This could be done either in the laboratory or in the field. By doing this in the second 24 hours, no volume would be lost due to analysis of ammonium (Item no. 7).

When all increments for the total 48 hours were analyzed for conductivity and total phosphorus, the data were also here subjected to variographic evaluation. This would give indications of the heterogeneity at the sampling point, uncertainty for the sampling unit (Item no. 1), and the importance of frequency of extracting increments for the composite sample (Item no. 9). By analyzing the increments from a period of 48 hours it would also be possible to see if the start time of sampling (composite sample for a period of 24 hours) had influence on the composition of the composite sample (Item no. 8a).

Main Experiment 3 – Variographic Analysis of Waste Water Before the Weir

This experiment covered item no. 1 and 9 when the sampling was done before weir. The experiment was broadly identical to main experiment 1:

Two sampling units were placed, so the sampling points were as close as acceptable and the delivery point was placed in the same height above the waste water stream. From the one sampling unit a composite sample was collected over a period of 24 hours with at least six increments per hour according to DS/ISO 5667-10. From the second sampling unit similar increments were collected with the same interval as for the first sampling unit, but here each increment was analyzed separately. The sampling frequency for the two sampling units should be the same to ensure complete comparability. Before placement of sampling units and regularly during the experiments the reservoir should be cleaned from sediments to avoid clotting of the hoses and sampling units.

When all increments were analyzed, the increment series data were subjected to variographic analysis in order to describe the variability of the composition of the waste water stream. This were to see if sampling before a weir gave rise to higher sampling uncertainty compared to sampling after a weir (which was described in DS/ISO 5667-10 to be the correct sampling location). This would give indications of the intrinsic heterogeneity at the sampling point, a breakdown of the uncertainty for the sampling unit (Item no. 1), and the importance of the frequency of extracting increments for the composite sample (Item no. 9).

Minor Experiment 1 – Volume Reduction and Sub-sampling

This experiment covered item no. 5, and can be done with any composite sample from a time period of 24 hours. The experiment was as follows:

Shake the composite sample well. Replicate taking at least 10 sub-samples of the required amount of volume for the analysis (This is the current procedure in the laboratory). Analyze each for the different parameters selected in the experimental plan.

Calculate the mean value, the standard deviation and the derived "Relative Sampling Variance" (RSV).

$$RSV = \frac{STD}{\bar{x}} \cdot 100$$

If the RSV is acceptable (less than 5 %) [56], the sub-sampling technique is adequate. If the RSV is higher than acceptable, optimization of the current volume reduction technique must be carried out according to the principles in Theory of Sampling (TOS).

Optimization of the volume reduction can be done by shaking the composite sample well and using a problem-dependent version of the "riffle-splitter" principle (in the so-called "bed blending" modus), see Figure 44. In this way the volume can be representatively reduced into several sub-samples.

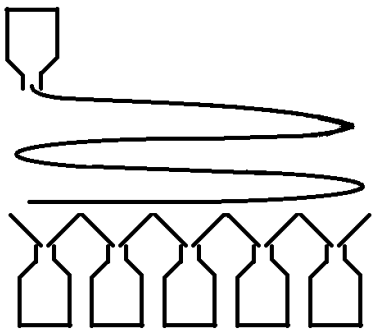

Figure 44 Bed blending "Riffle-splitter" principle for volume reducing liquid samples

By repeating this on randomly selected sub-samples to end up with sub-sub-sub-samples until the required volume is obtained, the final volume for analysis should be as representative as possible.

The data for volume reduction will be compared statistically.

Weather Conditions During Sampling Period

During the sampling period the rainfall period was unusually high for the season. Precipitation for each day is shown in Figure 45. The national average was 126 mm through November 2009, 47 mm higher than the meteorological normal. November 2009 ranks as the 4th highest month in rainfall since 1874. Southern Denmark received the most rain with 154 mm compared to the normal 98 mm for the region [57]. In total, it rained on 27 days in November; in the sampling period there were only 8 days without rain. This extraordinary amount of rain had a definite influence of the results, which will be described in the discussion of the data obtained.

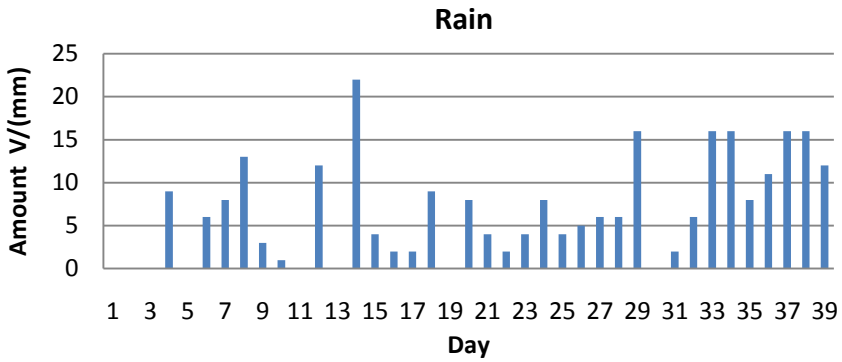

Figure 45 Daily precipitation in the sampling period. Data not available for the first three days

In the 48 hours o f incremental sampling it started raining after approx 15 hour. Therefore only increments from the first 15 hours were used in the variographic evaluation.

Sampling Procedure

Sampling Points

Figure 46 shows an overview of the sampling setup and a schematic overview of the sampling locations. Sampling points D, A, and B are positioned before the weir, while points E, F, and G are located after the weir. Sampling point C is co-located with point A, but positioned 30 cm lower.

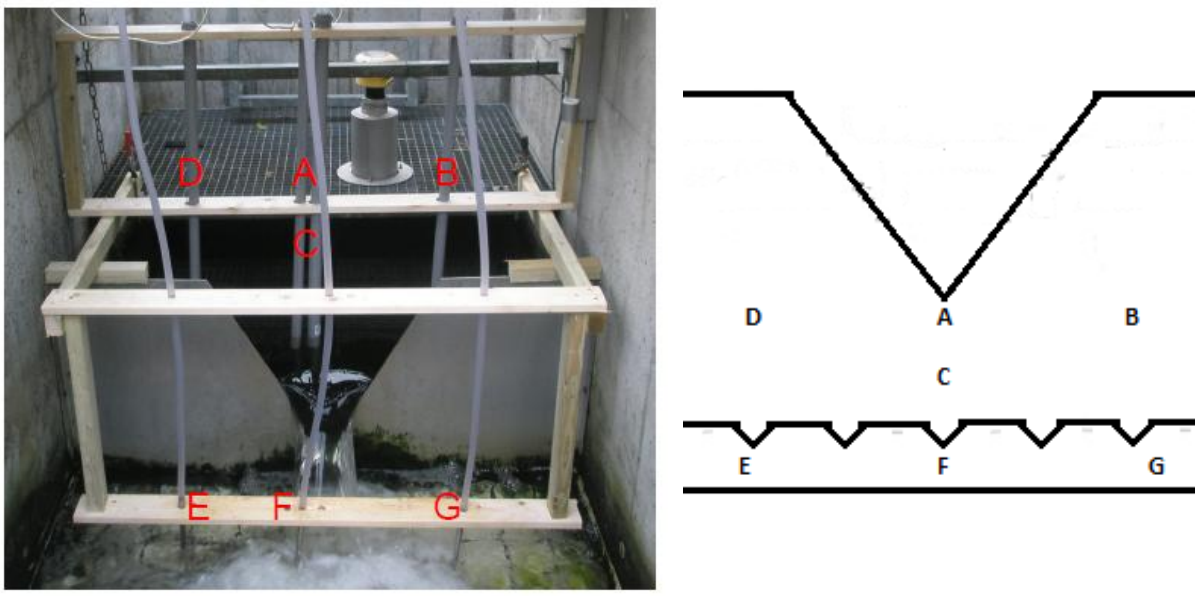

Figure 46 Photographic (left) and schematic overview (right) of the sampling station

The height from the sample intake to the measuring chamber (equals the length of suction hose) was 2.15 m for F, E and G. It was 2.20 m for A, D and B. It was 2.50 m for C. The distance from A, D and B to the V-weir plate was 30 cm and the distance from F, E and G to the V-weir plate was 35 cm. The distances A - D, A - B, F – E, and F - G were 35 cm. The sample intake for A was placed 5 cm below the V-weir and C was placed 30 cm lower. The water level at the sample intakes for F, E, and G was approximately 10 cm and intakes were placed 5 cm from the bottom.

The influx to the reservoir before the weir was located beneath point D opposite sampling point B. At both points the water appears stagnant at the surface. Point A was located just upstream of the weir and the velocity on the surface seemed higher here compared to points D and B. At Point F, located just after the weir, the velocity and turbulence in the water was at maximum. Point E and G were situated after the weir respectively left and right of point F. The turbulence was a little less here than at point F. At low velocity the water at points E and G seemed almost stagnant, but at high(er) velocities the conditions were more similar to that at point F.

When the central control system of the facility measuring a passing of 1 m^3 water it sent a signal to the automated sampling equipment in sampling point A. Each time the equipment received seven signals it began to sample, and at the same time it sent a signal further to the other sampling points. From A it went to C. From here the signal went to D, then E, then F, and finally it split up and ended at B and G. Thus, all sampling equipment samples simultaneously.

Sampling Cycle

An overview of the sampling cycle is shown in Figure 47. The sampling cycle starts by purging the sampling hose to remove any remaining still standing water from earlier sampling suctions (1). Then the water is pulled up by vacuum from the sampling point to the measuring chamber (2). When the chamber is full, suction stops and is reversed. Then excess water is discarded until the selected volume of water is reached in the chamber (3). The last step is discharge of sample from the measuring chamber to the storage container (4). A video of the sampling cycle can be seen on the enclosed CD-rom.

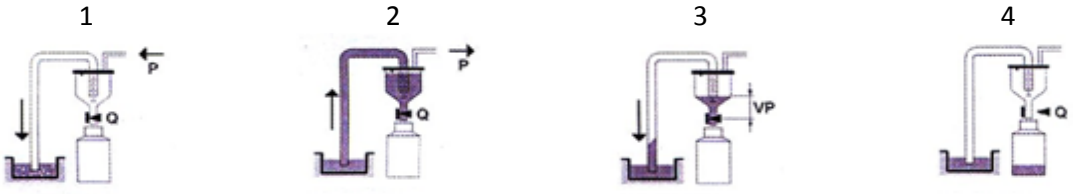

Figure 47 Sampling cycle for vacuum sampling unit [49]

Sampling Scheme

From all sampling points 24-hours composite samples were extracted and analyzed with regards to total phosphorus (TP) and conductivity. The 24-hours samples were extracted with a time interval of 24 hours ± 2 hours [50]. Increments were extracted from sampling point F over a period of 48 hours and from sampling point A over a period of 24 hours. The increments were also analyzed for TP and conductivity. The increments from sampling point F were in the first 24 hours also analyzed for ammonium-nitrogen (NH_4-N). Increments were collected for every 7 m^3 giving a time interval between extracting increments from 3 min to 12 min depending on the flow velocity of the waste water stream. The sampling scheme is listed in Table 26.

Table 26 Sampling scheme for the parameters TP, conductivity and NH_4-N

Parameter	Sample type	Sampling point	Time between samples
TP	Increments	A + F	3 min to 12 min (7 m^3)
	24-hour	A, B, C, D, E, F, G	24 ± 2 hours
Conductivity	Increments	A + F	3 min to 12 min (7 m^3)
	24-hour	A, B, C, D, E, F, G	24 ± 2 hours
NH_4-N	Increments	F	3 min to 12 min (7 m^3)
	24-hour	F	24 ± 2 hours

Experiment to Validate Representative Volume Reduction

An experimental approach to determine if the techniques used for volume reduction of the 24-hour samples (and increments) were representative was performed as minor experiment 1. This was done to see if 1) the technique for volume reduction used was satisfactory and 2) to determine the uncertainty contribution from the volume reduction. The experiment was done at Eurofins Environment A/S and at Esbjerg Institute of Technology, Aalborg University (EIT AAU), since both laboratories were involved in the analysis of the increments and the 24-hours samples.

The volume reduction was performed at Eurofins Environment A/S by placing a hose in the storage container and then connecting the hose to a pump to ensure good mixing of the sample. From the container a sub-sample was extracted. In the analytical apparatus a further aliquot was extracted, which underwent the relevant pre-treatment and was analyzed for the content of TP. This step was repeated 12 times and the samples were analyzed in duplicate.

At EIT AAU the volume reduction was performed by shaking the storage container several times and then extracting 100 ml into a sub-sample container. The sub-sample was shaken well and a second sub-sub-sample of 15 ml was extracted, which underwent pre-treatment. From this pre-treated sub-sample an aliquot of 400 µl was analyzed for the content of TP. This was repeated 10 times and the samples were analyzed in duplicate. The sub-samples were also analyzed for conductivity.

The measurements from the experiments for volume reduction are shown in Appendix 14. In Table 27 the results for mean value, standard deviation, and the derived "relative sampling variance" (RSV) are listed.

Table 27 Mean value, standard deviation and RSV for TP and conductivity

	Eurofins TP		EIT AAU TP		EIT AAU Conductivity	
Mean value	196.182	µg/L	143.487	µg/L	291	µS/cm
Standard deviation	2.693	µg/L	6.558	µg/L	3.77	µS/cm
RSV	1.37	%	4.57	%	1.30	%

For both Eurofins Environment A/S and EIT AAU the RSV were below 5 %, which states that the techniques for volume reduction was acceptable and that no further optimization of the techniques were needed [56]. Additionally, it shows that the uncertainty from the volume reduction (including the analytical uncertainty) does not contribute with more than 4.57 % to the global estimation error for TP and 1.30 % for conductivity.

Total Phosphorous in Increments

The sampling points used for the analysis of increments were sampling point F and A. These points were chosen because F was the correct sampling point according to ISO 5667-10 and A was the point used commonly. First sampling point F is discussed, than sampling point A, and afterwards the two sampling points are compared. The data for TP in increments are listed in Appendix 15.

Variografic Analysis of Total Phosphorous in Increments

The increments were taken with a flow-distance of 7 m^3, which for the shortest time interval was approximately 3 min and for the longest time interval was approximately 12 min. For data processing, increments were analyzed for the first 15 hours before the heavy rain came down.

Sampling Point F

The analytical concentration measurements for sampling point F are shown in Figure 48. The blue curve is the original measurement and the red curve is an interpolation after the dataset was corrected for missing data and possible outliers (due to errors in the sampling process, which are listed and discussed later). There was a small trend to increasing concentrations over the period.

To calculate the experimental variogram the analytical concentration had to be corrected for missing data. This was done by replacing missing data by a mean value of the immediately adjacent measurements on either side. A linear regression was applied to the data and the mean trend values for all measurements were calculated to be used for “de-trending”. The de-trended data are shown in Figure 49 (Note the difference in scale between the two figures). The resulting time series was calculated and imported into the program “Vario”, which can be downloaded from www.acabs.dk. This de-trended data series forms the basis for the experimental variogram, which is shown in Figure 50.

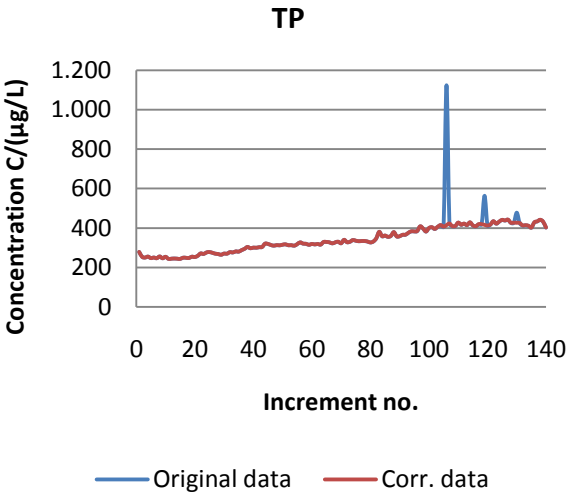

Figure 48 TP analytical concentration development in increments at sampling point F

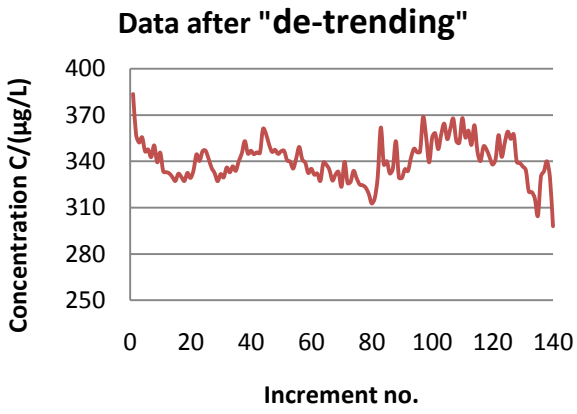

Figure 49 TP analytical concentration in increments after "de-trending" at sampling point F. Excluded points are no. 106, 119, and 130.

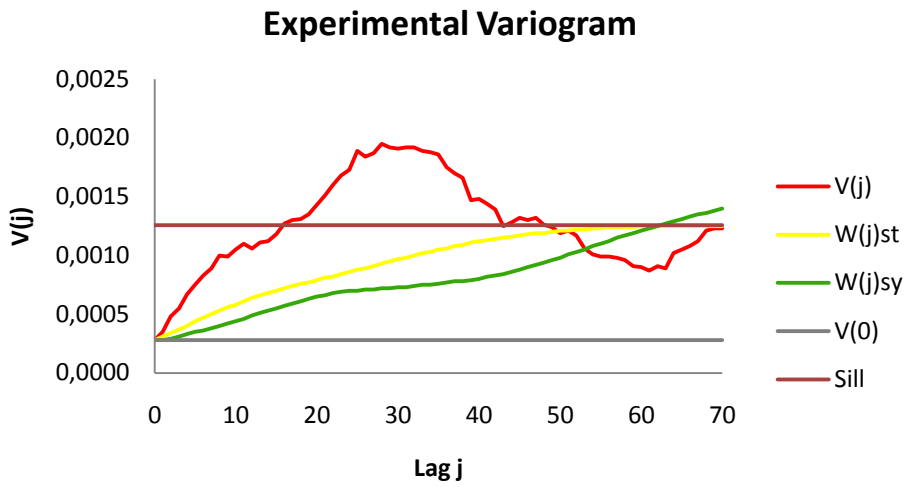

Figure 50 Experimental variogram and auxiliary functions for increments in sampling point F. Data series F was subjected to linear de-trending before variogram calculation.

In Figure 50 the red curve is the variogram, and the yellow and green curves are auxiliary functions. The yellow curve is the error generating function of the stratified random sampling and the green curve is the error generating function for systematic sampling.

From the variogram, see Figure 50, a cyclic variation with period of j = 60 (= 420 m^3) was indicated, but more increments must be analyzed to confirm this (see further below).

The volume of waste water and the concentrations of matter varied during the day and night. The amount of water and concentration of matter was highest during the day [58]. This was expected to be seen from the analytical concentrations, but this is not clear from Figure 48; however it is more significant in the variogram, where a cycle is seen for lag of 420 m^3. Usually the waste water facility treats 1000 m^3 per day [55]. Less water is used during the night than during the day and the sampling period started during the day, when water from the night was discharged. The cyclic variation could be explained by the variation in the water composition over 24 hours.

Sampling Point A

The analytical concentration measurements for sampling point A are shown in Figure 51. The blue curve is the original measurement and the red curve is an interpolation after the dataset was corrected for missing data and possible outliers. There is a trend of increasing concentrations over the period.

After “de-trending” the time series was calculated, see Figure 52, and then used for the basis for the experimental variogram shown in Figure 53.

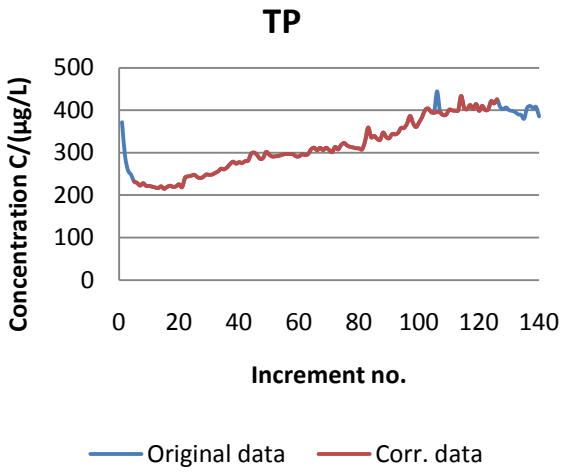

Figure 51 TP analytical concentration development in increments at sampling point A

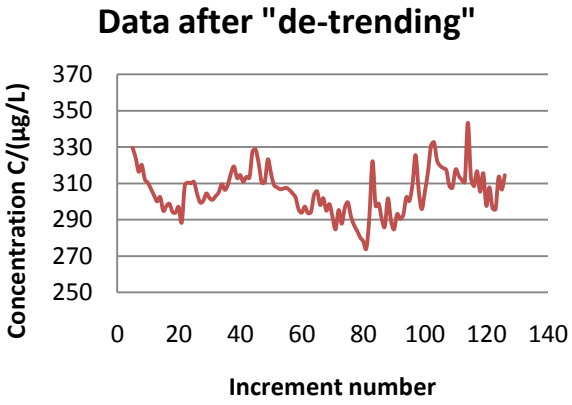

Figure 52 TP analytical concentration in increments after "de-trending" at sampling point A. Excluded points are 1-4, 106, and 127-140.

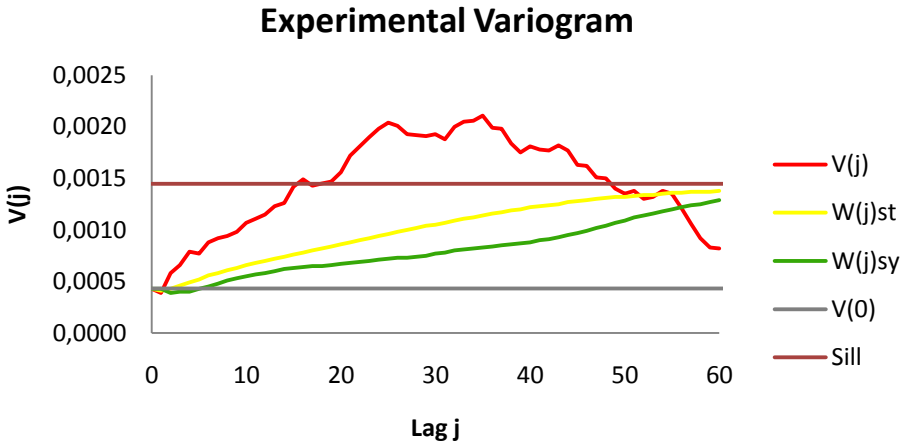

Figure 53 Experimental variogram and auxiliary functions for increments in sampling point A. Data series A was subjected to linear de-trending before variogram calculation.

From the variogram, a cyclic variation with period of j = 60 (= 420 m^3) was again observed, see Figure 10. This could again be explained by the variation from over 24 hours.

Nugget Effect and Sill for Total Phosphorous in Increments

The nugget effect, sill, and relative proportions for sampling point F and A are listed in Table 28.

Table 28 Nugget effect, sill level and relative proportions for increments from sampling points F and A

Sampling Point	V(0)	Sill	V(0)/Sill [%]
F	0.00028	0.0013	22
A	0.00043	0.0015	30

The nugget effect for sampling point F amounted to 0.00028 and the sill was 0.00136; therefore, the total 0-D sampling variation corresponded to 22 % of the total process variability.

The nugget effect for sampling point A amounted to 0.00043 and the sill was 0.0015; therefore the total 0-D sampling variation corresponded to 30 % of the total process variability.

Comparing the results for sampling point F to those for sampling point A, gives that sampling point F had the smallest nugget effect and process variability, yet the differences were small. From this it was seen that sampling point F was slightly more suitable than sampling point A, which confirm that the structure and composition of sampling point F was better than that of sampling point A.

Total Sampling Error for Total Phosphorous in Increments

The TSE estimates for sampling point F and A are shown in Figure 54 and Figure 55, respectively. N.B. Due to the programmers labs, the TSE calculated in Vario and shown on top of the bars in the figures is equal to $3 \cdot s_{TSE}$. Therefore all values in figures for TSE were divided with a factor three before they were used in the evaluation of TSE.

Sampling Point F

The smallest TSE for the measuring of TP in sampling point F was found for j = 1 and Q = 96, where the TSE was equal to 0.17 %, see Figure 54. For j = 1 and Q = 1 the TSE was 1.7 %. Thus, the standard deviation for the result of measuring each increment is 1.7 %. When extracting a composite sample with more than 96 increments the TSE estimation was in the same range for j = 1 to j = 6. This gives that the standard deviation to the average result of measuring 96 increments (combined to a composite sample) extracted with 7 m^3 between each increment (j = 1) or with 42 m^3 between each increment (j = 6) was in the same range. This will give that the TSE will be in the same range when sampling with a flow-distance of 7 m^3 to 42 m^3. The TSE increased when the number of increments was decreased from 96 to 1. Therefore, a composite sample was better than one increment (or spot-sample). For further information of the combinations of j and Q see Appendix 14.

According to the Danish EPA, the sampling scheme should extract a minimum of 3 increments, but preferably 5 to 6 increments per hour to compensate for the fluctuations in flow and concentration during night and day. This gave a minimum of 72 increments, but it was preferred to have 120 to 144 increments per 24 hours. With this in mind, the TSE was 0.20 % for sampling point F (j = 1 and Q = 72). At Bramming Nord, j = 2 was closest to the normal procedure, and provided a TSE of 0.20 %.

For incremental sampling (based upon the TSE simulations) it would be better to increase the number of increments in the composite sample than to decrease the distance between the increments. This is seen in Figure 54 where the steepest descending is in the direction of increasing Q. Therefore it is better with regards to TSE to use 24-hour composite samples than to use a spot-sample (so-called grab sample).

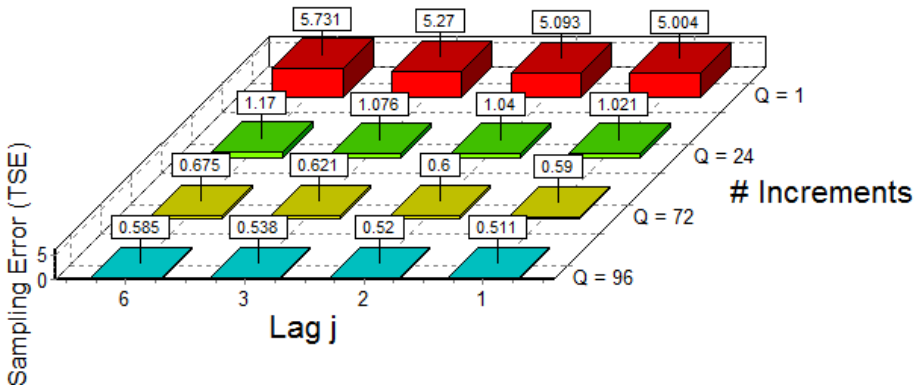

Figure 54 Total Sampling Error for measuring TP in increments from sampling point F. j = lag, Q = number of increments

Sampling Point A

The smallest TSE for the measuring of TP in sampling point A was found for j = 2 and Q = 96, where the TSE was equal to 0.20 %, see Figure 55. For j = 1 and Q = 1, when each increment is analyzed separately, the TSE was 2.1 %.This was slightly higher than for j = 2, but was most likely because of an artefact in the data analysis, because the TSE for j = 1 should, according to the theory, be the smallest.

As for sampling point F, the TSE when extracting a composite sample with more than 96 increments was in the same range for j = 1 to j = 6. When following the guidelines from the Danish EPA, the sampling scheme would give rise to an TSE of 0.23 % for sampling point A (j = 2 and Q = 72).

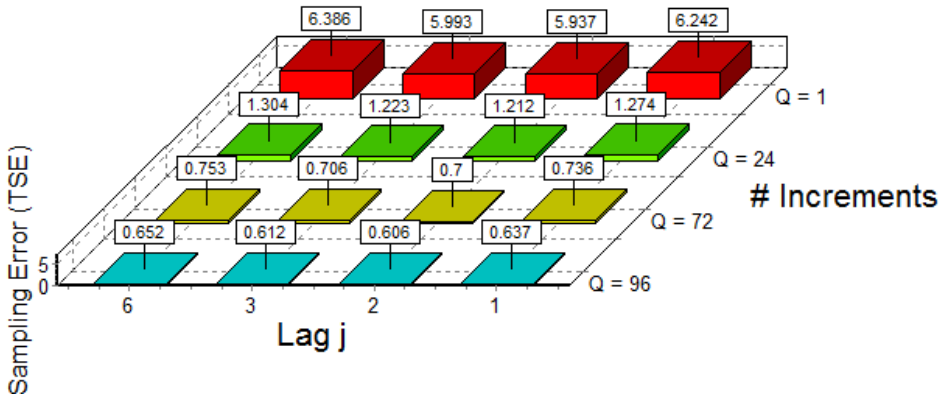

Figure 55 Total Sampling Error for measuring TP in increments from sampling point A. j = lag, Q = number of increments

TSE were in the same range for both sampling points, but the standard uncertainty arising from sampling was only slightly smaller for sampling point F (0.20%) compared to sampling point A (0.23 %). To see if the difference between the standard uncertainties was significant a F-test could be made. This gave that the difference may be significant, but this could not be stated with certainty. Therefore the difference seen between sampling point F and A could be a coincidence and not a real difference.

Global Estimation Error for Total Phosphorous in Increments

Uncertainty is not only limited to sampling and materialization of the increments or 24-hour samples, but is composed from all of the steps from primary sampling through mass/volume reducing until the amount of an aliquot is reach. Therefore, the global estimation error (GEE) is the summation of TAE and TSE [59].

When the optimal sampling point (F) was used the results for TSE and TAE were as follows

- TSE for 72 increments (j = 2, Q = 72): 0.20 %
- TAE: 0.84 %

This gave a GEE of 0.86 % ($\sqrt{0.20^2 + 0.84^2}$) for increments.

Comparison with Previous Study

From the baseline pilot survey [51], where waste water was evaluated from three different waste water facilities, the nugget effect was estimated and found to be between 0.00117 and 0.00517, see Table 29. The uncertainty from the analysis ($CV_{analysis}$), the measurement (CV(0)), and the sampling ($CV_{sampling}$) is also listed in Table 29.

In this present survey where Bramming Nord waste water treatment facility was investigated, it was found that the nugget effect was smaller than those claimed in the previous survey [51]. One reason for the difference could have been caused by the differences in analytical uncertainty. Another reason could be mis-calculations or interpretations of the nugget effect, which could give an incorrect to high/small result. A third reason could be the representativity of the sampling procedure, where the procedure used in Bramming might have been more representative and minimized the sampling errors, which might have resulted in a more correct result. One factor to influence the representativity was that in the previous survey the increments were extracted time proportional, and in this study the increments were extracted flow proportional. The differences between the two studies were related to the large difference in analytical uncertainty, and to some degree the interpretation of the nugget effect. Since the interval between extracting increments were small the uncertainty contributions from extracting either time or flow proportional are negligible.

Table 29 Estimation of variance in the outlet and nugget effect for increments analyzed for TP[4].

TP	Variance – mass reduction, pretreatment and analysis $CV_{analysis}$ [%]	Variography from sampling each 2 min – 24 samples		Variance – material + sampling
		V(0)	CV(0) [%]	$CV_{sampling}$ [%]
Lynetten, serie A	3.6	0.00121 (0.00042)	3.47 (2.05)	n.s. (n.s.)
Lynetten, serie B		0.00125 (0.00187)	3.53 (4.32)	n.s. (2.40)
Karup		0.00117 (0.00119)	3.41 (3.45)	n.s. (n.s.)
Mejlby 2006		0.00517 (0.00346)	7.19 (5.88)	6.2 (4.65)
Mejlby 2007		0.00140 (0.00119)	3.74 (3.45)	1.0 (n.s.)
Bramming Nord	0.84	0.00028*	1.67	1.45

***140 samples extracted with intervals of 7 m^3. The calculations of the results in the table are shown in Appendix 8. Values in brackets are calculations on basis of the variograms made with Vario.**

Total Phosphorous in 24-hour Composite Samples

All seven previously described sampling points were used for the analysis of 24-hour composite samples. First, the analytical concentration is directly compared for all sampling points, than the points are discussed on the basis of experimental variograms. First points F, E and G after the weir are discussed as they are the most correct locations according to ISO 5667-10, followed by sampling points A, D and B, and at last sampling point C is discussed. After an individual description, the variograms are compared according to position of the sampling points. The journal for the sampling procedure for all sampling points can be found on the enclosed CD-rom, and a reduced report can be found in Appendix 17-23. The data for TP in 24-hours samples are listed in Appendix 24.

Analytical Concentrations of Total Phosphorous in 24-hour Composite Samples

When comparing the analytical concentrations directly after correction for mixing data and outliers, see Figure 56, only sampling point A stands out with more fluctuations than the rest of the sampling points. For sampling point A three points differed greatly from the rest of the results, samples no. 1, 4 and 13, but there are no obvious reasons for this with regards to errors in the sampling procedures.

The remaining six sampling stations showed essentially the same tendency; it was not possible to observe distinctive differences between these stations. Up to day 15 the results were almost identical, but after 15 days the results differed slightly from each other and the concentration range became more stable. It was generally raining during the duration of the sampling period, especially in the last four weeks; therefore, the waste water was diluted more than usual giving the result shown, see Figure 45.

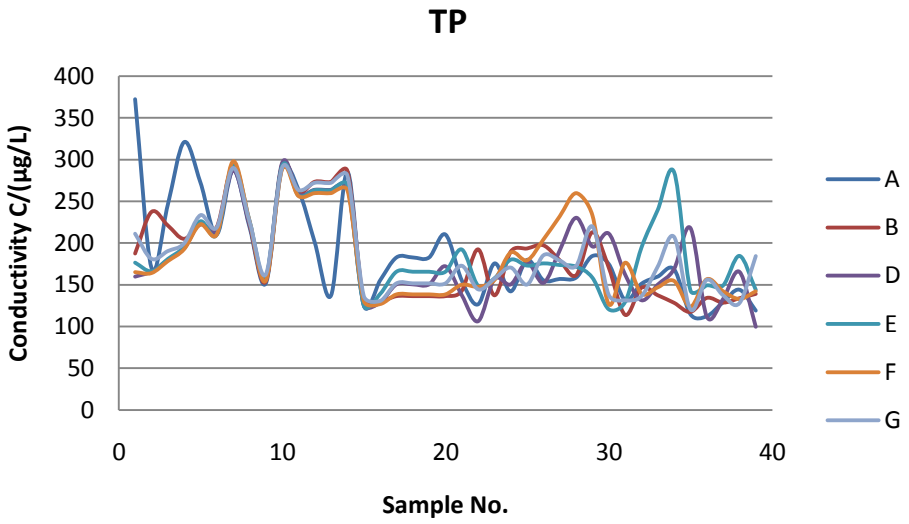

Figure 56 Analytical concentration of TP measured in 24-hour samples from sampling points A - G

Variografic Analysis of Total Phosphorous in 24-hour Composite Samples

Samples (24-hour composite samples) were volume-reduced to the required analytical volume and analyzed for TP. First, the analytical concentration and experimental variogram for TP were discussed in relation to the individual sampling points (Sampling points F and A are examined thoroughly here, the other sampling points are described in Appendix 25). Then the results from all the sampling points were compared (grouped as *before*, *after* and *across* the weir). The same layout was used when subsequently discussing the results for conductivity.

Sampling Point F

The analytical concentration measurements for sampling point F are shown in Figure 57. The blue dots are the original measurements. The red curve shown is an interpolation after the dataset was corrected for missing data (due to errors in the sampling process). Individual measurements differed from each other, while there was a slightly decreasing trend overall. In the first two weeks the measurements fluctuated significantly, while in the last four weeks concentrations became more similar.

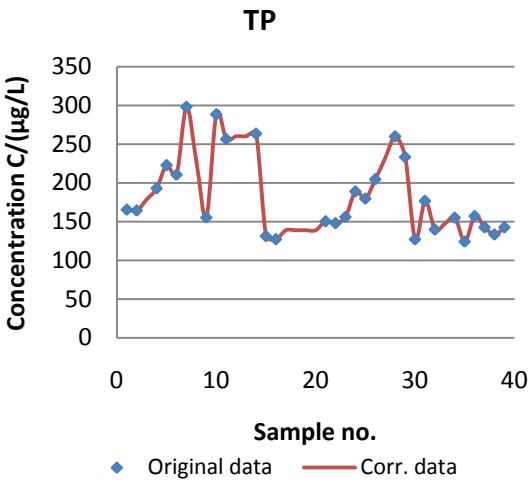

Figure 57 TP analytical concentration development in 24-hour samples at sampling point F.

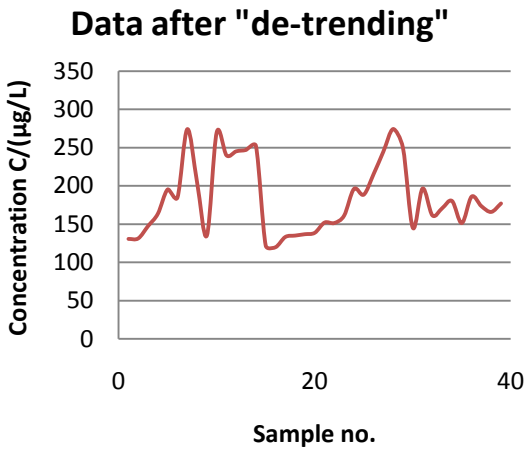

Figure 58 De-trended data for TP in 24-hour samples at sampling point F. Excluded points are 3, 8, 12, 13, 17-20, and 27

The data for F is corrected for missing data and shown in Figure 57. After "de-trending" the time series is calculated, see Figure 58, and then used for the basis for the experimental variogram which is shown in Figure 59.

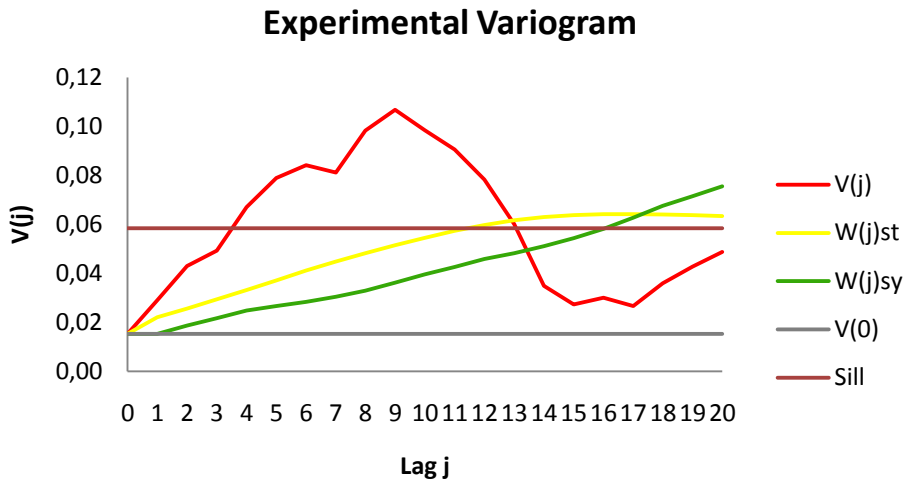

Figure 59 Experimental variogram and auxiliary functions for 24-hour samples at sampling point F. Data series F was subjected to linear de-trending before variogram calculation.

From the variogram a cyclic variation with a period of 15 days to 17 days was observed due to the distinct distribution of rainfall periods. There may also (perhaps) be a possible small indication of a cyclic variation of 7 days. The nugget effect, V(0) was estimated by linear extrapolating the first five points to intercept the ordinate axis. The nugget effect amounted to 0.015 and the sill was 0.058 (the grand mean of all variogram values). Thus, this states that the total 0-D sampling variation corresponds to 26 % of the total process variability.

Sampling Point A

The analytical concentration measurements are shown in Figure 60 as an interpolation after the dataset is corrected for missing data. The fluctuations in analytical concentration are most likely due to the amount of rain as described before for previous datasets.

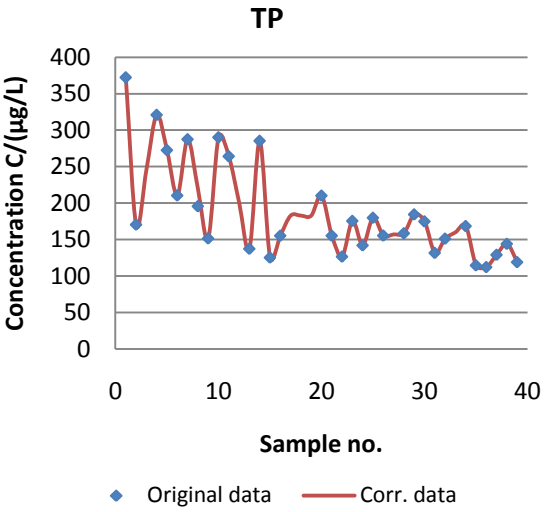

Figure 60 TP analytical concentration development in 24-hour samples at sampling point A

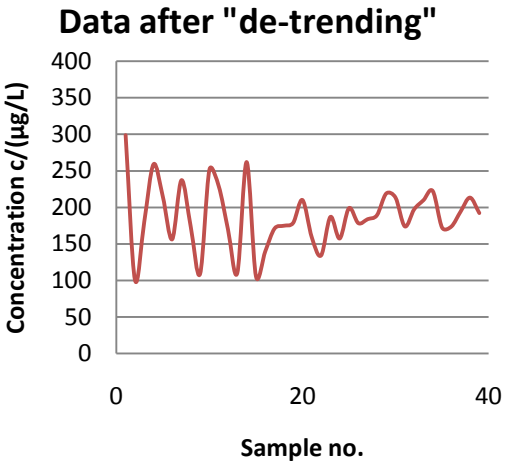

Figure 61 De-trended data for TP in 24-hour samples at sampling point A. Excluded points are 3, 8, 12, 17-19, 27, and 33.

After "de-trending" the time series, see Figure 61, was calculated and then used for the basis for the experimental variogram, which is shown in Figure 62.

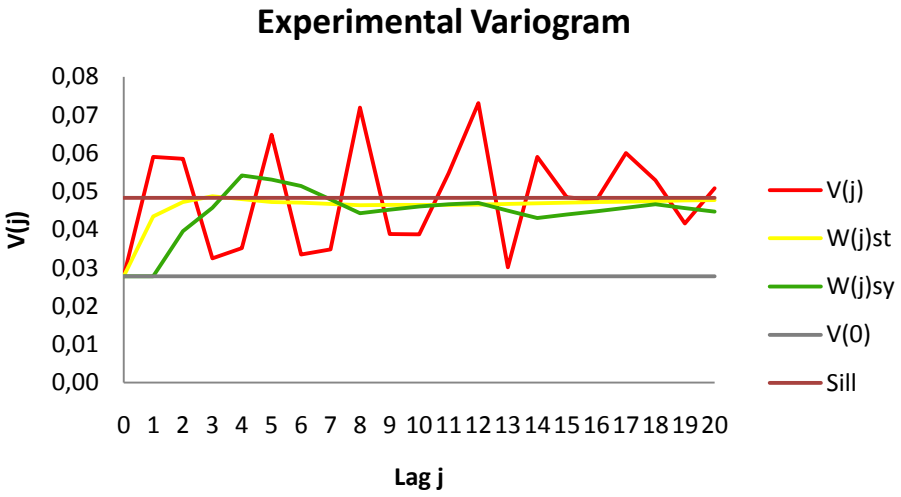

Figure 62 Experimental variogram and auxiliary functions for 24-hour samples in sampling point A. Data series A was subjected to linear de-trending before variogram calculation.

From the variogram a cyclic variation with a period of 3 days to 4 days was very prominent. The nugget effect amounted to 0.028 and the sill was 0.048. This allows to state that the total 0-D sampling variation corresponded to 58 % of the total process variability (sill).

Comparison of Sampling Points E, F, G, D, A, and B

Figure 63 shows a synoptic overview of all variograms for sampling points E, F, G, D, A, and B. The blue vertical line shows the cyclic period for each sampling point.

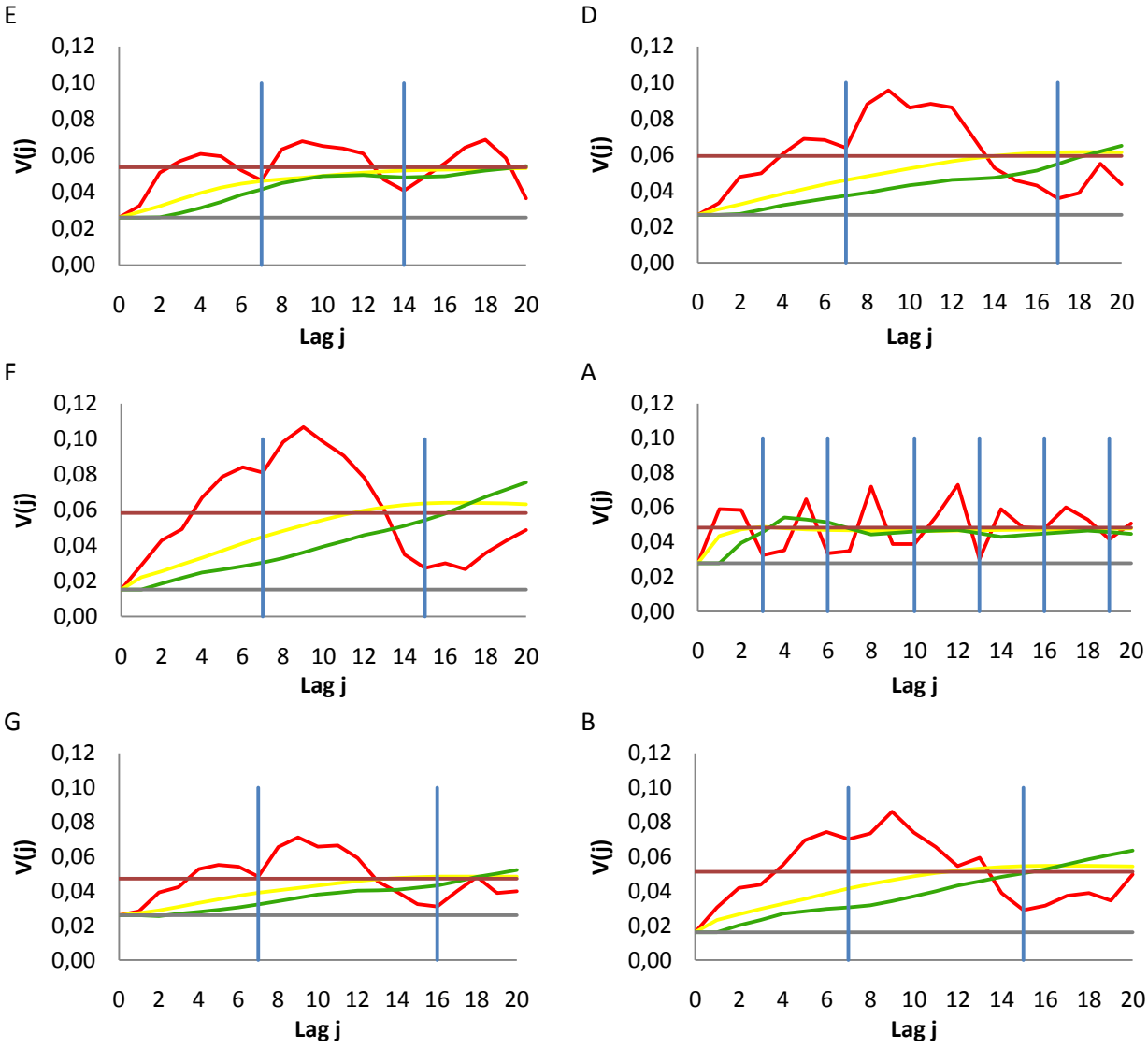

Figure 63 Synoptic presentation of experimental variograms for TP in 24-hour samples for sampling points E, F, G, D, A, and B

A comparison of the variograms for all six sampling points shows clearly how the trend of sampling point A is dramatically different from the rest of the points. The cyclic period of 3 days to 4 days is too distinct to be a coincidence; however, there is no logical explanation to the variations in A. Some suggestions are made later when possible errors which could have occurred in the sampling process are discussed. If the cycle in A is due to large concentration variation it should have also been recognizable in the other sampling points. In the other variograms this cycle of 3 days to 4 days is not clear.

With respect to cyclic variation the remaining five sampling points showed a broadly similar cyclic variations with a period of 15 days to 18 days, except for sampling point E, where the cyclic variation

appears to have been characterized by a period of 14 days. These cyclic variations are most likely pseudo-variations caused by the amount of rain in the first vs. the second part of the sampling period. As seen on Figure 45 there were much more rain in the second period from day 18 to 39.

There was also an interesting indication in all these variograms of a cyclic variation of 7 days. The possible reason for this cyclic variation could be the differences in use of water and overload of pollutants on weekdays and weekend. The waste water was a combination of water from household and industry and from drainage water. The water from household and industrial use were supplied in a constant rhythm day and night with weekends differing from weekdays. The drainage water was supplied more steadily during all hours of the day and night. During periods of rain, the drainage water was supplied in more influencing proportions. Due to the amount and distribution of rain in the experimental period the variation of 7 days was not as evident as expected. This might be more significant if the composition of water was not influence/diluted by the large amount of rain water.

When comparing points before, after, and across the weir while taking the above into considerations, it was shown that sampling point E and G are similar to F as expected. Sampling D and B was expected to show similarities, but they were slightly different in indication of the cyclic period where D were more distinct than B. This could be due to the water entered below point D in the direction of B; therefore, the water at point D was more stagnant than at point B. Sampling points A and F were expected to have some kind of similarities. A was the point where (from a practical point of view) samples are taken commonly and F was the point which fulfilled most of the guidelines from the Danish EPA [49] and ISO 5667-10 [50]. Since A was so distinctly different from the rest of the sampling points with regards to TP, the results could be an A location specific coincidence, or it could be related to the measurements of TP alone or related to the composition of suspended matter in the waste water . This unique “A feature” was concluded not to be related to the sampling equipment or procedure, since A was the point where the time interval of sampling was controlled and registered. If the difference is due to the equipment controlling, the tendencies should also be recognizable for all other sampling points. This A feature remains a mystery in spite a considerable amount of detective work.

The placement of point B provides a very interesting sampling point to investigate as an alternative which shows similarities to point F. Point B is also, from a practical point of view, an alternative to F, since it is easier to secure the hose in exactly the same point without regard to the velocity and amount water.

Nugget Effect and Sill for Total Phosphorous in 24-hour Composite Samples

Table 30 shows the nugget effects, sill levels, and relative proportions between them for the first six sampling points.

Table 30 Nugget effect, sill level and relative proportions for TP in 24-hour samples from sampling points F, E, G, D, A, and B

Sampling Point	V(0)	Sill	V(0)/Sill [%]
F	0.015	0.058	26
E	0.026	0.054	49
G	0.026	0.047	55
A	0.028	0.048	58
D	0.027	0.059	45
B	0.016	0.051	31

By comparing the nugget effect it can be seen that there is a slight indication of two groups; below and above 0.02.

- Below: B, F
- Above: E, G, D, and A

For sampling points B and F the lowest percentage ratio of the sill for the sampling points was found. Point F also had the lowest nugget effect of 0.015, which showed that for this point the 0-D-sampling variation has the lowest influence on the total sampling error. The relative proportion between the nugget effect and the sill is 26 % for sampling point F.

Comparison of the nugget effect across the weir for D and E, A and F, and B and G gave no systematic variations. For D vs. E the nugget effect was equal and for A vs. F it was lowest after the weir. For B vs. G the nugget effect was lowest before the weir. The latter could be an indications that B could be an alternative sampling point compared to F since the nugget effect for B is 0.016, only slightly higher than F.

The sill level describes the total variability in the process; therefore, a low level of sill is wanted if one is looking for a sampling position with a minimum variability in the process. The sill levels for the nugget effect also indicated a division in two groups; below and above 0.05.

- Below: A, G
- Above: D, B, F, and E

The sill for the sampling points were 0.047 to 0.059 and showed no systematic variations across the weir when comparing D and E, A and F, B and G. When the sampling points before the weir are compared, it showed that D and B both had a higher sill than A. Comparison of the sampling points after the weir showed that E and G had a lower sill than F. B and F were similar in nugget effect, but not in sill, but still had a lower relative proportion between the nugget effect and sill compared to the rest of the points. This made B and F more suitable sampling points.

With regards to the range of the variograms, which is a reflection of autocorrelation between 24-hour samples, it was not possible to make a conclusion based of these datasets. It requires more samples to provide a larger dataset before anything could be said about the autocorrelation. This is due to the pseudo cyclic variation which gives a decrease in the variogram before it stabilizes with maximum approximately equal to the sill.

Comparison of Sampling Points A and C

The difference in structure of the sampling point is that C was placed 30 cm below A. To ensure that the vertical axis was the same, the hoses were attached together with tape. With regards to analytical concentration for point A and C there are the same differences as when A is compared to the rest of the sampling points, see Figure 64.

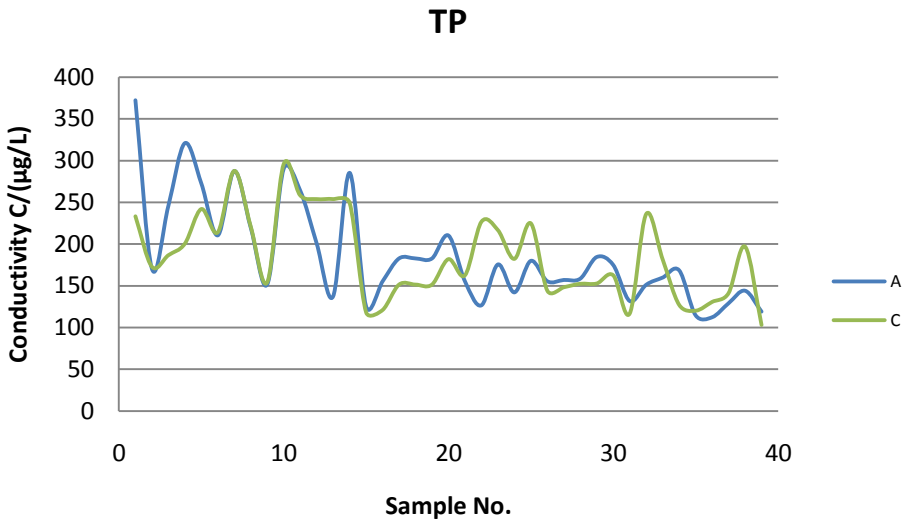

Figure 64 Sampling positions A and C with regards to measurements of TP in 24-hour samples. The data are corrected for extreme values and missing data

The concentrations between the points are compared in a scatter plot of where A is plotted as a function of C, see Figure 65. This alternative scatter plot does not reveal any systematic deviations between the sampling locations, since the points are equally placed around a line through (0,0) and (1,1).

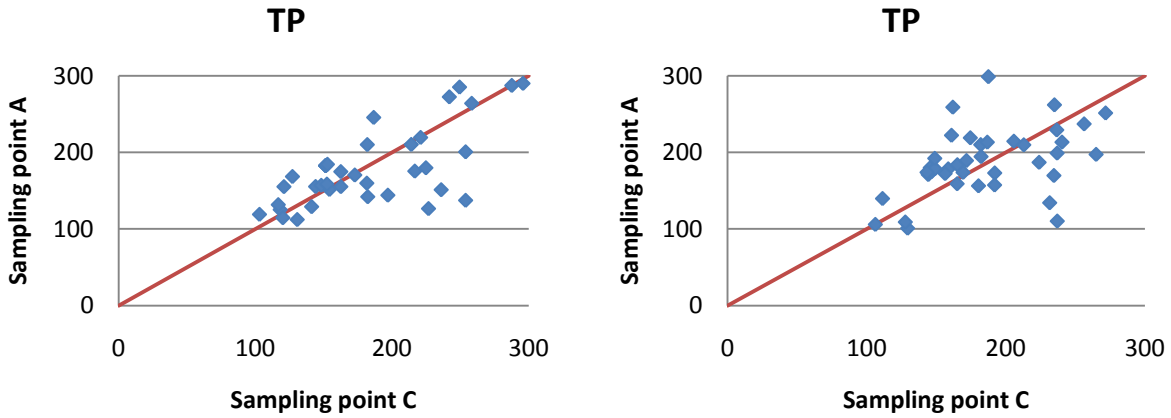

Figure 65 Scatter plot of the concentration from sampling point A and C as a function of each other (left: before correction of data, right: after correction of data)

A comparison of the experimental variograms for points A and C also provides the same differences as seen when A is compared to the rest of the sampling points, see Figure 66. The blue vertical line shows the cyclic period for each sampling point.

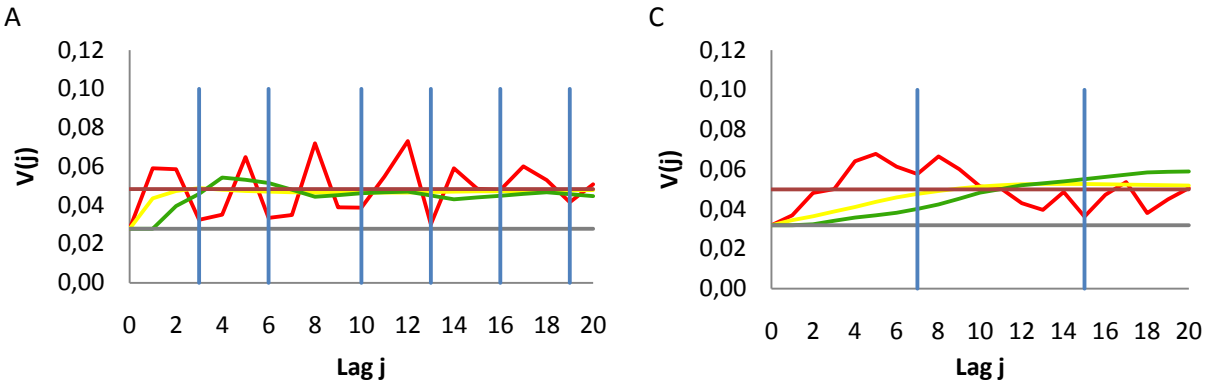

Figure 66 Experimental variograms for TP in 24-hour samples from sampling points A and C

It was seen that for point A there was a cyclic variation of 3 days to 4 days, where for C the cyclic variations were at 7 days and 15 days. The variation in points A and C showed that the sill was the same for both points, but the nugget effect was slightly smaller at point A than at C, but in the same range, see Table 10. The nugget effect is highest for point C when compared to all sampling points, which states that the 0-D-sampling variation was highest in point C. This also was as expected, since the water stems upstream of the weir. Due to this the water is more stagnant than at the other points and the uncertainty from sampling to the final measurements would become higher.

Table 31 Nugget effect, sill and the ration between them for 24-hour samples from sampling points A and C

Sampling Point	V(0)	Sill	V(0)/Sill [%]
A	0.028	0.048	58
C	0.032	0.050	64

Total Sampling Error for Total Phosphorous in 24-hour Composite Samples

In the following TSE for all seven sampling points is described. Sampling points F and A are examined here, the other sampling points are described in Appendix 26.

Sampling Point F

A 3-D histogram was made of TSE (The TSE calculated in Vario and shown on top of the bars in the figures is equal to $3 \cdot s_{TSE}$) with relative values for TSE as a function of different values for j and Q, see Figure 67, where for j = 1 which was equal to 24 hours, then Q = 1 was equal to 24 hours, Q = 2 was equal to 48 hours, Q = 7 was equal to one week.

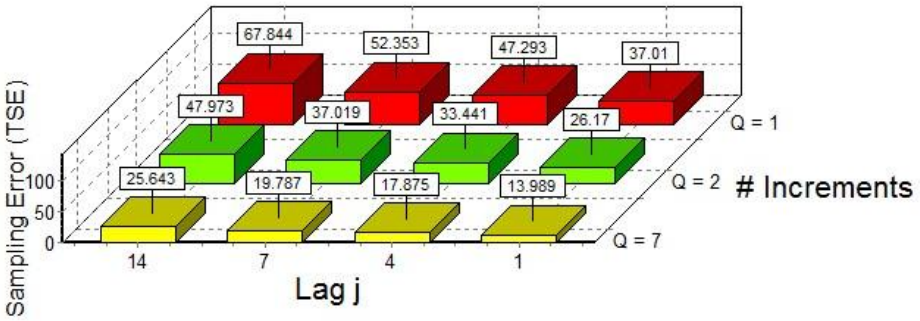

Figure 67 TSE for TP in 24-hour samples from sampling point F

As expected the TSE had the smallest value for j = 1 and Q = 7 of 4.66 %. This meant that with a lag of 1 and a composite sample of seven 24-hour samples (this case is called a week-sample), the smallest

TSE was found. Thus, a week-sample had a smaller TSE than a 24-hour sample. From a practical point of view, sampling of a week-sample was not optimal, since this meant that the technicians should have more equipment for sampling, and be at the sampling point once a day to change the container and bring it to the lab for storage until all 24-hour samples have been collected. For many parameters other than TP, samples would not be stable for a week.

As sampling was done commonly with j = 1 and Q = 1 (24-hour sample), this would for point F give an TSE of approx 12.3 %. It is seen that by increasing j the TSE increases and by increasing Q the TSE decreases. Therefore TSE can be minimized by increasing Q, as in using more 24-hour samples for a composite sample or composite evaluation, and using j = 1.

Sampling Point A

A 3D histogram was made of the relative values for TSE as a function of different values for j and Q, see Figure 68.

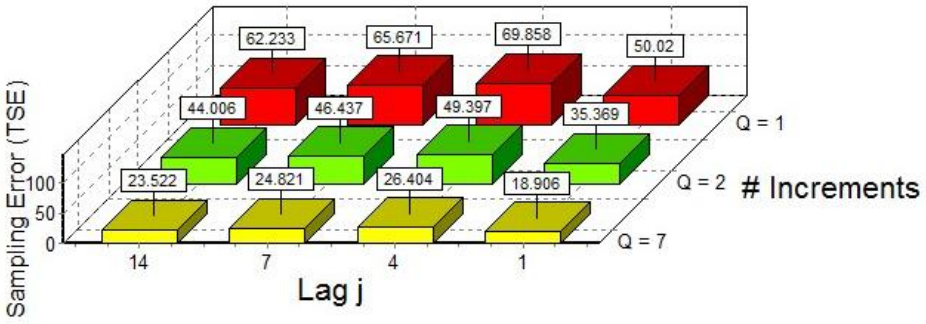

Figure 68 TSE for TP in 24-hour samples from sampling point A

As expected the TSE had the smallest value for j = 1 and Q = 7 of 4.81 %. As sampling was done commonly with j = 1 and Q = 1, the TSE for point A would give an error of 16.7 %.

Comparison of Total Sampling Error for Total Phosphorous in 24-hour Composite Samples

When comparing all the sampling points with regard to TSE, it is seen that, as expected, sampling point C had the highest TSE and 0-D-proces variation due to the structure of the sampling point, see Table 11. Point A, from the experimental variogram was shown to have the worst position for sampling, yet shows it had the next highest TSE and 0-D-proces variation. When comparing F, which was the correct and best sampling position, with B, which was a possible alternative based upon the variograms, it shows that the TSE and 0-D process variation were in the same percentage range. This indicates that B again could be an alternative to F.

Table 32 TSE for j = 1 and Q = 1 and 0-D process variation for 24-hour samples at each sampling point

Sampling point	TSE [%]	V(0)/Sill [%]
F	12.3	26
E	16.2	49
G	16.2	55
A	16.7	58
D	16.3	45
B	12.7	31
C	17.9	64

Dividing Total Sampling Error into Different Error Contributions

From the variogram when the optimal sampling point (F) was used the results for the nugget effect, sill, and relative ratio between them is listed in Table 33.

Table 33 Nugget effect, sill and relative proportional ratio between them for results from sampling point F

	24-hour samples
Nugget effect	0.015
Sill	0.058
Nugget effect/sill	26 %

This showed that the 0-D – process variation for 24-hour samples accounted for 26 % of the sill and the 1-D – process variation accounted for 74 % of the sill.

The uncertainty from 1-D – process variation was seen as the differences in concentrations over the whole period.

Global Estimation Error for Total Phosphorous in 24-hour Composite Samples

The GEE was as described before the summation of TAE and TSE [59].

When the optimal sampling point (F) was used the results for TSE and TAE were as follows

- TSE for 24-hour sample: 12.3 %
- TAE - Eurofins: 0.842 %
- TAE – EIT AAU: 4.55 %

This gave a GEE of 12.3 % and 13.1 % for 24-hour samples at Eurofins and EIT AAU, respectively.

From a previous literature [51] study it was found that the standard uncertainty could be expected to be between 24 % to 48 % depending on the parameter and level of concentration. For TP the standard uncertainty was expected to be between 24 % to 39 %; therefore, a standard uncertainty of 12.3 % and 13.1 % was below the expected range. It might be easy to reduce this standard uncertainty by extracting a larger volume of water in each increment [54]. In this project 50 ml was extracted, which was the smallest amount recommended.

The concentrations measured at sampling point F in the 24-hour composite samples were 123.92 µg/L to 298.01 µg/L. The mean value was 183.29 µg/L and the standard deviation was 51.077 µg/L, see Appendix 24. The standard uncertainty of 12.3 % equals an expanded uncertainty of 24.6 % with a coverage factor of 2 (equal to 95 % confidence level, when normal probability is assumed). When t-testing was used for the calculations of confidence intervals, it resulted in a 95 % confidence range of 183.29 µg/L ± 18.03 µg/L. This stated that in this range the true mean value was found with 95 % certainty.

Conductivity in Increments

The sampling points used for the TP analysis of increments were points F and A. These were chosen because F was the correct sampling point according to ISO 5667-10 and A was the point used commonly. First sampling point F is discussed, than sampling point A: afterwards the two sampling points are compared. The data for conductivity in increments are listed in Appendix 27.

Variografic Analysis of Conductivity in Increments

The increments extracted were analyzed for conductivity. To recall, the increments were taken with a flow-distance of 7 m^3, which for the shortest time interval was approximately 3 min and for the longest time interval was approximately 12 min. The data processing increments were analyzed for the first 15 hours before the persistent rain came down.

Sampling point F

The conductivity measurements for sampling point F are shown in Figure 69. The blue curve shows the original measurements and the red curve is an interpolation after the dataset was corrected for possible outliers. This shows a trend to ascending conductivity over the period.

After “de-trending” the time series was calculated, see Figure 70, and then used for the basis for the experimental variogram which is shown in Figure 71. The “de-trending” was done in the same way as described for TP.

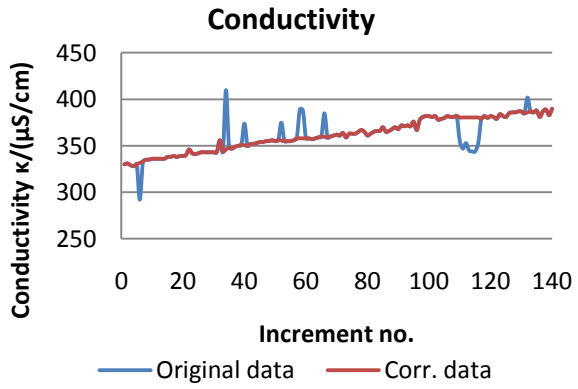

Figure 69 Conductivity development in increments at sampling point F

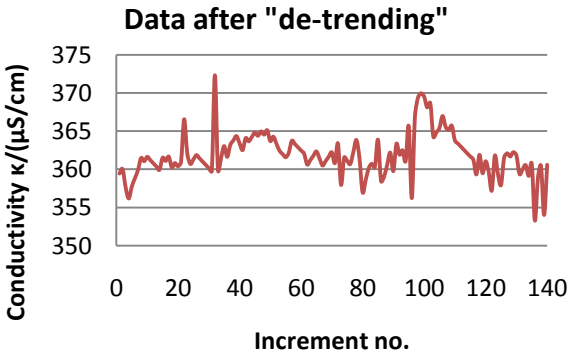

Figure 70 Conductivity in increments after "de-trending" at sampling point F. Excluded points are no. 6, 34, 39, 52, 58, 59, 66, 110-116, and 132.

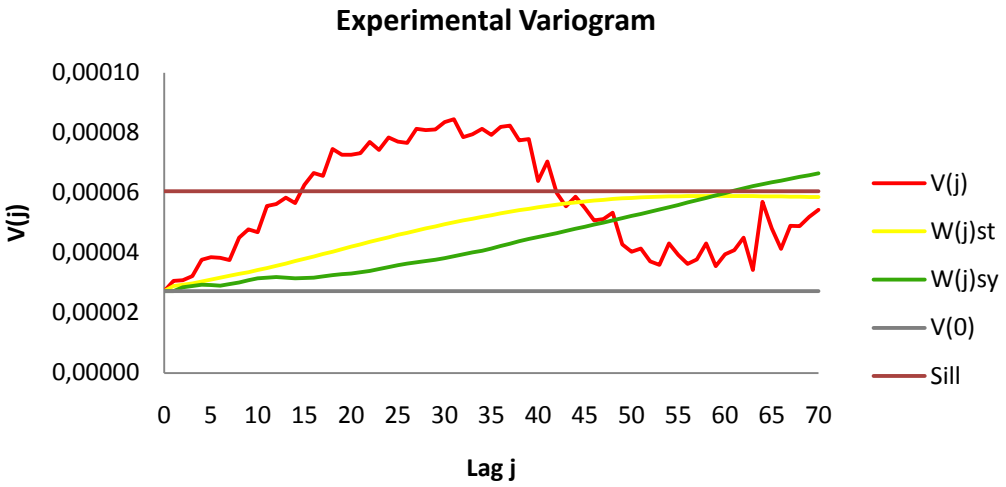

Figure 71 Experimental variogram and auxiliary functions for conductivity in increments at sampling point F. Data series F was subjected to linear de-trending before variogram calculations

From the variogram a cyclic variation with period of 52 to 63 increments (= 364 m^3 to 441 m^3) was observed. Usually the waste water facility treats 1000 m^3 per day [55] with the same day and night variations of cyclic variation as seen for TP. The confirmation of this cyclic variation could be done by analyzing increments from at least two times 24 hours.

Sampling point A

The analytical concentration measurements for sampling point A are shown in Figure 72. The blue curve is the original measurements and the red curve is an interpolation after the dataset is corrected for possible outliers. Again there is a trend to ascending conductivity over the period.

After "de-trending" the time series was calculated, see Figure 73, and then used for the basis for the experimental variogram which is shown in Figure 74.

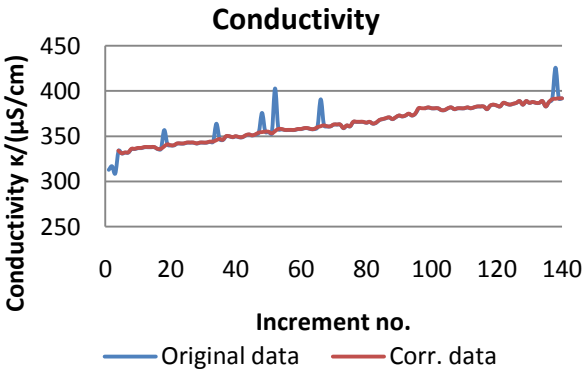

Figure 72 Conductivity development in increments at sampling point A

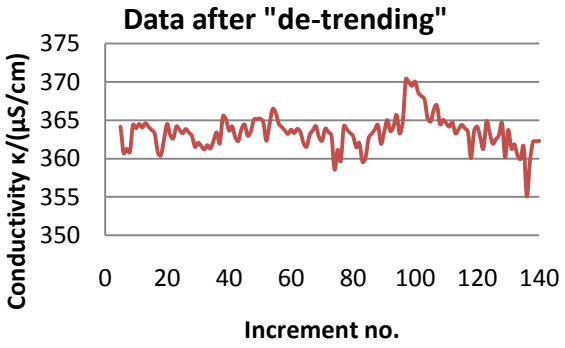

Figure 73 Conductivity in increments after "de-trending" at sampling point A. Excluded points are no. 1-3, 18, 34, 48, 52, 66, and 138.

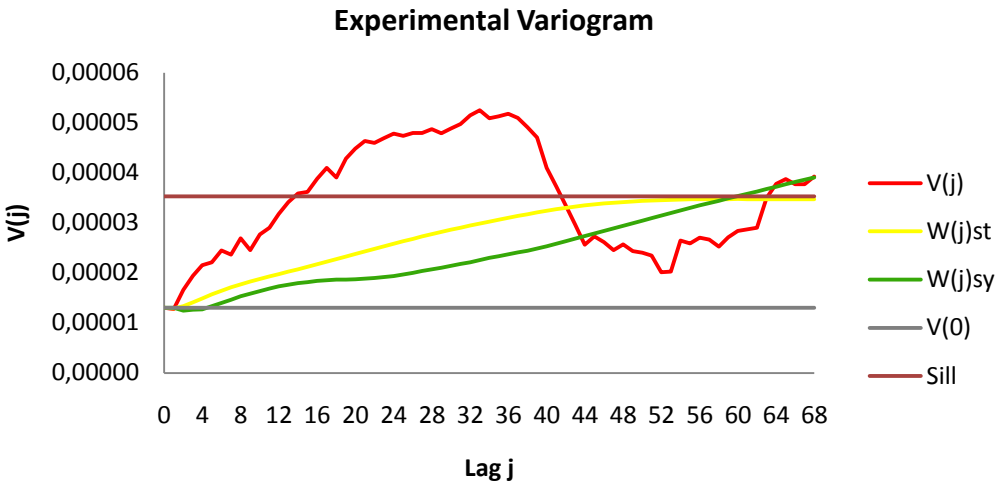

Figure 74 Experimental variogram and auxiliary functions for conductivity in increments at sampling point A. Data series A was subjected to linear de-trending before variogram calculations

From the variogram a cyclic variation with period of 44 to 62 increments (= 308 m^3 to 434 m^3) was observed. Again the cyclic variation could be explained by the variation from day to night over 24 hours. The large interval could be due to the amount of rain, since the increments were diluted to a degree that would have influenced the results.

Nugget Effect and Sill for Conductivity in Increments

The nugget effect, sill, and relative proportions for sampling point F and A is listed in Table 34.

Table 34 Nugget effect, sill level and relative proportions for increments from sampling points F and A

Sampling Point	V(0)	Sill	V(0)/Sill [%]
F	0.000027	0.000061	45
A	0.000013	0.000035	37

The nugget effect for sampling point F amounted to 0.000027 and the sill was 0.000061; therefore, the total 0-D sampling variation corresponded to 45 % of the total process variability.

The nugget effect for sampling point A amounted to 0.000013 and the sill was 0.000035; therefore, a the total 0-D sampling variation corresponded to 37 % of the total process variability.

Comparing the results for sampling point F to those for sampling point A, gives that sampling point A has the smallest nugget effect and process variability. This shows that sampling point A was slightly more suitable than sampling point F with regards to sampling of increments and analyzing them for conductivity. This was the opposite of the results for TP, where sampling point F gave lower values than sampling point A. The differences for conductivity was so small that it could not with certainty be stated that they were really different.

Total Sampling Error for Conductivity in Increments

The TSE is a sum of seven error contributions; FSE, GSE, IDE, IEE, IPE, TFE, and CFE. In the following the TSE for increments from sampling point F and A are described. The TSE estimates for sampling point F and A are shown in Figure 75 and Figure 76, respectively. (The TSE calculated in Vario and shown on top of the bars in the figures is equal to $3 \cdot s_{TSE}$)

The smallest TSE for the measuring of conductivity in sampling point F is found for j = 1 and Q = 96, where the TSE was equal to 0.053 %. For j = 1 and Q = 1 the TSE was 0.52 %.

According to the Danish EPA the sampling scheme should extract a minimum 3 increments, but preferably 5-6 increments per hour to compensate for the fluctuations in flow during night and day. This gives a minimum of 72 increments, but preferably 120 to 144 increments per 24 hours. With this in mind, the TSE would be below 0.061 % for sampling point F (j = 1 and Q = 72). At Bramming Nord j = 2 was closest to the normal procedure, and this gave a TSE of 0.063 %

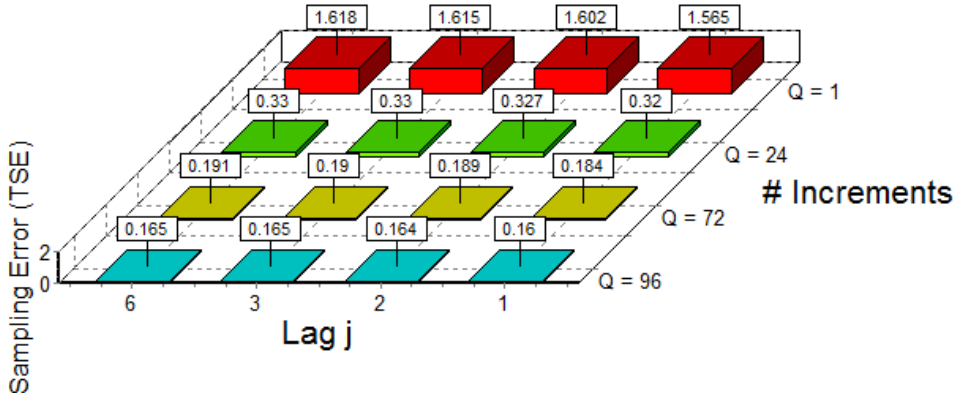

Figure 75 Total Sampling Error for measuring conductivity in increments from sampling point F. J = lag, Q = number of increments

The smallest TSE for the measuring of conductivity in sampling point A was found for j = 2 and Q = 96, where the TSE was equal to 0.037 %, see Figure 76. For j = 1 and Q = 1 when each increment was analyzed separately, the TSE was 0.36 %.

When following the guidelines from the Danish EPA the sampling scheme would result in a TSE below 0.042 % for sampling point A (j = 2 and Q = 72). When sampling point A are compared to sampling point F, it is shown that the smallest TSE were for sampling point A.

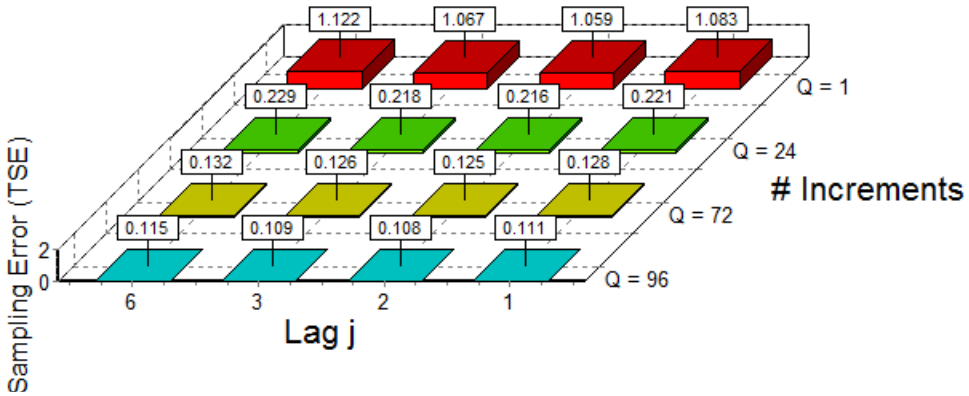

Figure 76 Total Sampling Error for measuring conductivity in increments from sampling point A. J = lag, Q = number of increments

The TSE was in the same range for both sampling points, yet the standard uncertainty arising from sampling was slightly smaller for sampling point A (0.042 %) when compared to sampling point F (0.063 %). The differences were so small, that it could not be stated with certainty that the differences were real.

The TSE when extracting a composite sample at sampling point F and A with more than 96 increments was in the same range for j = 1 to j = 6. This indicated that in situations where the weather conditions causes a higher flow it was possible to sample with a lower frequency and still obtain a small TSE. The lower frequency will ensure that the total amount of water sampled did not exceed the volume of the storage container in the sampling equipment.

Global Estimation Error for Conductivity in Increments

The GEE was as described before as the summation of TAE and TSE [59].

When the best sampling point for conductivity in increments (A) was used the results for TSE and TAE were as follows

- TSE for increments: 0.042 % (j = 2, Q = 72)
- TAE: 0.91 %

This gave a GEE of 0.91 % for increments. For sampling point F the GEE was also 0.91 % due to the small value of TSE.

Comparison with Previous Study

From the earlier baseline survey the nugget effect was estimated and found to be between $0.24 \cdot 10^{-6}$ to $6.37 \cdot 10^{-6}$, see Table 35. The uncertainty from the analysis ($CV_{analysis}$), the measurement (CV(0)), and the sampling ($CV_{sampling}$) are also listed in Table 35.

In this survey where Bramming Nord waste water treatment facility was investigated, the nugget effect was higher than those from the previous survey. Comparing the uncertainty from the analysis to the uncertainty from sampling and material heterogeneity, it was found that the uncertainty from sampling and material heterogeneity were insignificant when sampling increments. This was the case for both the previous and present study with only one exception in Mejlby 2007, where the CV(0) was higher than the $CV_{analysis}$[4].

Table 35 Estimation of variance in the outlet and nugget effect for increments analyzed for TP [51].

Conductivity	Variance – mass reduction, pretreatment and analysis $CV_{analysis}$ [%]	Variography from sampling each 2 min – 24 samples		Variation – material + sampling
		V(0)	CV(0) [%]	$CV_{sampling}$ [%]
Lynetten, serie A	0.2	0.00000024	0.05	n.s.
Lynetten, serie B		0.00000074	0.09	n.s.
Karup		0.00000154	0.12	n.s.
Mejlby 2006		0.00000019	0.04	n.s.
Mejlby 2007		0.00000637	0.25	0.15
Bramming Nord	0.91	0.000013*	0.36	n.s.

***140 samples extracted with intervals of 7 m^3. n.s. means not significant. The calculations of the results in the table are shown in Appendix 8.**

The difference in conductivity could have been because of the same reasons as previously listed for TP.

- The analytical uncertainty
- Mis-calculations or interpretations of the nugget effect
- The representativity of the sampling procedure

Conductivity in 24-hour samples

Analytical Variations for Conductivity in 24-hour Composite Samples

The same 24-hour samples that were previously were analyzed for TP were also analyzed with regards to conductivity. After volume reduction to obtain the aliquot for measuring TP, the sub-sample are used to measure conductivity. When comparing the conductivity in 24-hour samples directly after correction for missing data, but before removal of outliers, see Figure 77, there are no distinct differences between the sampling points. Therefore it was difficult to make any reflections to conductivity with regards to sampling point. Therefore variographic analysis applied to the data in the following. The journal for the sampling process can be found on the enclosed CD-rom, and a reduced report can be found in Appendix 17 - 23. The data for conductivity in 24-hours samples are listed in Appendix 28.

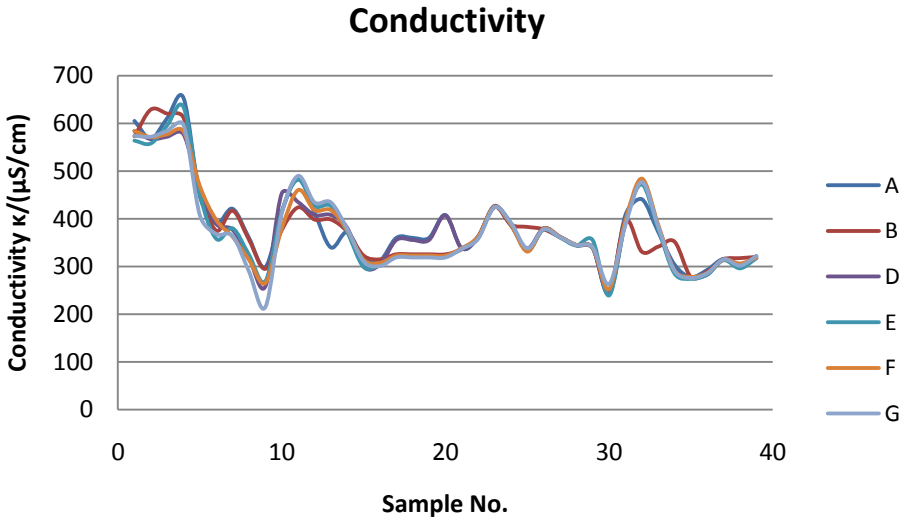

Figure 77 Conductivity measured in 24-hour samples from sampling points A - G

Variographic Analysis of Conductivity in 24-hour Composite Samples

First, the directly measured conductivity and experimental variogram for conductivity are discussed in relation to sampling point (Sampling points F and A are examined thoroughly here, the other sampling points are described in Appendix 29). Then the results from sampling point F, E, G, A, D, and B are compared and later A and C.

Sampling Point F

The conductivity measurements from sampling point F are shown in Figure 78. The curve shown is an interpolation after the dataset was corrected for outliers. Individual measurements differ from each other, while there was a slightly decreasing trend overall. While it was quite raining during the entire sampling period, especially in the last four weeks, the waste water were more diluted than usual; therefore, the results were expected to be more stabile and non-fluctuating than under circumstances where no rain was present.

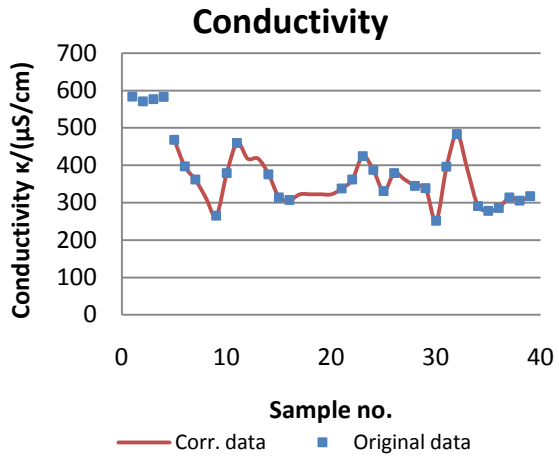

Figure 78 Conductivity development in 24-hour samples at sampling point F

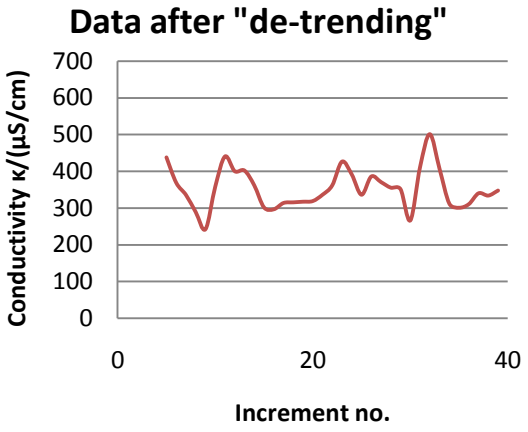

Figure 79 Conductivity in 24-hour samples after "de-trending" at sampling point F. Excluded points are 1-4, 8, 12, 13, 17-20, 27, and 33.

To calculate the experimental variogram the conductivity measurements had to be corrected for missing data. This was done by replacing missing data by a mean value of the immediately adjacent measurements on either side. The corrected curve is the red curve shown in Figure 78. Linear regression was applied to the data and the mean trend values for all measurements were calculated to be used for "de-trending". The de-trended data are shown in Figure 79 for the experimental variogram which is shown in Figure 80.

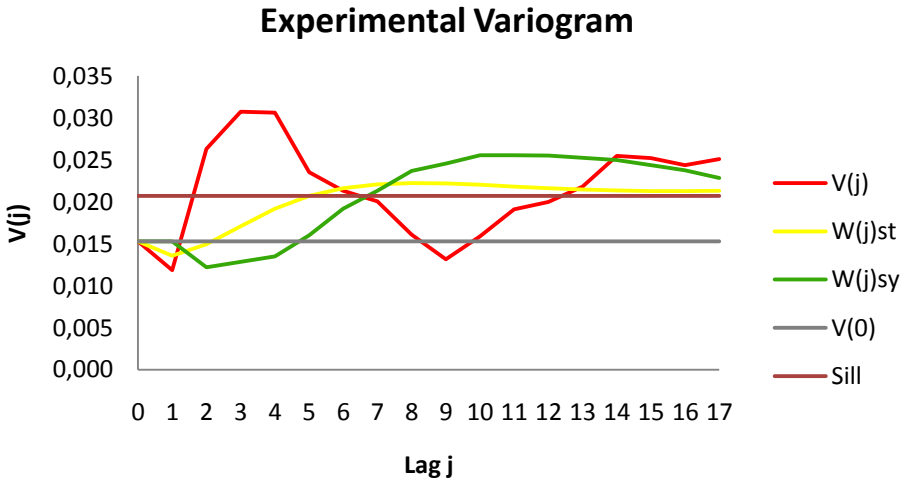

Figure 80 Experimental variogram and auxiliary functions for conductivity in 24-hour samples at sampling point F. Data series F was subjected to linear de-trending before variogram calculations

From the variogram a cyclic variation with period of 9 days was observed, which was most likely due to the amount of rain. The nugget effect, V(0), was estimated by linear extrapolating the first three points to intercept the ordinate axis. The nugget effect amounted to 0.0153 and the sill was 0.0207. Hence, the total 0-D sampling variation corresponds to 74 % of the total process variability.

Sampling Point A

The conductivity measurements from sampling point A are shown in Figure 81 as an interpolation after the dataset was corrected for outliers. The fluctuations in conductivity were most likely due to the amount of rain as described before for the previous datasets.

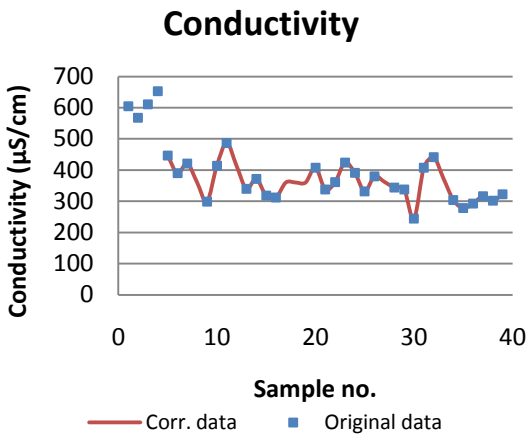

Figure 81 Conductivity development in 24-hour samples at sampling point A

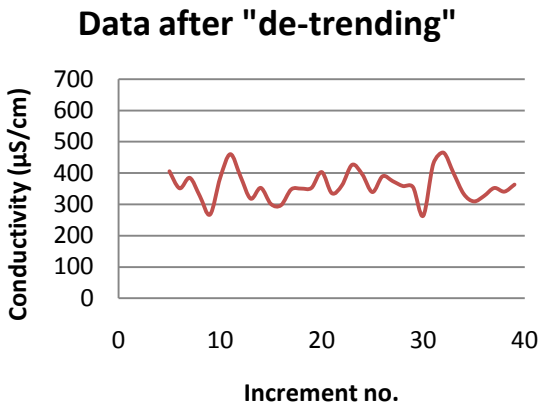

Figure 82 Conductivity in 24-hour samples after "de-trending" at sampling point A. Excluded points are 1-4, 8, 12, 17-19, 27, and 33

After “de-trending” the time series was calculated, see Figure 82, and then used for the basis for the experimental variogram which is shown in Figure 83.

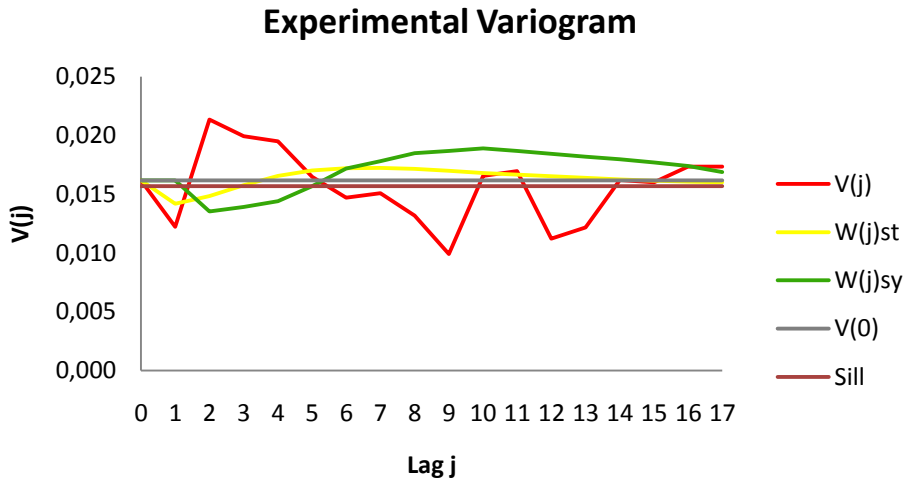

Figure 83 Experimental variogram and auxiliary functions for conductivity in 24-hour samples at sampling point A. Data series A was subjected to linear de-trending before variogram calculations

From the variogram a cyclic variations with a period of 9 days was observed. The nugget effect amounted to 0.0162 and the sill was 0.0157. Thus, the total 0-D sampling variation corresponded to 103 % of the total process variability. The reason to that A was above 100 % were due to uncertainties in determining the nugget effect and the sill.

Comparison of Variograms for Conductivity in 24-hour Composite Samples

Figure 84 shows a synoptic overview of variograms for sampling points E, F, G, D, A, and B. The blue vertical line shows the cyclic period for each sampling point.

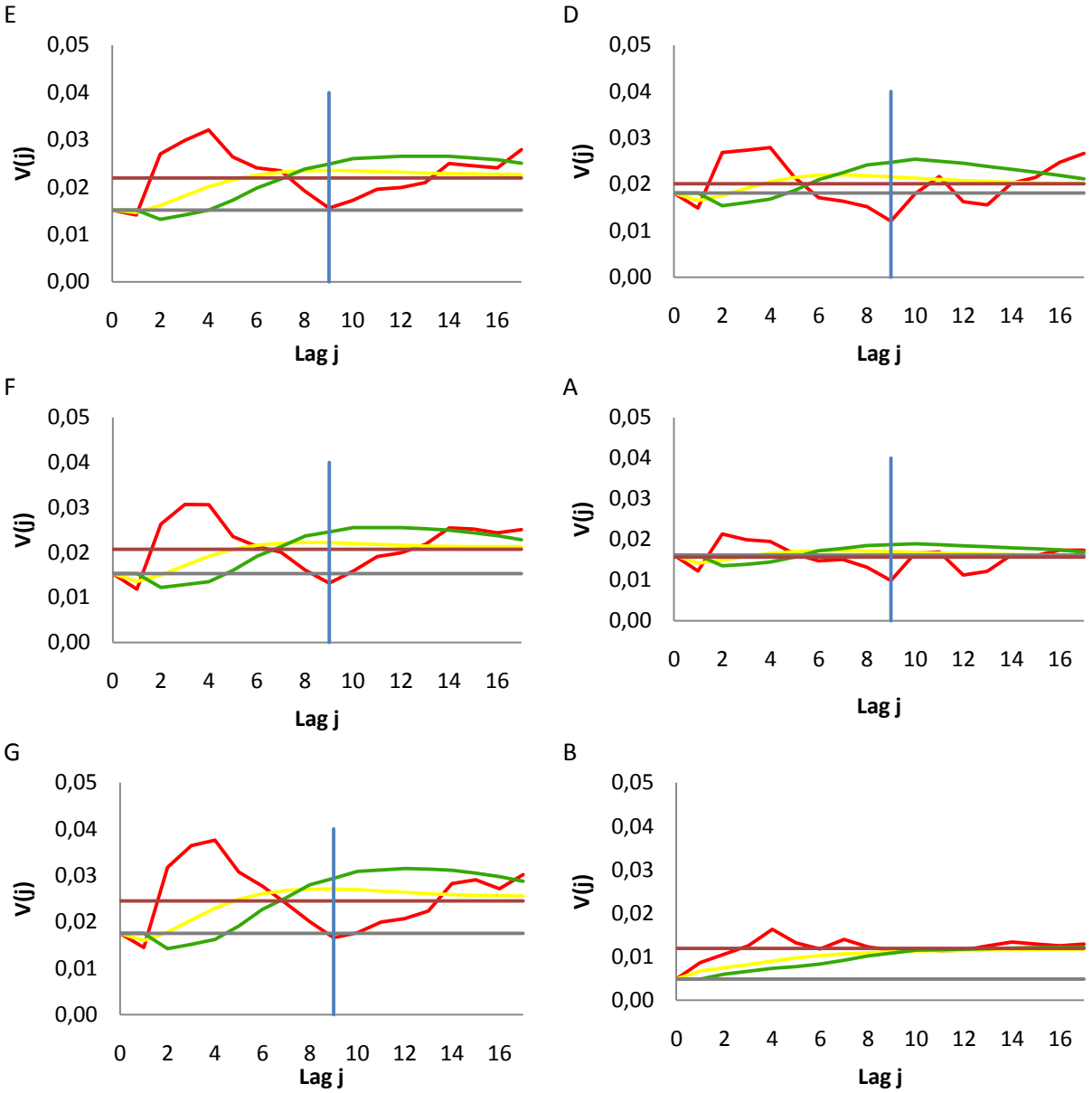

Figure 84 Synoptic presentation of experimental variograms for conductivity in 24-hour samples for sampling points E, F, G, D, A, and B

A comparison of the variograms for the six sampling points showed that the variograms were similar in structure and all were essentially flat, see Figure 84. They showed an indication of a cyclic variation of 9 days, except B, which showed no cyclic variation. The cyclic variation was most likely a pseudo-variation caused by the amount of rain in the sampling period, since no logical explanation could be found.

Comparing points before, after, and across the weir (as is done for TP), the pattern was not the same for conductivity as for TP, where there were differences according to location of the sampling point. For conductivity it was seen that all sampling points showed similar tendencies.

Point A was where (from a practical point of view) samples were taken commonly and F was the point which fulfils most of the demand in ISO 5667-10 [50]. Because of the similarities, there was no indications of that F should be a better point than A.

Nugget Effect and Sill for Conductivity in 24-hour Composite Samples

The nugget effect, sill and relative proportions for sampling points F, E, G, A, D, and B are listed in Table 36.

Table 36 Nugget effect, sill level and relative proportions for 24-hour samples from all sampling points

Sampling Point	V(0)	Sill	V(0)/Sill [%]
F	0.0153	0.0207	74
E	0.0152	0.0219	69
G	0.0175	0.0245	71
A	0.0162	0.0157	103
D	0.0181	0.0201	90
B	0.00480	0.0119	40

When comparing the values of the nugget effect for all sampling points it was found that sampling points F, E, G, A, and D were in the same range. Only sampling points B stood out.

When comparing the level of the sill only B and A were really different from the rest of the sampling points, by having significantly lower values than the rest.

The relative proportions between the nugget effect and sill were high for all sampling points, except B. For sampling point F, E, and G the values were similar, which was to expect since they were similar in structure. The reason to that A was above 100 % and B was very low were due to uncertainties in determining the nugget effect and the sill.

Comparison of Sampling Points A and C

With regards to conductivity for point A and C, see Figure 85, there was only a very minor difference.

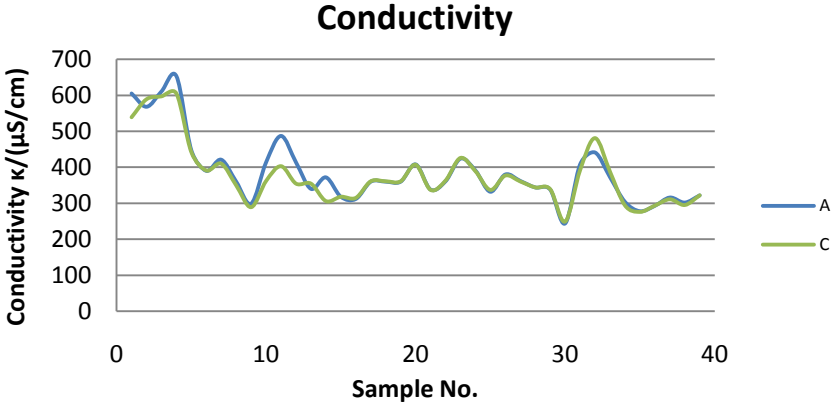

Figure 85 Sampling positions A and C with regards to measurements of conductivity in 24-hour samples. The data are corrected for extreme values and missing data

A comparison of the experimental variograms for points A and C, see Figure 86, showed that there was no clear difference between the points either, fully as expected. The blue vertical line shows the cyclic period for each sampling point.

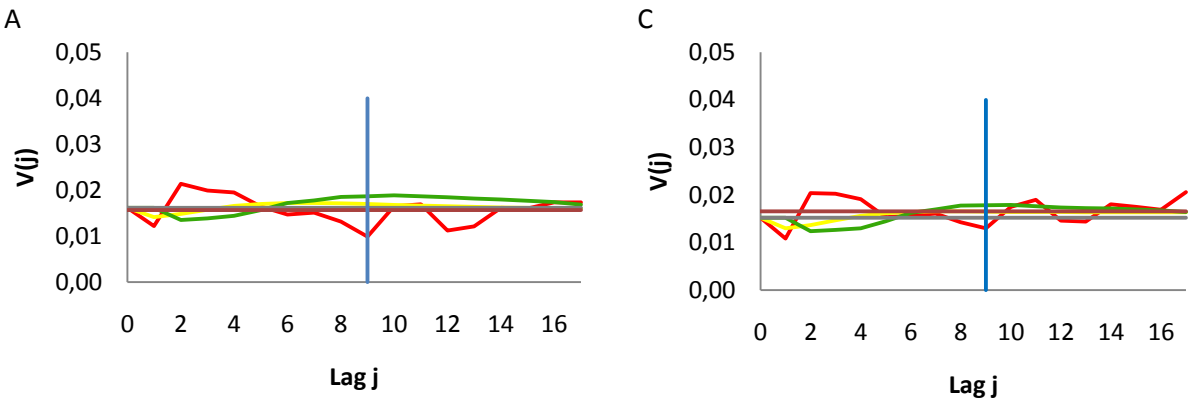

Figure 86 Experimental variograms for conductivity in 24-hour samples from sampling points A and C

It was seen that for point A and C there was a tendency of a periodicity of 9 days. The relative proportions between the nugget effect and sill was approximately equal, see table 16. Therefore it seemed to be of no importance to where the sampling took place with regards to the height of the sampling point.

Table 37 Nugget effect, sill and the ration between them for 24-hour samples from sampling points A and C

Sampling Point	V(0)	Sill	V(0)/Sill [%]
A	0.0162	0.0157	103
C	0.0152	0.0166	92

Total Sampling Error for Conductivity in 24-hour Composite Samples

For increments the TSE is a sum of seven error contributions; FSE, GSE, IDE, IEE, IPE, TFE, and CFE. In the following, the TSE for two of the seven sampling points are described. Sampling points F and A are examined here, while the other sampling points are described in Appendix 30.

Sampling Point F

A 3-D histogram was made of the TSE (The TSE calculated in Vario and shown on top of the bars in the figures is equal to $3 \cdot s_{TSE}$) with relative values for TSE as a function of different values for j and Q, see Figure 87, where for j = 1 which is equal to 24 hours, than Q = 1 is equal to 24 hours, Q = 2 is 48 hours, Q = 7 is one week.

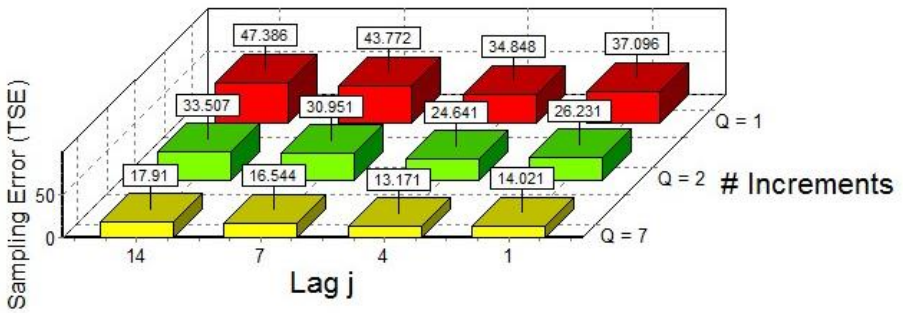

Figure 87 Total Sampling Error for measuring conductivity in 24-hour samples from sampling point F. j = lag, Q = number of increments

As expected the TSE had the smallest value for j = 1 and Q = 7 of 4.73 %. This meant that with a lag of 1 and a composite sample of seven 24-hour samples, the smallest TSE was found. As stated before for TP, this was not optimal from a practical point of view, so the sampling was done with j = 1 and Q = 1. This gave an error of approx. 12.4 %. It was seen that by increasing j the TSE increases and by increasing Q the TSE decreases. Therefore, TSE could be minimized by increasing Q, as in using more 24-hour samples for a composite sample. This was not practical nor economical, so the sampling scheme was a compromise between the price, what was practical, and what level of uncertainty was acceptable.

Sampling Point A

A 3D histogram was made of the TSE with relative values for TSE as a function of different values for j and Q, see Figure 88.

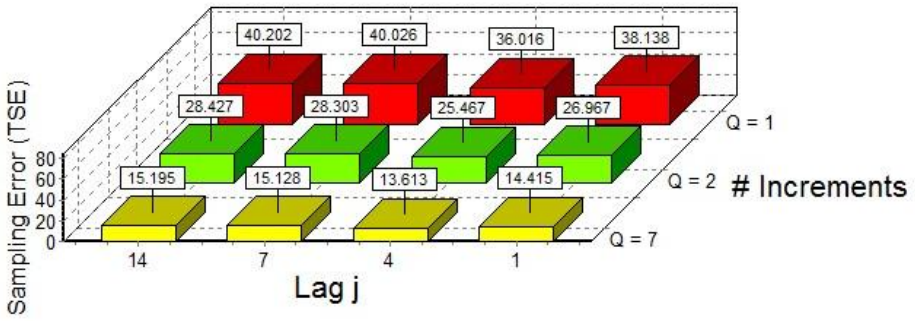

Figure 88 Total Sampling Error for measuring conductivity in 24-hour samples from sampling point A. j = lag, Q = number of increments

As expected the TSE had the smallest value for j = 1 and Q = 7 of 4.81 %. As sampling was done commonly with j = 1 and Q = 1, the TSE for point A would give an error of 12.7 %.

Comparison of Total Sampling Error for Conductivity in 24-hour Composite Samples

When comparing all the points with regard to TSE, it was seen that all sampling points, except B, have equally values of sampling errors, see Table 38. The low TSE for sampling point B was due to the previous described low value for the nugget effect and the sill.

When comparing sampling point F, which was the correct sampling point, with sampling point B, which was a possible alternative when measuring TP, it was shown that the TSE was lowest for B as so was also the 0-D - process variation. Since TSE and the 0-D - process variation were for B below those for F, B could also be an alternative when measuring conductivity.

Table 38 TSE for j = 1 and Q = 1 and 0-D process variation for 24-hour composite samples at each sampling point

Sampling point	TSE [%]	V(0)/Sill [%]
F	12.4	74
E	12.3	69
G	13.2	71
A	12.7	103
D	13.5	90
B	6.93	40
C	12.3	92

Dividing Total Sampling Error into Different Error Contributions

To recall the meaning of TSE, as previously described: the TSE is a sum of the seven errors and can be divided into two main contribution arising from the 0-D - and 1-D – process variation. The 0-D - process variation is the contribution from FSE, GSE, ISE and TAE. The 1-D – process variation is the uncertainty contribution from the process. The 1-D – process variation is the difference between the sill and nugget effect in the variogram.

An example of this was used in the variogram from sampling point F and the results for the nugget effect, sill, and relative ratio between them is listed in Table 33.

Table 39 Nugget effect, sill and relative proportional ratio between them for results from sampling point F

	24-hour samples
V(0)	0.0153
Sill	0.0207
V(0)/sill [%]	74

This showed that the 0-D – process variation for 24-hour samples accounted for 74 % of the sill and the 1-D – process variation accounted for 26 % of the sill.

Global Estimation Error for Conductivity in 24-hour Composite Samples

The GEE is as described before the summation of TAE and TSE [59].

When the sampling point F was used the results for TSE and TAE were as follows

- TSE for 24-hour sample: 12.4 %
- TAE: 0.91 %

This gave a GEE of 12.4 % for 24-hour samples.

The baseline study [59] found that the standard uncertainty could be expected to be between 24 % to 48 % depending on the parameter and level of concentration. For conductivity the standard uncertainty was not stated in the literature, but was expected to be in the same range as the parameters examined in the study (SS, COD, BOD, Total-N and TP). Therefore, a standard uncertainty of 12.4 % were below the expected range.

The conductivity measured at sampling point F in the 24-hour samples were 252 µS/cm to 484 µS/cm. The mean value was 353 µS/cm and the standard deviation was 57.0 µS/cm, see Appendix 28. The standard uncertainty of 12.4 % equals an expanded uncertainty of 24.8 % with a coverage factor of 2 (equal to 95 % confidence level, when normal probability is assumed). By applying t-testing, this resulted in a 95 % confidence range of 353 µS/cm ± 19.6 µS/cm. This states that in this range the true mean value was found with 95 % certainty.

NH_4-N in Increments

Sampling point F was chosen for the analysis of increments for the content of NH_4-N since this sampling point was the correct sampling point according to ISO 5667-10.

First a variographic analysis was made. Afterwards the increments were compared to the corresponding 24-hour composite samples sample to see if any degradation took place during the period of sampling of a 24-hour composite sample.

Variographic Analysis of NH_4-N in Increments

The increments were the same as for TP and conductivity from sampling point F, so they were extracted with a flow-distance of 7 m^3, which for the shortest time interval was approximately 3 min and for the longest time interval was approximately 12 min. For the data processing increments were analyzed for the first 15 hours before persistent rain came down. The data are listed in Appendix 31.

The analytical concentration of measurements of NH_4-N are shown in Figure 89 as the blue curve. The red curve shows the measurements corrected for extreme values, outliers, and missing data, and they are used in the variographic analysis. The points from increment no. 1 to no. 33 are left out due to errors in the measurements and malfunctions of the equipment due to the temperature of the surroundings, which was too low for the equipment to function correctly. The increments from no. 125 to no. 140 were also left out due to irregularities in the measurement equipment. It could be seen that the analytical concentration differs only slightly, but had a descending tendency.

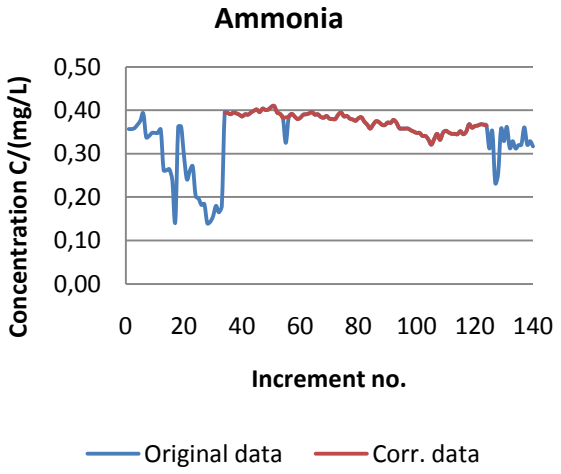

Figure 89 Ammonia analytical concentration development for increments at sampling point F

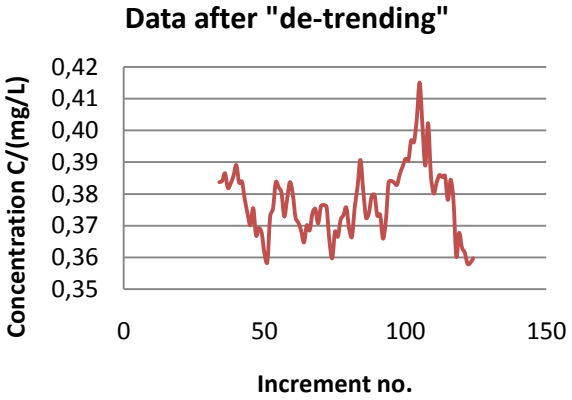

Figure 90 De-trended data for NH_4-N in increments at sampling point F. Excluded points are no. 1-33, 55, and 125-140.

The data for NH_4-N was corrected for missing data and de-trended. After “de-trending” the time series was calculated, see Figure 90, and then used for the basis for the experimental variogram which is shown in Figure 91. The time series was calculated with opposite sign than the corrected data series, this was due to that “Vario” only could calculate variograms upon positive numbers.

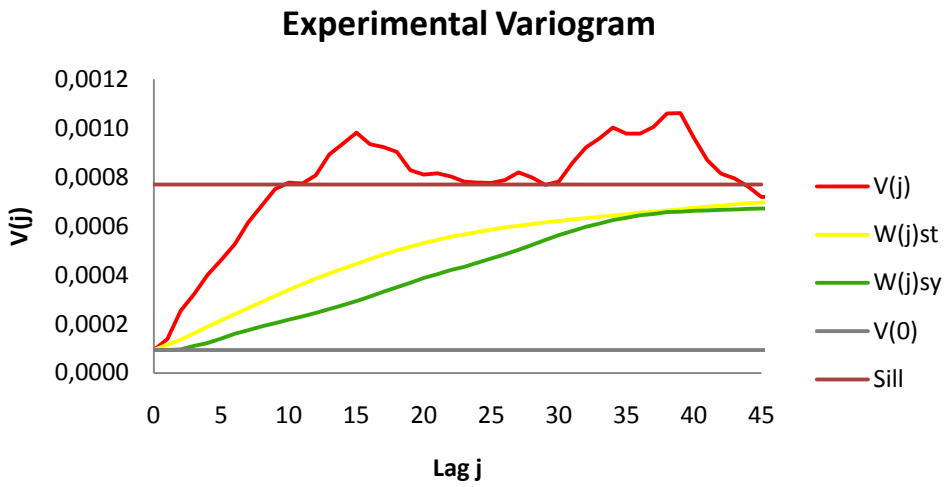

Figure 91 Experimental variogram and auxiliary functions for NH_4-N in increments from sampling point F. Data series F was subjected to linear de-trending before variogram calculation.

From the variogram there was indications of a cyclic variation of 12 increments (= 84 m^3 H_2O). The nugget effect amounted to 0.000094 and the sill was 0.00077. This allows to state that the total 0-D sampling variation corresponded to 12 % of the total process variability.

Total Sampling Error for NH_4-N in Increments

The TSE is, as stated previously, a sum of seven error contributions; FSE, GSE, IDE, IEE, IPE, TFE, and CFE.

A 3D histogram was made with relative values for TSE as a function of different values for j and Q, see Figure 92.

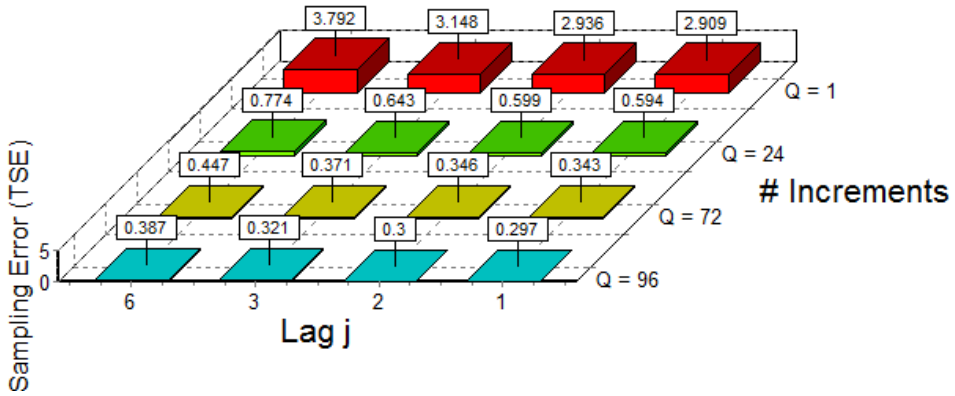

Figure 92 TSE for NH_4-N in increments from sampling point F

The smallest TSE for the measuring of NH_4-N in sampling point F was found for j = 1 and Q = 96, where the TSE was equal to 0.099 %, see Figure 92. For j = 1 and Q = 1, which was when each increment is analyzed separately, the TSE was 0.97 %.

The TSE when extracting a composite sample with more than 96 increments was in the same range for j = 1 to j = 6. When following ISO 5667-10 the sampling scheme would give rise to an TSE 0.12 % for sampling point F (j = 2 and Q = 72).

Global Estimation Error for NH_4-N in Increments

The GEE was as described before the summation of TAE and TSE [59].

When sampling point F was used for measuring NH_4-N in increments, results for TSE and TAE were as follows

- TSE for increments: 0.12 %
- TAE: 2.7 %

This gave a GEE of 2.7 % for increments.

Degradation of NH_4-N during Storage

The waste water came from household and industry and had a certain background content of NH_4. To avoid that excess NH_4 was released to the environment in high concentrations a nitrification process was used, where the NH_4 was converted to NO_3^- [58]. NH_4-N was one of the parameters in waste water which might undergo degradation during storage; therefore, it was interesting to investigate if the degradation began for the first increments during storage, when sampling of other increments to make up the final composite sample took place. Degradation could be found by extracting increments parallel to a 24-hour composite sample and measuring both NH_4-N in increments and the 24-hour composite samples. This was done by comparing the mean of the analytical concentration in increments to the analytical concentration in the composite sample. The calculations were based upon increments extracted during the entire 24 hours (276 increments) at sampling point F. The comparison and calculations were done with reservations since of the 140 samples used for variographic evaluation, the first 33 and the last 17 samples were discarded due to analytical difficulties.

The results were as follows:

- Mean concentration of 276 increments: 0.283 mg/L
- Concentration in 24-hour sample (3 measurements): 0.326 mg/L

This provided a deviation of 0.044 mg/L between the mean values. The deviation was higher than the allowed total analytical standard uncertainty to the results, which was given to 5 % for concentrations above 0.6 mg/L and to 0.03 mg/L for concentrations below 0.6 mg/L [56].

Since the mean concentration of the increments was lower than the concentration in the 24-hour composite sample, it was not possible to state if degradation had occurred.

The standard deviation for the results were as follows

- Increments: 0.090 mg/L
- 24-hour samples: 0.004 mg/L

This gave 95 % confidence intervals as follows

- Increments: 0.280 mg/L ± 0.011 mg/L (0.269 mg/L to 0.291 mg/L)
- 24-hour samples: 0.326 mg/L ± 0.010 mg/L (0.316 mg/L 0.336 mg/L)

The confidence intervals were not overlapping; therefore, it could be stated with 95 % certainty that the mean concentrations of increments were not equal to the concentration of the 24-hour composite sample. The results showed that the difference was significant, but was affected to a

unknown degree by errors in the analytical measurements and exclusion of samples as previous mentioned during the variographic evaluation.

The global estimation error was found to be 2.70 % NH_4-N. The global estimation error covers both analytical and sampling uncertainty. Since the confidence intervals were not overlapping and the deviation could not be covered by the global estimation error found in this project, the concentrations were stated to be not equal. To investigate what has happened with regards to concentration of NH_4-N in the increments further investigations are required. A first experiment could be to repeat the process to see if the results are reproducible.

Sources of Errors for Waste Water Sampling

The following list provides possible errors or factors to consider when planning the sampling procedure, and for some of them a possible consequence is given. The errors could be for both increments and 24-hour samples. Afterwards, what most likely happened in this project is discussed.

- Electronic errors: sampling is done at incorrect interval or does not occur at all
    - Error in external measuring of the flow
    - Error in sending the flow measuring signal from the external controller to the sampling equipment
    - Error in the internal electronic controllers to determine when to sample
    - Error in the internal electronic controllers to send the signal further the next sampling equipment
    - Error in the internal controllers to manage the sampling cycle
    - Lack of power
- Sampling Equipment
    - The level probe in the measuring chamber is calibrated incorrect
        - Incorrect increment volume is collected
    - Segregation in the measuring chamber before release to the storage container
        - The concentration of particulate matter becomes too high
    - The suction hose is not emptied before sampling of the next increment
        - Carry-over from one increment to another
    - The measuring chamber is not emptied between two increments
        - Carry-over from one increment to another
    - The velocity of the water in the suction hose is different from that of the water stream at the sampling point
        - Too high:
            - Suction effect occurs from the sampling intake and the concentration of particulate matter becomes too high
        - Too Low:
            - Gas bubbles in the hose occurs due to pressure drop in the sampling intake, which causes the concentration of particulate matter to be too high in the first part of the increment
    - The open/close valve from the measuring chamber to the storage container has a mal-function
        - Always closed: Overflow of the measuring container
        - Always open: The water goes directly to the storage container
    - Overflow of the storage container
        - The composite sample is not representative for the waste water stream

- The suction hose is partly/fully blocked
  - Less or no water is collected due to that the suction time expired before the measuring chamber is full
- The suction hose is too long
  - Segregation in the hose and the concentration of particulate matter becomes too low in the sample
- The hose from the measuring chamber is not placed correctly in the storage container
  - The water does not go into the storage container

- Other
  - Time proportional sampling is used when flow proportional sampling was optimal or vice versa
  - Mix up of the sampling equipments with regards to sampling point
  - Biofilm in the suction hose or measuring chamber causing contamination of the samples
  - No cleaning of the surroundings of the sampling intake if it is close to the wall/bottom of the reservoir
    - Particulate matter or the like could contaminate the sample or block the suction hose
  - Weather conditions, which could have importance for the composition of the sample
    - Rain: Downpours could be a problem, since they would diluted the waste water stream
    - High/low temperature: Degradation of the matter in waste water stream would give too low a concentration of the matter
  - Distance from water surface to sampling intake, due to shift in high and low water flow
    - If the distance is too short, there is a risk of the water surface being below the sample intake
  - Differences in turbulence in the water stream at the sampling point caused by
    - Differences between night and day
    - Differences between rain or no rain
  - Composition of the waste water
    - Suspended, colloidal or particulate matter in the water
  - Sampling period
    - Variations of the seasons with regards to both temperature and downpour
  - Sampling frequency
    - Too low: Variations in the composition of the water stream may not be found
    - Too high: The volume of the composite sample becomes larger than the volume of the storage container
  - Procedure to mass/volume reduce the sample
    - Incorrect mass/volume reducing the sample can make a representative primary sample to be non representative secondary sample
  - Pre-treatment and preparation of sample
    - Incorrect conservation, storage and preparation of sample prior to analysis
  - Training of sampler is important to ensure that the sampling equipment is placed and working correctly

All of the above mentioned errors are possible in an automated sampling procedure as the one used in this project. In this project some of the mentioned errors did occur, and some of these are described below or can be found in the journal for the sampling points in Appendix 17 - 23.

The following examples are given:

1. The water overflowed the storage container due to the size of the increment being larger than 50 ml.
2. The hose from the measuring chamber was incorrectly placed, so increments did not enter the storage container.
3. Errors in the internal electronic controllers which should send the signal further to the next sampling equipment or errors in the internal controllers to manage the sampling cycle.
4. Lack of power to the sampling equipment due to water in the wiring.

All of these errors caused the samples to be discarded and left out of the data analysis.

One thing not taken into account in this project, which may also result in errors in the sampling process, was the velocity of the water both in the water stream and in the suction hose. The velocity in the suction hose was fixed, whereas flow velocity in the water stream is changing due to variations in the flux of water passing. Another error associated with this velocity error is that the turbulence in the water at the sampling points is of importance to the actual velocity of the water in the suction hose. Large turbulence causes air bubbles to be present in the water which also are sucked up in the suction hose, and since air is lighter than water this will cause a lower velocity of the water. This may aggravate the previous mentioned error resulting from the velocity difference of the water in the water stream and the suction hose.

Sampling point A was seen to be very different from expected and from the rest of the sampling points when they were analyzed with regards to the TP content of the waste water. It was expected to see differences in sampling points across the weir and differences in C compared to A. The main error to the differences in A compared to the rest could be a mix-up in the placement of the suction hose, so A perhaps was erroneously designated as C (since C was similar to the rest of the points). This was checked twice during the sampling period and was found not to be the case. However, the differences could also be due to differences in the composition of the water, but there was no obvious reason to why there should be differences in composition of the water at sampling point A compared to D and B. The differences could be caused by some electric malfunction of the sampling equipment, but this had to be of internal nature in the sampling cycle, since A controls when the other sampling points start sampling. There had been no registration of electrical errors with the sampling equipment and the number of extracted increments and amount of water was similar to the rest of the point; therefore, this error to the representativity of the sampling procedure was equally unlikely. A reason for the cyclic period of 3 days to 4 days could be that some sector of the industry in the area cleans or flushes internal water reservoirs, and on certain days with intervals of 3 days to 4 days, lead their waste water to the waste water treatment facility.

The differences in A must perhaps be explained by other errors types. This was also the case for the cyclic variation of four days, which there is no obvious explanation as well.

Discussion

Time Resolution for Increments vs. 24-hour Samples

As previously described the "24-hour" samples are a composite of increments acquired over a period of 24 hour. The increments are extracted for each 7 m^3 H_2O, which passes the sampling locations. The resolution difference is shown in Figure 43. The time interval for increments was much smaller than that for the 24-hour samples; in fact, every single 24 hour period equals 150 to 200 increments, depending on the varying water flux. Therefore, it is not possible to compare these two sampling regimes directly, and neither does it make sense to compare their variograms directly.

The analytical concentrations for the 24-hour composite samples and the increments are shown in Figure 93. In these figures two blue boxes are delineated, which showed that the increments series was extracted only in a very narrow part of the analytical variations for the 24-hour samples. Note that the concentration intervals are not identical in these two figures.

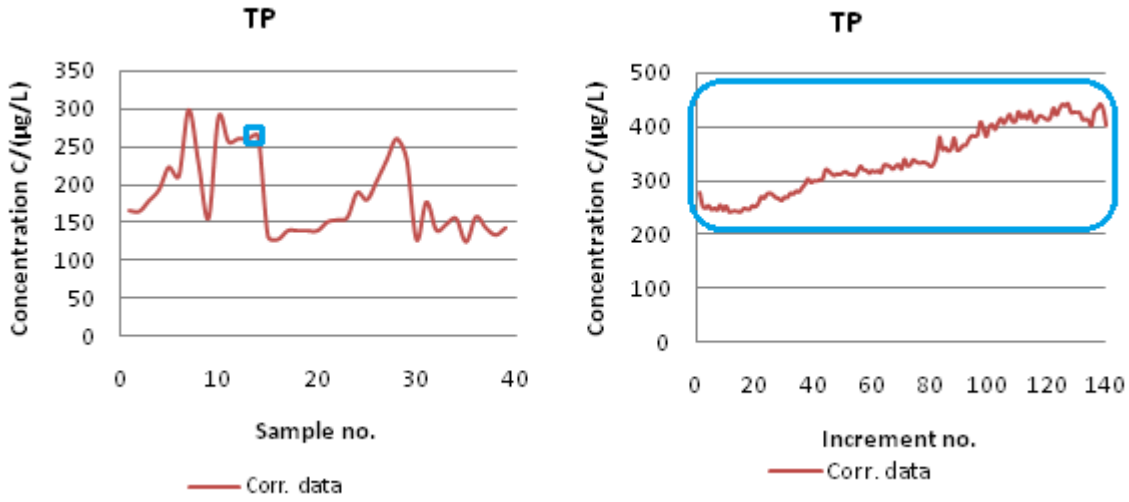

Figure 93 TP analytical concentration in 24-hour samples (left) and in increments (right). The blue boxes outline the same time interval

Variogram Comparison for Increments and 24-hour Samples

Figure 94 is a drawing of the experimental variograms for the 24-hour samples and for the increments respectively. The blue area in the variogram for 24-hour samples (top) signifies the single lag in which the variogram for the increments fits in. From the 24 hour sample variogram it is not possible to discern what really happens in the first 24 hour interval before the first sample is extracted. In the 24-hour variogram a red square indicates the interval where increments variogram may show some detailed light on the situation for j = 0 in the variogram for the 24-hour samples. This is not completely correct since the sample type and volume is not the same, see above, but it may give an *indication* of the ultimate sampling and analysis resolution possible at this vastly smaller resolution. It is, however, not physically meaningful to compare the nugget effects from two variograms with such dramatically different sample supports (sample volume differences).

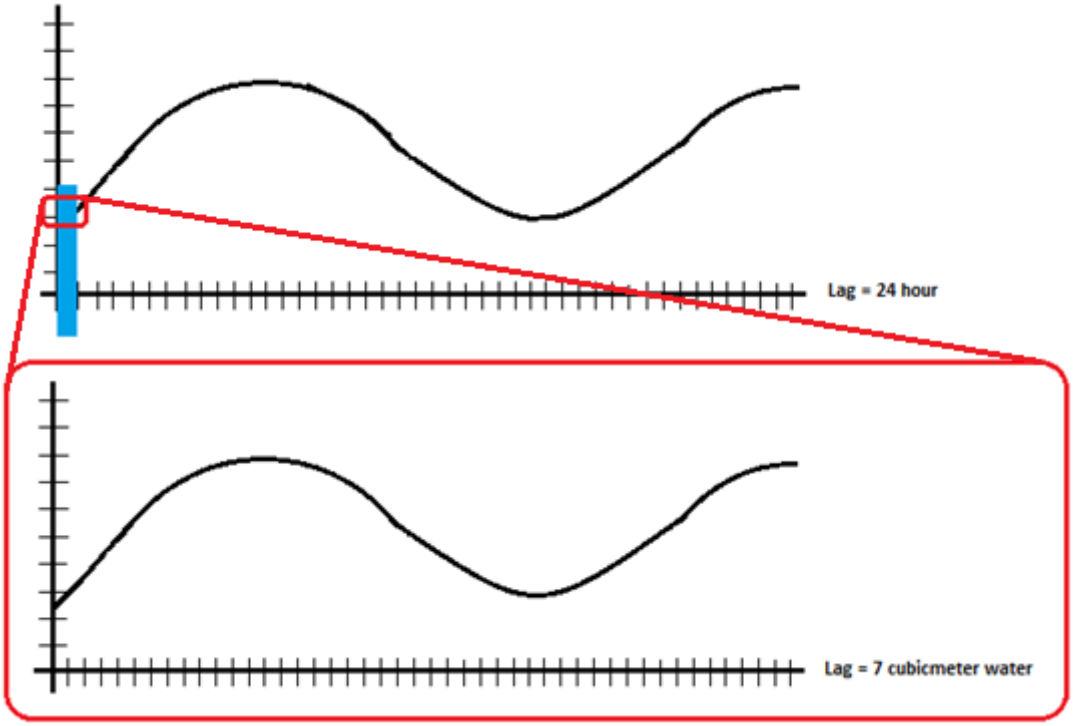

Figure 94 Experimental variogram for 24-hour samples (top) compared to that for increments (bottom)

Prerequisite for the Calculation of V(0)

To evaluate the variograms found in the present study, the concentration range and variance from the previous literature [51] and the present studies can be compared. An illustration of the principal comparison options are shown in Figure 95. The concentration range and V(0) for increments are in the same range in this and the previous studies both for TP and conductivity. The 24-hour sampling had not been evalutated before, so there was no available comparison here, but the concentration range was of the same magnitude as expected compared to previous measurements.

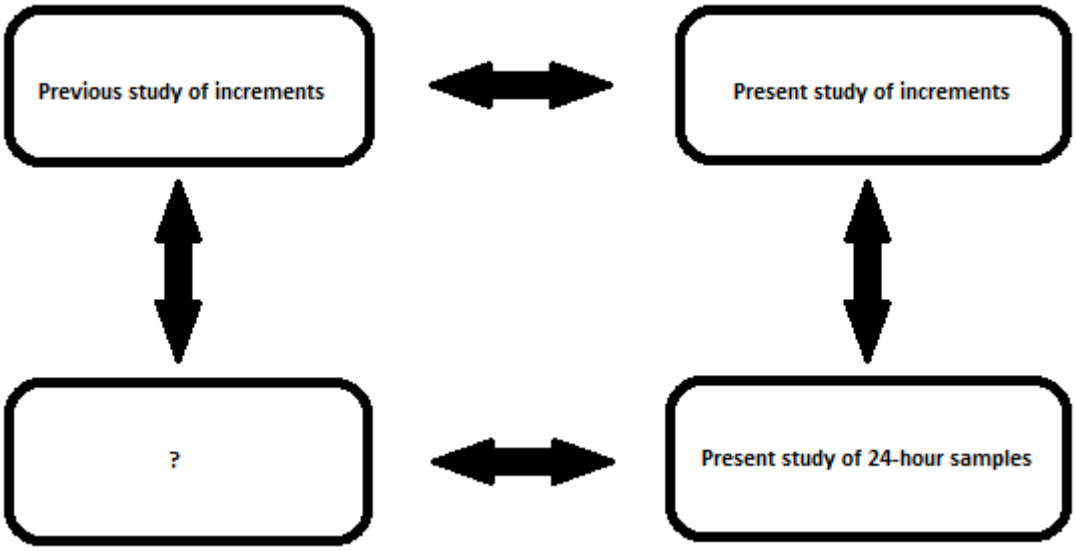

Figure 95 Illustration of possible ways to compare variograms for increments and 24-hour samples

Another way of checking the calculations of V(0) would be to compare CV % from the variogram with the mean value of the relative variance for each day at all sampling point over the entire period, see Table 40 (increments) and Table 41 (24-hour samples) in which these CV % are listed. This can be done since water passing the sampling points should be of the closely comparable type, i.e., it is equally mixed and has the same concentration over the entire sampling location.

It is seen that CV % calculated from the corrected raw data (outliers are removed, but the data are not de-trended) and from the variogram were in the same range, even though there was a minor deviation for TP in increments and for conductivity in 24-hour samples. In spite of this the relative variance and the empirical V(0) were in the same range. From this, the variograms could be said to be as expected based on the TP and conductivity measurement magnitudes.

Table 40 CV % from variogram and from calculation of relative variance for increments

	TP		Conductivity	
Sampling Points	**CV % -variogram**	**CV % - calculated**	**CV % -variogram**	**CV % - calculated**
A + F	1.88	5.56	0.447	0.536

Table 41 CV % from variogram and from calculation of relative variance for 24-hour samples

	TP		Conductivity	
Sampling Point	**CV % -variogram**	**CV % - calculated**	**CV % -variogram**	**CV % - calculated**
A – F	15.6	16.1	12.1	5.63

Total Phosphorous in Increments

Two sampling points (F and A) were compared to elucidate if there was any difference of importance for the sampling process. This was evaluated by a variographic analysis.

The variographic analysis of increments found a cyclic variation of 420 m^3, which was given by the differences in use of water during night or day. Therefore, a composite sample, where increments were extracted for a period of 24 hours, compared to one increment would give a reliable representative picture of the waste water stream. When the sampling points were compared with regards to nugget effect and sill, it was seen that the indications of that sampling point F was slightly better than sampling point A. The difference was so small that it cannot be stated with certainty if the difference was a real difference or not.

The total sampling error (TSE) for F of 0.20 % was slightly smaller than that of sampling point A of 0.23 %. But again the differences were so small that it could not be stated with certainty that there was a real difference. The variographic analysis and the total analytical uncertainty (TAE) found that the global estimation error (GEE) for the results was 0.86 % when each increment was analyzed.

Total Phosphorous in 24-hour Composite Samples

For a period of 39 days 24-hour composite samples were collected to see if the sampling location in the outlet at one waste water treatment facility had influence on the sampling uncertainty and to what degree the uncertainty were quantified.

The samples were collected from seven different points at the same outlet stream. The sampling points were individually analyzed variographically and afterwards compared before, after, and across the weir. The variographic analysis showed that sampling point A gave very different results than the

rest of the sampling points by having a unexplainable cyclic variation of 4 days. The other sampling points showed a cyclic variation of 14 days to 18 days, which could be explained by the amount rain in the first and the second part of the sampling period; therefore, the variation was said to be a pseudo-cyclic variation. Also in the variograms there was an indication of a cyclic variation of 7 days. This variation could be explained by the variations of water use during weekdays and the weekend.

When comparing the nugget effect and sill for points before, after, and across the weir it was seen that sampling point E and G were similar to F as was expected, since they were similar in structure. Sampling point D and B was expected to show similarities, but they did not. This could be because the water entering below point D in the direction of B; therefore, the water in point D was more stagnant than in point B. Sampling points A and F were expected to have some kind of similarities, but they did not mainly due to the differences in cyclic variations. An interesting aspect of the variograms was that sampling point B could be an alternative to sampling point F, since it showed similar results. Sampling point F was the sampling point which in structure met most of the guidelines from the Danish EPA and ISO 5667-10. Sampling point B was easier to sample from, since in structure the accessibility was easier.

The TSE for the best sampling point (F) gave a TSE of 12.3 %. It can be minimized by using more than one 24-hour sample and making a composite sample since the TSE for a week-sample (seven 24-hour samples combined) gave a TSE of 4.66 %. When measuring a single 24-hour sample the GEE was 12.3 %.

From a previous study [54] it was found that the standard uncertainty for TP was expected to be between 24 % to 39 %, therefore a standard uncertainty of 12.3 % was below the expected range. The standard uncertainty might be higher, since the samples extracted in this study were diluted by the heavy rainfall. The dilution might have caused the material heterogeneity to be less distinct than it would usually be.

Conductivity in Increments

Conductivity in increments were evaluated in the same way as for TP. Increments results for conductivity showed the same results as for TP, meaning a cyclic variation, which could be explained by the differences during night and day. The only difference between the results for conductivity and TP was that sampling point A was indicated to be slightly better than F when comparing the nugget effect and sill, but it could not be stated with certainty, since the difference was very small.

The TSE was in the same range for both sampling points, but the standard uncertainty arising from sampling was slightly smaller for sampling point A (0.042 %) compared to sampling point F (0.063 %). Again, the differences were so small, that it could not be stated with certainty that the differences were real. The GEE for increments from sampling point A was calculated to be 0.91 %.

Conductivity in 24-hour Composite Samples

Conductivity in 24-hour samples were evaluated in the same way as for TP. Sampling point A, which was very different for TP, was similar to all the other sampling points when measuring conductivity. The variograms showed cyclic variations of 9 days. The cycle was different from that of TP, but since conductivity and TP were related to different parameters in the waste water, the cyclic variations could both be explained by the amount of rain in the sampling period. All the variograms showed similar results, but sampling point B was slightly more stable and showed no clear cyclic variation. This indicates that B could be an alternative to the correct sampling point F, since B was not as influenced by varying amounts of rain water. Overall it could be stated that when measuring

conductivity the sampling point was not as important as for TP, since almost all of the values for nugget effect and sill were in the same range.

The TSE were in the same range for all points, so no specific sampling point stood out to be better than the rest, even though sampling points after the weir had a lower percentage of 0-D process variation when comparing the nugget effect and sill. A TSE in the range of 12.4 % gave a GEE of 12.4 % when measuring conductivity in 24-hour samples. In the previous study conductivity was not quantified with regards to sampling uncertainty.

Possible Relationship Between V(0) for Increments and 24-hour Samples

This project showed that the V(0) for increments was much smaller than V(0) for the 24-hour composite samples in which sampling point F was used as an example, Table 42. For TP there was approximately a factor 50 difference and for conductivity approximately a factor 550. The other sampling points also showed that the factor for conductivity was significantly larger than that of TP.

Table 42 V(0) for TP and conductivity and the relationship between the values. Sampling point F is used as example

	TP	Conductivity	TP/conductivity
Increments	0.00028	0.000027	10
24-hour samples	0.015	0.015	1
24-hour/increment	54	567	

The variation in concentration for TP is larger than for conductivity as seen in Figure 96 and Figure 97, again using sampling point F for comparison. TP and conductivity measurements are shown after removal of outliers and after de-trending.

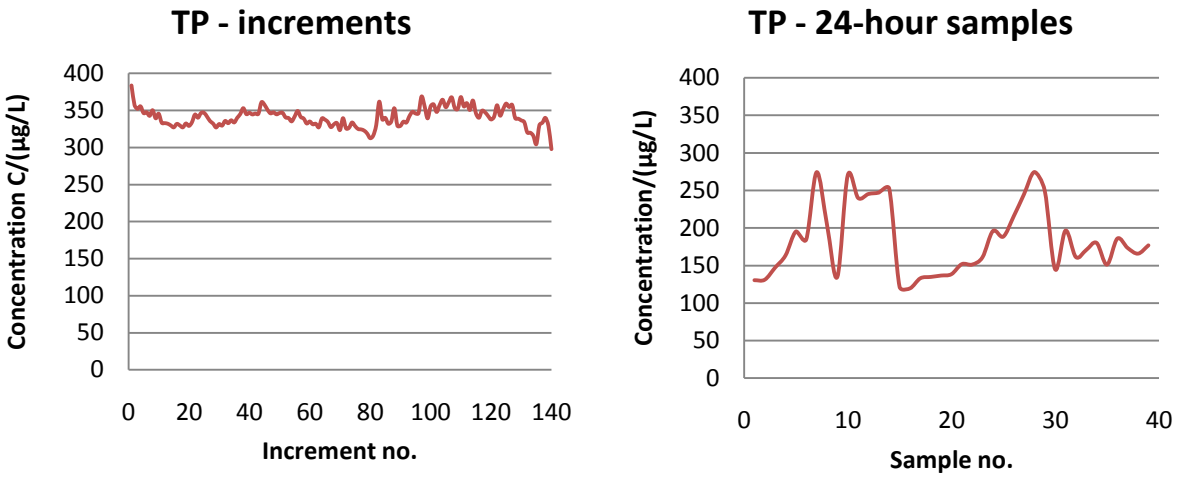

Figure 96 Analytical concentrations for TP after removal of outliers and de-trending of data from sampling point F. Left: Increments, right: 24-hour samples

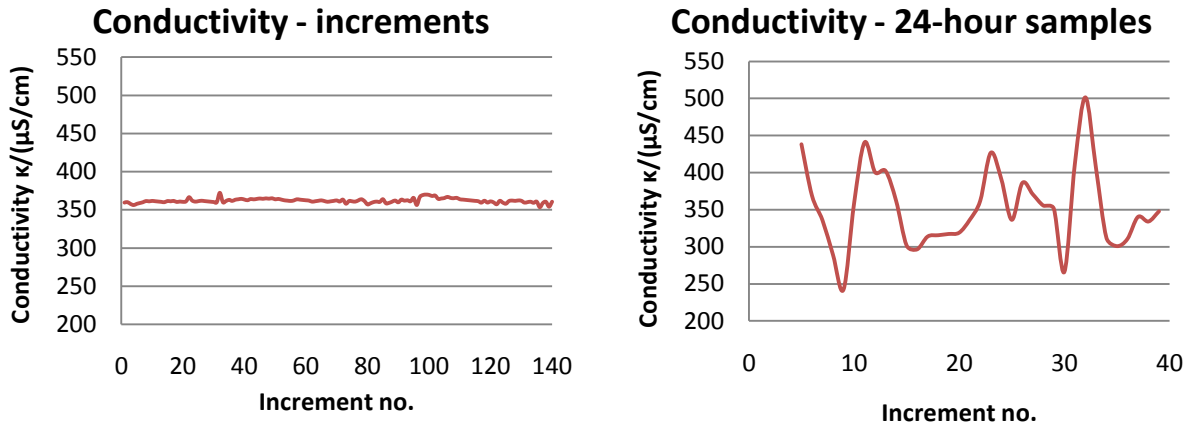

Figure 97 Measurements of conductivity after removal of outliers and de-trending of data from sampling point F. Left: Increments, right: 24-hour samples

For TP the interval was approx 300 µg/L to 385 µg/L in the increments and 125 µg/L to 275 µg/L in the 24-hour composite samples. For conductivity the interval was approx 355 µS/cm to 370 µS/cm in the increments and 250 µS/cm to 500 µS/cm in the 24-hour composite samples.

Possible Relationship Between V(0) for TP and Conductivity

When comparing the V(0) between increments for TP and conductivity it was shown that V(0) of TP was larger than for conductivity, which could be explained by the fact that the variations in TP were larger than those in conductivity. This was the same for V(0) for 24-hour samples.

On the basis of the present study, it was not possible to say anything about whether or not there was a relationship between V(0) for increments and V(0) for 24-hour samples from one parameter to another, since only two parameters were evaluated. Whether or not this linkage can be made has not previously been described.

NH_4-N in Increments

Increments from sampling point F were evaluated with regards to NH_4-N to quantify the uncertainty and compared to the related 24-hour sample to see if degradation during storage was seen. The variogram showed indication of a cyclic variation of approx 12 increments. The cyclic variation might be a pseudo-variation due to practical issues during the process of sampling and analysis. For practical reasons a "group" of increments were brought from the location of sampling to location of analysis instead of each individual increment. Therefore, some degradation may have occurred in the first increments in each group before analysis and give rise to a pseudo-cyclic variation. The number of increments in such a group varied between 10 and 15.

For NH_4-N the TSE was found to be 0.12 % when sampling increments. This gave a GEE of 2.7 % when measuring conductivity in each increment.

Since the mean concentration of all the increments extracted in the 24 hours was lower than the concentration in the 24-hour sample, it was not possible to state if degradation occurred during storage.

Conclusion

Variographic analysis of waste water emission at Bramming Waste Water Treatment Facility North on TP and conductivity (7 m^3 increments) showed cyclic variation of approx 420 m^3, which equals day-to-night compositional load variations. A composite sample taken over 24 hour is thus concluded to provide reliable results for emission monitoring.

Variographic analysis of TP and conductivity in 24-hour composite samples from seven sampling points in the outlet from the waste water treatment facility resulted in a cyclic variation of respectively 7 days and 9 days. The 7 day cycle equals the week-to-weekend variations in composition of the waste water. The indicated 9-day period remains unexplainable at the ending of the project period. There was also a cyclic variation for TP of 14 days to 18 days, this was concluded to be a pseudo-cyclic variation due to the amount of rainfall in the experimental period. The project confirms that sampling point F, directly after the weir was a representative sampling point, but an equally good alternative was sampling point B (results from these two points are similar for both TP and conductivity). The variographic analysis resulted in an estimate for the TSE for TP and conductivity at sampling point F as 12.3 % and 12.4 % respectively, compared to which the TAE was insignificant for both parameters.

Variographic analysis of NH_4-N in increments from sampling point F showed indication of a cyclic variation of approx 12 increments, which could be explained as a pseudo-variation due to practical issues during the process of sampling and analysis. It was not possible to investigate to which degree degradation of NH_4-N was occurring during the sampling period of 24 hours.

Perspective

Optimal Sampling Outline

The perspective of this project was to come up with the optimal sampling procedure, which could be used at all facilities. This is not possible, due to all the different factors, which is of importance in a sampling process. Some of the important factors are the composition of the waste water, the amount of water and the flow velocity in the water stream. Als, the structure of the sampling points is of importance; the distance to walls and bottom and/or weir, the possibility of turbulence in the water stream and the ease to which it is to reach the sampling point.

The experimental setup used in this project can with alterations and in a reduced form be used as a inspiration for facilities which are similar in structure to that of Bramming Nord. This meaning that the water enters in a reservoir and passed a weir followed by a point where there is large turbulence in the water stream. The reduction in sampling points in the experimental setup and finding the optimal sampling point can be done on the basis of an evaluation of the structure of the facility and then comparing only two or three possible sampling points to find the one which gives a representative sampling process. This should preferably be done for each waste water treatment plant to find a representative sampling point in each case.

When the possible sampling points are identified a variographic experiment should be carried out for a period of minimum twice the time period between two scheduled samplings. This meaning that for a facility like Bramming Nord, which is characterized to take 12 samples each year (one per month) the period should be at least 62 days. This will give a representative sampling point to describe the

waste water stream. It will also give a better determination of a cyclic variation in the composition of the water, so sampling could be scheduled around the cyclic variation.

When the representative sampling point is identified, and if it is possible to sample each day over a period of a year, the variographic analysis in addition to the cyclic variation will also give findings for the season variation. This could show if one sample per month gives a representative picture of the water or if in some periods there should be extracted more samples.

The evaluation of the experimental variogram and the TSE will give the optimal combination of j and Q for each sampling point. This could help to plan the optimal sampling schedule for the waste water treatment facility. The time period should be at least 62 days to ensure enough degrees of freedom in the calculation of the variogram and TSE to be able to count on the results when j and Q have high values.

On the basis of the data for the time period of 39 days in this project it is only possible in "Vario" to simulate TSE for 24-hour composite samples for j in the interval; $1 < j < 19$. If one had 24-hour composite samples for a longer time period it could be possible to simulate the TSE based upon the demands the waste water treatment plants are subjected to from the Danish Agency of Spatial and Environmental Planning (*By- og Landskabsstyrelsen*). The levels of j needed between samples and for simulation of TSE are listed in Table 43.

Table 43 Levels of j (lag) needed between samples and for simulation of TSE according to demands from BLST

Demand	$j_{between\ samples}$	$j_{simulation}$
6 samples per year; 1 each second month	60	120
12 samples per year; 1 per month	30	60
24 samples per year; 2 per month	15	30

From Table 43 it can be seen that for the smallest waste water treatment plants there is needed at least 120 days of sampling to make a simulation to see if the demand of only one sample each second month gives an acceptable TSE. For the largest plants the demand is 2 samples per month, and this demands sampling of at least 30 days to see if it gives an acceptable TSE.

Q is the number of 24-hour composite samples to make up a composite sample, therefore for this simulation Q should always equal 1. This is because all the 24-hour samples are measured as one sample each time and not made up of more samples.

Reproducible Findings

For Bramming Nord it could be interesting to repeat the experimental setup for sampling points A, B and F. Sampling points A to see if the findings, which were very different from the rest of the sampling points, were reproducible or if they were caused by some unexpected and as yet unexplainable factors. Sampling points B and F, to see if the findings were reproducible, but also to see if B was really an alternative to F.

Outlet vs. Influx

The outlet water stream is most important, since the water is directly discharged to the surrounding environment, but it could also be interesting to make a sampling process in the influx water stream. This could be interesting when the cleaning process was to be evaluated to see what kind of treatment and to what degree treatment is needed. Therefore, a setup of sampling point(s) in the influx and outlet should be evaluated to see if the cleaning was optimal. The evaluation of the outlet

would show if the cleaning of the water was sufficient and the evaluation of the influx would tell what kind of treatment is needed.

Lifting Height

As a supplement to this study of evaluating the importance of the location of the sampling point, the lifting height could also be evaluated. In ISO 5667-10 [50]and "*Teknisk anvisning for punktkilder*" [49] stated that the lifting height of the increments from the sampling intake to measuring chamber should be no higher than 3 m. To evaluate the importance of the lifting height and the uncertainty contribution to the results, an experimental setup like the following could be made which covers item no. 3b in the first presented problem statement:

3. Which variations in the composite sample can be expected with regards to the used equipment and its use?
    b. Lift of samples to required height – normal altitude of sample unit is 1 m to 3 m [49]

Lifting Height of Increments until Delivery Point

The lifting height could be evaluated by taking composite samples from a time period of 3 hours collected over a period of 48 hours. This should be repeated with three different height of delivery point.

The experiment could be done by using three sampler units, where the sampling points should be located as close together as found acceptable to obtain the same concentrations of the parameters in question for all composite samples within acceptable deviations. The delivery point should be placed in different heights to find the uncertainty arising from varying heights to lift the increments

Data analysis would be based upon comparing the timeseries and the standard deviations of the composite samples. The dataset would consist of 16 timeseries with three composites samples from each timeseries.

This experiment would indicate if segregation in the hose gives rise to measurable excess variability in the concentrations of the composite samples, and show if the lifting height is of importance for the representativity in the sampling process. This would expectedly give rise to different V(0)/sill proportions.

Bibliography

1. R. Bauer, H. Nieuwoudt, F. Bauer, J. Kossmann, K. Koch and K. H. Esbensen; Spectroscopy for Grape and Wine Analysis; Analytical Chemistry; 2008, pp. 1371 - 1379
2. V. Baeten and P. Dardenne; Spectroscopy: Developments in Instrumentation and Analysis; Grasas y Aceites; 2002, vol. 53, pp. 45 – 63
3. D. W. Lachenmeier, R. Godelmann, M. Steiner, B. Ansay, J. Weigel and G. Krieg; Rapid and mobile determination of alcoholic strength in wine, beer and spirits using a flow-through infrared sensor; Chemistry Central Journal, 2010, vol. 4
4. P. L. Mahia, J. S. Gándara and P. P. Losada; Validation of ethanol determination in alcoholic beverages by infrared spectrophotometry using orthogonal and derivative functions to correct for water absorption; Vibrational Spectroscopy; 1992, vol. 3, pp. 133 – 138
5. M. Gallignani, S. Garrigues and M. de la Guardia; Direct Determination of Ethanol in all Types of Alcoholic Beverages by Near-Infrared Derivative Spectroscopy; Analyst; 1993, vol. 118, pp. 1167 – 1173
6. R. Cocciardi, A. A. Ismail and J. Sedman; Investigation of the Potential Utility of Single-Bounce Attenuated Total Reflectance Fourier Transform Infrared Spectroscopy in the Analysis of Distilled Liquors and Wines; Journal of Agricultural and Food Chemistry; 2005, vol. 53, pp. 2803 – 2809
7. D. W. Lachenmeier; Rapid quality control of spirit drinks and beer using multivariate data analysis of Fourier transform infrared spectra; Food Chemistry; 2007, vol. 101, pp. 825 – 832
8. Y. Shao and Y. He; Nondestructive measurement of the internal quality of bayberry juice using Vis/NIR spectroscopy; Journal of Food Engineering; 2007, vol. 79, pp. 1015 – 1019
9. L. Saavedra, A. Garcia and C. Barbas; Development and validation of a capillary electrophoresis method for direct measurement of isocitric, citric, tartaric and malic acids as adulteration markers in Orange juice; Journal of Chromatography A; 2000, vol. 881, pp. 395 – 401
10. E. Lopez-Tamames, M. A. Puig-Deu, E. Teixera and S. Buxadera; Organic acids, sugars, and glycerol content in white winemaking products determined by HPLC: relationship to climate and varietal factors; American Journal of Enology Viticulture; 1996, vol. 47, pp. 193 – 198
11. A. Urtubia, J. R. Pérez-Correa, M. Meurens and E. Agosin; Monitoring large scale wine fermentations with infrared spectroscopy; Talanta; 2004, vol. 64, pp. 778 – 784
12. R. Schindler, R. Vonach, B. Lendl and R. Kellner; A rapid automated method for wine analysis based upon sequential injection (SI)-FTIR spectrometry; Fresenius Journal of Analytical Chemistry; 1998, vol. 362, pp. 130 - 136
13. M. A. Brescia, I. J. Kosir, V. Caldarola, J. Kidric, and A. Sacco; Chemometric Classification of Apulian and Slovenian Wines Using 1H-NMR and ICP-OES Together with HPICE Data; Journal of Agricultural and Food Chemistry; 2004, vol. 51, pp. 21 - 26
14. I. Moret, G. Scarponi and P. Cescon; Chemometric characterization and classification of five venetian white wines; Journal of Agricultural and Food Chemistry; 1994, vol. 42, pp. 1143 – 1153
15. F. H. Larsen, F. van den Berg, and S. B. Engelsen; An exploratory chemometric study of 1H-NMR spectra of table wines; Journal of Chemometrics; 2006, vol. 20, pp. 198 – 208
16. M. Gallignani, S. Garrigues and M. de la Guardia; Derivative Fourier transform infrared spectrometric determination of ethanol in alcoholic beverages; Analytica Chimica Acta, 1994, vol. 287, pp. 275 – 283
17. M. Urbano-Cuadrado, M. D. Luque de Castro, P. M. Pérez-Juan, J. Garcia-Olmo and M. A. Gómez-Nieto; Near infrared reflectance spectroscopy and multivariate analysis in enology –

Determination or screening of fifteen parameters in different types of wines; Analytica Chimica Acta, 2004, vol. 527, pp. 81-88
18. P. L. Mahia, J. S. Gándara, and P. P. Losada; Validation of ethanol determination in alcoholic beverages by infrared spectrophotometry using orthogonal and derivative functions to correct for water absorption; Vibrational Spectroscopy, 1992, vol. 3, pp. 133 – 138
19. R. Nagarajan, A. Gupta, R. Mehrotra and M. M. Bajaj; Quantitative Analysis of Alcohol, Sugar, and Tartaric Acid in Alcoholic Beverages Using Attenuated Total Reflectance Spectroscopy, Journal of Automated Methods and Management in Chemistry; vol. 2006, pp. 1- 5
20. Commission Regulation (EC) No 753/2002 of 29 April 2002 laying down certain rules for applying Council Regulation (EC) No 1493/1999 as regards the description, designation, presentation and protection of certain wine sector products
21. Commission Directive 87/250/EC of 15 April 1987 on the indication of alcoholic strength by volume in labelling of alcoholic beverages for sale to the ultimate consumer
22. S. K. Schreyer; Determination of Ethanol in Wine; available 17.05.2010 online through www.polychromix.com/PDF/wine.pdf
23. J. Hirsch and L. Tenkl; FT-NIR Analysis of Wine; available 17.05.2010 online through www.thermo.com/eThermo/CMA/PDFs/Articles/articlesFile_1192.pdf
24. M. Blanco and D. Valdés; Influence of temperature on the predictive ability of near infrared spectroscopy models; Journal of Near Infrared spectroscopy; 2004, vol. 12, pp. 121 – 126
25. D. Cozzolino, L. Liu, W. U. Cynkar, R. G. Dambergs, L. Janik, C. V. Colby and M. Gishen; Effect of temperature variation on the visible and near infrared spectra of wine and the consequences on the partial least square calibrations developed to measure chemical composition: Analytica Chimica Acta; 2007, vol. 588, pp. 224 – 230
26. H. Abe, C. Iyo and S. Kawano; A study on the universality of a calibration with sample temperature compensation; Journal of Near Infrared Spectroscopy; 2000, vol. 8, pp. 209 – 214
27. F. D. Barboza and R. J. Poppi; Determination of alcohol content in beverages using short-wave near-infrared spectroscopy and temperature correction by transfer calibration procedures; Analytical and bioanalytical chemistry; 2003, vol. 377, pp. 695 – 701
28. H. Maeda, Y. Wang, Y. Ozaki, M. Suzuki, M. A. Czarniecki and M. Iwahashi; A near-infrared study of hydrogen bonds in alcohols – comparison of chemometrics and spectroscopic analysis; Chemometrics and Intelligent Laboratory Systems; 1999, vol. 45, pp. 121 – 130
29. M. A. Czarnecki and Y. Ozaki; The temperature-induced changes in hydrogen bonding of decan-1-ol in the pure liquid phase studied by two-dimensional Fourier transform near-infrared correlation spectroscopy; Physical Chemistry Chemical Physics, 1999, vol. 1, pp. 797-800
30. W. G. Hansen, S. C. C. Wiedemann, M. Snieder and V. A. L. Wortel; Tolerance of near infrared calibrations to temperature variations; a practical evaluation; Journal of Near Infrared Spectroscopy; 2000, vol. 8, pp. 125 – 132
31. C. K. Hansen; Arbeidsledige ble vingründere; Nordlys; available 05.08.2006 online through www.nordlys.no/nyheter/article2224367.ece
32. Guttorm Isaksen, De 5 Vinmakeran, Tromsø, Norway
33. De 5 Vinmakeran; Forretningsplan for De 5 Vinmakeran AS; 09.06.2009
34. Alessandro Spatafora; Vinification Protocol; Poggibonsi, Siena, Italy
35. De 5 Vinmakeran; Product Presentations; available 17.05.2010 online through www.de5.no
36. K. Henriksen and G. K. Bjørn; Sorter og kloner af rabarber - Sortsforsøg med rabarber ved Årslev 1997-1998; DJF rapport havebrug nr. 31, Januar 2004; available 19.05.2010 online through http://www.agrsci.dk/djfpublikation/djfpdf/djfha31.pdf
37. P. S. Holoway; Managing Wild Bog Blueberry, Lingonberry, Cloudberry and Crowberry Stands in Alaska; University of Alaska Fairbanks; August 2006

38. M. V. Moreno-Arribas and M. C. Polo; Wine Chemistry and Biochemistry; Springer, 2009, ISBN 0-387-74116-1, 736 pages
39. P. Ribéreau-Gayon, Y. Glories, A. Maujean and D. Dubourdieu; Handbook of Enology vol. 2: The Chemistry of Wine Stabilization and Treatments; John Wiley & Sons Ltd., 2006, ISBN 0-471-97363-7, Chapter 1
40. Professor Kim H. Esbensen, Esbjerg Institute of Technology Aalborg University
41. E. Skibsted; PAT and Beyond; Ph.D. dissertation; University of Amsterdam; 2005; available 23.05.2010 online through http://dare.uva.nl/record/169022
42. A. Savitsky and M. J. E. Golay; Smoothing and Differentiation of Data by Simplified Least Squares Procedures; Analytical Chemistry; 1964, vol. 36, no. 8, pp. 1627 - 1639
43. K. H. Esbensen; Multivariate Data Analysis - in practice; 5th ed.; CAMO process AS, ISBN 82-993330-3-2, 598 pages
44. T. Næs, T. Isaksson, T. Fearn and T. Davies; A user-friendly guide to Multivariate Calibration and Classification; NIR Publications, 2002, ISBN 0-9528666-2-5, 344 pages
45. K. Beebe, R. J. Pell and M. B. Seasholtz; Chemometrics – A Practical Guide; John Wiley & Sons, 1998, ISBN 0-471-12451-6, 348 pages
46. K. H. Esbensen and P. Geladi; Principles of Proper Validation: use and abuse of re-sampling for validation; Journal of Chemometrics; 2010, vol. 24, pp. 168 – 187
47. P. Jørgensen, J. G. Pedersen, E. P. Jensen and K. H. Esbensen; On-line batch fermentation process monitoring (NIR) – introducing ”biological process time”; Journal of Chemometrics; 2004, vol. 18, pp. 81 - 91
48. Waste Water Engineering: treatment and reuse; Tchobanoglous, G., Burton, F. and Stensel, H. D.; McGraw-Hill; 4th edition, 2003, ISBN 0070418780, 1848 pages
49. Teknisk anvisning for punktkilder; Miljøstyrelsen, version 3, October 2004
50. DS/ISO 5667-10; Water Quality – Sampling – Part 10: Guidance on sampling of waste waters; 1st ed. 2004
51. By- og Landskabsstyrelsens Reference Laboratorium; Bestemmelse af usikkerhed ved automatisk prøvetagning af spildevand – II. Variografisk analyse på flere renseanlæg; November 2007
52. Miljøstyrelsens Reference Laboratorium; Bestemmelse af usikkerhed ved automatisk prøvetagning af spildevand – I. Pilotundersøgelse af variografisk analyse; May 2007
53. C. Dehlendorff; Robust estimation af nugget effect i spildevandsprøver; IMM Statistical Consulting Center, Technical University of Denmark; Report 16th March 2007
54. DHI – Institut for Vand og Miljø (for Eurofins A/S); Usikkerhed/fejl ved automatisk prøvetagning af spildevand – litteraturundersøgelse og forsøgsskitse; Report February 2003, rev. November 2005
55. Hans Jæger, Manager of Bramming Nord Renseanlæg
56. BEK nr. 1353 af 11/12/2006; Bekendtgørelse om kvalitetskrav til miljømålinger udført af akkrediterede laboratorier, certificerede personer m.v.
57. Dansk Meterologisk Institut (DMI); available 11.01.2010 online through http://www.dmi.dk/dmi/vejret-i-danmark-november_2009
58. L. Winther, J. J. Linde-Jensen, I. Mikkelsen, H. T. Jensen and M. Henze; Spildevands teknik; Polyteknisk Forlag 1978, ISBN 87-502-0479-3, 445 pages
59. K. H. Esbensen, H. H. Friis-Petersen, L. Petersen, J. B. Holm-Nielsen and P. P. Mortensen; Representative process sampling – in practice: Variographic analysis and estimation of total sampling errors (TSE); Chemometrics and Intelligent Laboratory Systems; 2007, vol. 88, pp. 41-59
60. IT Tutor, Perkin Elmer
61. L. Petersen and K. H. Esbensen; Representative process sampling for reliable data analysis – a tutorial; Journal of Chemometrics; 2005, vol. 19, pp. 625-647

62. P. M. Gy; Sampling for Analytical Purposes; John Wiley & Sons; 1998, ISBN 0471979562, 172 pages
63. K. Bakeev; Process Analytical Technology; 2nd ed., Blackwell Publications, 2010; ISBN 0470722077, 576 pages
64. L. Petersen; Pierre Gy's Theory of Sampling (TOS) – in Practice: Laboratory and Industrial Didactics; Ph.D. Thesis; January 2005; Aalborg University Esbjerg
65. L. Petersen, C. K. Dahl and K. H. Esbensen; Representative mass reduction in sampling—a critical survey of techniques and hardware; Chemometrics and Intelligent Laboratory Systems; 2004, vol. 74, pp. 95– 114
66. L. Petersen, P. Minkkinen and K. H. Esbensen; Representative sampling for reliable data analysis: Theory of Sampling, Chemometrics and Intelligent Laboratory Systems; 2005, vol. 77, pp. 261-277
67. F. F. Pitard; Pierre Gy´s Theory of Sampling and C. O. Ingamell´s Poisson Process Approach; Doctoral Thesis; June 2009, 309 pages
68. Polychromix MEMS NIR – How does this technology work? AN99-MEMS-Technology Overview; available 26.04.2010 online through www.polychromix.com
69. S. D. Senturia; MEMS-Enabled Products: A Growing Market Segment; available 26.04.2010 online through www.polychromix.com

Table of Content - Appendix

Appendix 1 – The Theory of Infrared Spectroscopy

Spring Movements

A simple diatomic molecule can be described as a spring with a force constant *k* attached to two balls of mass *m*, see Figure 98.

Figure 98 Model of a simple molecule [60]

The spring has zero potential energy at equilibrium with the length d. If the spring is stretched or compressed the potential energy increases along a parabola, which is called the harmonic potential, see Figure 99.

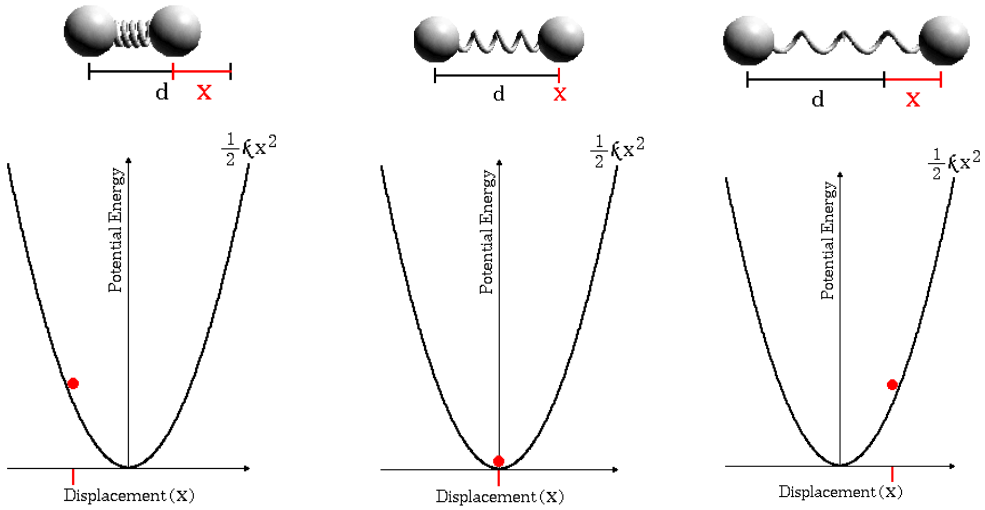

Figure 99 The harmonic potential of a simple molecule [60]
Left: compressed molecule; centre: equilibrium; right: stretched molecule

The force constant of the spring and the mass of the atoms are related to the vibration frequency v by the following equation [60]

$$\nu = \frac{1}{2\pi}\sqrt{\frac{k}{m}}$$

From the equation it is seen that at a larger force constant the frequency will be higher, and at a lower force constant the frequency will be lower. An increase or decrease in mass will result in a lower or higher frequency, but the potential energy will remain constant, since the mass has no influence to the potential energy.

The total energy for the molecule vibration is equal to the potential energy at the stretched or compressed position. If the spring is stretched to a length of x_{max} the total energy is

$$E = \frac{1}{2}k\ x_{\max}^2$$

This simple model of a diatomic molecule indicates that a molecule can vibrate at any total energy. This is not completely true and therefore we have to use quantum mechanics to get the accurate model. [60]

Vibration Quantum Mechanics

Quantum mechanics predicts the same relationship between mass of the molecules, force constant of the spring, and vibration frequency as the simple model, but the energy is quantized and therefore the molecules may vibrate only at energy levels which fit the following equation [60]

$$E_n = (n + \frac{1}{2})\ h\ \nu \qquad \text{n=0,1,2,3...}$$

where h = Planck's constant ($6.626 \cdot 10^{-34}$ J·s)

Energy Absorption

From the quantum mechanics we get that the molecules may only absorb or emit light with energy equal to the spacing between two levels of potential energy. According to the selection rule these transitions can only occur from one level to the next higher or lower level (Δn = ±1), see Figure 100.

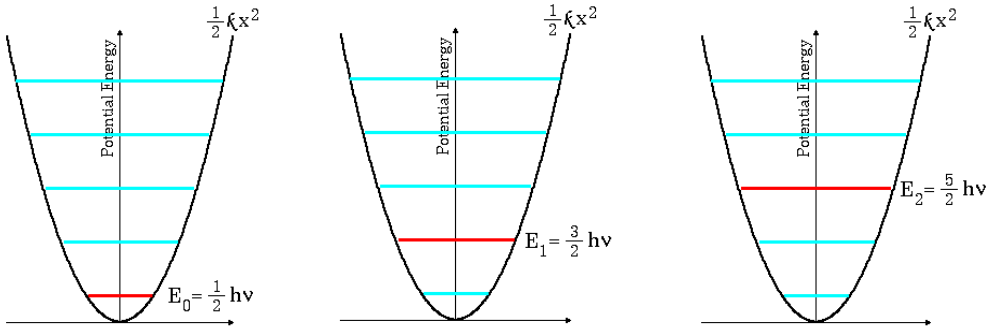

Figure 100 Schematic overview of the selection rule [60]

Due to the selection rule the molecule can only absorb light with energy level equal to *hν* and therefore the molecule will have a single peak in an infrared spectrum where the frequency correspond to the energy, see Figure 101. At a higher frequency there is a larger spacing between the energy levels which moves the peak to the left. At lower frequency the spacing is smaller and the peak moves to the right. [60]

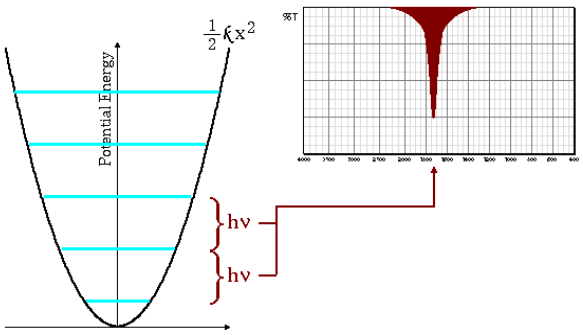

Figure 101 Infrared spectrum of a simple molecule [60]

The example is a simple model and the actual spectrum is more complicated than described in the above. The actual model and spectrum is better described by an an-harmonic potential. This is due to

the fact that when two molecules are forced together they will repel more strongly than a spring, and when they are pulled apart, the bond will break. In the more realistic model with the an-harmonic potential, the energy levels are only equal spaced when the potential is like the harmonic potential, see Figure 102.

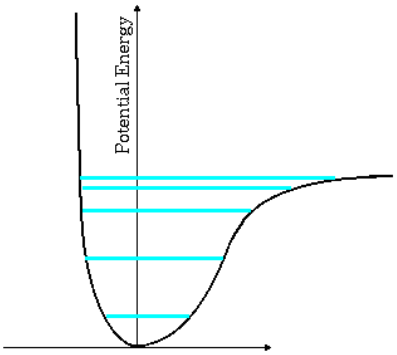

Figure 102 The an-harmonic potential [60]

For the more realistic model the selection rule is not rigorously true because a transition with $\Delta n = +2$ is also happening. This transition is called an overtone and responds to $\Delta E = 2 \cdot h\nu$. The band for the overtone appears at a little less than twice the frequency of the fundamental band, see Figure 103. The band for the overtone is less intense that the fundamental band and often it is so low in intensity that it cannot be found. [60]

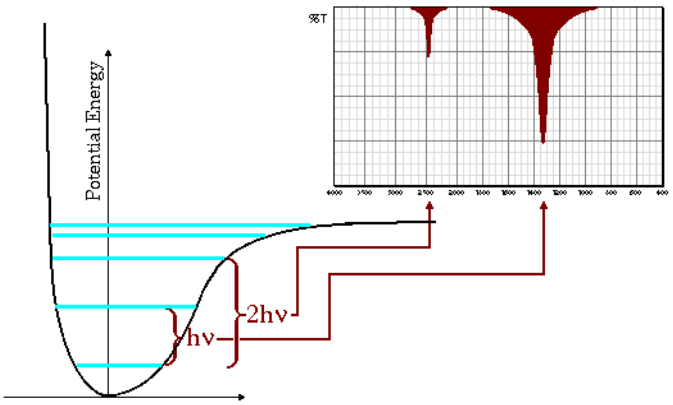

Figure 103 The fundamental band and the overtone band (~ 2 hv) in the IR-spectrum [60]

In order for the molecule to absorb light the molecular dipole charge much change when the transition occurs. H_2, which have a zero dipole, does not absorb infrared light. HCl has a change in the dipole charge when it stretches. If the dipole aligns with the electric field of a beam of the light, the light is absorbed. This will only occur when the frequency of the light is equal to the potential energy level for the stretching in the HCl molecule. [60]

The above mentioned infrared spectrum is for a simple diatomic molecule; molecules with more than two atoms have more complicated infrared spectra.

Description of Vibrations

In the following the vibrations in H_2O, CO_2, and pentane (C_5H_{12}) are described. [60]

H_2O

For H_2O the vibrations can be broken up into three simple motions, normal modes. For H_2O the normal modes are bend, symmetric stretch, and anti-symmetric stretch, see Figure 104. Each of the normal modes is associated to a simple potential energy curve and energy levels. Each normal mode has a change in dipole moment when it vibrates and therefore they absorb infrared light. When H_2O has three different normal modes there should also be three peaks in the infrared spectrum, see Figure 104.

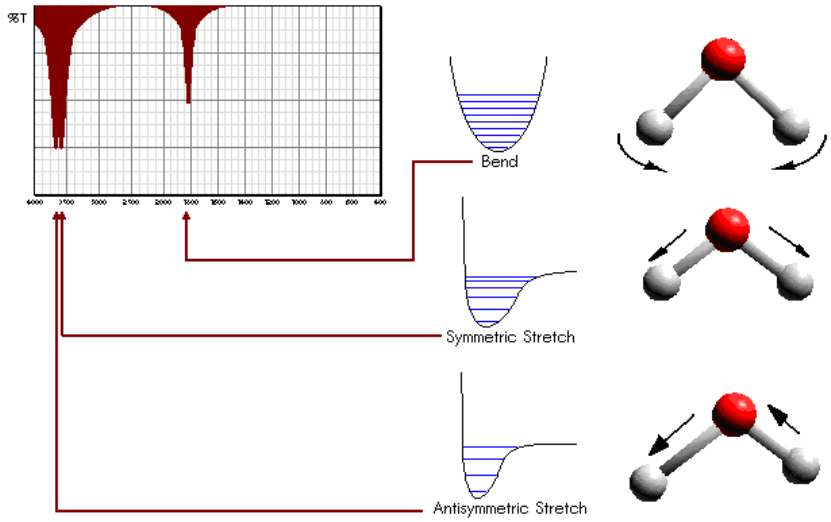

Figure 104 Vibration types and IR-spectrum of H_2O [60]

CO_2

CO2 is a linear molecule with four normal modes: in-plane and out-of-plane bends, symmetric and anti-symmetric stretch. By looking at the infrared spectrum there are only recognized two peaks, see Figure 105. This is because the two bends have the same frequency and the symmetric stretch does not have a dipole change when it vibrates.

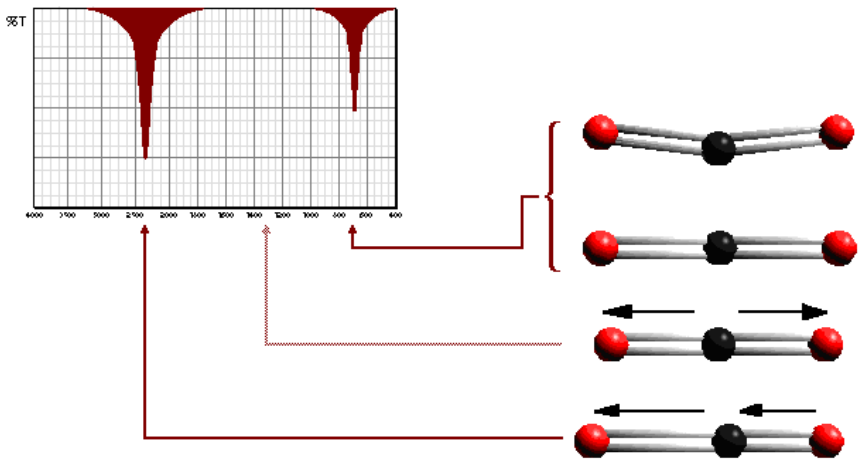

Figure 105 Vibrations and IR-spectrum for CO_2 [60]

Pentane

For pentane, which have 17 atoms, there are 46 normal modes (3N-6 = 3·17-6 = 46, N is the number of atoms). To simplify this situation an assumption is made that each functional group can be treated independently and has the same normal modes no matter where the group is attached. When this is applied there are only two functional groups in pentane; -CH3 and -CH2. Each of these functional groups has a set of group frequencies which corresponds to the normal modes for the group, see Figure 106.

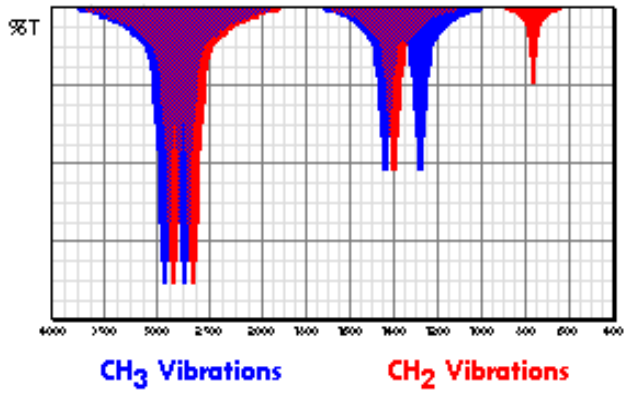

Figure 106 The IR-spectrum for pentane with regards to CH_3 and CH_2 vibrations [60]

Appendix 2 – Theory of Sampling

Pierre Gy has since the early 1950s worked the development of a theory of correct sampling on how to obtain a correct sample. The theory is called "Theory of Sampling" (TOS) and defines seven sampling errors and seven sampling unit operations, which is described in the following, but first some basic definitions.

Basic definitions

The basic definitions to understand TOS and the error contributions are [61]
Lot: Defined as the total volume/mass of material to be sampled
Fragment: defined as the smallest possible part of the lot
Increment: defined as a spatially coherent group of fragments extracted simultaneously by the same sampling equipment
Sample: defined as the amount of correctly extracted material from the lot
Specimen: defined as the product of a non-correct selection and is structurally biased
Sub-sample: a sample reduced properly by a representative mass reduction process
Composite sample: a sample made up of more than one increment
Grab-sample: A specimen, which can only be said to be representative for the material in this particularly specimen. In grab-sampling the specimen is extracted directly from the lot as one large increment.

The **relative sampling error**, e, is defined as

$$e = \frac{a_S - a_L}{a_L}$$

where
a_s: analytical grade of the sample ($a_S = \frac{m_a}{m_S}$, mass of analyte divided by total mass of sample)
a_L: average concentration of the lot

A process of sampling is **accurate** it the average sampling error, m_e, is equal to zero. The process is **reproducible** if the variance of the sampling error is less than a small predetermined value, $s_e^2 \leq s_0^2$. The notation **representative** is a combination of the property of the mean square error including both a systematic and random part of the sampling error [62]

$$r_e^2 = m_e^2 + s_e^2$$

From TOS a sampling process is correct if it is accurate. For the sampling process also to be representative, it also has to be reproducible. Only then it can be qualified as being representative.

Material heterogeneity

All materials are heterogeneous at two levels; composition and spatial. Composition is defined by the different fragments of the lot, and spatial define to what degree the fragments are distributed in the lot. As help to describe the heterogeneity is defined the constitutional (CH) and distributional (DH) heterogeneity. The CH expresses all between-fragment compositional variations in the lot and DH expresses all between-increments compositional variations in the lot.

Constitutional Heterogeneity

The CH is a property of the material to be sampled where the individual units are considered to be fragments, which are unalterable and indivisible.
The heterogeneity carried by one fragment is defined as [62, 63]

$$h_i = \frac{(a_i - a_L)}{a_L} \cdot \frac{M_i}{M_{\bar{i}}}$$

where
i = 1, 2, 3, … N_F
N_F : number of fragments
$M_{\bar{i}} = \frac{M_L}{N_F}$; M_L: mass of lot

The CH of the lot, CH_L, can be described as the variance of h_i [62, 63]

$$CH_L = s^2(h_i) = \frac{1}{N_F}\sum_i h_i^2$$

The CH_L is defined as the variance of all heterogeneity contributions from all fragments which together make up the whole lot. The CH is a non-constant material heterogeneity and is also notated as the Fundamental Sampling Error (FSE) and therefore

$$s^2_{FSE} = CH_L$$

Distributional Heterogeneity

The DH occurs when dealing with increments and their interrelationships. The DH is related to CH and takes into account the spatial heterogeneity between the increments.

The heterogeneity carried by one increment is described as [62, 63]

$$h_n = \frac{(a_n - a_L)}{a_L} \cdot \frac{M_n}{M_{\bar{n}}}$$

Where
n = 1, 2, 3, … N_I
N_I : number of increments
a_n: analytical grade of the increment n
M_n: mass of increment n
$M_{\bar{n}}$: average mass of all increments in the lot

The DH of the lot, DH_L, can be described as the variance of h_n [62, 63]

$$DH_L = s^2(h_n) = \frac{1}{N_I}\sum_n h_n^2$$

The DH_L is defined as the variance of all heterogeneity contributions from all increments which together make up the whole lot.

The DH can also be expressed as a derived function of the CH, where the spatial DH is described using the grouping factor Y and the segregation factor Z, see later.

$$\mathrm{DH_L} = \mathrm{s^2(h_n)} = \mathrm{CH_L} \cdot \frac{1+\mathrm{YZ}}{1+\mathrm{Y}}$$

This formula gives that $\mathrm{DH_L} > 0$ and that $\mathrm{CH_L} \geq \mathrm{DH_L}$.

The error associated with the spatial distribution of increments in a lot is notated as the Grouping and Segregation error (GSE) and therefore

$$\mathrm{s^2_{GSE}} = \mathrm{DH_L}$$

This gives that

$$\mathrm{s^2_{GSE}} = \frac{1+\mathrm{YZ}}{1+\mathrm{Y}} \cdot \mathrm{s^2_{FSE}}$$

Sampling Errors

The seven sampling errors are listed and discussed below, where the first two is correct sampling errors, the next three is incorrect sampling errors, and the last two only is present in1-D sampling.

- Correct Sampling Errors
  - FSE: Fundamental Sampling Errors
  - GSE: Grouping and Segregation Errors
- ISE: Incorrect Sampling Errors
  - IDE: Incorrect Delimination Errors
  - IEE: Incorrect Extraction Errors
  - IPE: Incorrect Preparation Errors
- TFE: Time Fluctuation Errors
- CFE: Cyclic Fluctuation Errors

In addition to the above seven errors is also the Total Analytical Error (TAE) of importance. The sum of all eight errors gives the Global Estimation Error (GEE).

Correct Sampling Errors

The correct sampling errors are FSE and GSE. They are always present and cannot be avoided. They can be minimized, but never completely eliminated.

Fundamental Sampling Error

FSE is characterized by the material heterogeneity and inherent to the material properties such as particle size, shape and density etc. The contribution from FSE is constant for a given lot. The only way to minimize the FSE is by applying comminution to reduce the particle size.

The FSE can be estimated by "Gy's Formula" [62]

$$\mathrm{s^2(FSE)} = \mathrm{Cd^3}\left(\frac{1}{\mathrm{M_s}} - \frac{1}{\mathrm{M_L}}\right) \approx \frac{\mathrm{Cd^3}}{\mathrm{M_s}}$$

where
C: "Sampling constant", it is a product of four material parameters: c, f, g and β.

c: "constitutional parameter" (dimensionless) of specific gravity [g/cm^3], and can be calculated from the following formula

$$c = \frac{\left(1 - \frac{a_L}{\alpha}\right)^2}{\frac{a_L}{\alpha}} \rho_c + \left(1 - \frac{a_L}{\alpha}\right) \rho_m$$

where
a_L: average concentration of the lot
α: concentration of the particles of interest
ρ_s: density of the particles of interest
ρ_m: density of the matrix

f: "Particle shape factor" (dimensionless), describing the deviation from the ideal shape of a square

$f_{square} = 2$, $f_{sphere} = 0.52$, $f_{flat\ disc} = 0.1$

g: "Size distribution factor" (dimensionless), describing the span of particles in the lot

g = 1; all particles have the same size
g = 0.75; $1 < d/d_{0.05} < 2$,
g = 0.5; $2 < d/d_{0.05} < 4$
g = 0.25; $d/d_{0.05} > 4$

β: "Liberation factor" (dimensionless), describing the degree of liberation (separation) of the particle of interest from the rest of the matrix

β = 1; fully separated particles
β = 0; completely homogenized
$0 < \beta < 1$; $\beta = \left(\frac{d_L}{d}\right)^{0.5}$

where
L: Liberation size
d: "Top particle size", defined as the square-mesh screen that retains 5 % of the material [cm]

d: measure of the coarset fragment size
M_L: mass of the lot, M_L is far larger in size than M_s, and is therefore almost always cancelled out of the calculations.
M_S: mass of the sample

Grouping and Segregation Error

GSE is a combination of the material heterogeneity and the sampling process. The GSE is always present and arises when the sampling of increments is not ideal; fragments are not sampled individually and/or have not equal probability of being selected. GSE decreases when the size of the selected group decreases and reaches its minimum when individual fragments are collected to make up the sample. GSE depends on fragment segregation and is almost always occurring when

particulate matter is to be sampled. GSE can be minimized by communition (to avoid grouping) and mixing or blending (to avoid segregation).

The GSE are calculated by [62]

$$s_{GSE} = \sqrt{s_{FSE}^2 YZ}$$

where

Y: grouping parameter, and can be calculated approximately as $Y = \frac{N_F - N_G}{N_G - 1} \approx \frac{N_F}{N_G}$
(number of fragments in the lot divided with the number of groups of fragments in the lot)
Z: segregation parameter, which cannot be easily defined mathematically, but it is the measure of extent of the local and global segregation and/or stratification of the fragments in the lot [62]

Y can be minimized by using a smaller number of fragments in the groups, which gives a higher number of groups. Z can be minimized by mixing the lot.

The calculation of GSE can be difficult by the previous mentioned formula, but it can also be determined experimentally by determine FSE and TSE when all incorrect errors are eliminated. Then GSE can be calculated as

$$s_{GSE} = \sqrt{s_{TSE}^2 - s_{FSE}^2}$$

The Minimal Practical Error (MPE) is the sum of FSE and GSE when all other error contributions is equal to zero. This is the minimum error which always is present.

$$s_{MPE} = \sqrt{s_{FSE}^2 + s_{GSE}^2}$$

Incorrect Sampling Errors

All the incorrect sampling errors can be highly minimized and in many process eliminated. The incorrect sampling errors are divided in three groups; Incorrect Delimitation Error (IDE), Incorrect Extraction Error (IEE), and Incorrect Preparation Error (IPE). The occurrence of incorrect sampling errors is minimized by using correct sampling.

Incorrect Delimitation Error

The IDE occurs when the actual shape of the increment extracted deviates from the correct shape of the increment extracted. A good example is when one extract increments at the end of a conveyor belt. There it is important that the sampling device is constructed in a way so it have strictly parallel sides and that the cutter traverse the entire stream at uniform speed and in a parallel cut to ensure a equal representation of the entire width of the conveyor belt in the final increment. The deviation from the correct structure of the sampling equipment gives rise to the present of IDE in the sampling process.

Incorrect Extraction Error

The IEE occurs when using a correct sampling equipment, see above, but still does not take into account a set of practical extraction rules e.g. center of gravity. When the center of a fragment has its gravity in the delimitated increment the fragment belongs to the increment otherwise should be excluded from the increment. This also goes for samplers operated by vacuum, where the velocity in the sample cutter should be the same as in the matrix. The IEE can be difficult to eliminate, but can be minimized by obeying the rules and applying the sampling unit operations from TOS.

Incorrect Preparation Error

The IPE accounts for the errors occurring after extraction and before analysis. These errors occur when the sample undergo a number of steps before reaching the aliquot ready for analysis. The errors can be factors as human errors, spillage, contamination, degradation, loss of particles etc. One thing all these IPE factors have in common is that they cannot be treated by normal statistics, since they do not follow a specific distribution.

Time Fluctuation Error

The TFE is only present in 1-D sampling. The TFE describes the contributions due to the existence of trends in the process. The TFE is found by performing variographic analysis on the process. [61]

Cyclic Fluctuation Error

The CFE is also only present in 1-D sampling. The CFE describes the contributions due to the presence of periodic variations in the process. The CFE is also found by performing variographic analysis on the process.

Total Sampling Error

The Total Sampling Error (TSE) is the sum of all above mentioned seven error contributions

$$s_{TSE} = \sqrt{s_{FSE}^2 + s_{GSE}^2 + s_{IDE}^2 + s_{IEE}^2 + s_{IPE}^2 + s_{TFE}^2 + s_{CFE}^2}$$

Total Analytical Error

The TAE is the uncertainty to the measured result when analyzed for the parameter in question. It is normally expressed as a standard deviation.

Global Estimation Error

The GEE is the total sum of errors when sampling a sample and measuring a parameter for that sample

$$s_{GEE} = \sqrt{s_{TSE}^2 + s_{TAE}^2}$$

Sampling Unit Operations

The main objective in any sampling strategy is to obtain a representative sample capable of providing a valid estimate of the true value of the analyte in the lot from which the sample originates. The objective of the sampling and mass reduction procedure is to get from the lot to the analytical sample (the minute amount needed for analysis).

Any sampling operation has to obey the Fundamental Sampling Principle (FSP), which is defined in the following way

"All fragments, or groups of fragments, or increments of the lot, must have an equal, non-zero probability of ending up in the sample, while elements foreign to the lot must have a zero probability of ending up in the sample. The increment or the sample must not be altered in any way." [62]

For the sampling procedure to be carried out in a representative manner thus ensuring a reliable analytical result, a detailed plan over each step is required. As help to determine the correct

approach for obtaining a representative sample for analysis, there are seven sampling units (SUO) as listed below [63]. Each of them will be described in the following.

SUO 1. Always perform a heterogeneity characterization of new materials
SUO 2. Mix (homogenize) well before all further sampling steps
SUO 3. Use composite sampling instead of premature focus on the mass of the sample
SUO 4. Only use representative mass reduction
SUO 5. Comminution whenever necessary (reduction in grain size)
SUO 6. Perform variographic characterization of 1-D heterogeneity
SUO 7. Whenever possible turn 2-D and 3-D lots into 1-D equivalents

SUO 1. Always perform a heterogeneity characterization of new materials

To be sure that the sample is representative for the whole lot it is important to characterize the lot with respect to the heterogeneity. The characterization should be done with every new sampling operation from material with unknown heterogeneity.

An experimental approach for characterizing the heterogeneity is to make a multi-stage replication experiment. This replication experiment should be designed to yield an estimate of the variation at the scale-levels of interest. The replicates should have a sufficient number of samples at each sampling step to make a reliable statistical conclusion to the heterogeneity (minimum 10). [64]

SUO 2. Mix (homogenize) well before all further sampling steps

Homogenizing the lot before sampling is one of the most important practical steps in sampling together with SUO 3 and 4. The homogenizing step can be done by mixing or blending, and this is done to minimize the sampling error arising from grouping and segregation. The homogenizing step should be done before any increments are extracted to make up a composite sample.

SUO 3. Use composite sampling instead of premature focus on the mass of the sample

This sampling unit is closely related to SUO 2 since it also works on minimizing the contribution from segregation and grouping. A composite sample made up of several increments is better than extracting one large increment (also known as grab sampling), since the errors arising from segregation and grouping are minimized in the process. If the primary sample becomes unhandy large it can always be reduced later through representative mass reduction (SUO 4).

SUO 4. Only use representative mass reduction

When the secondary, tertiary or more sub-samples are made and the sub-sampling is carried out to end up with the analytical sample, the mass reduction is of great importance. The mass reduction has to be in a representative fashion, where the method and equipment are chosen with great care. Solid samples preferably should be mass reduced with some kind of riffle-splitter or similar, as described in an experimental survey of 17 currently used devices and methods. [65]

SUO 5. Comminution whenever necessary (reduction in grain size)

When the sampling process has been optimized through mixing and mass reduction, the only thing left to do to get the lowest sampling error is to comminute (crush or pulverize) the particles of the material to reduce the average particle size. This will result in a much easier mixable material and the material will become less heterogeneous.

SUO 6. Perform variographic characterization of 1-D heterogeneity

As with SUO 1 this unit operations should be used with every new material type and new sampling procedures. The variographic characterization is only applicable to 1-D lots. Variographic characterization is used to determine if there is periodicity in the production and to find the optimal

interval between extractions of increments (sampling frequency) to get a representative composite sample. The variographic analysis is described in more details in Appendix 10.

SUO 7. Whenever possible turn 2-D and 3-D lots into 1-D equivalents

When working with TOS it is only possible to sample 0-D and 1-D lots correctly. Therefore 2-D and 3-D bodies have to be transformed into 1-D bodies. The differences in dimensionality is described below and illustrated schematically in Figure 107.

A lot can be defined as being of **0-D** on the basis of two conditions
The whole lot is taken as a sample
The expected value of the concentration of the analyte within a sample is independent on the location of the sample with regards to the lot from where it is taken

Ad 2: This implies that there is no intrinsic autocorrelation between the individual groups forming the lot. The correlation is regarding both spatially, physically and chronological considerations, this means that it should be possible to reach and extract all fragments without any modifications to the lot's spatially appearance.

A lot is **1-D** if it consists of strings of fragments or groups that have a distinct autocorrelation. The extracted samples have to cover the two dimensions (width and height) of the lot completely.

A lot is **2-D** if the basis is a layout of a plane with finite but small thickness. The samples from a 2-D lot have to cover the entire third dimension of the lot.

A lot is **3-D** when the extracted sample cannot cover any of the dimensions of the lot in full.

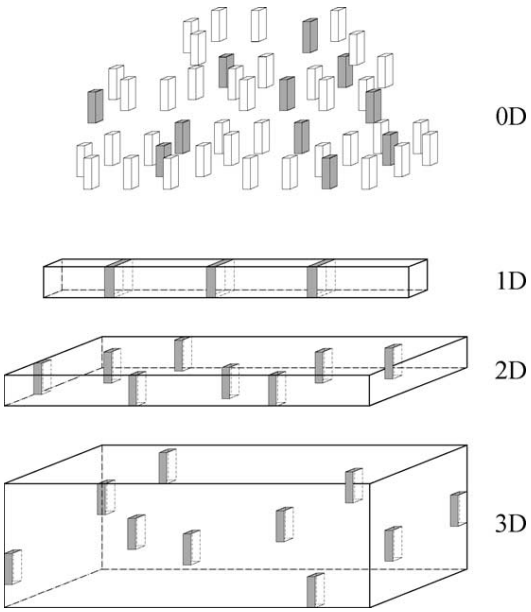

Figure 107 Schematically illustration of the lot dimensionalities in sampling [66]. The gray-shaded boxes indicate increments to be extracted, white boxes indicates the remaining lot material.

A lot should preferably be reduced to 1-D lot before sampling and this may be done by transporting/moving the lot from one place to another on a conveyor belt or with equipment so increments can be extracted to form a composite sample. When a conveyor belt is used increments should be taken as full cross-sectional areas of the lot.

Experiments to Validate Representative Sampling

An experimental approach to determine the correct sampling procedure and the correct number of increments in the primary or any sub-sampling is described below in three small experiments.

Experiment 1 – Replicate Experiment

Take a primary sample from a lot with the current procedure. Perform all sub-sampling and mass reduction steps according to FSP and measure for the analyte of interest. Repeat this at least 10 times.

Calculate the mean value, the standard deviation and the derived "Relative Sampling Variance" (RSV).

$$RSV = \frac{STD}{\bar{x}} \cdot 100$$

If the is smaller than 20 % (16 %) [67], the sampling technique is adequate. If higher than 20%, optimization of the current sampling procedure must be carried out according to the principles in TOS. A RSV of 20 % is acceptable for solids, but it should be much lower for liquids, since it is easier to mix liquids in an attempt to make the lot homogeneous.

Experiment 2 – Optimal number of increments in the composite sampling process

Take representative primary composite samples from the lot with 1 – 10 or more increments (one sample with one increment, one sample with two increments etc.). Perform sub-sampling and mass reduction according to FSP and measure for the analyte of interest. Repeat, for each number of increments, the sampling procedure at least three times.
Plot the standard deviation as a function of number of increments. When the curve is approaching a constant value, the optimal number of increments is reached.

Experiment 3 – Replicate Experiment (new sampling procedure)

Take a representative primary sample from the lot using the indicated number of increments calculated previously. Do sub-sampling and mass reduction according to FSP and measure for the analyte of interest. Repeat this at least 10 times, preferably more.

Calculate the RSV. If it is smaller than 20 % (16 %), the sampling technique is adequate, if higher, than 20 %, optimization of the current sampling procedure must be carried out according to the principles in TOS, e.g. use more increments – or reduce errors arising from grouping and segregation further.

If the RSV in Experiment 3 is satisfactory, the sampling and measuring procedure is in statistical control, and will result in samples which are representative of the lot. If the RSV is not satisfactory, redo Experiment 2 and 3 after each optimization of the sampling procedure until the RSV is satisfactory.

Appendix 3 – Conversion Table; g/L to % vol. for Ethanol

Density of ethanol = 0.789 g/ml = 789 g/L

Conversion: $\frac{Concentration\ [g/L] \cdot 100\ [\%]}{789\ g/L} = Concentration\ [\%\ vol]$

g/L	% vol	g/L	% vol	g/L	% vol
0.50	0.0634	15.5	1.96	30.5	3.87
1.00	0.127	16.0	2.03	31.0	3.93
1.50	0.190	16.5	2.09	31.5	3.99
2.00	0.253	17.0	2.15	32.0	4.06
2.50	0.317	17.5	2.22	32.5	4.12
3.00	0.380	18.0	2.28	33.0	4.18
3.50	0.444	18.5	2.34	33.5	4.25
4.00	0.507	19.0	2.41	34.0	4.31
4.50	0.570	19.5	2.47	34.5	4.37
5.00	0.634	20.0	2.53	35.0	4.44
5.50	0.697	20.5	2.60	35.5	4.50
6.00	0.760	21.0	2.66	36.0	4.56
6.50	0.824	21.5	2.72	36.5	4.63
7.00	0.887	22.0	2.79	37.0	4.69
7.50	0.951	22.5	2.85	37.5	4.75
8.00	1.01	23.0	2.92	38.0	4.82
8.50	1.08	23.5	2.98	38.5	4.88
9.00	1.14	24.0	3.04	39.0	4.94
9.50	1.20	24.5	3.11	39.5	5.01
10.0	1.27	25.0	3.17	40.0	5.07
10.5	1.33	25.5	3.23	40.5	5.13
11.0	1.39	26.0	3.30	41.0	5.20
11.5	1.46	26.5	3.36	41.5	5.26
12.0	1.52	27.0	3.42	42.0	5.32
12.5	1.58	27.5	3.49	42.5	5.39
13.0	1.65	28.0	3.55	43.0	5.45
13.5	1.71	28.5	3.61	43.5	5.51
14.0	1.77	29.0	3.68	44.0	5.58
14.5	1.84	29.5	3.74	44.5	5.64
15.0	1.90	30.0	3.80	45.0	5.70

Appendix 4 – Reference Measurements for Calibration and Test Set

White Wine

Glas nr.	Sucrose		Glucose		Fructose		Glycerol		Ethanol	
	Cal g/L	Test g/L	Cal g/L	Test g/L	Cal g/L	Test g/L	Cal g/L	Test g/L	Cal g/L	Test g/L
1	4.049	4.646	12.36	15.04	11.93	14.32	11.14	13.95	16.06	19.66
2	3.278	3.450	9.651	9.963	9.308	9.492	9.125	9.601	13.22	12.47
3	3.686	2.392	9.148	9.660	8.695	9.054	8.677	8.706	11.21	11.45
4	3.575	2.942	8.700	7.332	8.133	6.821	7.879	6.752	10.62	8.994
5	2.975	1.557	7.186	4.341	6.794	4.186	7.166	3.930	8.666	5.446
6	2.616	1.221	6.397	3.529	6.020	3.442	6.122	3.223	8.469	4.238
7	2.29	0.7592	5.875	2.557	5.492	2.318	5.499	1.977	6.892	2.769
8	1.81	0.6030	4.771	1.860	4.605	1.568	4.508	1.373	6.070	1.664
9	1.41	0.4981	4.085	1.370	3.990	1.195	3.925	1.020	5.231	1.162
10	1.28	0.3392	3.635	0.704	3.500	0.693	3.444	0.690	4.660	0.843
11	0.6656		3.298		3.194		2.998		4.148	
12	0.6335		2.668		2.506		2.491		3.155	
13	0.6791		2.458		2.165		2.016		2.567	
14	0.6868		2.262		2.149		1.739		2.015	
15	0.5266		1.600		1.439		1.385		1.998	
16	0.5205		1.666		1.381		1.176		1.598	
17	0.3104		0.9151		0.9113		0.8719		1.196	
18	0.2645		0.7744		0.7728		0.7645		0.9911	
19	0.2355		0.6791		0.6684		0.6400		0.8975	
20	0.1756		0.5445		0.5376		0.5239		0.7078	
21	0.2203		0.4645		0.4582		0.4420		0.5778	
22	0.1206		0.4165		0.4049		0.3848		0.4774	
23	0.07975		0.2902		0.2858		0.2862		0.3554	
24	0.07450		0.2331		0.2280		0.2262		0.3140	
25	0.04570		0.1801		0.1760		0.1650		0.2306	
26	0.03490		0.1394		0.1370		0.1409		0.1638	
27	0.01975		0.08195		0.08480		0.08145		0.1197	
28	0.01400		0.06305		0.04750		0.06665		0.08615	
29	0.00870		0.03340		0.03430		0.04400		0.04845	
30	0.00590		0.02255		0.02365		0.03290		0.03190	

White Wine

Glas nr.	Citric acid		Tartaric acid		Malic acid		Succicinic acid		Lactic acid		Acetic acid	
	Cal	Test	Cal	Test	Cal	Test	Cal	Test	Cal	Test	Cal	Test
	mg/L	mg/L	mg/L	mg/L	mg/L	mg/L	mg/L	mg/L	mg/L	mg/L	mg/L	mg/L
1	68.08	82.40	938.8	887.4	1255	1254	328.5	340.7	58.53	64.00	534.5	539.6
2	60.24	44.91	834.7	607.0	1124	821.2	283.7	209.4	49.13	39.19	496.7	356.5
3	54.72	42.94	728.8	532.8	990.2	722.8	249.2	189.8	41.75	32.51	448.0	298.6
4	49.46	35.20	667.8	427.5	896.0	584.0	227.9	141.9	40.41	23.40	381.7	278.8
5	42.99	21.76	605.6	312.4	802.9	428.1	200.7	106.5	30.10	18.17	324.2	200.6
6	38.43	16.64	550.7	215.8	744.5	304.6	192.5	89.06	29.36	14.03	353.8	141.2
7	35.30	11.28	468.8	160.7	624.7	219.4	158.2	85.51	26.93	-	291.5	104.8
8	29.47	11.74	402.4	110.5	542.1	148.0	150.2	35.53	24.41	5.816	257.3	64.01
9	25.76	5.787	360.7	80.85	470.8	108.9	112.6	29.91	23.96	16.35	214.2	54.84
10	26.83	3.301	313.6	54.22	429.1	72.90	108.4	17.35	18.03	3.085	186.7	35.21
11	18.14		275.7		368.9		94.72		14.99		164.7	
12	16.23		219.1		298.8		74.58		12.93		129.0	
13	14.49		183.6		248.4		63.53		11.58		106.6	
14	10.17		156.7		211.0		55.27		10.34		100.5	
15	11.08		135.9		181.6		47.19		8.99		80.09	
16	7.367		106.9		142.5		43.54		m		82.26	
17	6.410		89.39		116.9		31.05		6.10		42.91	
18	5.809		73.04		96.82		26.47		6.25		36.81	
19	3.713		63.30		84.65		21.09		3.42		34.68	
20	-		73.76		80.98		13.98		2.69		30.54	

Rose Wine

Glas nr.	Sucrose		Glucose		Fructose		Glycerol		Ethanol	
	Cal	Test	Cal	Test	Cal	Test	Cal	Test	Cal	Test
	g/L	g/L	g/L	g/L	g/L	g/L	g/L	g/L	g/L	g/L
1	-	-	10.97	10.79	10.73	10.31	2.993	2.415	25.17	16.99
2	-	-	9.684	8.486	9.503	8.143	2.673	1.752	22.01	13.71
3	-	-	8.620	6.791	8.439	6.665	2.380	1.483	19.63	11.30
4	-	-	7.518	5.875	7.570	5.641	2.068	1.302	17.87	9.443
5	-	-	6.821	4.191	6.837	4.012	1.833	0.9221	16.20	6.737
6	-	-	5.723	3.145	5.682	3.126	1.623	0.7305	13.23	5.211
7	-	-	4.887	2.533	4.832	2.508	1.255	0.5866	11.52	4.185
8	-	-	4.231	1.845	4.208	1.845	1.082	0.4152	9.991	3.074
9	-	-	3.698	1.405	3.697	1.425	0.9599	0.3172	8.681	2.381
10	-	-	2.831	1.153	2.788	1.161	0.748	0.2542	6.598	1.997
11	-	-	2.274	0.8666	2.253	0.8571	0.5939	0.1817	5.356	1.437
12	-	-	1.901	0.6688	1.857	0.6839	0.489	0.1445	4.408	1.104
13	-	-	1.630	0.5650	1.589	0.5697	0.4095	0.1113	3.733	0.9649
14	-	-	1.249	0.4146	1.244	0.3925	0.3097	0.0856	2.929	0.6954
15	-		1.022		1.011		0.2657		2.376	
16	-		0.8356		0.8364		0.2039		1.984	
17	-		0.6365		0.6276		0.1611		1.478	
18	-		0.5127		0.5095		0.1127		1.206	
19	-		0.4347		0.3945		0.0918		0.9455	
20	-		0.2999		0.2804		0.0697		0.6926	
21	-		0.2281		0.2387		0.0534		0.5548	
22	-		0.1981		0.1803		0.0375		0.4664	

Rose Wine

Glas nr.	Citric acid		Tartaric acid		Malic acid		Succicinic acid		Lactic acid		Acetic acid	
	Cal	Test	Cal	Test	Cal	Test	Cal	Test	Cal	Test	Cal	Test
	mg/L	mg/L	mg/L	mg/L	mg/L	mg/L	mg/L	mg/L	mg/L	mg/L	mg/L	mg/L
1	1617	1492	m	312.2	710.8	601.6	830.4	878.4	103.6	105.8	m	145.2
2	1485	1201	m	251.2	605.8	467.9	769.7	707.0	153.0	93.49	m	119.9
3	1270	952.7	m	196.5	552.8	379.4	658.1	564.4	108.7	84.12	m	106.0
4	1143	805.4	m	166.3	468.8	322.6	576.8	479.5	86.51	66.35	m	130.3
5	1014	579.4	m	118.7	411.2	232.7	526.3	370.4	85.45	97.53	m	61.46
6	828.4	447.4	m	91.73	335.7	182.1	483.3	324.5	73.40	60.98	m	43.91
7	681.2	364.6	m	74.21	281.4	146.8	363.3	214.8	40.24	30.50	m	56.39
8	614.9	262.4	m	53.35	255.2	102.7	316.0	157.7	40.24	18.47	m	27.02
9	516.7	206.9	m	43.09	218.8	87.63	276.5	125.6	43.76	16.44	m	18.90
10	386.5	168.9	m	34.07	166.2	67.19	209.2	100.5	32.67	17.21	m	29.78
11	310.9	124.3	m	25.29	134.5	50.50	167.6	75.82	26.24	11.61	m	12.61
12	262.2	96.57	m	19.28	113.3	38.25	140.8	58.84	22.29	6.524	m	10.07
13	219.6	81.85	m	17.52	96.79	33.43	120.9	33.43	19.25	6.870	m	9.496
14	172.6	61.09	m	12.01	73.81	23.76	91.25	23.76	14.45	4.224	m	9.556

Red Wine

Glas nr.	Sucrose		Glucose		Fructose		Glycerol		Ethanol	
	Cal	Test	Cal	Test	Cal	Test	Cal	Test	Cal	Test
	g/L	g/L	g/L	g/L	g/L	g/L	g/L	g/L	g/L	g/L
1	5.873	6.134	5.794	4.148	4.510	3.706	2.917	2.842	24.15	16.27
2	3.920	5.580	4.702	3.933	3.997	3.303	3.002	2.247	19.81	13.25
3	5.303	4.563	4.691	3.094	3.552	2.610	2.600	1.885	18.25	10.66
4	4.787	3.863	4.206	2.598	3.162	2.169	2.390	1.627	16.07	9.037
5	4.389	2.957	3.789	2.130	2.881	1.657	2.228	1.174	14.26	6.522
6	3.357	2.187	3.163	1.791	2.416	1.189	1.713	0.8894	12.42	4.982
7	3.172	1.482	2.676	1.463	2.086	0.9595	1.527	0.6894	10.33	3.984
8	2.745	1.020	2.308	1.004	1.790	0.6872	1.380	0.4756	8.839	2.894
9	2.354	0.8008	2.044	0.7873	1.551	0.5262	1.153	0.3891	7.909	2.243
10	1.301	0.7075	1.244	0.6760	1.153	0.4306	0.8835	0.3366	5.963	1.836
11	1.006	0.4636	1.000	0.4944	0.9518	0.3175	0.7270	0.2357	4.799	1.402
12	0.7219	0.3371	0.8174	0.2490	0.7738	0.2392	0.5785	0.1746	4.100	1.079
13	0.6325	0.3131	0.7108	0.2173	0.6542	0.1901	0.4696	0.1516	3.442	0.881
14	0.4956	0.2144	0.5333	0.1423	0.5204	0.1223	0.3932	0.1077	2.564	0.65
15	0.5243		0.4505		0.4212		0.2917		2.183	
16	0.4375		0.3766		0.3305		0.2565		1.759	
17	0.3060		0.2399		0.2176		0.1965		1.317	
18	0.2300		0.2052		0.1943		0.1679		1.050	
19	0.2253		0.1841		0.1201		0.1045		0.9022	
20	0.1651		0.1346		0.1387		0.0897		0.6181	
21	0.09675		0.0955		0.0978		0.0567		0.4805	
22	0.08155		0.07255		0.07670		0.4060		0.4224	

Red Wine

Glas nr.	Citric acid		Tartaric acid		Malic acid		Succicinic acid		Lactic acid		Acetic acid	
	Cal	Test	Cal	Test	Cal	Test	Cal	Test	Cal	Test	Cal	Test
	mg/L	mg/L	mg/L	mg/L	mg/L	mg/L	mg/L	mg/L	mg/L	mg/L	mg/L	mg/L
1	546.6	554.4	1075	1010	364.4	323.6	825.8	919.6	239.6	152.7	205.7	160.2
2	492.5	466.7	997.7	1009	319.5	273.5	719.0	748.3	153.8	139.1	185.1	130.9
3	410.4	400.1	865.7	818.7	263.6	262.0	613.9	608.9	109.9	104.3	142.4	98.27
4	371.0	321.9	774.8	722.2	240.5	190.1	556.1	579.6	104.3	153.3	133.5	99.84
5	338.9	222.0	700.1	505.7	225.7	133.0	519.1	404.4	111.4	108.3	136.1	53.11
6	286.4	170.2	586.6	389.2	191.2	116.3	437.1	276.0	95.64	44.73	140.9	42.08
7	243.9	134.3	474.3	311.1	159.2	78.65	313.3	226.8	79.25	62.93	91.11	44.31
8	209.3	86.91	419.2	217.4	136.5	51.79	269.5	157.7	67.20	23.89	106.5	29.26
9	181.1	72.73	362.1	173.3	118.5	45.23	234.8	124.3	57.43	20.84	67.36	20.80
10	134.3	60.32	277.3	141.4	87.91	34.70	177.8	101.2	46.51	18.07	53.66	17.81
11	106.9	43.07	223.3	103.9	70.83	25.86	142.6	75.38	33.62	14.10	41.77	12.49
12	87.25	33.84	185.8	81.57	57.25	20.11	122.0	58.15	37.59	10.54	35.09	9.095
13	74.53	28.18	158.3	67.82	49.47	17.02	102.3	52.83	24.03	12.90	28.89	8.419
14	56.87	20.90	122.0	50.14	37.72	13.15	83.22	38.58	18.85	8.758	22.51	8.394

Appendix 5 – Theory of Micro-Electromechanical Systems

The Micro-Electromechanical Systems (MEMS) features the construction and manufacture of an inexpensive, rugged, precise, and low powered miniaturized NIR spectrometer. The MEMS components are silicon chips with micro-mechanical elements, which respond to physical variable such as pressure, acceleration, flow, sound, and for NIR spectrometers – to light.

The MEMS Chip

The MEMS chips is built up of micromechanical elements attached to a silicon substrate with micro fabrication technique. By this means it is possible to create a diffractive grating structure with electrically movable elements. The structure can be programmed to filter light in specific regions of a spectra very rapidly.

The MEMS chip is a 1-D array of micro-mirrors, which are programmable so they can be raised and lowered to form a micro-programmable diffraction grating. A schematic illustration of the MEMS chip and the operation as an diffraction grating is shown in Figure 108.

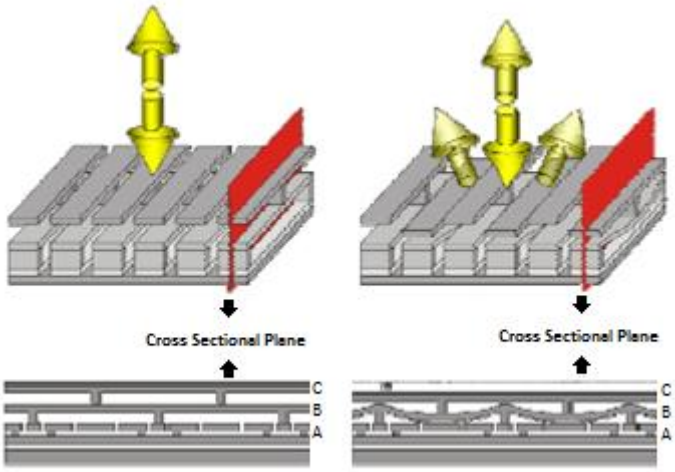

Figure 108 Schematic illustration of the MEMS chip and its operation [68]

The “A” layer is a silicon substrate that supports a series of micro-post which support the “B” layer. This layer is again a silicon layer with micro-post which support the “C” layer. The surface of the “C” layer is a gold reflective coating. The MEMS chip is actuated by applying a voltage between the layers “A” and “B”, which results in a raise or lowering of the “C” layer. The required actuation is a movement of only a fraction of a micron. During the entire process the “C” layer continuous to have a optically flat surface necessary for the desired optical characteristics for the spectroscopy. [68]

When all the micro-mirrors are in the all-up position, the chip is a mirror. When alternate micro-mirrors are depressed the light impinging on the chip is diffracted away from the chip at an angle, which depends on the ratio of the wavelength of the light to the width of the micro-mirrors. A change for the all-up to the alternate down states are achieved en less than one millisecond, which make the measurement of a whole spectra very fast.

The light is dispersed by wavelength using the micro-mirrors as a fixed diffracting grating, this gives that each wavelength range hits a different set of micro-mirrors giving a pixel. The MEMS chip is able to have 100 pixels, resulting from the possible to pre-code 100 different settings of up and down positions of the micro-mirrors. When the light is reflected from the chip it is sent to a detector. If

a pixel is set in diffraction mode, the light hitting that pixel is diffracted away and does not reach the detector. [69]

Digital Transform Spectroscopy

By using Digital Transform Spectroscopy (DTS) the spectrum collected from the sample is dispersed across the MEMS chip. The 100 pre-coding controls when the chip should block the light in specific regions of the spectrum while other regions are reflected, collected and recombined onto a single photo-detector, see Figure 109.

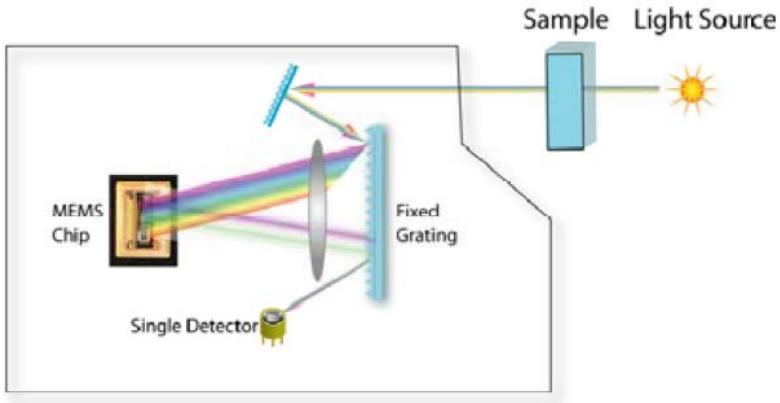

Figure 109 Schematic of Digital Transform Spectrometer [68]

The chip is driven through 100 pre-coded sequences of up-and-down settings (pixels), which create a unique time signature at the detector. The DTS matrix represents a time sequenced set of spectral mask, which is represented by rows, created using the MEMS chip. The columns represents pixels, which is corresponding to the spectral ranges. In Figure 110 is shown such a DTS matrix, where the green areas are the transmitted spectral regions and the white areas represents the diffracted spectral regions. By measuring the total power with one single detector at individual spectral mask in the matrix it yields a transform. Then the transform is collected it is easily inverted resulting in the full spectrum for the sample.

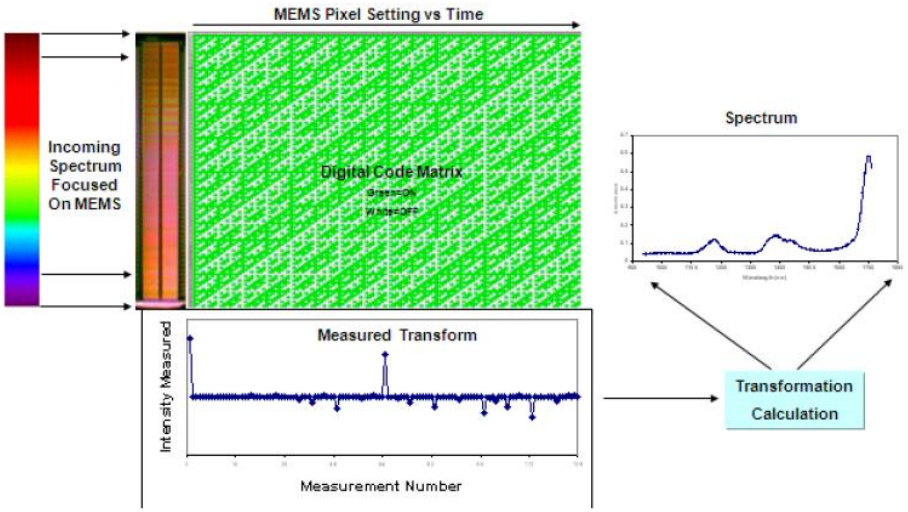

Figure 110 The DTS transform matrix representing af time sequenced set of spectral masks, and the transformation from Digital Code Matrix to Spectrum [68]

Since the MEMS chip is very fast to change between the different up-and-down setting, the entire operation from collecting to displaying the spectrum takes less than one second.

The operation of a spectrometer using DTS and MEMS chip is insensitive to stray of light and drifts in the detector.

MEMS Requirements

There are three critical MEMS co-design requirements
The length of the micro-mirrors must match the spot size produced by the overall optical design
The voltage required to change the micro-mirrors from up to down settings must be within the voltage range of available low-power electronics chips, and
The structure of the MEMS must create a diffraction angle large enough to permit exclusion of the unwanted light from the optical path to the detector.

The PHAZIR™

The PHAZIR™ is small, light, and only requires sufficiently low power to be built as a battery-operated hand-held spectrometer using DTS and a MEMS chip. In Figure 111 is shown a schematic structure of the PHAZIR™ where the placement of the optical module with the MEMS chip is shown. The optics module including the MEMS chip and the DTS segment is the heart of the PHAZIR™ spectrometer. The PHAZIR™ also has a light source (similar to a normal tungsten light ball), a sampling head (directs the light onto the sample and collects the reflected light), a battery, a display, control electronics for the MEMS chip, and a small computer. The computer controls the spectrometer and the analysis of the spectrum.[69]

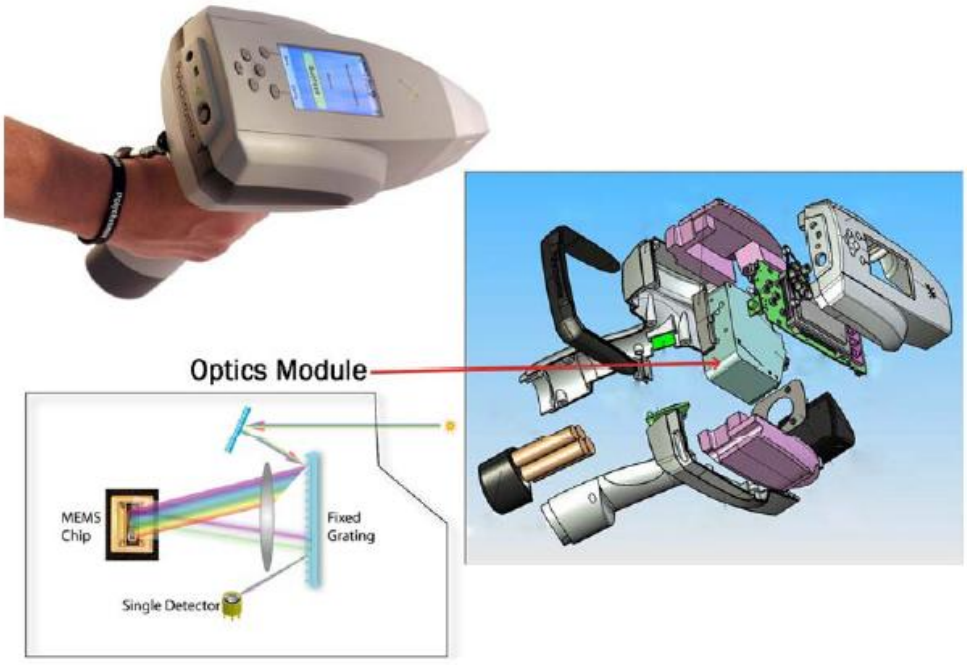

Figure 111 The PHAZIR™ (top left) with a exploded view (right) of the inside showing the placement of the optics module (bottom left) with the MEMS chip inside [68]

Appendix 6 – Multivariate Data Analysis

Basic definitions of data analysis

The data matrices used for multivariate data analysis consists of [43]
objects, which are observations;
n, the number of objects in the matrix;
p, the number of X-variables in the matrix;
q, the number of Y-variables in the matrix;
X-variables, independent variables or observations on the same object; and
Y-variables, dependent variables or observations on the same object.

Principal Components Analysis

Principal components analysis (PCA) is the decomposition of the **X** matrix into a structure part and a noise part. The structure part is where the important information are hidden (information correlated to the properties), and the noise is the rest of the information hidden in the raw data. The **X** matrix is therefore a sum of the data structure and the noise.

The **X** matrix with p variables and n objects can be presented in an orthogonal coordinate system with p dimensions. If the data in the **X** matrix are plotted in the orthogonal coordinate system, it might give a data swarm, in which a line would describe the data swarm almost as accurate as the data swarm itself. This line is the first principal component (PC1). For a 3-D example see Figure 112.

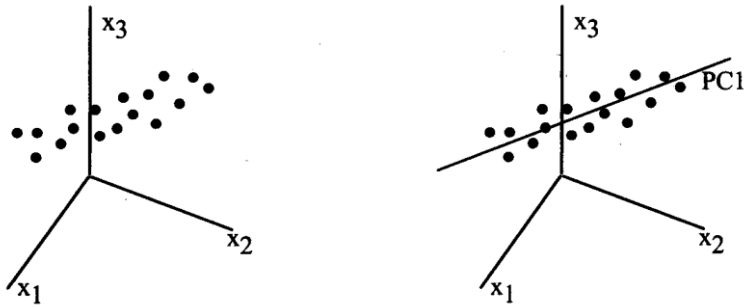

Figure 112 Left: Data swarm in 3-D. Right: Data swarm with PC1 [43]

The PC1 lies along the direction of maximum variance. If the points on PC1 are like a planar in appearance, the second principal component (PC2) will lie orthogonal to PC1 and in the direction of the second largest variance, see Figure 113. Continuing with PC3, then PC3 will lie orthogonal to both PC1 and PC2 and have the third largest variance and so on for PC4 and PC5 etc.

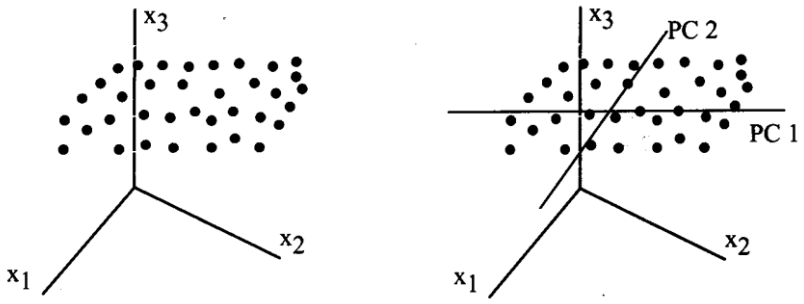

Figure 113 Left: Data swarm in a planar. Right: Data swarm with 2 PCs [43]

The approach by finding orthogonal PCs of increasing order which lie along a maximum variance of decreasing order will result in a new coordinate system. The origin of this new coordinate system is the average point in the data swarm: [43]

$$(\bar{x}_1, \bar{x}_2, \ldots, \bar{x}_p), \text{ where } \bar{x}_k = \frac{\sum_{i=1}^{n} x_{ij}}{n}$$

A linear combination of each PC contains p coefficients, where p is equal to the number of unit vectors. These coefficients are also the loadings. The loadings give information regarding the relationship between the p variables in the original **X** matrix and the PCs in the new coordinate system. A loading plot is a pair of coefficients plotted against each other. The loading plots are used to give an overview over how much each variable contributes to each PC.

When objects in the original coordinate system are projected on the PC we get a score, where the score is equal to the distance of the projection, see Figure 114. By doing this to all the points and PCs we get a score matrix **T**. The score vector is a column in **T**. The score plots, which are used to simplify a many dimensional coordinate system to 2- D or 3-D, are two pair of score vectors plotted against each other. The score plots are used to give an overview of the data.

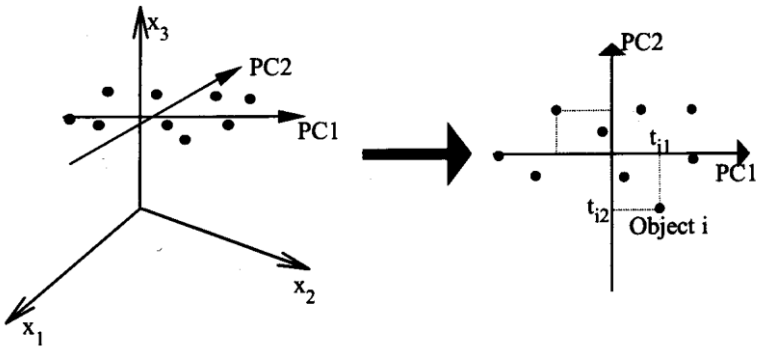

Figure 114 Scores as PC-coordinates [43]

When loading and score plots are compared for the same PCs, they give valuable information about the interrelationship between both objects and variables.

The PC model decomposites **X** into data structure and noise, and can be describe by the following equation

$$\boldsymbol{X} = \boldsymbol{TP}^T + \boldsymbol{E} = Data\ Structure + Noise$$

For the equation apply that **T** is the score matrix, $\mathbf{P}^T$ is the transposed loading matrix and **E** is the error component. The PC model is described as the $\mathbf{TP}^T$, where **E** not is a part of the model. **E** is the buildup residual matrix and the part that is not explained by the model.

When **E** is equal to zero the residual variance (unexplained variance) is equal to 0 % and then the $\mathbf{TP}^T$ is the explained variance by the model and is equal to 100 %. When $\mathbf{TP}^T$ increases, **E** decreases, as seen in Figure 115. The sum of % explained variance and % residual variance is always equal to 100 %.

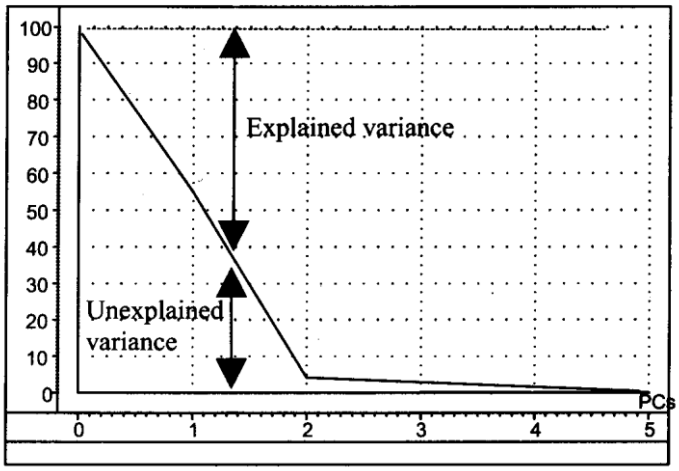

Figure 115 Explained and unexplained residual variance [43]

Multivariate Calibration

Multivariate calibration is the relating of two sets of data, **X** and **Y**, where the **X** consists of independent variables and the **Y** consists of dependent variables. The **Y** is a description of the desired property as a function of the measured variables, **X**. The two matrices are organized as shown in Figure 116. To get the most out of multivariate data analysis, **X** has to be measured with one method that can give results which can replace many single analyses. The **Y** matrix is measured with one or more analyses where the wish is to replace them all with the analysis of **X**. The **X** matrix and the corresponding **Y** matrix are called the calibration set or training set.

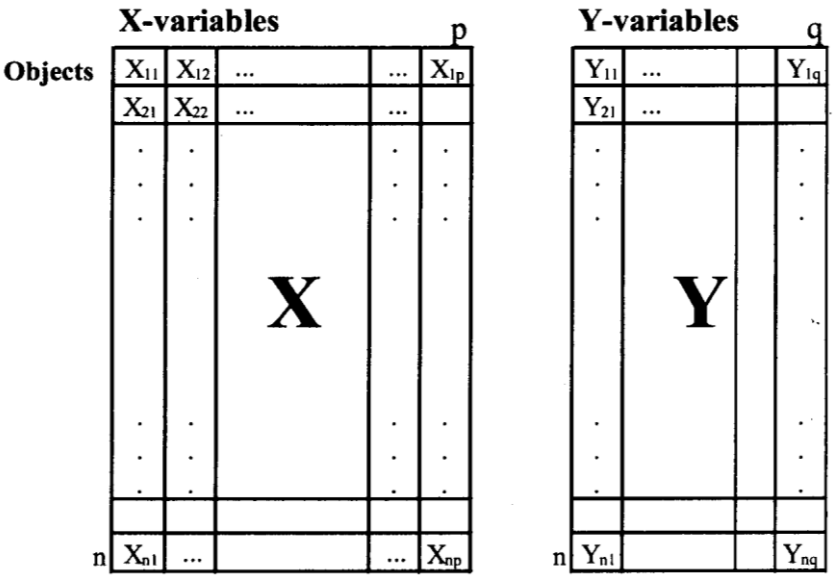

Figure 116 Overview of the X- and Y-matrices [43]

Partial Least Squares Regression

Partial Least Squares Regression (PLS) uses the y-data structure as a guiding hand when the **X**-matrix is decomposed. A schematic overview of the PLS is shown in Figure 117.

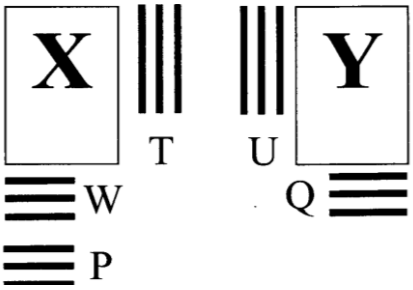

Figure 117 Schematic overview of PLS [43]

PLS connects the **X**- and the **Y**-spaces by letting the **u**-score vector act as the starting point for the **t**-score vectors in the X-space decomposition. This means that $\mathbf{u_1}$ replaces $\mathbf{t_1}$ in the regression. Afterwards $\mathbf{u_1}$ is substituted by $\mathbf{t_1}$ in the relevant stage in the PLS-algorithm in which the **Y**-space is decomposed.

The first influence to the **X**-decomposition is the $\mathbf{u_1}$, this leading to calculation of the **X**-loadings, termed **w**. The **t**-vectors of the **X**-space are now calculated (like in PCA) and based on the **w**-vector. The **t**-vector is then used as the starting point for the $\mathbf{u_1}^*$-vector (instead of $\mathbf{u_1}$) leading to calculation of the **Y**-loadings, termed **q.** The **u**-vectors of the **Y**-space are now calculated and based on the **q**-vector. The approach continues until the correlation, r^2, has the maximum value obtainable for the dataset. In this way the **X**- and **Y**-spaces are modelled interdependently. By using and balancing the information from both **X**- and **Y**-spaces the PLS model reduces the influence of large variations in **X** which have no correlations with **Y**. Now the PLS model is finish. [43]

Calibration Set Requirements

To be a good calibration set, the data must be representative for both the samples at hand and for the future collected samples. The measuring conditions should also be as similar as possible. The calibration set should representative covers all aspects of variations that could occur in real life. Here should be covered the natural variety in real samples, this means that real samples are better than artificial laboratory samples. Another way of saying the same thing is that the calibration set must span the **X** and the **Y**, in a way that is as representative as possible.

Minimizing the Prediction Error

The prediction error is the residual **Y**-variance based on the validation, see later. In Figure 118 is shown a plot of the Root Mean Square Error of Prediction (RMSEP). The y-axis is the prediction error in terms of RMSEP and the x-axis is the number of principal components for the prediction model.

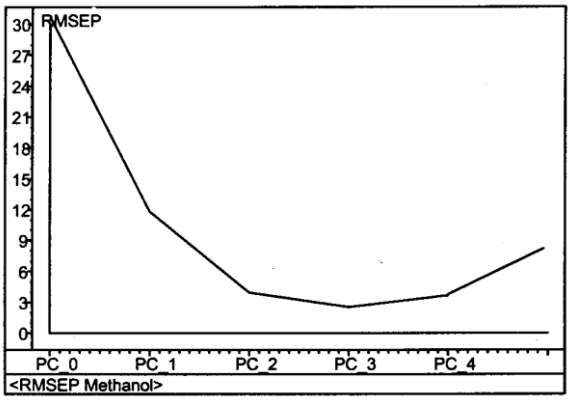

Figure 118 RMSEP vs. number of PCs [43]

The RMSEP is calculated as [43]

$$RMSEP = \sqrt{\frac{\sum_{i=1}^{n}(\hat{y}_{i,pred} - y_{i,ref})^2}{n}}$$

It is seen in the equation for RMSEP, that the prediction ability is best when the prediction error is lowest. This gives that the best prediction is when the deviation between predicted values and reference values is as low as possible. In Figure 118 the lowest RMSEP is for three PLSs and this is therefore the number of PLSs at which the prediction error is minimized. Since the curve increases for more PLSs than three, the model may be improved with more PLSs but the prediction ability will be reduced. From this it can be concluded that the minimum RMSEP gives the optimal complexity of the model with the number of PLSs corresponding to the minimum RMSEP.

To be able to compared models a relative RMSEP has to be calculated.

$$relRMSEP = \frac{RMSEP}{\bar{Y}} \cdot 100\ [\%], \text{ where } \bar{Y} = Y_{max} - Y_{min}$$

The values of Y should be for the test set, since it is the error from the prediction of the test set, which is interesting.

As an alternative to RMSEP the squared error of prediction (SEP) is used. The RMSEP is the sum of bias and the SEP, where the bias should be as small as possible and preferably equal to zero.

$$RMSEP^2 = bias^2 + SEP^2$$

The SEP is the error without bias. The SEP is a very used parameter to say if a model is good or not, but since the bias may have changed since the calibration has been made. When bias has change once it may very well do it again, therefore it is better to use RMSEP to say if a model is good or not.

In general the optimal complexity of the model can be described as shown in Figure 119, where the empirical prediction error is shown as the sum of the modelling and the estimation errors. For a low number of PLSs the model will be under-fitted and for a high number of PLSs the model will be over-fitted. The optimal number of PLSs is marked with an arrow. If a model is over-fitted, it will be too detailed in the prediction. It will fail in predicting new objects with an optimal accuracy because it also describes the noise in the model.

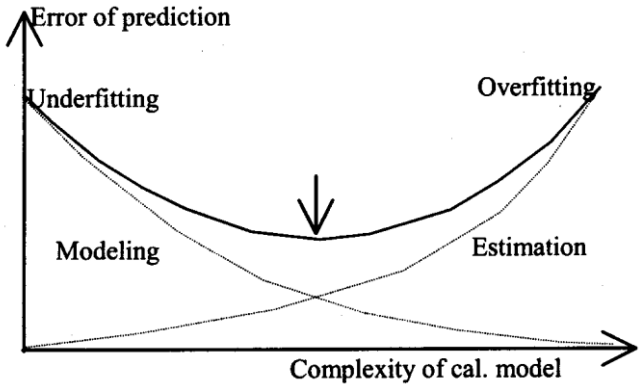

Figure 119 Empirical Prediction Error [43]

Predicted vs. Measured

When the models is made it is described by a plot of the predicted values against the measured values. A regression curve is calculated from the data points. The slope of this regression line is the accuracy of the model (closeness to the actual result) and the squared correlation coefficient (R^2) of the regression curve is the precision of the model (degree of reproducibility).

The R^2 is modelled by the specific relation, where the proportion of total variation in the values of Y that may be accounted for by a linear relationship with values of X

$$R^2 = \frac{S_{xy}^2}{\sqrt{S_{xx}S_{yy}}}$$

Where the entries S_{xy}, S_{xx}, and S_{yy} are defined by

$$S_{xy} = \sum_{1=1}^{n}(x_i - \bar{x})(y_i - \bar{y})$$

$$S_{xx} = \sum_{1=1}^{n}(x_i - \bar{x})^2$$

$$S_{yy} = \sum_{1=1}^{n}(y_i - \bar{y})^2$$

Validation

Validation is testing the models performance according to a given set of test results. The validation testing is concerned with the models ability to predict on a new data set, which has not been used for the calibration. Before the validation can take place, we need to know the Y-values for the new data set to make a comparison between the predicted and the reference values. The validation can be done in several ways such as e.g. test set validation or cross validation. [43]

Test Set Validation

In test set validation the model is calibrated on one set of data, and then validated on one or more new sets of data, which have been kept out of the modelling so far. In test set validation the calibrated model predict a Y-value (Y_{pred}) and then compare the Y_{pred} with known reference Y-values (Y_{ref}) from the new data set.

The optimal test set validation is carried out as follows

1. Collecting samples for one or more training sets (independent first sampling).
2. Measurements of **X** and **Y**.
3. Calibration of the model.
4. Collecting one or more test set (independent second sampling).
5. Measurements of **X** and **Y**.
6. Validation of the model.

Both the training and test set has to be large in number of samples and representative for both **X** and **Y**.

Test set validation is the best and optimal validation method, because it uses two different sets of data for calibration and validation. In real life it can be problematic or even impossible to get two large and independent sets of samples, f. ex. because of the difficulties in sampling or preparations of samples, expensive measurements of **Y**-values, or unacceptably dangerous test-methods etc. If for some reasons the test set validation can't be chosen, there is an alternative method called cross validation. [43]

Cross Validation

In cross validation there is only used one set of data, the same data set are used for calibration and validation. There are two types of cross validation; full and segmented cross validation.

Full cross validation is when there are made as many sub-models as there are objects. For every time you calibrate the model, you leave one object out of the data set, and then use this one object for testing. Full cross validation should only be used when there are a minimum of samples accessible so there are too few samples to make test set or segmented cross validation.

Segmented cross validation is when you divide the calibration set into segments with more than one sample in each. Then you make the model by leaving out one segment and calibrate on the remaining samples. Afterwards you test the model with the left-out segment. By repeating this for all the segments, the model is both calibrated and validated at the same time. The best model is obtained with as few segments as possible, because then it is the best simulation of test set validation. [43]

Prediction

After the model is satisfactory validated it can be used for predicting new results. In a prediction situation the new data for X is projected onto the A model components, and then Y is estimated using the projected scores and loading matrices, T and P.

To check the models ability to predict, the Y values are to be known for the data set. The X data are used to make the prediction, and then the known Y values can be used for a comparison between Y_{pred} and Y_{ref}. By plotting the predicted values against the measured values it can be seen how good the prediction ability of the model is. If the slope of the regression line for the points is close to 1, the prediction is good. An estimation of the uncertainty to the predicted value is represented by the value of RMSEP. [43]

Appendix 7 – First Modelling Campaign

White wine (890 - 1691 nm)							# Outliers		
Parameter	**Pre-treatment**	**Slope**	**R^2**	**RMSEP [g/L]**	**# PLS**	**Outliers**	**Cal**	**Test**	**Outliers [%]**
Sucrose	1st derivative	0.934	0.979	$2.29 \cdot 10^{-1}$	2	LT03, L28	1	1	5
Glucose	Raw data	0.993	0.946	$7.10 \cdot 10^{-1}$	2	LT01, LT03, LT10, L25, L28, L29, L30	4	3	18
Fructose	Raw data red.	0.995	0.973	$4.78 \cdot 10^{-1}$	3	LT01, LT03, LT10, L25, L28, L29, L30	4	3	18
Glycerol	Raw data red.	0.925	0.977	$4.59 \cdot 10^{-1}$	3	LT01, LT03, LT10, L23, L28, L29, L30	4	3	18
Ethanol	2nd derivative	0.931	0.981	$5.27 \cdot 10^{-1}$	1	LT01, LT03, LT04, LT10, L20, L23, L28, L29	4	4	20
Citric Acid	1st derivative	1.03	0.963	$2.91 \cdot 10^{-3}$	1	LT01, LT02	0	2	7
Tartaric Acid	MSC - full	1.08	0.959	$5.44 \cdot 10^{-2}$	2	LT04, LT10	0	2	7
Malic Acid	MSC - full	1.03	0.972	$6.21 \cdot 10^{-2}$	2	LT04, LT10	0	2	7
Succicinic Acid	MSC - full	0.991	0.973	$1.63 \cdot 10^{-2}$	2	LT04, LT10	0	2	7
Lactic Acid	Raw data red.	0.982	0.969	$2.17 \cdot 10^{-3}$	2	LT01, LT04, LT09, LT10, L01, L16	2	4	20
Acetic Acid	1st derivative	0.989	0.962	$2.39 \cdot 10^{-2}$	1	LT01, LT02, LT03	0	3	10

White wine (1596 – 1691 nm)							# Outliers		
Parameter	**Pre-treatment**	**Slope**	**R^2**	**RMSEP [g/L]**	**# PLS**	**Outliers**	**Cal**	**Test**	**Outliers [%]**
Sucrose	1st derivative	0.974	0.967	$1.83 \cdot 10^{-1}$	1	LT01, LT03, LT04, L22, L23, L25, L28, L30	5	3	20
Glucose	MSC - common amplification	0.994	0.971	$5.14 \cdot 10^{-1}$	1	LT01, LT04, L21, L23, L24, L26, LT03	4	3	18
Fructose	MSC - common amplification	0.987	0.969	$5.21 \cdot 10^{-1}$	1	LT01, LT04, L21, L23, L24, L26, LT03	4	3	18
Glycerol	Raw data red.	1.03	0.962	$6.47 \cdot 10^{-1}$	1	LT01, LT04, L21, L23, L24, L26	4	2	15
Ethanol	Raw data	0.974	0.959	$8.79 \cdot 10^{-1}$	1	LT01, LT04, L21, L23, L24, L26	4	2	15
Citric Acid	1st derivative	0.939	0.961	$2.99 \cdot 10^{-3}$	1	LT01, LT02	0	2	7
Tartaric Acid	1st derivative	0.975	0.987	$3.12 \cdot 10^{-2}$	1	LT02, LT03	0	2	7
Malic Acid	MSC - common amplification	0.986	0.985	$4.60 \cdot 10^{-2}$	1	LT02, LT03	0	2	7
Succicinic Acid	Raw data red.	1.02	0.956	$2.01 \cdot 10^{-2}$	1	LT02	0	1	3
Lactic Acid	1st derivative	1.05	0.978	$1.84 \cdot 10^{-3}$	1	LT01, LT03, LT09	0	3	10
Acetic Acid	1st derivative	0.992	0.985	$1.95 \cdot 10^{-2}$	2	LT02, LT03	0	2	7

Rosé wine (890 - 1691 nm)							# Outliers		
Parameter	**Pre-treatment**	**Slope**	**R^2**	**RMSEP [g/L]**	**# PLS**	**Outliers**	**Cal**	**Test**	**Outliers [%]**
Sucrose	-			-	-		-	-	-
Glucose	1st derivative	0.904	0.982	$4.28 \cdot 10^{-1}$	1	T06, T17, T20, T22	4	0	11
Fructose	MSC - full	0.906	0.967	$4.59 \cdot 10^{-1}$	3	TT01	0	1	3
Glycerol	MSC - full	1.01	0.972	$1.17 \cdot 10^{-1}$	3	T01, T19	2	0	6
Ethanol	1st derivative	1.05	0.956	$8.62 \cdot 10^{-1}$	1	T11, T17, T20, T22, TT01, TT12, TT13, TT14	4	4	22
Citric Acid	1st derivative	0.935	0.991	$3.90 \cdot 10^{-2}$	1	T06, TT01, TT12, TT13, TT14	1	4	18
Tartaric Acid	-			-	-		-	-	-
Malic Acid	1st derivative	0.940	0.985	$2.59 \cdot 10^{-2}$	1	T06	1	0	4
Succicinic Acid	MSC - full	0.863	0.982	$3.40 \cdot 10^{-2}$	3	TT01, TT02	0	2	7
Lactic Acid	Raw data red.	0.944	0.980	$5.59 \cdot 10^{-3}$	2	T02, TT05, TT06	1	2	11
Acetic Acid	-	-	-	-	-		-	-	-

Rosé wine (1596 - 2396 nm)							# Outliers		
Parameter	**Pre-treatment**	**Slope**	**R^2**	**RMSEP [g/L]**	**# PLS**	**Outliers**	**Cal**	**Test**	**Outliers [%]**
Sucrose	-	-	-	-	-		-	-	-
Glucose	2nd derivative	0.999	0.961	$6.25 \cdot 10^{-1}$	2		0	0	0
Fructose	2nd derivative	1.04	0.960	$6.11 \cdot 10^{-1}$	2		0	0	0
Glycerol	2nd derivative	0.989	0.970	$1.08 \cdot 10^{-1}$	2	TT01, TT02, TT03	0	3	8
Ethanol	Raw data red.	1.19	0.952	1.23	3	T11, T19, T22, TT13, TT14	3	2	14
Citric Acid	2nd derivative	0.937	0.970	$8.94 \cdot 10^{-2}$	1		0	0	0
Tartaric Acid	-	-	-	-	-		-	-	-
Malic Acid	2nd derivative	0.987	0.945	$4.40 \cdot 10^{-2}$	2	T01, TT11, TT14	1	2	11
Succicinic Acid	2nd derivative	1.00	0.978	$4.00 \cdot 10^{-2}$	2	TT01, TT06, TT14	0	3	11
Lactic Acid	2nd derivative	1.04	0.973	$6.26 \cdot 10^{-3}$	2	T02, TT05, TT06, TT14	1	3	14
Acetic Acid	-	-	-	-	-		-	-	-

Red wine (890 - 1691 nm)							# Outliers		
Parameter	**Pre-treatment**	**Slope**	**R^2**	**RMSEP [g/L]**	**# PLS**	**Outliers**	**Cal**	**Test**	**Outliers [%]**
Sucrose	MSC - full	0.956	0.939	$5.02 \cdot 10^{-1}$	2	S15, S17, S18, S21	4	0	11
Glucose	MSC - full	1.11	0.917	$4.01 \cdot 10^{-1}$	2	S15, S17, S18, S21, ST01, ST03	4	2	17
Fructose	Raw data	1.03	0.974	$1.89 \cdot 10^{-1}$	3	S18, ST11, ST12, ST14	1	3	11
Glycerol	MSC - full	1.05	0.899	$2.78 \cdot 10^{-1}$	2	S18	1	0	3
Ethanol	MSC - full	1.10	0.854	1.93	2	S18, ST01, ST02, ST03	1	3	11
Citric Acid	MSC - full	0.902	0.968	$3.32 \cdot 10^{-2}$	2		0	0	0
Tartaric Acid	MSC - full	0.926	0.959	$7.39 \cdot 10^{-2}$	4	S11	1	0	4
Malic Acid	MSC - full	0.993	0.974	$1.86 \cdot 10^{-2}$	2		0	0	0
Succicinic Acid	MSC - full	0.898	0.978	$4.51 \cdot 10^{-2}$	5	ST04, ST05, ST13, ST14	0	4	14
Lactic Acid	MSC - common amplification	0.979	0.960	$1.12 \cdot 10^{-2}$	2	ST04, ST05, ST11, ST14	0	4	14
Acetic Acid	Raw data	0.923	0.947	$1.59 \cdot 10^{-2}$	3	ST03	0	1	4

Red wine (1596 - 2396 nm)							# Outliers		
Parameter	**Pre-treatment**	**Slope**	**R^2**	**RMSEP [g/L]**	**# PLS**	**Outliers**	**Cal**	**Test**	**Outliers [%]**
Sucrose	Raw data red.	0.969	0.965	$4.10 \cdot 10^{-1}$	2	S02, S15, ST11, ST12, ST13, ST14	2	4	17
Glucose	2nd derivative	1.00	0.935	$3.02 \cdot 10^{-1}$	1	S02, S12, S21, ST01, ST13	3	2	14
Fructose	2nd derivative	0.920	0.959	$2.11 \cdot 10^{-1}$	2	S21, ST01, ST13	1	2	8
Glycerol	2nd derivative	1.03	0.967	$1.60 \cdot 10^{-1}$	2	S21, ST07, ST13	1	2	8
Ethanol	2nd derivative	1.11	0.893	1.64	2	S21, ST01	1	1	6
Citric Acid	Raw data	0.875	0.956	$3.99 \cdot 10^{-2}$	2	ST06	0	1	4
Tartaric Acid	Raw data	0.945	0.953	$7.47 \cdot 10^{-2}$	2	ST02	0	1	4
Malic Acid	Raw data	1.01	0.960	$2.35 \cdot 10^{-2}$	2	ST03	0	1	4
Succicinic Acid	2nd derivative	0.824	0.915	$8.10 \cdot 10^{-2}$	2	ST02, ST04, ST12, ST13	0	4	14
Lactic Acid	2nd derivative	0.853	0.895	$1.95 \cdot 10^{-2}$	2	ST04	0	1	4
Acetic Acid	Raw data	1.12	0.962	$1.26 \cdot 10^{-2}$	2	ST05, ST06, ST11, ST13	0	4	14

Appendix 8 – Second Modelling Campaign

White wine (890 - 1691 nm)						# Outliers			Range			
Parameter	Slope	R^2	RMSEP [g/L]	# PLS	Outliers	Cal	Test	% outliers	min	max		relRMSEP [%]
Sucrose	1.09	0.965	$1.91 \cdot 10^{-1}$	1	LT01, LT04, LT10, L20, L22, L27 - L30	6	3	23	0.50 -	3.45	g/L	12.9
Glucose	0.971	0.980	$6.92 \cdot 10^{-1}$	1	LT03, L28, L29, L30	3	1	10	0.70 -	15.0	g/L	9.66
Fructose	0.970	0.981	$6.28 \cdot 10^{-1}$	1	LT03, L28, L29, L30	3	1	10	0.69 -	14.3	g/L	9.22
Glycerol	0.952	0.980	$6.41 \cdot 10^{-1}$	1	LT03, L28, L29, L30	3	1	10	0.69 -	13.9	g/L	9.67
Ethanol	0.942	0.983	$8.29 \cdot 10^{-1}$	1	LT03, L28, L29, L30	3	1	10	0.84 -	19.7	g/L	8.81
Citric Acid	1.10	0.994	$1.75 \cdot 10^{-3}$	1	LT02	0	1	3	3.30 -	82.4	mg/L	4.44
Tartaric Acid	1.07	0.980	$2.89 \cdot 10^{-2}$	2	LT01, LT02	2	0	7	54.2 -	533	mg/L	12.1
Malic Acid	1.10	0.973	$4.51 \cdot 10^{-2}$	1	LT01, LT02	0	2	7	72.9 -	723	mg/L	13.9
Succicinic Acid	1.09	0.952	$1.47 \cdot 10^{-2}$	1	LT01, LT02	0	2	7	17.4 -	190	mg/L	17.1
Lactic Acid	1.05	0.976	$2.95 \cdot 10^{-3}$	1	LT07, LT09, L16	1	2	10	3.09 -	64.0	mg/L	9.68
Acetic Acid	0.993	0.990	$1.21 \cdot 10^{-2}$	1	LT01, LT02, LT03	0	3	10	35.2 -	279	mg/L	10.0
Mean	1.03	0.978	$2.81 \cdot 10^{-1}$	1				10				10.7

White wine (1596 - 2396 nm)						# Outliers			Range			
Parameter	Slope	R^2	RMSEP [g/L]	# PLS	Outliers	Cal	Test	% outliers	min	max		relRMSEP [%]
Sucrose	0.974	0.967	$1.83 \cdot 10^{-1}$	1	LT01, LT03, LT04, L22, L23, L25, L28, L30	5	3	20	0.34 -	3.45	g/L	11.8
Glucose	0.879	0.963	$5.61 \cdot 10^{-1}$	2	LT01, LT03, LT04, L23	1	3	10	0.70 -	9.96	g/L	12.1
Fructose	0.865	0.958	$5.75 \cdot 10^{-1}$	2	LT01, LT03, LT04, L23	1	3	10	0.69 -	9.49	g/L	13.1
Glycerol	0.854	0.956	$7.42 \cdot 10^{-1}$	3	LT01, LT04, LT09, L23	1	3	10	0.69 -	9.60	g/L	16.7
Ethanol	0.856	0.966	$8.19 \cdot 10^{-1}$	2	LT01, LT04, L23	1	2	8	0.84 -	12.5	g/L	14.1
Citric Acid	0.939	0.961	$2.99 \cdot 10^{-3}$	1	LT01, LT02	0	2	7	3.30 -	42.9	mg/L	15.1
Tartaric Acid	0.975	0.987	$3.12 \cdot 10^{-2}$	1	LT02, LT03	0	2	7	54.2 -	887	mg/L	7.48
Malic Acid	0.929	0.986	$4.40 \cdot 10^{-2}$	1	LT02, LT03	0	2	7	72.9 -	1254	mg/L	7.46
Succicinic Acid	0.914	0.989	$1.09 \cdot 10^{-2}$	2	LT02, LT03, LT07	0	3	10	17.4 -	341	mg/L	6.76
Lactic Acid	1.05	0.978	$1.84 \cdot 10^{-3}$	1	LT01, LT03, LT09	0	3	10	3.09 -	39.2	mg/L	10.2
Acetic Acid	0.992	0.985	$1.95 \cdot 10^{-2}$	2	LT02, LT03	0	2	7	35.2 -	540	mg/L	7.74
Mean	0.930	0.972	$2.72 \cdot 10^{-1}$	2				9				11.1

Rosé wine (890 - 1691 nm)						# Outliers			Range			
Parameter	**Slope**	**R^2**	**RMSEP [g/L]**	**# PLS**	**Outliers**	**Cal**	**Test**	**% outliers**	**min**	**max**		**relRMSEP [%]**
Sucrose	-	-	-	-		-	-	-	-	-	-	-
Glucose	0.929	0.971	$4.43 \cdot 10^{-1}$	2	TT01	0	1	3	0.42 -	8.49	g/L	11.0
Fructose	0.949	0.973	$4.13 \cdot 10^{-1}$	2	TT01	0	1	3	0.39 -	8.14	g/L	10.7
Glycerol	1.08	0.921	$1.99 \cdot 10^{-1}$	2	TT02, T11	1	1	6	0.086 -	2.42	g/L	17.1
Ethanol	1.10	0.974	$8.19 \cdot 10^{-1}$	1	T01, TT02, TT03, TT13, TT14	1	4	14	1.10 -	17.0	g/L	10.3
Citric Acid	1.04	0.982	$7.16 \cdot 10^{-2}$	2	T11	1	0	4	61.1 -	1492	mg/L	10.0
Tartaric Acid	-	-	-	-		-	-	-	-	-	-	-
Malic Acid	1.06	0.979	$2.95 \cdot 10^{-2}$	2	TT13, TT14, T11	1	2	11	38.3 -	602	mg/L	10.5
Succicinic Acid	0.894	0.970	$4.63 \cdot 10^{-2}$	3	TT01, T11	1	1	7	23.8 -	707	mg/L	13.5
Lactic Acid	1.06	0.945	$9.94 \cdot 10^{-3}$	2	TT01, TT05, T11	1	2	11	4.22 -	93.5	mg/L	22.3
Acetic Acid	-	-	-	-		-	-	-	-	-	-	-
Mean	1.01	0.964	$2.54 \cdot 10^{-1}$	2				7				13.2

Rosé wine (1596 - 2396 nm)						# Outliers			Range			
Parameter	**Slope**	**R^2**	**RMSEP [g/L]**	**# PLS**	**Outliers**	**Cal**	**Test**	**% outliers**	**min**	**max**		**relRMSEP [%]**
Sucrose	-	-	-	-		-	-	-	-	-	-	-
Glucose	0.999	0.961	$6.25 \cdot 10^{-1}$	2		0	0	0	0.42 -	10.8	g/L	12.0
Fructose	1.04	0.960	$6.11 \cdot 10^{-1}$	2		0	0	0	0.39 -	10.3	g/L	12.3
Glycerol	0.989	0.970	$1.08 \cdot 10^{-1}$	2	TT01, TT02, TT03	0	3	8	0.086 -	1.30	g/L	17.7
Ethanol	1.19	0.952	1.23	3	T11, T19, T22, TT13, TT14	3	2	14	1.10 -	170	g/L	15.5
Citric Acid	0.937	0.970	$8.94 \cdot 10^{-2}$	1		0	0	0	61.1 -	1492	mg/L	12.5
Tartaric Acid	-	-	-	-		-	-	-	-	-	-	-
Malic Acid	0.987	0.945	$4.40 \cdot 10^{-2}$	2	T01, TT11, TT14	1	2	11	33.4 -	468	mg/L	20.2
Succicinic Acid	1.00	0.978	$4.00 \cdot 10^{-2}$	2	TT01, TT06, TT14	0	3	11	33.4 -	707	mg/L	11.9
Lactic Acid	1.04	0.973	$6.26 \cdot 10^{-3}$	2	T02, TT05, TT06, TT14	1	3	14	6.87 -	106	mg/L	12.6
Acetic Acid	-	-	-	-		-	-	-	-	-	-	-
Mean	1.02	0.964	$3.44 \cdot 10^{-1}$	2				7				14.4

Red wine (890 - 1691 nm)						# Outliers			Range			
Parameter	**Slope**	**R^2**	**RMSEP [g/L]**	**# PLS**	**Outliers**	**Cal**	**Test**	**% outliers**	**min**	**max**		**relRMSEP [%]**
Sucrose	0.933	0.971	$3.20 \cdot 10^{-1}$	2	ST02, ST09, ST13, S02, S15, S18	3	3	17	0.21 -	6.13	g/L	10.8
Glucose	1.06	0.970	$2.26 \cdot 10^{-1}$	2	ST01, ST03, ST09, S18, S20	2	3	14	0.14 -	3.93	g/L	11.9
Fructose	1.01	0.992	$1.00 \cdot 10^{-1}$	1	ST01, ST09, S18, S20	2	2	11	0.12 -	3.30	g/L	6.29
Glycerol	0.993	0.987	$9.94 \cdot 10^{-2}$	1	ST09, ST20	1	1	6	0.11 -	2.84	g/L	7.27
Ethanol	1.12	0.891	1.27	1	ST01, ST02, ST03, ST09, ST10, ST11, ST13, ST14, S18	1	8	25	0.65 -	13.3	g/L	20.1
Citric Acid	0.962	0.980	$2.72 \cdot 10^{-2}$	3	ST09, S14	1	1	7	28.2 -	554	mg/L	10.3
Tartaric Acid	1.02	0.942	$8.69 \cdot 10^{-2}$	3	ST02, ST09, S14	1	2	11	50.1 -	1010	mg/L	18.1
Malic Acid	1.03	0.964	$2.27 \cdot 10^{-2}$	1	ST09, S14	1	1	7	13.2 -	324	mg/L	14.6
Succicinic Acid	0.930	0.927	$7.68 \cdot 10^{-2}$	4	ST02, ST09, ST14, S14	1	3	14	52.8 -	920	mg/L	17.7
Lactic Acid	0.896	0.966	$1.01 \cdot 10^{-2}$	1	ST04, ST05, ST09, S01	1	3	14	8.76 -	153	mg/L	14.1
Acetic Acid	1.13	0.990	$7.78 \cdot 10^{-3}$	1	ST01, ST02, ST03, ST09, S14	1	4	18	8.39 -	131	mg/L	12.7
Mean	1.01	0.962	$2.04 \cdot 10^{-1}$	2				13				13.1

Red wine (1596 - 2396 nm)						# Outliers			Range			
Parameter	**Slope**	**R^2**	**RMSEP [g/L]**	**# PLS**	**Outliers**	**Cal**	**Test**	**% outliers**	**min**	**max**		**relRMSEP [%]**
Sucrose	0.864	0.890	$6.69 \cdot 10^{-1}$	1	S02, S21	2	0	6	0.21 -	6.13	g/L	22.6
Glucose	1.00	0.935	$3.02 \cdot 10^{-1}$	1	S02, S12, S21, ST01, ST13	3	2	14	0.14 -	3.93	g/L	15.9
Fructose	0.920	0.959	$2.11 \cdot 10^{-1}$	2	S21, ST01, ST13	1	2	8	0.12 -	3.30	g/L	13.3
Glycerol	1.03	0.967	$1.60 \cdot 10^{-1}$	2	S21, ST07, ST13	1	2	8	0.11 -	2.84	g/L	11.7
Ethanol	1.09	0.881	1.81	2	S21, ST01	1	1	6	0.65 -	13.3	g/L	28.8
Citric Acid	0.837	0.945	$4.26 \cdot 10^{-2}$	2	ST13	0	1	4	20.9 -	554	mg/L	16.0
Tartaric Acid	0.913	0.935	$8.55 \cdot 10^{-2}$	2	ST02, ST13	0	2	7	50.1 -	1010	mg/L	17.8
Malic Acid	0.961	0.981	$1.57 \cdot 10^{-2}$	2	ST03, ST13	0	2	7	13.2 -	324	mg/L	10.1
Succicinic Acid	0.824	0.915	$8.10 \cdot 10^{-2}$	2	ST02, ST04, ST12, ST13	0	4	14	52.8 -	920	mg/L	18.7
Lactic Acid	0.853	0.895	$1.95 \cdot 10^{-2}$	2	ST04	0	1	4	8.76 -	153	mg/L	27.1
Acetic Acid	0.992	0.902	$1.96 \cdot 10^{-2}$	2	S06, ST13	1	1	7	8.39 -	160	mg/L	25.9
Mean	0.935	0.928	$3.11 \cdot 10^{-1}$	2				8				18.9

Appendix 9 – Modelling Campaign for Total Models

White wine (890 - 1691 nm)						# Outliers			Range			relRMSEP
Parameter	**Slope**	**R^2**	**RMSEP [g/L]**	**# PLS**	**Outliers**	**Cal**	**Test**	**% outliers**	**min**	**max**		**[%]**
Total Sugar	0.992	0.980	1.57	1	LT03, L29	1	1	5	1.74 -	34.0	g/L	9.72
Glycerol	0.952	0.980	0.641	1	LT03, L28, L29, L30	3	1	10	0.690 -	13.9	g/L	9.67
Ethanol	0.942	0.983	0.829	1	LT03, L28, L29, L30	3	1	10	0.843 -	19.7	g/L	8.81
Ethanol			0.105						0.107 -	2.49	% vol	
Total Acid	1.02	0.989	0.0721	3	LT01, LT02	0	2	7	0.186 -	1.82	g/L	8.83

Rosé wine (890 - 1691 nm)						# Outliers			Range			relRMSEP
Parameter	**Slope**	**R^2**	**RMSEP [g/L]**	**# PLS**	**Outliers**	**Cal**	**Test**	**% outliers**	**min**	**max**		**[%]**
Total Sugar	0.892	0.961	1.07	2	TT01, TT09, T11	1	2	8	0.812 -	17.6	g/L	12.8
Glycerol	1.08	0.921	0.199	2	TT02, T11	1	1	6	0.086 -	2.42	g/L	17.1
Ethanol	1.10	0.974	0.819	1	T01, TT02, TT03, TT13, TT14	1	4	14	1.10 -	17.0	g/L	10.3
Ethanol			0.104						0.140 -	2.15	% vol	
Total Acid	0.923	0.972	0.156	3	TT01, TT02	0	2	7	0.134 -	2.28	g/L	14.6

Red wine (890 - 1691 nm)						# Outliers			Range			relRMSEP
Parameter	**Slope**	**R^2**	**RMSEP [g/L]**	**# PLS**	**Outliers**	**Cal**	**Test**	**% outliers**	**min**	**max**		**[%]**
Total Sugar	1.00	0.979	0.659	2	ST09, S18, S20	2	1	8	0.479 -	14.0	g/L	9.76
Glycerol	0.993	0.987	0.0994	1	ST09, S20	1	1	6	0.108 -	2.84	g/L	7.27
Ethanol	1.12	0.891	1.27	1	ST01, ST02, ST03, ST09 - ST11, ST13, ST14, S18	1	8	25	1.08 -	9.04	g/L	31.9
Ethanol			0.161						0.0824 -	1.68	% vol	
Total Acid	0.944	0.967	0.198	3	ST01, ST09, S11, S14	2	2	13	0.140 -	2.77	g/L	15.1

Appendix 10 – Variography

Sampling

1-D sampling can be done in three ways; Systematic, stratified random, and random of which the systematic is used in variographic analysis. Systematic sampling is sampling with the same distance between increments. Random sampling is sampling at random intervals. Stratified random is the random sampling within a systematic distance which is kept constant and repeated for the whole sampling period. Systematic sampling is used when variographic analysis is perform. The chronological order of the increments has to be known and included in the analysis. [59, 61, 63]

Heterogeneity

Sampling of a 1-D lot requires a characterization of the non-random heterogeneity fluctuations along the extended dimension of the lot (heterogeneity between increments). The heterogeneity is comprised of three parts [63]

- Short range fluctuation contributions: the heterogeneity within a particular increment being delineated for extraction (correct 0-D sampling + FSE + GSE), called PIE1
- Long range fluctuation contributions: the longer term trends in the process (Time fluctuation error, TFE), called PIE2
- Cyclic term: periodic variation of the lot (cyclic fluctuation error, CFE), called PIE3

Lag

At least 60 increments has to be extracted to give a reliable variographic analysis. This is of course depending on the process, but is a rule of thumb.

The distance between extracted increments are process depending and are measured in e.g. minutes or m^3. The normalized distance between the increments is a dimensionless parameter for the lag, j

$$j = \frac{\theta}{\theta_{min}}$$

θ is the inter-sample interval and θ_{min} is the smallest interval sampled, which is supposed to be smaller than the most probable sampling frequency. Lags higher than $j = N_u/2$ are not used in practice, since this will result in calculations were not all experimental values are included in the evaluation. N_u is the number of units (increments) combined to a composite sample (also called the sample pairs). An illustration of the lag and extraction of increments are shown in Figure 120. The lag starts from one, since a lag of zero would corresponds to extracting the same increment twice and this is not possible in practice.

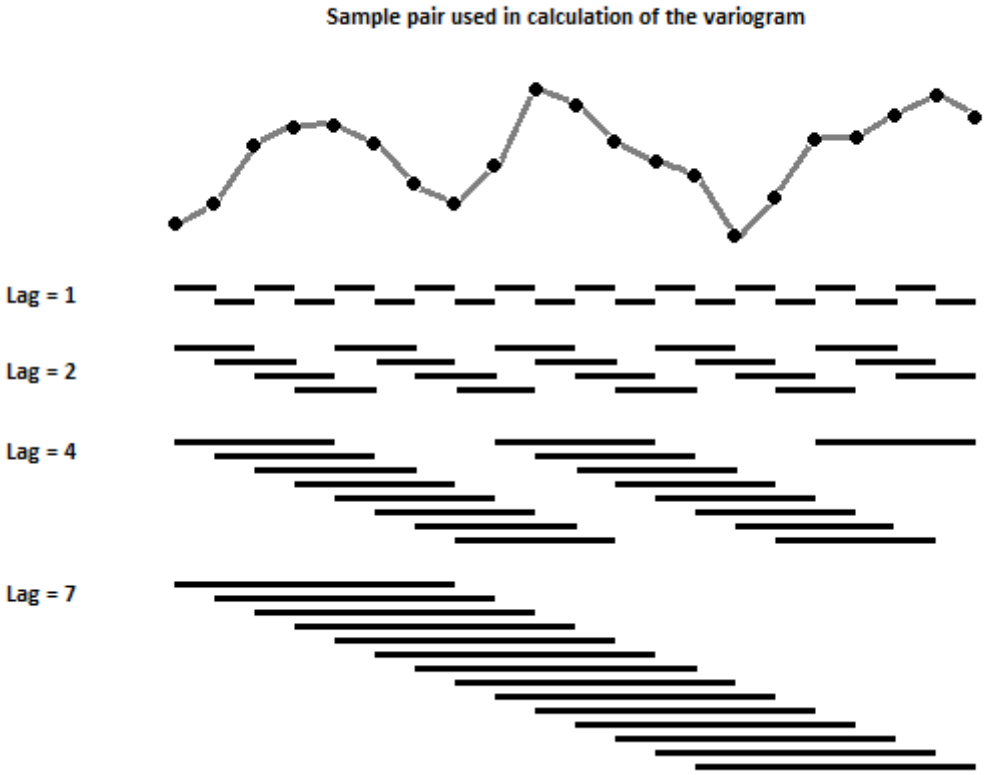

Figure 120 Increments used for the variographic analysis.
Effective lags of 1, 2, 4, and 7 are illustrated

Variographic Analysis

Variography is a heterogeneity characterization of the 1-D lot and is used to characterize the autocorrelation of 1-D lots as a function of the distance between extracted increments. Variography is also used for identifying ascending or decreasing trends and cycles in the process data.

The Function for the Variogram

The function for the variogram is defined as ½ times the average squared difference in heterogeneity contributions between the sum of pairs of increments as a function of j [61]

$$V(j) = \frac{1}{2(N_u - j)a_L^2}\sum_m (a_{m+j} - a_m)^2$$

The above equation is the relative variogram based upon the heterogeneity distribution. The variogram can also be based upon concentration, which is called the absolute variogram [61]

$$V(j) = \frac{1}{2(N_u - j)}\sum_m (h_{m+j} - h_m)^2$$

Shape of the variogram

When analysis of the experimental variogram is made the first approach is to identify the form and level of the variogram. This will give valuable information on the process variation and the quality of the sampling process. [59, 61, 63]

There are only three principal types of variogram, where all variograms are like one of them or a combination of more of them. The types are (see Figure 121)

- The increasing variogram
- The flat variogram
- The periodic variogram

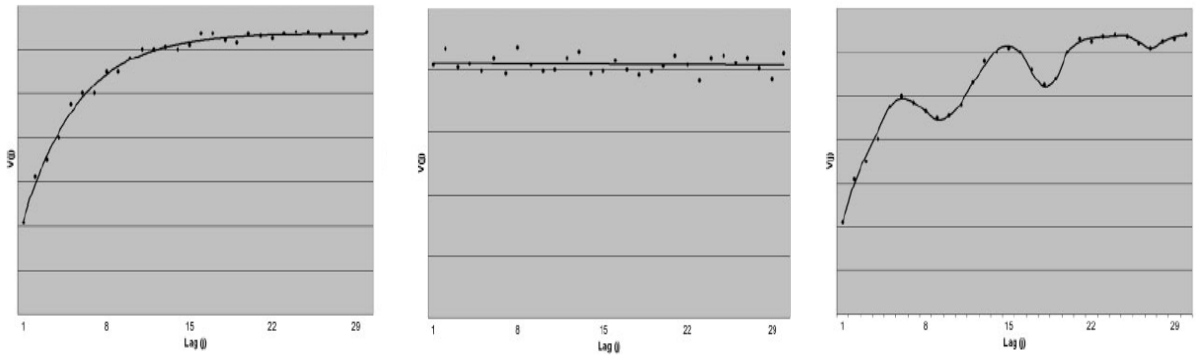

Figure 121 Three types of variograms; left: increasing variogram, center: flat variogram and right: periodic variogram [61]

The increasing variogram is the most often found variogram, the flat variogram shown no autocorrelation along the x-axis and the periodic variogram shows fluctuations along the x-axis. The periodic variogram in Figure 121 is shown on a increasing variogram, but can also be seen on a flat variogram.

Nugget effect, Sill and Range

The next approach is to identify the nugget effect, sill and range of the process, see Figure 122. They describe different aspects of the process variation of to what degree the incorrect sampling errors is included in the process variation. [59, 61, 63]

- **Nugget effect:** This is an estimate for the minimal practical error which is present in the process variation. The nugget effect is in TOS calculated as back-extrapolated of the first five points to intercept the ordinate axis of the variogram. The nugget effect include the FSE, GSE, TAE and all ISE, which has not be eliminated or minimized.
- **Sill:** This provides information about the expected maximum process variation if autocorrelation between increments is not taken into account.
- **Range:** This is found as the lag beyond which no autocorrelation is present. Autocorrelation increases when the inter-sample lag becomes smaller. This meaning when decreasing the lag down to one the grade of the slope of the variance (the slope of a line between the points from zero to the sill in the variogram) from the sill level is a affirmation of more and more autocorrelation in the process data.

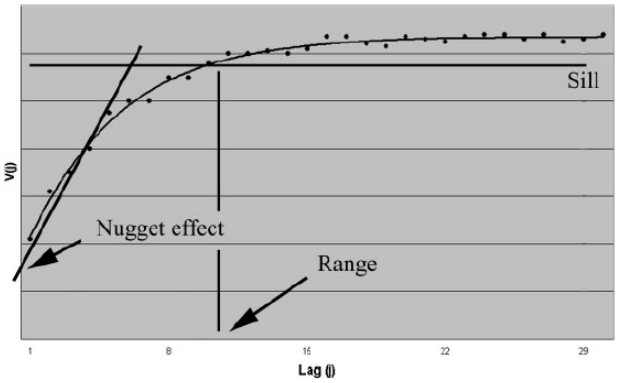

Figure 122 Variogram, showing nugget effect, sill and range [61]

Optimal Sampling Scheme

When the variographic analysis is made, the optimal sampling scheme can be derived by [63]

- Avoiding to sample at the period of a periodic variogram. If a periodic variogram is found it is important not to sample with a frequency equal or close to the period. The sampling process in that case would not be representative for the whole process variability and result in an underestimation of the true variation.
- Using the systematic sampling strategy. Stratified random sampling strategy will lead to optimal results, but the systematic sampling strategy is in many cases just as effective. The advantage is that it is easier to incorporate for automatic sampling.
- Sampling with a frequency below the range. This will ensure that the autocorrelation in the process will effectively reduce the sampling variation. This is further more ensured if increments are combined to a composite sample before analysis.
- Ensuring that the nugget effect is as small as possible (equal to the minimal practical error) by elimination all incorrect sampling errors and minimizing FSE and GSE.
- Finding the correct combination of distance between the increments extracted and the correct number of increments to combine in a composite sample. This is done by calculation of the total sampling error for the sampling process.

Total Sampling Error

After the variographic analysis is made with regards to the variogram it is possible to make a simulation of the total sampling error (TSE) for all combinations of j and Q, where j is the distance between the increments and Q is the number of increments combined to a composite sample. The simulation is made on basis of the same data as the variogram, so no further sampling is necessary. [59, 61, 63]

The TSE in TOS is split into seven error components and they characterize the material and the sampling procedure.

- FSE: Fundamental Sampling Errors
- GSE: Grouping and Segregation Errors
- ISE: Incorrect Sampling Errors
    - IDE: Incorrect Delimination Errors
    - IEE: Incorrect Extraction Errors
    - IPE: Incorrect Preparation Errors
- TFE: Time Fluctuation Errors
- CFE: Cyclic Fluctuation Errors

FSE and GSE are always present and are material specific. The sum of the two is the Minimal Practical Error (MPE). The variance of the MPE (s^2_{MPE}) is equal to the nugget effect in the variogram. The ISE can all be eliminated from the sampling procedure. It is probably not an easy task to do, but they should be minimized as much as possible. TFE and CFE are only present in 1D sampling. When discussing TSE for the variographic experiments it is the sum of all seven errors.

$$s_{TSE} = \sqrt{s^2_{FSE} + s^2_{GSE} + s^2_{IDE} + s^2_{IEE} + s^2_{IPE} + s^2_{TFE} + s^2_{CFE}}$$

The TSE is by the software often shown graphically as 3-D histograms of different combinations of j and Q. In this 3-D histogram the TSE is the standard deviation to the result for the particular combination of j and Q.

A starting point in designing the optimal sampling plan with the help of TSE is to compare different combinations of j and Q and than work in the direction where there is seen steepest descending in the results.

In practice when both the variogram and the TSE are calculated, they are based upon one set of samples extracted in one run. The different combinations of lag and increments are only a simulation based on the one dataset and not a new dataset for each combination.

Since TSE is a sum of the seven errors it can be divide into two main contributions arising from the 0-D - and 1-D – process variation. The 0-D - process variation is the contribution from FSE, GSE, ISE and TAE and is named minimum process error (MPE). The variance for the MPE is equal to the nugget effect (V(0)) in the variogram. This is the uncertainty from the sampling procedure.

$$s^2_{MPE} = s^2_{FSE} + s^2_{GSE} + s^2_{ISE} + s^2_{TAE} = V(0)$$

The 1-D – process variation is the uncertainty contribution from the process, here it is the variation in composition of the waste water stream (material heterogeneity). The 1-D – process variation is the difference between the sill and nugget effect in the variogram.

Appendix 11 – Experimental Variograms from Vario and IMM

Experimental variograms made upon basis of the results obtained in a previous study of three waste water treatment facilities[4]. In the experimental variograms each lag was equal to 2.5 minutes.

Vario (TOS)

Lynetten, serie A

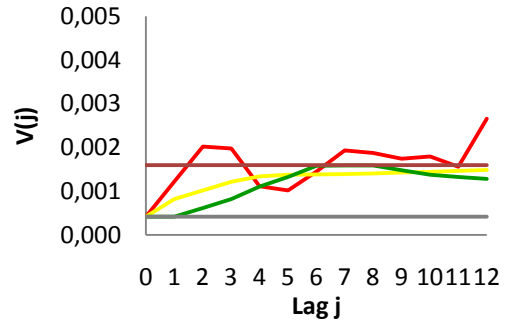

Lynetten, serie B

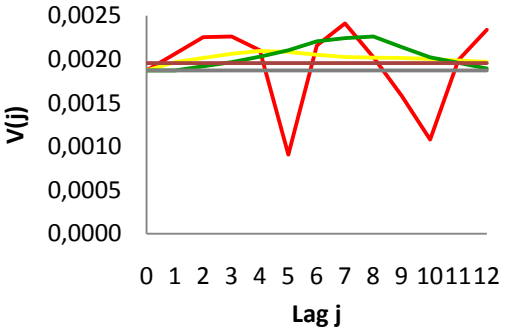

Karup

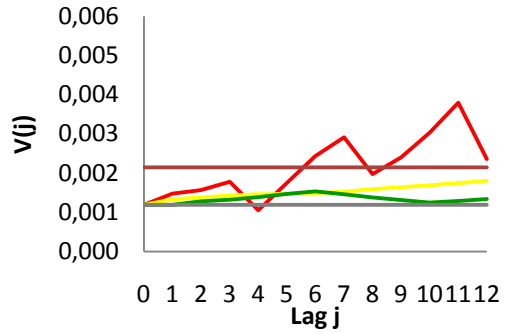

IMM [51, 53]

Lynetten, serie A

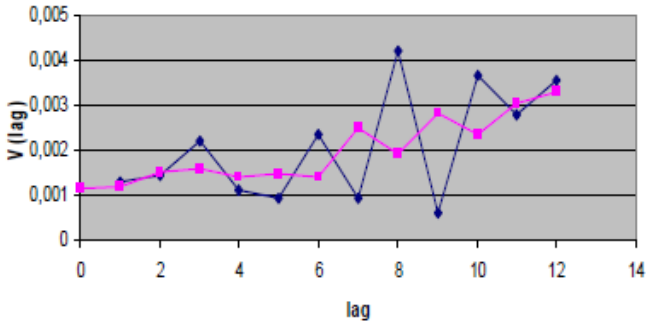

Lynetten, serie B

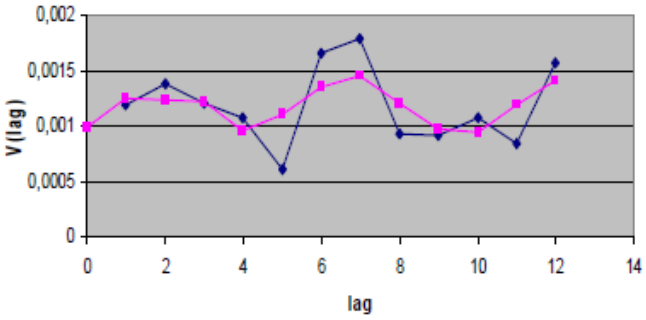

Karup

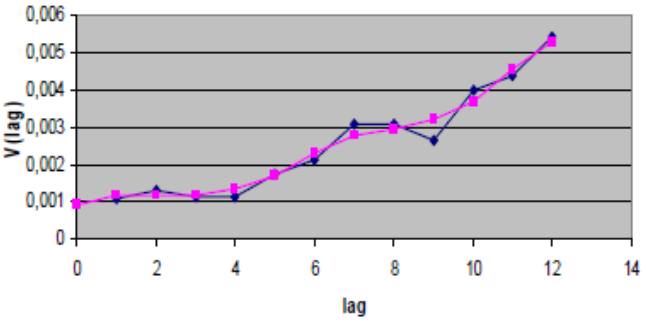

Mejlby, 2006

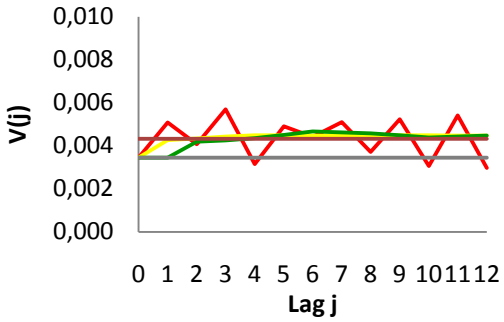

Mejlby, 2006

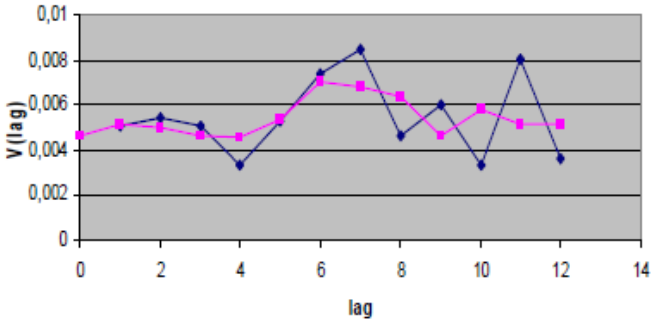

Mejlby, 2007

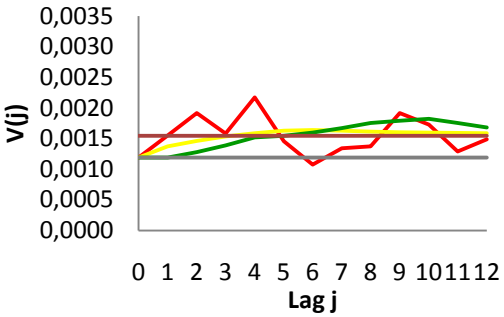

Mejlby, 2007

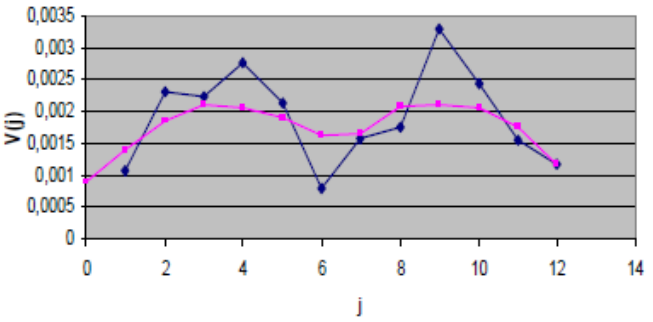

Red: V(j)
Yellow: W(j)st
Green: W(j)sy
Gray: V(0)
Braun: Sill

Blue: Estimated
Pink: Fitted

Appendix 12 – Analytical Uncertainty

TP

Eurofins Environment A/S		
#	Measurement	
1	223.861	µg/L
2	218.110	µg/L
3	218.943	µg/L
4	218.883	µg/L
5	222.398	µg/L
6	218.670	µg/L
7	221.106	µg/L
8	220.337	µg/L
9	220.256	µg/L
10	221.773	µg/L
Mean	220.434	µg/L
Std dev.	1.857	µg/L
CV	0.842	%

EIT AAU		
#	Measurement	
1	133.199	µg/L
2	141.834	µg/L
3	147.344	µg/L
4	135.204	µg/L
5	140.887	µg/L
6	144.797	µg/L
7	135.136	µg/L
8	149.141	µg/L
9	138.703	µg/L
10	151.946	µg/L
Mean	140.694	µg/L
Std dev.	6.402	µg/L
CV	4.55	%

Conductivity

EIT AAU		
#	Measurement	
1	137.6	µS/cm
2	135.9	µS/cm
3	137.2	µS/cm
4	136.6	µS/cm
5	137.5	µS/cm
6	136.9	µS/cm
7	135.8	µS/cm
8	133.2	µS/cm
9	137.1	µS/cm
10	135.9	µS/cm
11	137.6	µS/cm
12	135.9	µS/cm
Mean	136.4	µS/cm
Std dev	1.24	µS/cm
CV	0.91	%

NH_4-N

EIT AAU		
#	Measurement	
1	0.121	mg/L
2	0.121	mg/L
3	0.121	mg/L
4	0.124	mg/L
5	0.127	mg/L
6	0.131	mg/L
7	0.119	mg/L
8	0.122	mg/L
9	0.122	mg/L
10	0.120	mg/L
11	0.124	mg/L
12	0.123	mg/L
Mean	0.123	mg/L
Std dev.	0.003	mg/L
CV	2.70	%

Appendix 13 – Mass of Increments

#	Mass (Container) [g]	Mass (Container + water) [g]	Mass (water) [g]
1	11.289	54.029	42.740
2	11.326	54.163	42.837
3	11.199	55.017	43.818
4	11.276	55.654	44.378
5	11.194	57.788	46.594
6	11.286	55.835	44.549
7	11.291	56.665	45.374
8	11.329	56.331	45.002
9	11.168	54.892	43.724
10	11.279	55.153	43.874
		Mean	44.289 g
		Stdafv	1.169 g
		CV	2.64 %

Appendix 14 – Volume Reduction

Eurofins Environment A/S

Sample no.	1st measurement TP [µg/L]	2nd measurement TP [µg/L]	Mean TP [µg/L]	Stddev TP [µg/L]
1	193.528	199.691	196.609	4.358
2	194.096	198.209	196.153	2.909
3	199.972	199.837	199.904	0.096
4	197.612	200.071	198.842	1.739
5	195.003	197.075	196.039	1.466
6	194.282	193.099	193.691	0.836
7	198.198	196.516	197.357	1.190
8	196.534	194.875	195.705	1.173
9	194.173	191.401	192.787	1.960
10	200.093	200.211	200.152	0.084
11	189.573	193.157	191.365	2.534
12	197.544	193.619	195.581	2.776
		Mean	196.182	µg/L
		Stddev	2.693	µg/L
		RSV	1.37	%

EIT AAU

Sample no.	1st measurement TP [µg/L]	2nd measurement TP [µg/L]	Mean TP [µg/L]	Stddev TP [µg/L]	Conductivity [µS/cm]
1	136.582	134.101	135.342	1.754	290
2	145.957	142.068	144.013	2.750	285
3	150.042	148.049	149.045	1.410	289
4	135.823	134.759	135.291	0.752	293
5	137.340	140.247	138.794	2.056	290
6	145.683	144.170	144.927	1.070	293
7	134.443	150.575	142.509	11.41	293
8	151.259	149.594	150.427	1.177	293
9	138.701	140.290	139.496	1.124	295
10	155.833	154.224	155.029	1.138	284

TP			**Conductivity**		
Mean	143.487	µg/L	**Mean**	291	µS/cm
Stddev	6.558	µg/L	**Stddev**	3.77	µS/cm
RSV	4.57	%	**RSV**	1.30	%

Appendix 15 –Total Phosphorous in Increments

Analytical data for TP in Increments From Sampling Point F

#	[µg/L]		#	[µg/L]		#	[µg/L]
1	279.103		49	312.467		97	408.686
2	254.364		50	315.688		98	397.231
3	250.630		51	317.473		99	382.186
4	255.537		52	312.828		100	399.840
5	247.889		53	313.487		101	404.107
6	250.676		54	310.489		102	395.271
7	247.178		55	318.560		103	406.388
8	256.342		56	327.559		104	414.835
9	246.876		57	320.987		105	406.283
10	254.631		58	320.312		106	(1123.87) 414.442
11	243.966		59	315.122		107	422.600
12	244.975		60	319.388		108	409.618
13	245.683		61	317.048		109	410.036
14	244.870		62	319.312		110	427.477
15	243.772		63	316.034		111	416.356
16	249.990		64	329.404		112	422.325
17	249.351		65	329.462		113	414.551
18	248.286		66	327.710		114	428.870
19	255.066		67	322.267		115	413.149
20	253.238		68	327.604		116	408.628
21	259.497		69	330.820		117	419.579
22	271.545		70	322.789		118	419.082
23	268.775		71	340.413		119	(563.896) 415.704
24	276.594		72	328.231		120	412.326
25	278.485		73	330.459		121	417.414
26	274.772		74	339.107		122	434.515
27	270.302		75	335.813		123	421.918
28	268.441		76	333.328		124	432.269
29	264.678		77	334.268		125	441.249
30	270.838		78	334.207		126	438.031
31	270.168		79	331.758		127	442.451
32	278.071		80	326.969		128	426.109
33	276.422		81	331.892		129	426.961
34	281.885		82	347.651		130	(478.275) 426.146
35	280.452		83	380.685		131	425.332
36	288.250		84	358.250		132	412.866
37	294.764		85	361.956		133	414.068
38	304.233		86	355.421		134	411.347
39	297.631		87	360.092		135	401.702
40	301.005		88	379.372		136	428.681
41	300.281		89	357.332		137	433.507
42	302.999		90	358.561		138	441.573
43	304.104		91	365.772		139	432.251
44	321.042		92	366.114		140	402.475
45	319.483		93	376.274			
46	314.172		94	383.542		**Mean [µg/L]**	340.699
47	310.776		95	382.819		**Stddev [µg/L]**	62.41
48	313.668		96	384.616		**CV [%]**	18.32

Analytical data for TP in Increments From Sampling Point A

#	[µg/L]		#	[µg/L]		#	[µg/L]
1	371.905		49	301.696		97	386.785
2	293.014		50	295.808		98	369.290
3	258.127		51	290.930		99	360.487
4	248.142		52	291.444		100	371.551
5	232.210		53	292.107		101	383.992
6	228.589		54	294.219		102	400.391
7	222.483		55	296.319		103	404.116
8	227.975		56	296.902		104	395.789
9	221.751		57	296.778		105	394.638
10	221.509		58	296.180		106	(444.577) 395.159
11	219.883		59	291.355		107	395.680
12	218.027		60	291.277		108	388.732
13	216.467		61	296.414		109	389.609
14	220.595		62	294.541		110	401.246
15	214.751		63	296.854		111	399.642
16	219.108		64	307.939		112	399.014
17	222.052		65	311.642		113	399.486
18	219.340		66	305.859		114	433.854
19	220.671		67	311.365		115	405.322
20	225.497		68	306.203		116	402.446
21	218.712		69	311.556		117	412.360
22	241.030		70	306.296		118	402.776
23	244.010		71	301.093		119	414.705
24	245.483		72	313.470		120	398.459
25	247.808		73	307.637		121	410.396
26	242.881		74	318.118		122	400.680
27	240.017		75	322.842		123	401.882
28	242.737		76	316.795		124	421.295
29	248.433		77	313.801		125	416.020
30	247.709		78	312.350		126	425.691
31	248.398		79	310.460		127	407.940
32	252.117		80	310.058		128	402.655
33	255.884		81	307.812		129	406.661
34	262.172		82	327.329		130	400.306
35	260.728		83	359.270		131	398.485
36	265.330		84	336.333		132	396.073
37	273.409		85	339.505		133	390.381
38	278.752		86	332.825		134	388.878
39	274.089		87	330.182		135	380.018
40	277.541		88	347.428		136	405.576
41	275.610		89	337.055		137	410.117
42	279.983		90	333.819		138	404.979
43	281.243		91	343.969		139	407.669
44	297.326		92	343.061		140	385.667
45	300.211		93	346.929			
46	294.303		94	358.394		**Mean [µg/L]**	312.153
47	285.495		95	358.107		**Stddev [µg/L]**	62.15
48	287.565		96	368.907		**CV [%]**	19.91

Blue numbers are outliers

Red numbers are calculated as the mean of the two surrounding results

Appendix 16 – Calculations of Coefficient of Variation

Calculations of Coefficient of Variation

The coefficient of variation (CV) for the analysis ($CV_{analysis}$)can be calculated from the standard deviation (s) and the mean concentration of the parameter ($\bar{x}$)

$$CV_{analysis} = \frac{s}{\bar{x}} \cdot 100$$

$CV_{measurement}$ is a sum of the variation from the analytical measurement ($CV_{analysis}$) and the variation from the sampling process ($CV_{sampling}$), not including time fluctuation errors.

$$CV^2_{measurement} = CV^2_{analysis} + CV^2_{sampling}$$

$CV_{measurement}$ can be calculated from the nugget effect (V(0)) in a variogram, since CV(0) is a estimate for $CV_{measurement}$ [51]

$$CV(0) = \sqrt{V(0)} \cdot 100 = \sqrt{s^2_{CSE} + s^2_{ISE} + s^2_{TAE}} \cdot 100 = CV_{measurement}$$

Where CSE is the Correct Sampling Errors (Fundamental Sampling Error and Grouping and Segregation Error) and ISE is the Incorrect Sampling Errors (Incorrect Delimitation Error, Incorrect Extraction Error and Incorrect Preparation Error).

With the above equations an estimate for the variation from sampling can be calculated as

$$CV_{sampling} = \sqrt{CV^2_{measurement} - CV^2_{analysis}}$$

Example of the calculations

For the calculations is used data from the present study when measuring TP in increments at sampling point F.

Coefficient of variation for the analysis

$$CV_{analysis} = \frac{s}{\bar{x}} \cdot 100 = \frac{1.857}{220.434} \cdot 100 = 0.842\ \%$$

Coefficient of variation for the measurement

$$CV_{measurement} = \sqrt{V(0) \cdot 100} = \sqrt{0.00028} \cdot 100 = 1.67\ \%$$

Coefficient of variation for the sampling

$$CV_{sampling} = \sqrt{CV^2_{measurement} - CV^2_{analysis}} = \sqrt{(1.67\ \%)^2 - (0.842\ \%)^2} = 1.45\ \%$$

Appendix 17 – Journal for Sampling Point F; 24-hour Samples

# Day	# Hours	Total H_2O [m^3]	H_2O per increment [m^3]	Rain [mm]	Approx. Vol. extracted [L]	# increments	Remarks
1	24:00	910	10	-	-	90	
2	24:00	920	10	-	-	90	
3	24:00	877	10	-	-	87	Discarded due to error in the sampling process
4	24:00	1793	10	9	-	179	
5	23:45	1530	10	-	8	153	
6	23:00	1590	10	6	8.6	159	
7	22:30	1293	10	8	7	129	
8	23:30	3503	10	13	10.6	200	Ended before recorded time, discarded
9	23:50	1761	15	3	6.8	117	
10	23:20	982	10	1	5	98	
11	23:30	1007	10	0	5.4	100	
12	23:50	2402	10	12	11	200	Ended before recorded time, discarded
13	23:45	2001	15	0	6.8	123	Discarded due to error in the sampling process. Increment volume adjusted
14	24:00	1945	7	22	14.3	276	Variography, 1st day
15	22:00	1624	7	4	12.9	232	Variography, 2nd day
16	24:00	3475	20	2	8.8	173	
17	22:30	1297	20	2	3.8	64	Too few increments
18	23:30	2882	12	9	10.2	200	Ended before recorded time, discarded
19	22:00	1282	15	0	4.6	82	Too few increments
20	22:40	2090	10	8	1.5	22	Discarded due to error in the sampling process
21	23:30	2459	15	4	8.3	163	
22	22:30	1353	15	2	5	90	
23	23:50	1491	15	4	5.2	99	
24	24:00	2972	15	8	9.9	198	
25	23:50	2022	15	4	7	134	
26	22:20	2058	12	5	8.7	171	
27	22:05	2429	12	6	10.1	200	Ended before recorded time, discarded
28	24:00	1982	15	6	6	132	
29	22:05	3564	20	16	9	178	
30	23:45	2215	20	0	5.9	110	
31	24:00	1676	15	2	5.9	111	
32	24:00	1973	12	6	8.4	164	
33	21:45	80	20	16	0	4	Discarded due to error in the sampling process
34	22:15	4000	20	16	10.2	200	
35	23:15	4000	20	8	10.2	200	
36	24:00	4000	20	11	10.1	200	
37	23:30	4000	20	16	10.2	200	
38	24:00	3943	20	16	10	197	
39	23:55	4000	20	12	10	200	Recorded error with one increment sampling

Appendix 18 – Journal for Sampling Point E; 24-hour Samples

# Day	# Hours	Total H_2O [m^3]	H_2O per increment [m^3]	Rain [mm]	Approx. Vol. extracted [L]	# increments	Remarks
1	24:00	910	10	-	-	90	
2	24:00	920	10	-	-	90	
3	24:00	877	10	-	-	-	Discarded due to error in the sampling process
4	24:00	1793	10	9	-	179	
5	23:45	1530	10	-	8	153	
6	23:00	1590	10	6	8.1	159	
7	22:30	1293	10	8	6.8	129	
8	23:30	3503	10	13	10.1	200	Ended before recorded time, discarded
9	23:50	1761	15	3	6.2	117	
10	23:20	982	10	1	5	98	
11	23:30	1007	10	0	5.1	100	
12	23:50	2402	10	12	1.1	200	Ended before recorded time, discarded
13	23:45	2001	15	0	6.4	123	Discarded due to error in the sampling process. Increment volume adjusted
14	24:00	1945	7	22	14.3	276	Variography, 1st day
15	22:00	1624	7	4	12.9	232	Variography, 2nd day
16	24:00	3475	20	2	8.8	173	
17	22:30	1297	20	2	4.8	64	Too few increments
18	23:30	2882	12	9	> 11	200	Ended before recorded time. Overflow of the storage container
19	22:00	1282	15	0	5.2	82	Too few increments
20	22:40	2090	10	8	1.4	104	Discarded due to error in the sampling process
21	23:30	2459	15	4	10	163	
22	22:30	1353	15	2	5.4	90	
23	23:50	1491	15	4	6	99	
24	24:00	2972	15	8	11	198	
25	23:50	2022	15	4	7	134	
26	22:20	2058	12	5	9	171	
27	22:05	2429	12	6	10.4	200	Ended before recorded time, discarded
28	24:00	1982	15	6	6.2	132	
29	22:05	3564	20	16	9.6	178	
30	23:45	2215	20	0	6	110	
31	24:00	1676	15	2	6	111	
32	24:00	1973	12	6	8.8	164	
33	21:45	80	20	16	0	4	Discarded due to error in the sampling process
34	22:15	4000	20	16	10.5	200	
35	23:15	4000	20	8	10.5	200	
36	24:00	4000	20	11	10.2	200	
37	23:30	4000	20	16	10.5	200	
38	24:00	3943	20	16	10.2	197	
39	23:55	4000	20	12	10.2	200	

Appendix 19 – Journal for Sampling Point G; 24-hour Samples

# Day	# Hours	Total H_2O [m^3]	H_2O per increment [m^3]	Rain [mm]	Approx. Vol. extracted [L]	# increments	Remarks
1	24:00	910	10	-	-	90	
2	24:00	920	10	-	-	90	
3	24:00	877	10	-	-	87	Discarded due to error in the sampling process
4	24:00	1793	10	9	-	179	
5	23:45	1530	10	-	8	153	
6	23:00	1590	10	6	8.6	159	Recorded error with one increment sampling
7	22:30	1293	10	8	7	129	
8	23:30	3503	10	13	10.2	200	Ended before recorded time, discarded
9	23:50	1761	15	3	6.7	117	
10	23:20	982	10	1	5.1	98	
11	23:30	1007	10	0	5.2	100	
12	23:50	2402	10	12	10.5	200	Ended before recorded time, discarded
13	23:45	2001	15	0	6.6	123	Discarded due to error in the sampling process. Increment volume adjusted
14	24:00	1945	7	22	14.5	276	Variography, 1st day
15	22:00	1624	7	4	12.9	232	Variography, 2nd day
16	24:00	3475	20	2	8.8	173	
17	22:30	1297	20	2	3.8	64	Too few increments
18	23:30	2882	12	9	10.2	200	Ended before recorded time, discarded
19	22:00	1282	15	0	4.8	82	Too few increments
20	22:40	2090	10	8	1.5	22	Discarded due to error in the sampling process
21	23:30	2459	15	4	8.5	163	
22	22:30	1353	15	2	5	90	
23	23:50	1491	15	4	5.4	99	
24	24:00	2972	15	8	10.1	198	
25	23:50	2022	15	4	7.1	134	
26	22:20	2058	12	5	9	171	
27	22:05	2429	12	6	10.2	200	Ended before recorded time, discarded
28	24:00	1982	15	6	6.2	132	
29	22:05	3564	20	16	9.2	178	
30	23:45	2215	20	0	6	110	
31	24:00	1676	15	2	6	111	
32	24:00	1973	12	6	8.6	164	
33	21:45	80	20	16	0	4	Discarded due to error in the sampling process
34	22:15	4000	20	16	10.2	200	
35	23:15	4000	20	8	10.2	200	
36	24:00	4000	20	11	10	200	
37	23:30	4000	20	16	10.2	200	
38	24:00	3943	20	16	10.1	197	
39	23:55	4000	20	12	10.1	200	

Appendix 20 – Journal for Sampling Point A; 24-hour Samples

# Day	# Hours	Total H_2O [m^3]	H_2O per Increment [m^3]	Rain [mm]	Approx vol. extracted [L]	# increments	Remarks
1	24:00	910	10	-	-	90	
2	24:00	920	10	-	-	90	
3	24:00	877	10	-	-	87	Discarded due to error in the sampling process
4	24:00	1793	10	9	-	179	
5	23:45	1530	10	-	6	153	
6	23:00	1590	10	6	8	159	
7	22:30	1293	10	8	6.7	129	
8	23:30	3503	10	13	10	200	Ended before recorded time, discarded
9	23:50	1761	15	3	6.2	117	
10	23:20	982	10	1	4.8	98	
11	23:30	1007	10	0	5	100	
12	23:50	2402	10	12	9.8	200	Ended before recorded time, discarded
13	23:45	2001	15	0	6.9	133	Increment volume adjusted
14	24:00	1945	7	22	14.4	276	Variography, 1. day
15	22:00	1624	7	4	12.5	232	Variography, 2. day
16	24:00	3475	20	2	8.6	173	
17	22:30	1297	20	2	3.8	64	Too few increments in 24-hour sample
18	23:30	2882	12	9	10.1	200	Ended before recorded time, discarded
19	22:00	1282	15	0	4.8	82	Too few increments
20	22:40	2090	10	8	10	200	
21	23:30	2459	15	4	8.5	163	
22	22:30	1353	15	2	5	90	
23	23:50	1491	15	4	5.3	99	
24	24:00	2972	15	8	10.1	198	
25	23:50	2022	15	4	7	134	
26	22:20	2058	12	5	8.9	171	
27	22:05	2429	12	6	10.2	200	Ended before recorded time, discarded
28	24:00	1982	15	6	6	132	
29	22:05	3564	20	16	9	178	
30	23:45	2215	20	0	5.9	110	
31	24:00	1676	15	2	5.9	111	
32	24:00	1973	12	6	8.7	164	
33	21:45	80	20	16	0	3	Discarded due to error in the sampling process
34	22:15	4000	20	16	10	200	
35	23:15	4000	20	8	10	200	
36	24:00	4000	20	11	10.1	200	
37	23:30	4000	20	16	10	200	
38	24:00	3943	20	16	10.1	197	
39	23:55	4000	20	12	10	200	

Appendix 21 – Journal for Sampling Point D; 24-hour Samples

# Day	# Hours	Total H_2O [m^3]	H_2O per increment [m^3]	Rain [mm]	Approx. Vol. extracted [L]	# increments	Remarks
1	24:00	910	10	-	-	90	
2	24:00	920	10	-	-	90	
3	24:00	877	10	-	-	87	Discarded due to error in the sampling process
4	24:00	1793	10	9	-		
5	23:45	1530	10	-	7	153	
6	23:00	1590	10	6	7.2	159	Increment volume adjusted
7	22:30	1293	10	8	6.8	129	
8	23:30	3503	10	13	10	200	Ended before recorded time
9	23:50	1761	15	3	6.2	117	
10	23:20	982	10	1	5	98	
11	23:30	1007	10	0	5	100	
12	23:50	2402	10	12	9.9	200	Ended before recorded time
13	23:45	2001	15	0	6.3	122	Discarded due to error in the sampling process. Increment volume adjusted.
14	24:00	1945	7	22	14.3	276	Variography, 1st day
15	22:00	1624	7	4	12.9	232	Variography, 2nd day
16	24:00	3475	20	2	8.8	173	
17	22:30	1297	20	2	3.8	64	Too few increments
18	23:30	2882	12	9	10.4	200	Ended before recorded time
19	22:00	1282	15	0	4.4	82	Too few increments
20	22:40	2090	10	8	10	200	
21	23:30	2459	15	4	8.5	163	
22	22:30	1353	15	2	4.9	90	
23	23:50	1491	15	4	5.3	99	
24	24:00	2972	15	8	10.1	198	
25	23:50	2022	15	4	7.1	134	
26	22:20	2058	12	5	8.8	171	
27	22:05	2429	12	6	10.2	200	Ended before recorded time
28	24:00	1982	15	6	56	132	
29	22:05	3564	20	16	9.6	178	
30	23:45	2215	20	0	6	110	
31	24:00	1676	15	2	6	111	
32	24:00	1973	12	6	8.8	164	
33	21:45	80	20	16	0	4	Discarded due to error in the sampling process
34	22:15	4000	20	16	10.3	200	
35	23:15	4000	20	8	10.3	200	
36	24:00	4000	20	11	10.2	200	
37	23:30	4000	20	16	10.3	200	
38	24:00	3943	20	16	10.3	197	
39	23:55	4000	20	12	10.3	200	

Appendix 22 – Journal for Sampling Point B; 24-hour Samples

# Day	# Hours	Total H_2O [m^3]	H_2O per increment [m^3]	Rain [mm]	Approx. Vol. extracted [L]	# increments	Remarks
1	24:00	910	10	-	-	90	
2	24:00	920	10	-	-	90	
3	24:00	877	10	-	-	87	Discarded due to error in the sampling process
4	24:00	1793	10	9	-	-	
5	23:45	1530	10	-	8	153	
6	23:00	1590	10	6	6.3	122	
7	22:30	1293	10	8	6.8	129	
8	23:30	3503	10	13	10	200	Ended before recorded time, discarded
9	23:50	1761	15	3	6.2	117	
10	23:20	982	10	1	5	98	
11	23:30	1007	10	0	5	100	
12	23:50	2402	10	12	< 1	106	Ended before recorded time, discarded
13	23:45	2001	15	0	6.3	123	Discarded due to error in the sampling process. Increment volume adjusted
14	24:00	1945	7	22	14.4	276	Variography, 1st day
15	22:00	1624	7	4	12.5	232	Variography, 2nd day
16	24:00	3475	20	2	8.6	173	
17	22:30	1297	20	2	3.8	64	Too few increments
18	23:30	2882	12	9	10.1	200	Ended before recorded time, discarded
19	22:00	1282	15	0	4.6	82	Too few increments
20	22:40	2090	10	8	1.4		Discarded due to error in the sampling process
21	23:30	2459	15	4	8.1	163	
22	22:30	1353	15	2	4.9	90	
23	23:50	1491	15	4	5.2	99	
24	24:00	2972	15	8	9.8	198	
25	23:50	2022	15	4	6.1	134	Discarded due to error in the sampling process; overflow of the storage container
26	22:20	2058	12	5	8.7	171	
27	22:05	2429	12	6	10.1	200	Ended before recorded time, discarded
28	24:00	1982	15	6	6	132	
29	22:05	3564	20	16	9.1	178	
30	23:45	2215	20	0	6	110	
31	24:00	1676	15	2	5.8	111	
32	24:00	1973	12	6	8.2	164	
33	21:45	80	20	16	0	4	Discarded due to error in the sampling process
34	22:15	4000	20	16	10.1	200	
35	23:15	4000	20	8	10.1	200	
36	24:00	4000	20	11	9.8	200	
37	23:30	4000	20	16	10.1	200	
38	24:00	3943	20	16	8.5	197	Discarded due to error in the sampling process; overflow of the storage container
39	23:55	4000	20	12	10	200	

Appendix 23 – Journal for Sampling Point C; 24-hour Samples

# Day	# Hours	Total H_2O [m^3]	H_2O per increment [m^3]	Rain [mm]	Approx vol. extracted [L]	# Increments	Remarks
1	24:00	910	10	-		90	
2	24:00	920	10	-		90	
3	24:00	877	10	-			Discarded due to error in the sampling process
4	24:00	1793	10	9		179	
5	23:45	1530	10	-	8	153	
6	23:00	1590	10	6	7.2	159	
7	22:30	1293	10	8	6	129	
8	23:30	3503	10	13	9	200	Ended before recorded time, discarded
9	23:50	1761	15	3	5.8	117	
10	23:20	982	10	1	4.8	98	
11	23:30	1007	10	0	5	100	
12	23:50	2402	10	12	9	200	Ended before recorded time, discarded
13	23:45	2001	15	0	6.1	123	Discarded due to error in the sampling process. Increment volume adjusted
14	24:00	1945	7	22	14.3	276	Variography, 1st day
15	22:00	1624	7	4	12.4	232	Variography, 2nd day
16	24:00	3475	20	2	8.5	173	
17	22:30	1297	20	2	3.5	64	Too few increments
18	23:30	2882	12	9	9.9	200	Ended before recorded time, discarded
19	22:00	1282	15	0	4.6	82	Too few increments
20	22:40	2090	10	8	10	200	
21	23:30	2459	15	4	8.1	163	
22	22:30	1353	15	2	4.8	90	
23	23:50	1491	15	4	5.1	99	
24	24:00	2972	15	8	9.8	198	
25	23:50	2022	15	4	6.85	134	
26	22:20	2058	12	5	8.5	171	
27	22:05	2429	12	6	10	200	Ended before recorded time, discarded
28	24:00	1982	15	6	5.9	132	
29	22:05	3564	20	16	8.9	178	
30	23:45	2215	20	0	5.8	110	
31	24:00	1676	15	2	5.7	111	
32	24:00	1973	12	6	8	164	
33	21:45	80	20	16	0	4	Discarded due to error in the sampling process
34	22:15	4000	20	16	10	200	

35	23:15	4000	20	8	10	200	
36	24:00	4000	20	11	4	200	Discarded due to error in the sampling process; overflow of the storage container
37	23:30	4000	20	16	10	200	
38	24:00	3943	20	16	9.8	197	
39	23:55	4000	20	12	9.8	200	

Appendix 24 – Total Phosphorous in 24-hour Composite Samples

Analytical Data for TP in 24-hour Composite Samples

	A	B	C	D	E	F	G
Day	[µg/L]	[µg/L]	[µg/L]	[µg/L]	[µg/L]	[µg/L]	[µg/L]
1	372.227	187.597	233.174	159.732	176.554	165.263	211.145
2	170.490	237.358	172.695	165.799	166.234	164.124	181.067
3	245.660	221.272	186.533	179.614	180.887	178.434	190.336
4	320.830	205.186	200.372	193.429	195.541	192.744	199.605
5	272.529	222.290	241.854	224.065	226.046	222.717	233.329
6	210.406	219.459	214.009	213.902	210.115	210.398	218.770
7	287.446	291.858	287.555	287.148	294.972	298.014	289.988
8	219.519	222.959	220.852	222.142	227.215	226.548	226.207
9	151.593	154.060	154.149	157.137	159.457	155.082	162.426
10	290.128	294.082	295.771	295.779	292.286	288.423	290.177
11	264.106	260.823	258.230	258.753	256.967	256.432	263.555
12	200.753	273.596	253.780	263.701	263.229	259.916	272.192
13	137.400	273.596	253.780	263.701	263.229	259.916	272.192
14	285.310	286.370	249.330	268.650	269.490	263.400	280.830
15	125.330	131.590	118.130	125.900	125.370	130.940	136.650
16	155.270	130.150	120.880	128.820	139.080	127.010	130.530
17	182.738	136.510	151.370	150.460	165.690	138.580	151.665
18	182.738	136.510	151.370	150.460	165.690	138.580	151.665
19	182.738	136.510	151.370	150.460	165.690	138.580	151.665
20	210.206	136.510	181.860	172.100	165.690	138.580	151.665
21	155.330	142.870	162.490	137.600	192.300	150.150	172.800
22	126.620	192.600	226.630	106.320	149.000	147.750	144.500
23	175.560	137.500	216.600	156.920	157.790	155.710	157.200
24	142.110	189.920	182.180	150.430	180.110	188.760	170.580
25	179.880	193.650	224.733	177.010	173.019	179.439	150.254
26	155.440	197.380	144.044	152.222	175.672	204.427	185.317
27	157.010	179.480	148.182	191.216	173.701	232.169	178.954
28	158.580	161.580	152.320	230.210	171.730	259.910	172.590
29	184.480	213.180	152.680	195.800	158.470	233.220	219.818
30	174.898	170.669	162.474	211.281	120.692	126.851	137.759
31	131.726	114.128	116.723	162.304	129.463	176.527	131.412
32	151.230	146.623	235.897	131.468	194.494	139.448	136.378
33	159.859	137.582	181.495	150.173	239.685	147.093	171.837
34	168.488	128.540	127.092	168.877	284.875	154.738	207.296
35	114.653	117.592	120.075	217.878	143.363	123.918	120.441
36	112.290	134.394	130.599	111.939	149.362	156.799	155.890
37	129.109	128.772	141.123	133.002	149.278	142.377	137.373
38	144.126	133.994	196.898	165.478	184.646	133.080	127.952
39	119.083	139.215	102.983	99.686	144.033	142.305	184.360
Mean [µg/L]	187.38	182.51	185.19	181.58	189.26	183.29	185.34
Stddev [µg/L]	62.03	54.37	51.25	51.08	48.53	51.08	49.49
CV [%]	33.1	29.8	27.7	28.3	25.64	27.9	26.7

Red numbers are missing data and calculated as the mean of the two surrounding results

Appendix 25 – Total Phosphorous; Variographic Analysis of Sampling Point E, G, D, B, and C

Sampling Point E

The analytical concentration measurements are shown in Figure 123 as an interpolation after the dataset is corrected for missing data. The fluctuations in analytical concentration are most likely due to the amount of rain as described before for previous dataset.

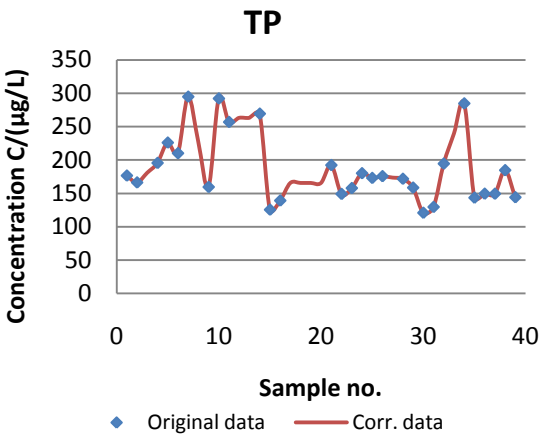

Figure 123 TP analytical concentration development in 24-hour samples at sampling point E

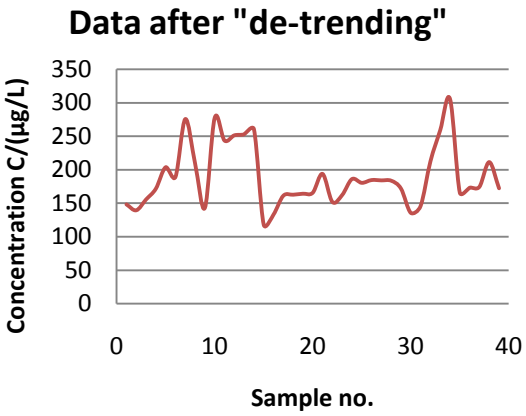

Figure 124 De-trended data for TP in 24-hour samples at sampling point E. Excluded points are 3, 8, 12, 13, 17-20, 27, and 33

After "de-trending" the time series is calculated, see Figure 124, and then used for the basis for the experimental variogram, which is shown in Figure 125.

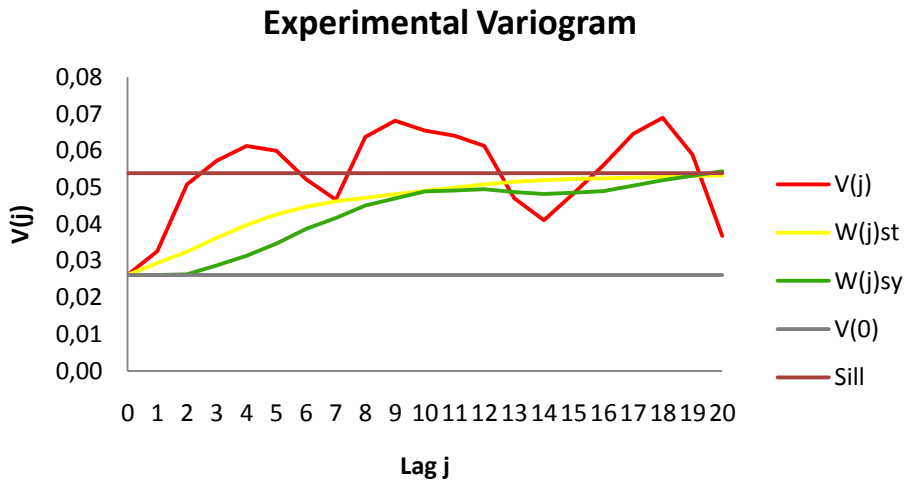

Figure 125 Experimental variogram and auxiliary functions for 24-hour samples at sampling point E. Data series E was subjected to linear de-trending before variogram calculation.

From the variogram a cyclic variation with period of 14 days was observed. There was here a somewhat more pronounced indication of a cyclic variation of 7 days. The nugget effect amounted to 0.026 and the sill was 0.054. This allows to state that the total 0-D sampling variation corresponded to 49 % of the total process variability.

Sampling Point G

The analytical concentration measurements are shown in Figure 126 as an interpolation after the dataset is corrected for missing data. The fluctuations in analytical concentration are most likely due to the amount of rain as described before for previous datasets.

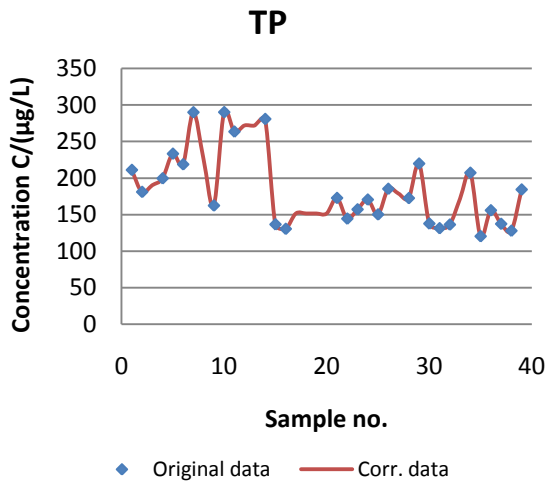

Figure 126 TP analytical concentration development in 24-hour samples at sampling point G

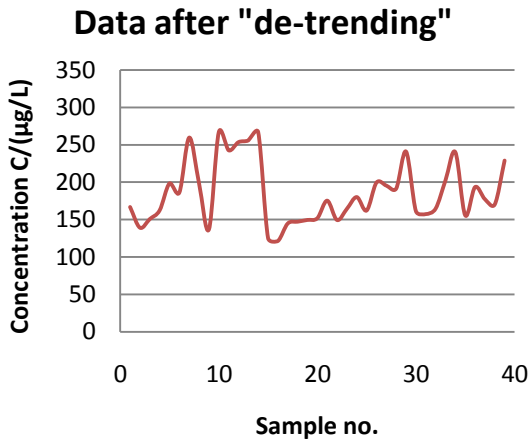

Figure 127 De-trended data for TP in 24-hour samples at sampling point G. Excluded points are 3, 8, 12, 13, 17-20, and 27

After "de-trending" the time series, see Figure 127, is calculated and then used for the basis for the experimental variogram, which is shown in Figure 128.

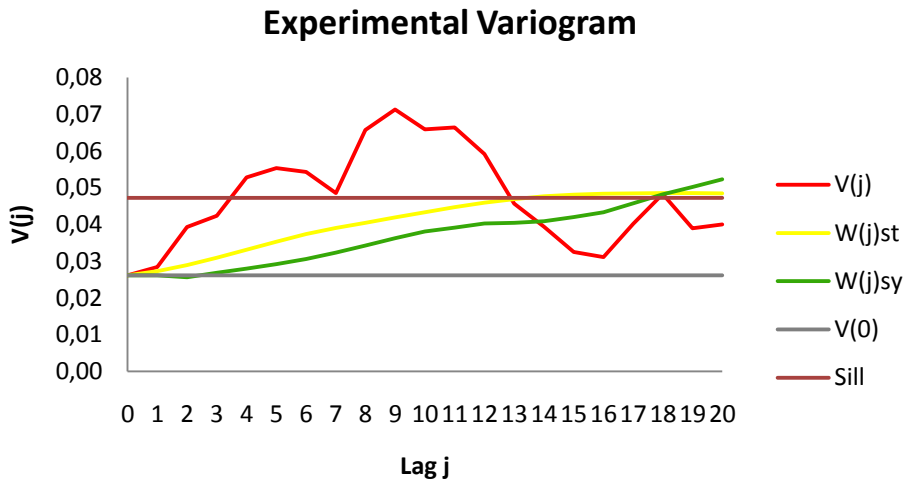

Figure 128 Experimental variogram and auxiliary functions for 24-hour samples at sampling point G. Data series G was subjected to linear de-trending before variogram calculation.

From the variogram a cyclic variation with period of 15 days to 16 days was observed. There was a clear indication of a cyclic variation of 7 days. The nugget effect amounted to 0.026 and the sill was 0.047. This allows to state that the total 0-D sampling variation corresponded to 55 % of the total process variability.

Sampling Point D

The analytical concentration measurements are shown in Figure 129 as an interpolation after the dataset is corrected for missing data. These fluctuations in analytical concentration are most likely due to the amount of rain as described before for previous datasets.

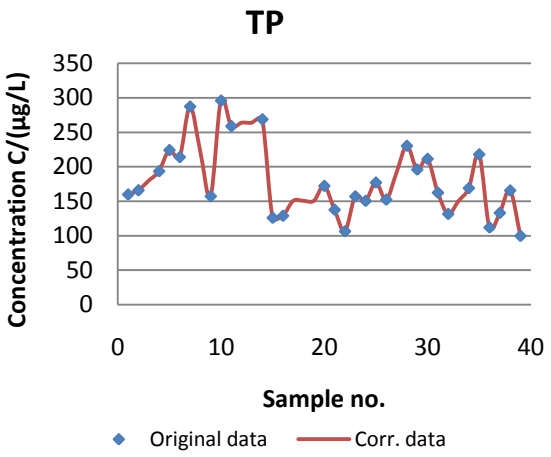

Figure 129 TP analytical concentration in 24-hour samples at sampling point D

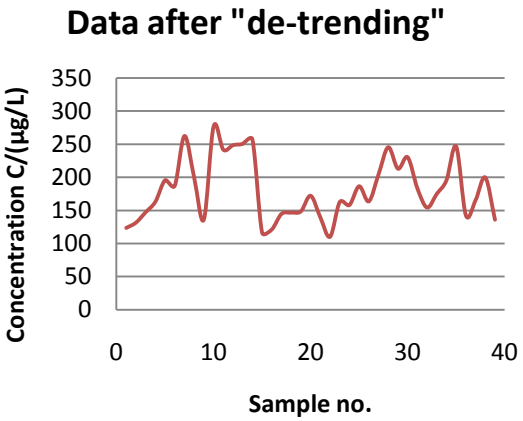

Figure 130 De-trended data for TP in 24-hour samples at sampling point D. Excluded points are 3, 8, 12, 13, 17-19, 27, and 33.

After "de-trending" the time series is calculated, see Figure 130, and then used for the basis for the experimental variogram, which is shown in Figure 131.

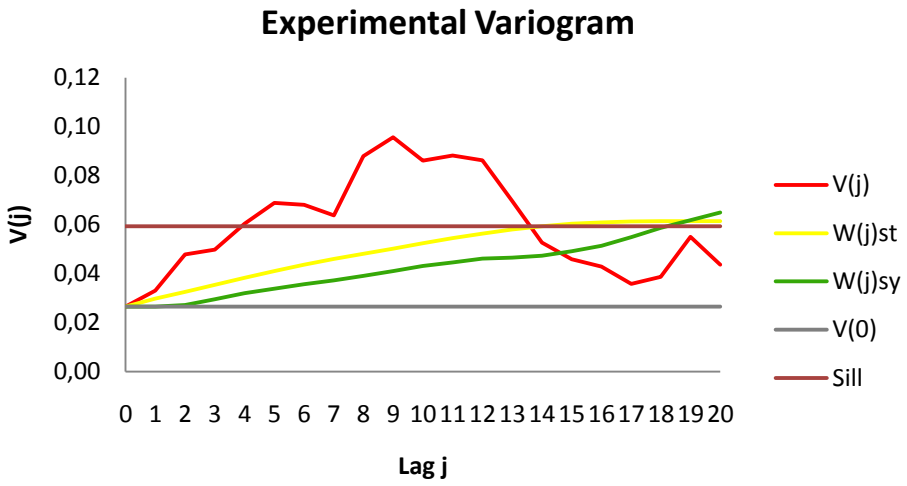

Figure 131 Experimental variogram and auxiliary functions for 24-hour samples at sampling point D. Data series D was subjected to linear de-trending before variogram calculation.

From the variogram a cyclic variation with period of 15 days to 18 days was observed. There was indications of a cyclic variation of 7 days. The nugget effect amounted to 0.027 and the sill was 0.059. This allows to state that the total 0-D sampling variation corresponded to 45 % of the total process variability.

Sampling Point B

The analytical concentration measurements are shown in Figure 132 as an interpolation after the dataset is corrected for missing data. The fluctuations in analytical concentration are most likely due to the amount of rain as described before.

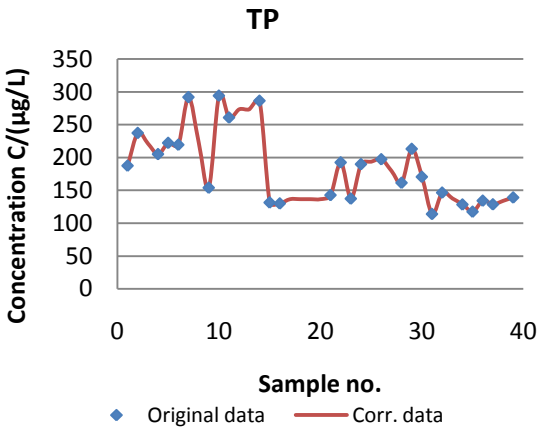

Figure 132 TP analytical concentration development in 24-hour samples at sampling point B.

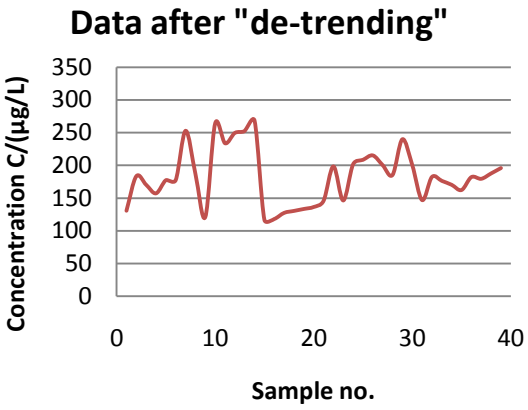

Figure 133 De-trended data for TP in 24-hour samples at sampling point B. Excluded points are 3, 8, 12, 13, 17-20, 25, 27, 33, and 38.

After "de-trending" the time series is calculated, see Figure 133, and then used for the basis for the experimental variogram, which is shown in Figure 134.

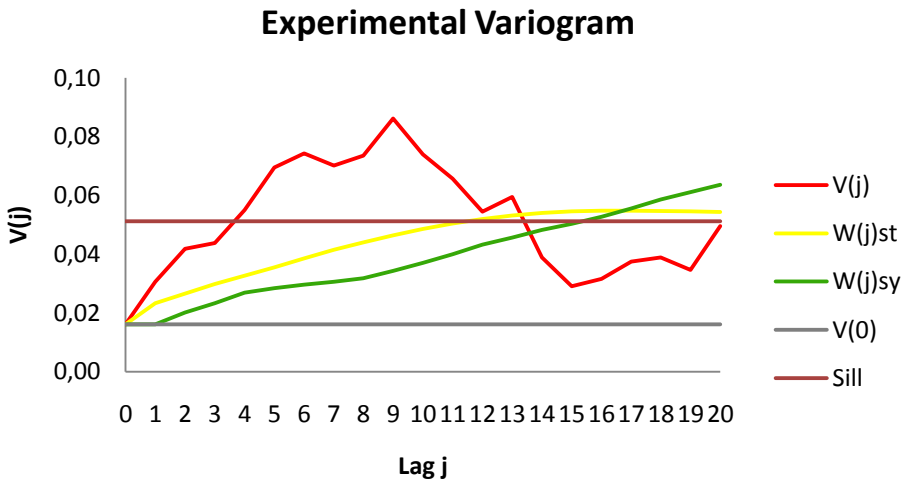

Figure 134 Experimental variogram and auxiliary functions for 24-hour samples at sampling point B. Data series B was subjected to linear de-trending before variogram calculation.

From the variogram a cyclic variation with a period of 15 days to 16 days was observed. There was a small indication of a cyclic variation of 7 days. The nugget effect amounted to 0.016 and the sill was 0.051. This allows to state that the total 0-D sampling variation corresponded to 31 % of the total process variability.

Sampling Point C

The analytical concentration measurements are shown in Figure 135 as an interpolation after the dataset is corrected for missing data. These fluctuations in analytical concentration are most likely due to the amount of rain as described before.

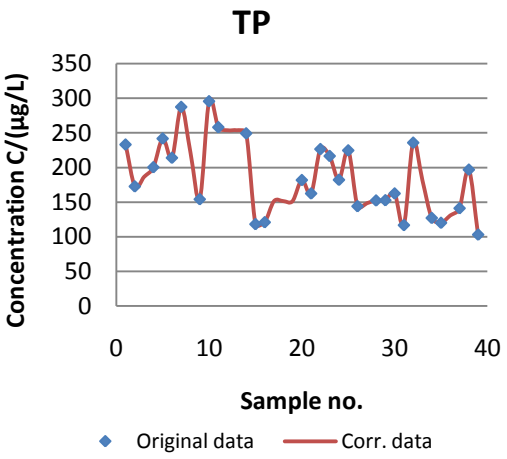

Figure 135 TP analytical concentration development in 24-hour samples at sampling point C.

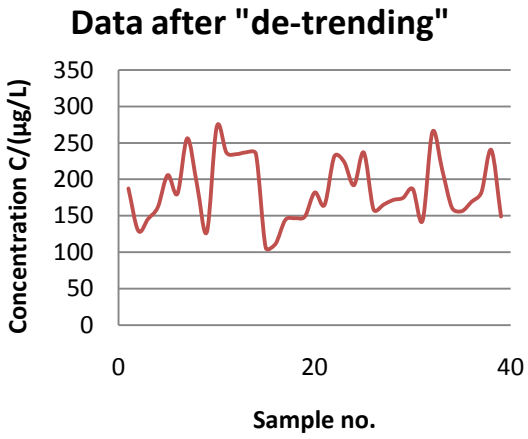

Figure 136 De-trended data for TP in 24-hour samples at sampling point C. Excluded points are 3, 8, 12, 13, 17-19, 27, 33, and 36.

After "de-trending the time series is calculated, see Figure 136,and then used for the basis for the experimental variogram, which is shown in Figure 137.

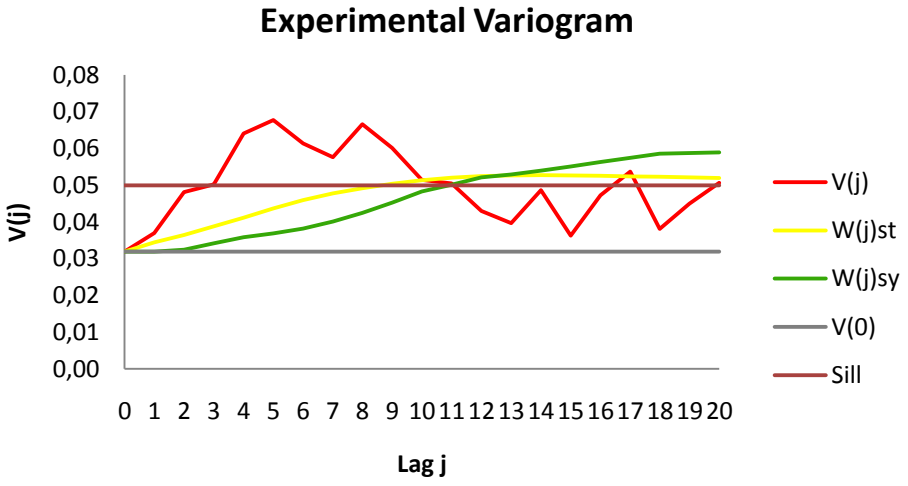

Figure 137 Experimental variogram and auxiliary functions for 24-hour samples at sampling point C. Data series C was subjected to linear de-trending before variogram calculation.

From the variogram cyclic variations with periods of 7 days and 13 days to 15 days were observed. The nugget effect amounted to 0.032 and the sill was 0.050. This allows to state that the total 0-D sampling variation correspondeds to 64 % of the total process variability.

Appendix 26 – Total Phosphorous; Total Sampling Error for Sampling Point E, G, D, B, and C

Sampling Point E

As before a 3D histogram is made of the TSE with relative values for TSE as a function of different values for j and Q, see Figure 138.

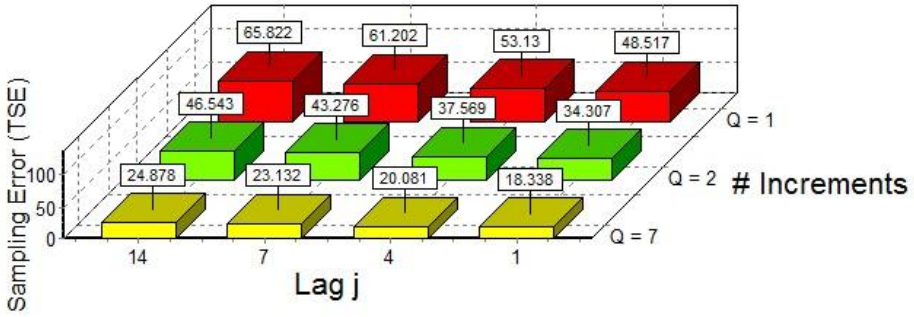

Figure 138 TSE for TP in 24-hour samples from sampling point E

Also as expected the TSE had the smallest value for j = 1 and Q = 7 of 6.11 %. As sampling was done commonly with j = 1 and Q = 1, the TSE for point E would give an error of 16.2 %.

Sampling Point G

As before a 3D histogram is made of the TSE with relative values for TSE as a function of different values for j and Q, see Figure 139.

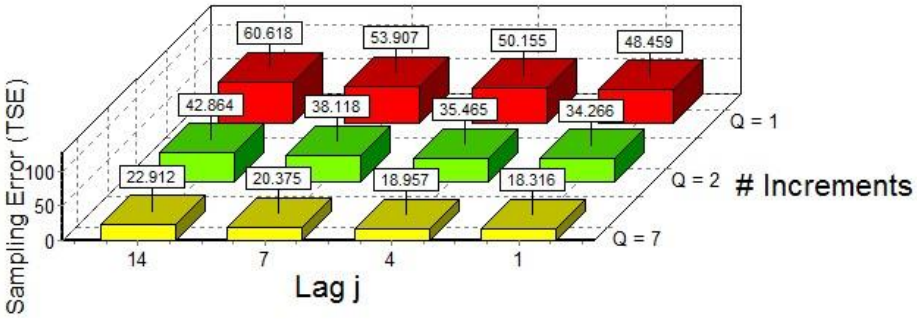

Figure 139 TSE for TP in 24-hour samples from sampling point G

Also as expected the TSE had the smallest value for j = 1 and Q = 7 of 6.11 %. As sampling was done commonly with j = 1 and Q = 1, the TSE for point G would give an error of 16.2 %.

Sampling Point D

As before a 3D histogram is made of the TSE with relative values for TSE as a function of different values for j and Q, see Figure 140.

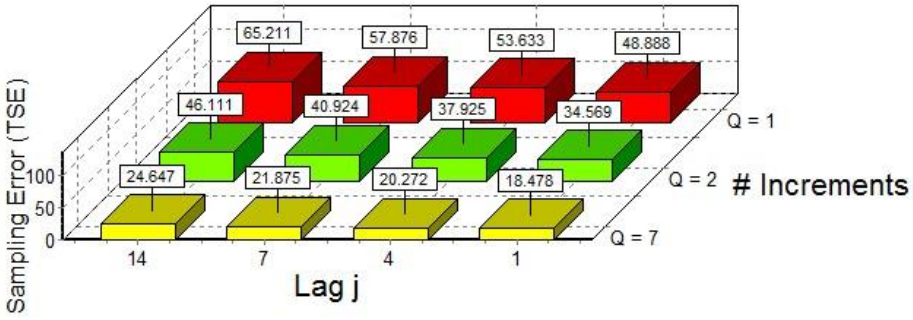

Figure 140 TSE for TP in 24-hour samples from sampling point D

Also as expected the TSE had the smallest value for j = 1 and Q = 7 of 6.16 %. As sampling was done commonly with j = 1 and Q = 1, the TSE for point D would give an error of 16.3 %.

Sampling Point B

A 3D histogram is made of the TSE with relative values for TSE as a function of different values for j and Q, see Figure 141.

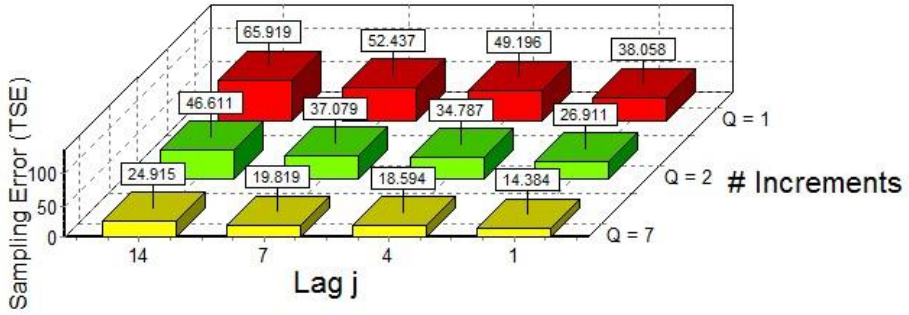

Figure 141 TSE for TP in 24-hour samples from sampling point B

Also as expected the TSE had the smallest value for j = 1 and Q = 7 of 4.79 %. As sampling was done commonly with j = 1 and Q = 1, the TSE for point B would give an error of 12.7 %.

Sampling Point C

As before a 3D histogram is made of the TSE with relative values for TSE as a function of different values for j and Q, see Figure 142.

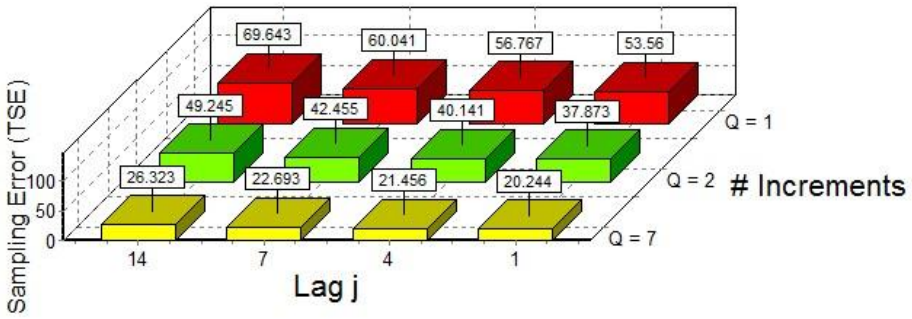

Figure 142 TSE for TP in 24-hour samples from sampling point C

Also as expected the TSE had the smallest value for j = 1 and Q = 7 of 6.75 %. As sampling was done commonly with j = 1 and Q = 1, the TSE for point C would give an error of 17.9 %.

Appendix 27 – Conductivity in Increments

Analytical Data for Conductivity in Increments from Sampling Point F

#	[µS/cm]		#	[µS/cm]		#	[µS/cm]
1	330		49	356		97	378
2	331		50	355		98	381
3	329		51	356		99	382
4	328		52	(375) 356		100	382
5	330		53	355		101	381
6	(292) 332		54	355		102	382
7	333		55	355		103	378
8	335		56	356		104	379
9	335		57	358		105	380
10	336		58	(389) 358		106	382
11	336		59	(388) 358		107	381
12	336		60	358		108	381
13	336		61	358		109	382
14	336		62	357		110	(355) 381
15	338		63	358		111	(347) 381
16	338		64	359		112	(353) 381
17	339		65	360		113	(345) 381
18	338		66	(385) 360		114	(344) 381
19	339		67	359		115	(344) 381
20	339		68	360		116	(353) 381
21	340		69	361		117	379
22	346		70	362		118	382
23	342		71	361		119	380
24	341		72	364		120	382
25	342		73	359		121	381
26	343		74	363		122	379
27	343		75	363		123	384
28	343		76	363		124	382
29	343		77	365		125	381
30	343		78	367		126	385
31	343		79	365		127	386
32	356		80	361		128	386
33	344		81	363		129	387
34	(410) 346		82	365		130	387
35	348		83	366		131	385
36	347		84	366		132	(402) 386
37	349		85	370		133	387
38	350		86	365		134	386
39	(374) 351		87	366		135	388
40	374		88	368		136	381
41	350		89	370		137	387
42	352		90	368		138	389
43	352		91	372		139	383
44	353		92	371		140	390
45	354		93	372			
46	354		94	371		**Mean [µS/cm]**	362
47	355		95	376		**Stddev [µS/cm]**	17.4
48	355		96	367		**CV [%]**	4.8

Analytical Data for Conductivity in Increments from Sampling Point A

#	[µS/cm]		#	[µS/cm]		#	[µS/cm]
1	313		49	355		97	381
2	317		50	355		98	381
3	309		51	353		99	382
4	334		52	(403) 356		100	381
5	331		53	358		101	381
6	332		54	358		102	381
7	332		55	357		103	379
8	336		56	357		104	379
9	336		57	357		105	381
10	337		58	357		106	382
11	337		59	358		107	380
12	338		60	358		108	381
13	338		61	359		109	381
14	338		62	359		110	381
15	338		63	358		111	382
16	336		64	358		112	381
17	336		65	360		113	382
18	(357) 339		66	(391) 361		114	383
19	341		67	362		115	383
20	340		68	361		116	383
21	340		69	361		117	380
22	342		70	363		118	384
23	342		71	363		119	385
24	342		72	363		120	384
25	343		73	359		121	383
26	343		74	362		122	387
27	343		75	361		123	386
28	342		76	366		124	385
29	343		77	366		125	386
30	343		78	366		126	387
31	343		79	366		127	389
32	344		80	365		128	385
33	344		81	366		129	389
34	(364) 346		82	364		130	387
35	347		83	365		131	388
36	346		84	368		132	387
37	350		85	369		133	387
38	350		86	370		134	389
39	349		87	371		135	383
40	350		88	369		136	388
41	349		89	371		137	391
42	349		90	373		138	(426) 392
43	351		91	372		139	392
44	352		92	373		140	392
45	351		93	375			
46	352		94	373		**Mean [µS/cm]**	363
47	354		95	375		**Stddev [µS/cm]**	19.9
48	(376) 355		96	381		**CV [%]**	5.5

Appendix 28 – Conductivity in 24-hour Composite Samples

Analytical Data for Conductivity in 24-hour Samples for Sampling Point A–G

Day	A [µS/cm]	B [µS/cm]	C [µS/cm]	D [µS/cm]	E [µS/cm]	F [µS/cm]	G [µS/cm]
1	605	573	539	584	564	584	574
2	568	629	589	567	558	571	572
3	611	621	597	572	596	577	585
4	653	612	605	577	634	583	597
5	447	460	442	459	451	468	407
6	390	375	391	389	358	397	368
7	421	417	410	377	380	362	364
8	360	356	350	318	325	314	290
9	299	295	289	258	269	265	215
10	414	376	362	453	415	379	411
11	487	424	403	435	482	460	490
12	414	399	355	408	427	418	435
13	340	399	355	408	427	418	435
14	372	373	306	381	372	376	379
15	318	323	318	300	299	314	311
16	312	315	315	304	304	307	301
17	360	326	361	356	321	323	319
18	360	326	361	356	321	323	319
19	360	326	361	356	321	323	319
20	408	326	407	407	321	323	319
21	338	336	337	338	338	338	337
22	361	363	363	363	361	362	358
23	424	425	426	427	425	425	424
24	391	388	389	386	389	388	392
25	332	383	337	338	334	331	338
26	380	378	377	380	377	379	378
27	362	362	361	363	361	362	362
28	344	345	344	345	344	345	345
29	338	339	339	340	355	339	340
30	244	247	249	242	239	252	263
31	408	396	392	391	393	396	387
32	441	331	481	477	472	484	477
33	373	342	388	385	379	388	384
34	304	352	294	292	285	291	291
35	278	278	276	277	274	278	276
36	293	289	294	283	283	286	286
37	316	315	311	316	313	314	315
38	302	318	295	304	296	306	302
39	322	320	322	318	317	318	322
Mean [µS/cm]	360	352	353	358	352	353	350
Stddev [µS/cm]	53.1	45.6	49.8	57.4	59.1	57.0	91.4
CV [%]	14.7	13.0	14.1	16.0	16.8	16.2	26.1

Blue numbers are outliers

Red numbers are missing data and calculated as the mean of the two surrounding results

Appendix 29 – Conductivity; Variographic Analysis of Sampling Point E, G, D, B, and C

Sampling Point E

The conductivity measurements from sampling point E are shown in Figure 143 corrected for outliers. The fluctuations in conductivity is most likely due to the amount of rain as described before for previous datasets.

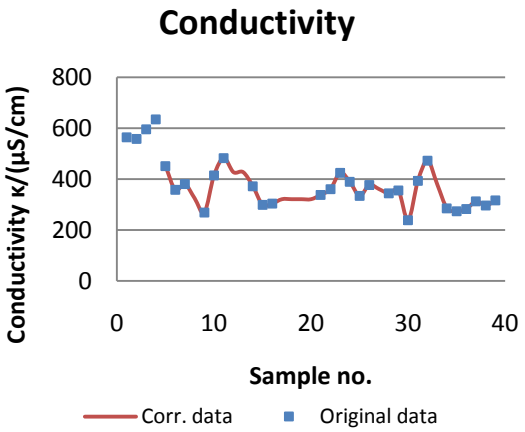

Figure 143 Conductivity development in 24-hour samples at sampling point E

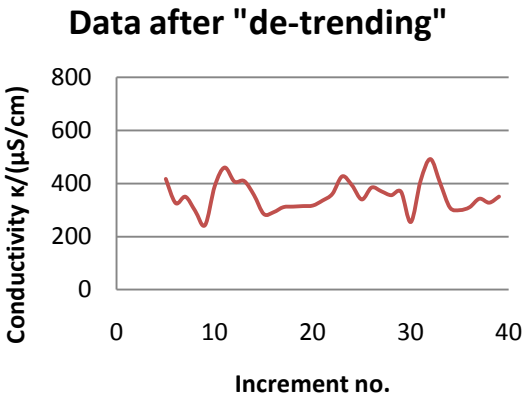

Figure 144 Conductivity in 24-hour samples after "de-trending" at sampling point E. Excluded points are 1-4, 8, 12, 13, 17-20, 27, and 33.

After “de-trending” the time series is calculated, see Figure 144, and then used for the basis for the experimental variogram which is shown in Figure 145.

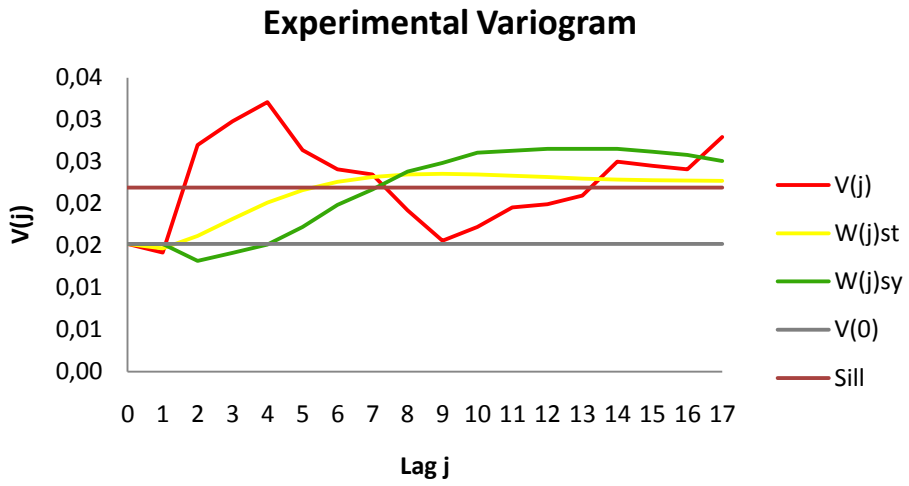

Figure 145 Experimental variogram and auxiliary functions for conductivity in 24-hour samples at sampling point E. Data series E was subjected to linear de-trending before variogram calculations

From the variogram a cyclic variation with a period of 9 days was observed. The nugget effect amounted to 0.0152 and the sill was 0.0219. This allows to state that the total 0-D sampling variation corresponded to 69 % of the total process variability.

Sampling Point G

The conductivity measurements from sampling point G are shown in Figure 146 as an interpolation after the dataset is corrected for outliers. The fluctuations in conductivity is most likely due to the amount of rain as described before for previous datasets.

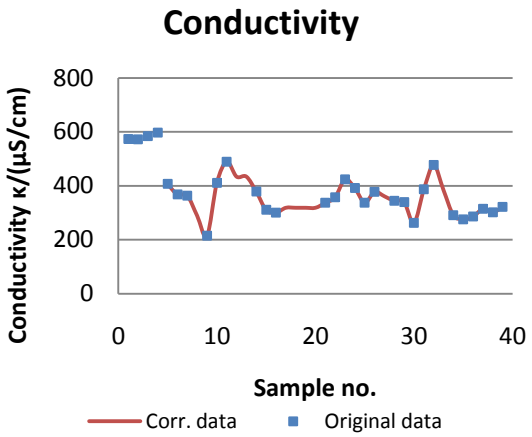

Figure 146 Conductivity development in 24-hour samples at sampling point G

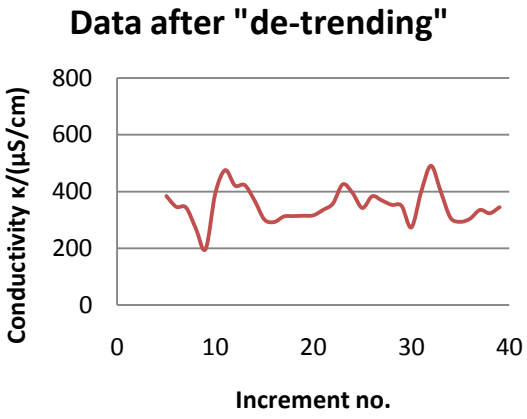

Figure 147 Conductivity in 24-hour samples after "de-trending" at sampling point G. Excluded points are 1-4, 8, 12, 13, 17-20, 27, and 33.

After “de-trending” the time series is calculated, see Figure 147, and then used for the basis for the experimental variogram which is shown in Figure 148.

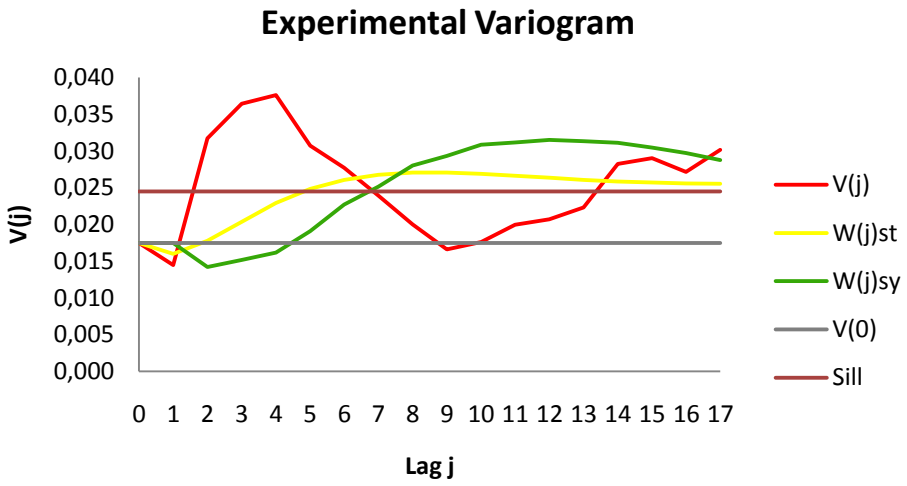

Figure 148 Experimental variogram and auxiliary functions for conductivity in 24-hour samples at sampling point G. Data series G was subjected to linear de-trending before variogram calculations

From the variogram a cyclic variations with period of 9 days was observed. The nugget effect amounted to 0.0175 and the sill was 0.0245. This allows to state that the total 0-D sampling variation corresponded to 71 % of the total process variability.

Sampling Point D

The conductivity measurements from sampling point D are shown in Figure 149 as an interpolation after the dataset is corrected for outliers. The fluctuations in conductivity is most likely due to the amount of rain as described before for previous datasets.

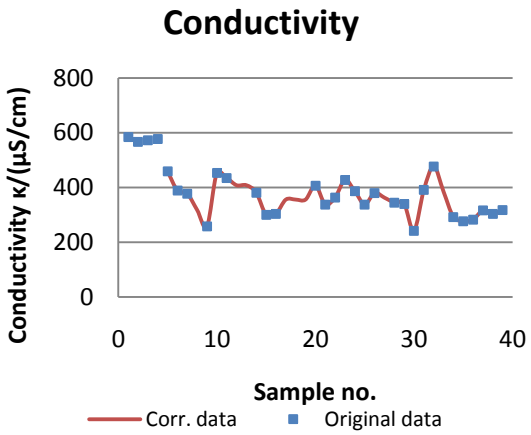

Figure 149 Conductivity development in 24-hour samples at sampling point D

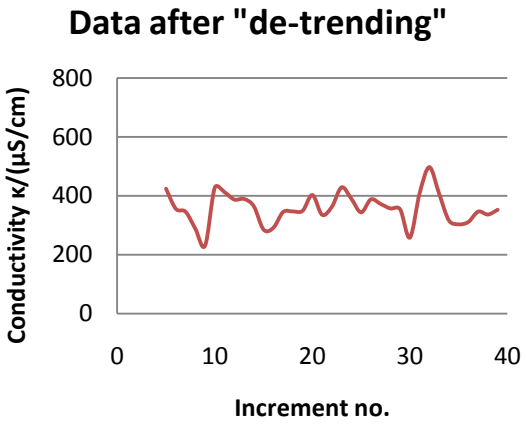

Figure 150 Conductivity in 24-hour samples after "de-trending" at sampling point D. Excluded points are 1-4, 8, 12, 13, 17-19, 27, and 33.

After “de-trending” the time series is calculated, see Figure 150, and then used for the basis for the experimental variogram which is shown in Figure 151.

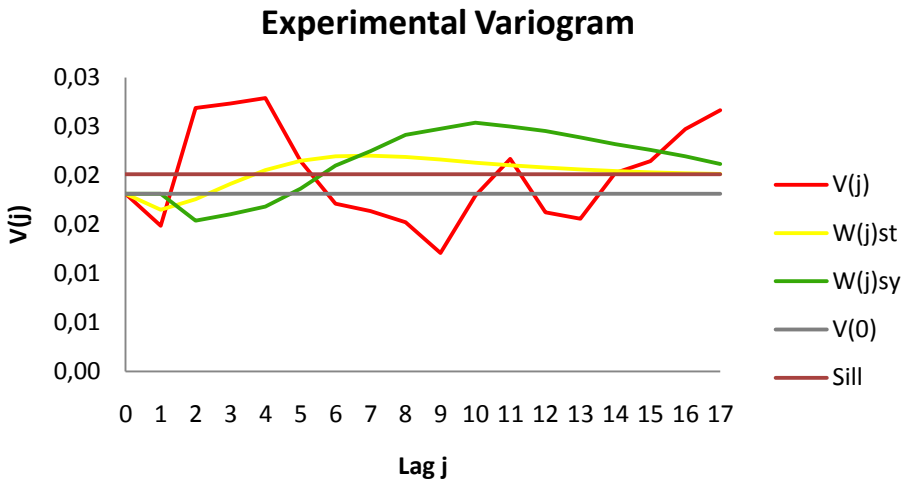

Figure 151 Experimental variogram and auxiliary functions for conductivity in 24-hour samples at sampling point D. Data series D was subjected to linear de-trending before variogram calculations

From the variogram a cyclic variation with period of 9 days was observed. The nugget effect amounted to 0.0181 and the sill was 0.0201. This allows to state that the total 0-D sampling variation corresponded to 90 % of the total process variability.

Sampling Point B

The conductivity measurements from sampling point B are shown in Figure 152 as an interpolation after the dataset is corrected for outliers. The fluctuations in conductivity is most likely due to the amount of rain as described before for previous datasets.

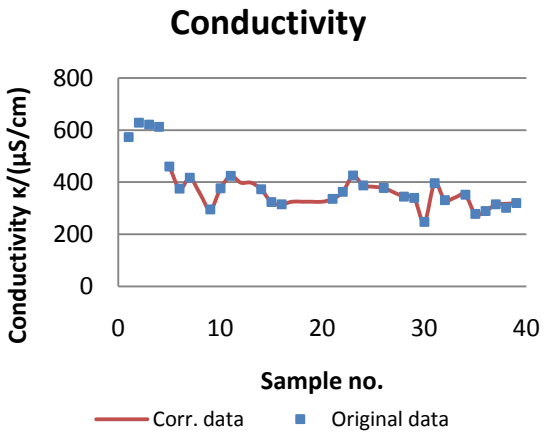

Figure 152 Conductivity development in 24-hour samples at sampling point B

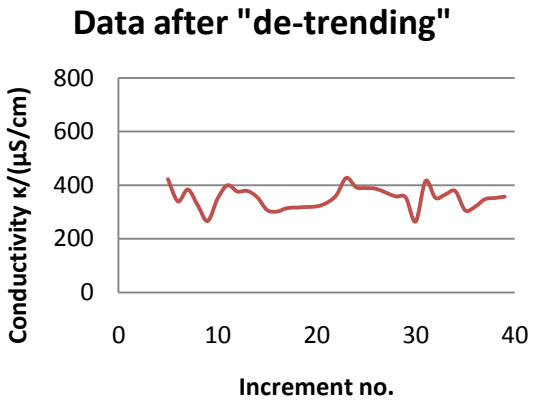

Figure 153 Conductivity in 24-hour samples after "de-trending" at sampling point B. Excluded points are 1-4, 8, 12, 13, 17-20, 25, 27, 33, and 38.

After “de-trending” the time series is calculated, see Figure 153, and then used for the basis for the experimental variogram which is shown in Figure 154.

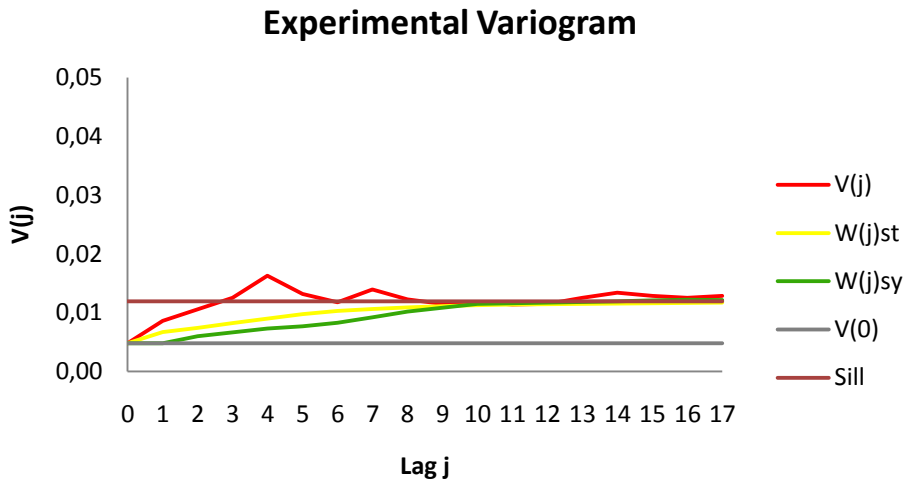

Figure 154 Experimental variogram and auxiliary functions for conductivity in 24-hour samples at sampling point B. Data series B was subjected to linear de-trending before variogram calculations

In the variogram no cyclic variation was observed. The variogram was flat with a range of two days. The nugget effect amounted to 0.00480 and the sill was 0.0119. This allows to state that the total 0-D sampling variation corresponded to 40 % of the total process variability.

Sampling Point C

The conductivity measurements from sampling point C are shown in Figure 155 as an interpolation after the dataset is corrected for outliers. The fluctuations in conductivity is most likely due to the amount of rain as described before for previous datasets.

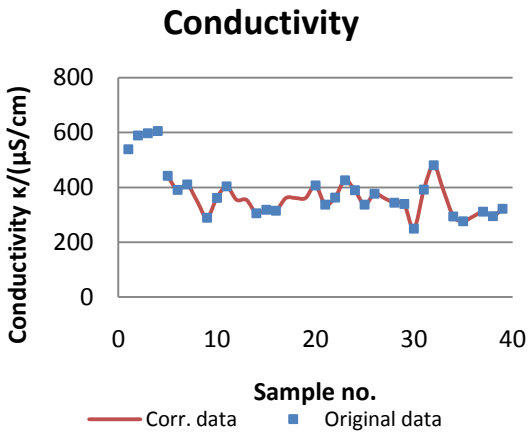

Figure 155 Conductivity development in 24-hour samples at sampling point C

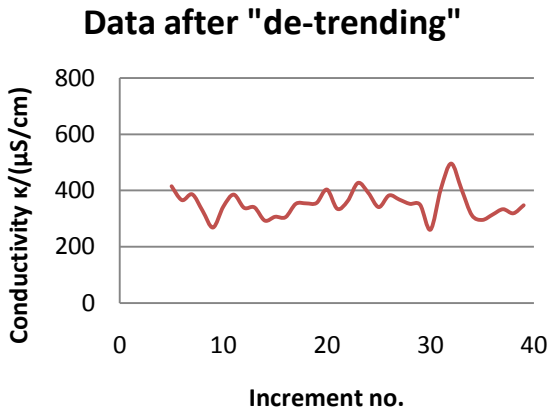

Figure 156 Conductivity in 24-hour samples after "de-trending" at sampling point C. Excluded points are 1-4, 8, 12, 13, 17-19, 27, 33, and 36.

After “de-trending” the time series is calculated, see Figure 156, and then used for the basis for the experimental variogram which is shown in Figure 157.

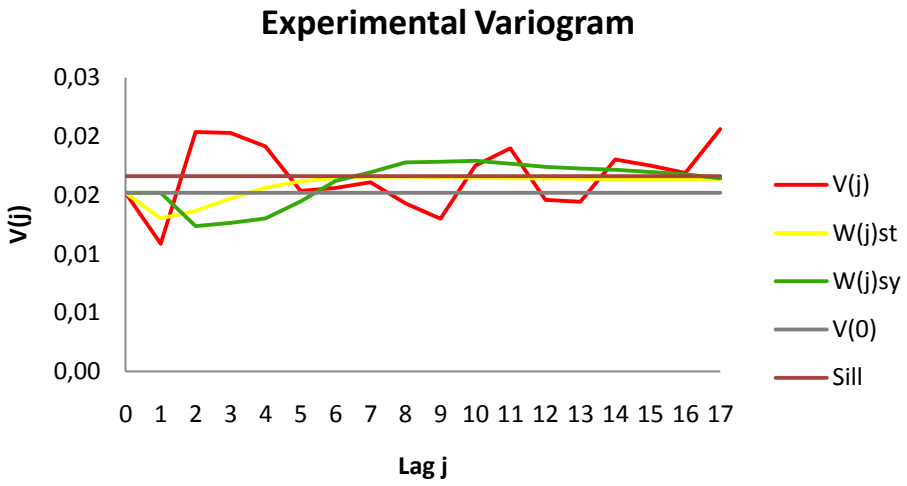

Figure 157 Experimental variogram and auxiliary functions for conductivity in 24-hour samples at sampling point C. Data series C was subjected to linear de-trending before variogram calculations

From the variogram an indication of a cyclic variation with period of 9 days was observed. The nugget effect amounted to 0.0152 and the sill was 0.0166. This allows to state that the total 0-D sampling variation corresponded to 92 % of the total process variability.

Appendix 30 – Conductivity; Total Sampling Error for Sampling Point E, G, D, B, and C

Sampling Point E

As before a 3D histogram is made of the TSE with relative values for TSE as a function of different values for j and Q, see Figure 158.

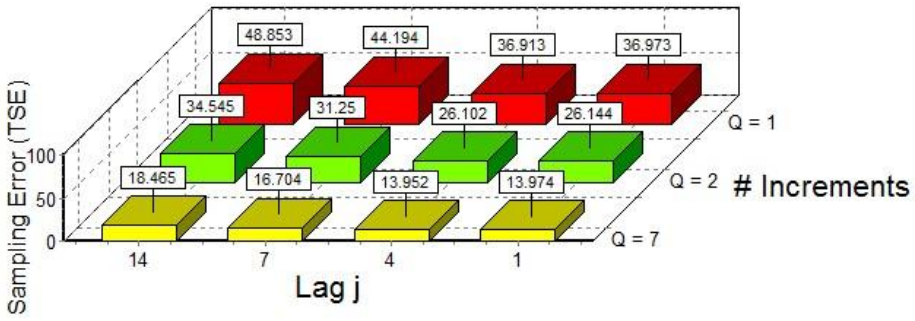

Figure 158 Total Sampling Error for measuring conductivity in 24-hour samples from sampling point E. j = lag, Q = number of increments

As expected the TSE had the smallest value for j = 1 and Q = 7 of 4.66 %. As sampling was done commonly with j = 1 and Q = 1, the TSE for point E would give an error of 12.3 %.

Sampling Point G

As before a 3D histogram is made of the TSE with relative values for TSE as a function of different values for j and Q, see Figure 159.

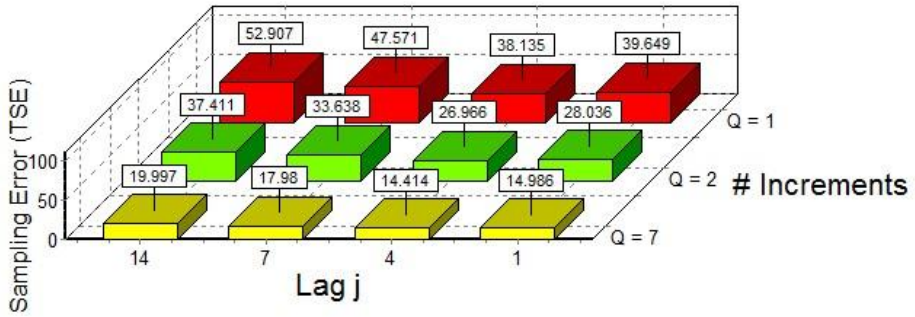

Figure 159 Total Sampling Error for measuring conductivity in 24-hour samples from sampling point G. j = lag, Q = number of increments

As expected the TSE had the smallest value for j = 1 and Q = 7 of 5.00 %. As sampling was done commonly with j = 1 and Q = 1, the TSE for point G would give an error of 13.2 %.

Sampling Point D

As before a 3D histogram is made of the TSE with relative values for TSE as a function of different values for j and Q, see Figure 160.

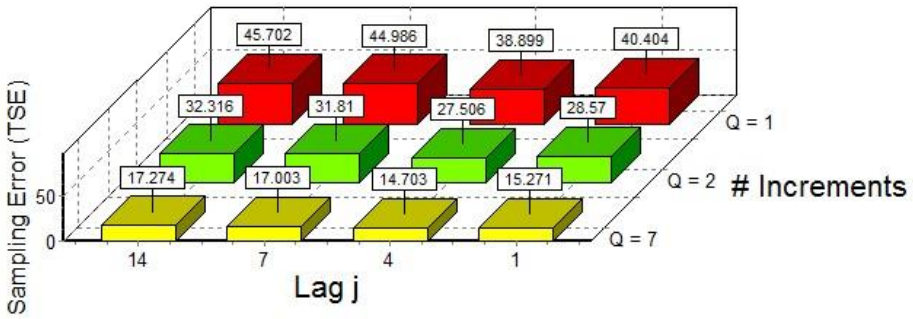

Figure 160 Total Sampling Error for measuring conductivity in 24-hour samples from sampling point D. j = lag, Q = number of increments

As expected the TSE had the smallest value for j = 1 and Q = 7 of 5.09 %. As sampling was done commonly with j = 1 and Q = 1, the TSE for point E would give an error of 13.5 %.

Sampling Point B

As before a 3D histogram is made of the TSE with relative values for TSE as a function of different values for j and Q, see Figure 161.

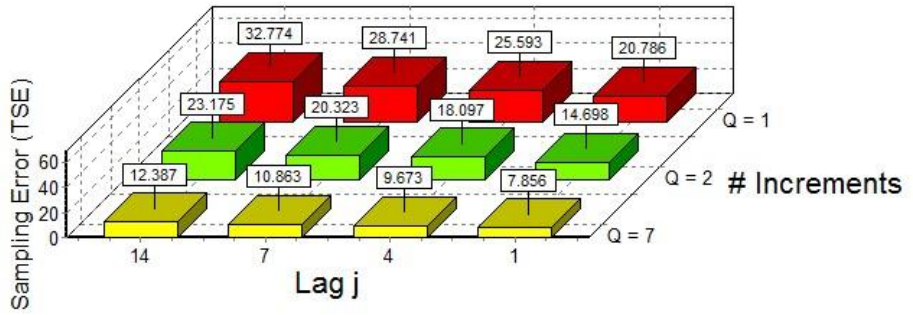

Figure 161 Total Sampling Error for measuring conductivity in 24-hour samples from sampling point B. j = lag, Q = number of increments

As expected the TSE had the smallest value for j = 1 and Q = 7 of 2.62 %. As sampling was done commonly with j = 1 and Q = 1, the TSE for point B would give an error of 6.93 %.

Sampling Point C

As before a 3D histogram is made of the TSE with relative values for TSE as a function of different values for j and Q, see Figure 162.

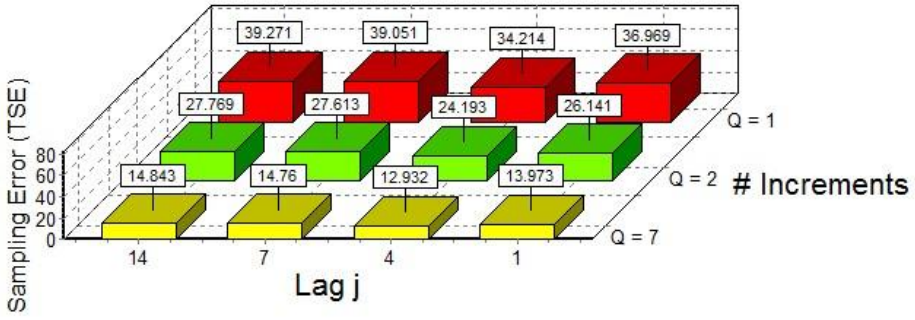

Figure 162 Total Sampling Error for measuring conductivity in 24-hour samples from sampling point C. j = lag, Q = number of increments

As expected the TSE had the smallest value for j = 1 and Q = 7 of 4.66 %. As sampling was done commonly with j = 1 and Q = 1, the TSE for point E would give an error of 12.3 %.

Appendix 31 – Ammonium in Increments

Analytical Data for NH_4-N in Increments from Sampling Point F

#	[mg/L]		#	[mg/L]		#	[mg/L]		#	[mg/L]		#	[mg/L]		#	[mg/L]
1	0.357		49	0.402		97	0.358		141	0.321		189	0.246		233	0.199
2	0.357		50	0.408		98	0.354		142	0.320		190	0.247		234	0.192
3	0.359		51	0.410		99	0.351		143	0.320		191	0.245		235	0.184
4	0.367		52	0.395		100	0.348		144	0.225		192	0.247		236	0.190
5	0.376		53	0.392		101	0.348		145	0.319		193	0.250		237	0.184
6	0.393		54	0.383		102	0.341		146	0.323		194	0.245		238	0.185
7	0.338		55	0.384		103	0.341		147	0.322		195	0.248		239	0.192
8	0.341		56	0.385		104	0.333		148	0.323		196	0.248		240	0.185
9	0.348		57	0.392		105	0.321		149	0.320		197	0.247		241	0.193
10	0.348		58	0.386		106	0.334		150	0.319		198	0.230		242	0.183
11	0.348		59	0.380		107	0.346		151	0.317		199	0.225		243	0.184
12	0.356		60	0.383		108	0.332		152	0.315		200	0.230		244	0.180
13	0.262		61	0.390		109	0.348		153	0.292		201	0.225		245	0.191
14	0.262		62	0.391		110	0.353		154	0.210		202	0.226		246	0.182
15	0.264		63	0.393		111	0.349		155	0.268		203	0.221		247	0.180
16	0.238		64	0.396		112	0.346		156	0.285		204	0.219		248	0.176
17	0.143		65	0.390		113	0.346		157	0.287		205	0.210		249	0.178
18	0.362		66	0.391		114	0.345		158	0.292		206	0.210		250	0.181
19	0.363		67	0.385		115	0.352		159	0.300		207	0.203		251	0.177
20	0.295		68	0.383		116	0.345		160	0.286		208	0.205		252	0.179
21	0.241		69	0.387		117	0.351		161	0.287		209	0.208		253	0.173
22	0.261		70	0.381		118	0.368		162	0.286		210	0.208		254	0.172
23	0.271		71	0.380		119	0.360		163	0.263		211	0.204		255	0.167
24	0.203		72	0.380		120	0.364		164	0.274		212	0.202		256	0.164
25	0.197		73	0.390		121	0.365		165	0.255		213	0.200		257	0.167
26	0.182		74	0.395		122	0.368		166	0.273		214	0.200		258	0.163
27	0.184		75	0.386		123	0.367		167	0.283		215	0.200		259	0.163
28	0.140		76	0.387		124	0.365		168	0.265		216	0.209		260	0.163
29	0.143		77	0.381		125	0.312		169	0.281		217	0.207		261	0.163
30	0.156		78	0.379		126	0.352		170	0.293		218	0.205		262	0.163
31	0.180		79	0.376		127	0.233		171	0.291		219	0.205		263	0.161
32	0.165		80	0.382		128	0.254		172	0.289		220	0.204		264	0.168
33	0.180		81	0.384		129	0.357		173	0.227		221	0.206		265	0.160
34	0.395		82	0.374		130	0.329		174	0.258		222	0.203		266	0.156
35	0.394		83	0.367		131	0.362		175	0.269		223	0.202		267	0.162
36	0.391		84	0.358		132	0.313		176	0.266		224	0.202		268	0.161
37	0.395		85	0.367		133	0.329		177	0.272		225	0.201		269	0.159
38	0.393		86	0.375		134	0.312		178	0.259		226	0.202		270	0.067
39	0.390		87	0.373		135	0.320		179	0.264		227	0.200		271	0.058
40	0.386		88	0.367		136	0.321		180	0.260		228	0.199		272	0.080
41	0.391		89	0.366		137	0.361		181	0.253		229	0.198		273	0.077
42	0.390		90	0.372		138	0.321		182	0.252		230	0.199		274	0.083
43	0.395		91	0.371		139	0.329		183	0.256		231	0.220		275	0.072
44	0.399		92	0.378		140	0.317		184	0.248		232	0.199		276	0.071
45	0.402		93	0.372					185	0.250						
46	0.396		94	0.359	**Mean [mg/L]**	0.374			186	0.250			**Mean [mg/L]**			0.283
47	0.404		95	0.358	**Stddev [mg/L]**	0.02			187	0.249			**Stddev [mg/L]**			0.86
48	0.401		96	0.358	**CV [%]**	5.4			188	0.249			**CV [%]**			30.58

Blue numbers are outliers. Red numbers are calculated as the mean of the two surrounding results.
Green numbers are the samples from after the variographic analysis is calculated